THE ROLE OF NAC TRANSCRIPTION FACTORS IN THE GENETIC REGULATION OF SENESCENCE TIMING AND GRAIN PROTEIN CONTENT IN WHEAT

by

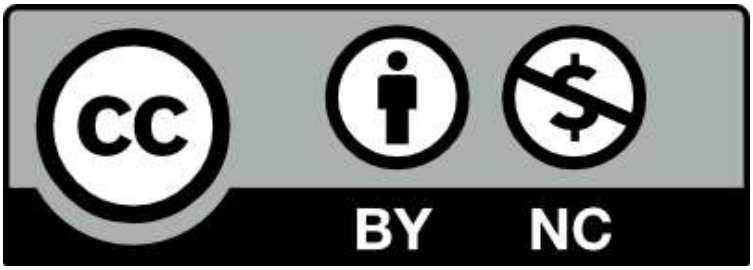
CATHERINE EMMA BLESSLEY EVANS

A thesis submitted to the University of Birmingham for the degree of
DOCTOR OF PHILOSOPHY

School of Biosciences
College of Life and Environmental Sciences
University of Birmingham
September 2023

UNIVERSITY OF BIRMINGHAM

University of Birmingham Research Archive
e-theses repository



This unpublished thesis/dissertation is under a Creative Commons Attribution-NonCommercial 4.0 International (CC BY-NC 4.0) licence.

You are free to:

Share — copy and redistribute the material in any medium or format

Adapt — remix, transform, and build upon the material

The licensor cannot revoke these freedoms as long as you follow the license terms.

Under the following terms:



Attribution — You must give appropriate credit, provide a link to the license, and indicate if changes were made. You may do so in any reasonable manner, but not in any way that suggests the licensor endorses you or your use.



NonCommercial — You may not use the material for commercial purposes.

No additional restrictions — You may not apply legal terms or technological measures that legally restrict others from doing anything the license permits.

Notices:

You do not have to comply with the license for elements of the material in the public domain or where your use is permitted by an applicable exception or limitation.

No warranties are given. The license may not give you all of the permissions necessary for your intended use. For example, other rights such as publicity, privacy, or moral rights may limit how you use the material.

Unless otherwise stated, any material in this thesis/dissertation that is cited to a third-party source is not included in the terms of this licence. Please refer to the original source(s) for licencing conditions of any quotes, images or other material cited to a third party.

I. Abstract

Wheat is the fourth most produced crop globally, and the first in the UK. High wheat grain protein content is important for both baking quality and nutritional value. A genetic trade-off between protein content and yield makes it a challenge to improve protein content without decreasing yield. In wheat, nitrogen remobilized from senescing leaves to developing grain contributes to grain protein content, and earlier leaf senescence correlates with increased protein and decreased yield. Transcription factors regulate the timing of leaf senescence in plants.

The aim of this thesis was to characterize the role of NAC transcription factors in regulating senescence timing in wheat. To achieve this, the progress of leaf and peduncle senescence was measured in wheat with overexpression or loss-of-function mutations of candidate NAC transcription factors. Results showed that *NAC5-1* and *NAM-2* promote earlier senescence, while *NAP-1* does not. *NAC5-1* and *NAM-2* promote decreased grain length and kernel weight respectively, but do not affect grain protein content. This provides some support to the model that transcriptional regulation of senescence timing mediates the trade-off between wheat protein content and yield. Showing that *NAC5-1* and *NAM-2* regulate senescence timing contributes to deciphering the transcription factor network of senescence in wheat. To explore application of transcription factors regulating senescence to wheat breeding, this thesis demonstrated that known senescence regulator *NAM-1* increases grain protein content in a UK field context. Allelic variants in candidate NAC transcription factors were identified and tracked in wheat breeding populations. Variation in senescence-regulating transcription factors such as *NAC5-1* and *NAM-2* could be targeted in wheat breeding to optimise the balance between wheat grain protein content and yield.

II. Acknowledgements

I am immensely grateful to supervisors Philippa Borrill and Juliet Coates, for supporting this project from start to finish, providing constructive advice, and encouraging me to develop skills and confidence as a researcher.

I would like to thank everyone in the Borrill Lab, not only for helping keep wheat plants alive and many other pieces of practical assistance, but also for being great company on this journey.

I would also like to thank industry supervisors Ruth Bryant and Chris Burt for facilitating exciting collaborative research projects, and, along with all the team at RAGT Ickleton, for welcoming me on placement and teaching me about the wheat breeding perspective.

I am grateful to technology platforms and support staff at University of Birmingham and John Innes Centre, without whom experiments would not have been possible. The MIBTP program and the JIC Women in Wheat network have provided enriching opportunities during this doctoral program which I will always remember.

Finally, to Mum, Dad, James, and too many friends to name – you believed in me; it means a lot.

This work was funded by Biotechnology and Biological Sciences Research Council (BBSRC) grant 2264969 and by RAGT Seeds Ltd. through a Midlands Integrative Biosciences Training Partnership (MIBTP) iCASE Studentship. Wheat transformation was funded by grant BB/R014876/1.

III. Contents listings

i. Table of contents

I. Abstract II

II. Acknowledgements III

III. Contents listings IV

i. Table of contents IV

ii. List of illustrations XI

iii. List of tables XXXIII

iv. List of definitions/abbreviations XLII

1 INTRODUCTION 1

1.1 Wheat production is key to global food security 1

1.2 The polyploid genome of modern wheat 1

1.2.1 Origin of the hexaploid genome of bread wheat 1

1.2.2 Implications of the hexaploid genome of bread wheat 2

1.3 Wheat grain protein content is important for human nutrition and bread quality 4

1.4 The challenge of improving wheat grain protein content 5

1.4.1 The trade-off between grain protein content and yield 5

1.4.2 The challenge 6

1.5 What is senescence? 7

1.5.1 The process of plant senescence 7

1.5.2 Nitrogen is remobilized from leaves to grain during senescence 8

1.5.3 Senescence timing is modulated by both developmental age and environmental stress 10

1.6 Wheat leaf senescence is linked to both grain yield and grain protein content 12

1.6.1 The link between senescence, yield and grain protein content 12

1.6.2 The impact of senescence on yield and protein content depends on the environment 14

1.6.3 The opportunity to improve nitrogen remobilization 15

1.7 Transcription factors regulate senescence in plants 16

1.7.1 The role of transcription factors in plant senescence 16

1.7.2 The NAC family of transcription factors in senescence 16

1.7.3 Advancing understanding of NAC transcription factors regulating senescence in wheat 18

1.8 The role of NAC transcription factors in regulating senescence in wheat 19

1.8.1 Senescence-associated NAC transcription factors in wheat, barley and rice 19

1.8.2 NAC transcription factors in this thesis 0

1.8.1 Technologies for wheat gene characterisation in this thesis 0

1.8.2 Senescence-regulating transcription factors as targets for improving senescence timing 4

1.9 Objectives 0

2 DOES *NAM-2* AFFECT THE TIMING OF SENESCENCE OR GRAIN PROTEIN CONTENT? 1

2.1 Introduction 1

2.1.1 Discovery of *NAM-1* de novo in wheat 1

2.1.2 Evolution of *NAM-1* and *NAM-2* 2

2.1.3 *NAM-1* increases grain protein by promoting the onset of senescence and nitrogen remobilization. 5

2.1.4 Further characterising the role of *NAM-2* in leaf senescence. 7

2.1.5 Objectives 8

2.2 Methods 9

2.2.1 Gene expression data 9

2.2.2 Development of *NAM-2* TILLING mutant lines 9

2.2.3 Working with TILLING lines 19

2.2.4 Plant growth 21

2.2.5 Phenotyping for glasshouse and CER experiments 24

2.2.6 Phenotyping for field experiments 30

2.2.7 Data analysis 32

2.2.8 Experimental Design 37

2.3 Results 45

2.3.1 Expression pattern of *NAM-2* during flag leaf senescence 45

2.3.2 Development of *NAM-2* TILLING lines 46

2.3.3 *NAM-2* TILLING lines show inconsistent senescence phenotypes in the glasshouse 66
2.3.4 Agronomic traits in *NAM-2* TILLING lines 75
2.3.5 Grain mass and protein content of *NAM-2* TILLING lines in the glasshouse 79
2.3.6 Effect of Cross and blocking factors on *NAM-2* dataset 89
2.3.7 Field trials of *NAM-2* TILLING lines 91
2.3.8 Senescence data for field trials 97
2.4 Discussion 104
2.4.1 Unravelling inconsistent senescence phenotyping data 104
2.4.2 There is some evidence that *NAM-2* promotes earlier senescence 107
2.4.3 The impact of *NAM-2* on grain mass and protein content 109
2.4.4 Conclusion 110
3 DO *NAC5-1* AND *NAP-1* AFFECT THE TIMING OF SENESCENCE? 112
3.1 Introduction: wheat orthologs of *OsNAC5* and *OsNAP* are candidate senescence regulators 112
3.1.1 *OsNAC5* plays a role in nutrient remobilization during senescence. 112
3.1.2 *OsNAP* promotes leaf senescence and osmotic stress tolerance in rice. 114
3.1.3 Objectives 114
3.2 Methods 115
3.2.1 Assessment of wheat orthologs of *OsNAC5* and *OsNAP* 115

3.2.2 Transformation of hexaploid wheat with constructs to overexpress *NAC5-A1* and *NAP-A1* 116

3.2.3 Development of tetraploid TILLING mutant lines for *NAC5-1* and *NAP-1* 121

3.2.4 Working with transgenic lines 123

3.2.5 Experimental design 127

3.3 Results 136

3.3.1 Identification of the orthologs of *OsNAC5* and *OsNAP* in wheat..... 136

3.3.2 Expression patterns of *NAC5-1* and *NAP-1* during flag leaf senescence 145

3.3.3 Overexpression of *NAC5-A1* in wheat 146

3.3.4 Mutations in *NAC5-1* in tetraploid wheat..... 164

3.3.5 Overexpression of *NAP-A1* in wheat 178

3.3.6 Mutations in *NAP-A1* in tetraploid wheat 191

3.4 Discussion 197

3.4.1 *NAC5-1* may promote earlier senescence in wheat..... 197

3.4.2 The role of *NAP-1* in wheat senescence..... 199

3.4.3 Strengths and caveats of these glasshouse experiments..... 201

3.4.4 Conclusion..... 202

4 APPLYING UNDERSTANDING OF SENESCENCE TO WHEAT BREEDING 204

4.1 Introduction..... 204

4.1.1 The challenge of improving wheat grain protein content 204

4.1.2 Senescence timing and grain protein content have changed through wheat breeding 205

4.1.3 Introgression of functional *NAM-B1* increases protein content in diverse germplasm and field conditions 205

4.1.4 Methods for phenotyping senescence vary across the literature. 208

4.1.5 Untapped genetic variation for senescence and grain protein content 209

4.1.6 Techniques in this chapter: exome capture and Near Isogenic Lines. 210

4.1.7 Allelic variation in *NAM-A1* 212

4.1.8 *NAM-2, NAC5-1* and *NAP-1* are candidate senescence regulators.... 213

4.1.9 Objectives 213

4.2 Methods 214

4.2.1 Experimental design 214

4.2.2 Genetic variation analysis 216

4.3 Results 226

4.3.1 Impact of *NAM-A1* and *NAM-B1* on senescence, yield and protein content in the field in the UK 226

4.3.2 Genetic diversity: From genes regulating senescence to selectable markers 239

4.4 Discussion 257

4.4.1 *NAM-A1* and *NAM-B1* promote earlier senescence and increased protein content in UK field conditions 257

4.4.2 Effect of *NAM-A1* and *NAM-B1* on yield 259

4.4.3 A pipeline to investigate and track allelic variation 260
4.4.4 Variation in NAC transcription factors 261
4.4.5 Implication of allelic variation in *NAM-A1* 263
4.4.6 Limitations of genetic variation analysis 264
4.4.7 Conclusion 265
5 DISCUSSION 266
5.1 Summary of main findings 266
5.2 Characterisation of NAC transcription factors 267
5.2.1 The role of three NAC transcription factors in senescence timing 267
5.2.2 Understanding of senescence regulation applied in a wheat breeding context 268
5.2.3 Expression profiles of NAC transcription factors in leaf senescence .. 270
5.3 Challenges and limitations 271
5.3.1 Senescence is environmentally variable 271
5.3.2 Challenges of TILLING lines 272
5.4 Implications for regulation of senescence timing in wheat 275
5.4.1 Understanding the protein-yield trade-off 275
5.4.2 The role of *NAM-A1* in wheat 275
5.4.3 The role of *NAP-1* in wheat 277
5.4.4 The regulatory network of senescence 278
5.4.5 Genetic redundancy and NAC transcription factors 280
5.5 Avenues for future research 282

5.5.1 Testing the impact of *NAC5-1* and *NAM-2* on nitrogen remobilization 282

5.5.2 Characterising novel candidate senescence regulators 283

5.5.3 Identifying downstream targets of senescence-regulating NACs..... 285

5.6 Applications for wheat breeding 288

5.6.1 A pipeline for applying allelic variation in wheat..... 288

5.6.2 Wheat germplasm 289

5.6.3 Scoring senescence 289

5.6.4 Applying understanding of senescence regulation to wheat improvement 290

5.7 Conclusion..... 292

6 References 293

ii. List of illustrations

Figure 1.1 The allohexaploid genome of bread wheat (Triticum aestivum ssp. aestivum, AABBDD) derives from two successive hybridization and whole genome duplication events. Most genes in bread wheat have three copies on the A, B and D subgenomes, known as homoeologs. 4

Figure 1.2 Conceptual diagram of the connection between senescence and the trade-off between protein content and yield. 13

Figure 1.3 Location of NAM-1, NAM-2, NAC5-1 and NAP-1 homoeologs in the bread wheat reference genome, Chinese Spring RefSeq v1.1 (Appels et al. 2018). NAM-B1 is not shown as the reference genome does not contain a functional gene copy. Figure generated with R package chromoMap (Anand and Rodriguez Lopez 2022). 2

Figure 1.4 Schematics of NAM-1, NAM-2, NAC5-1 and NAP-1 transcripts and peptide sequences. Transcripts taken from the bread wheat reference genome (IWGSC Refseq v1.1) (Appels et. al. 2018); except for NAM-B1 which is from Genbank DQ869673 (Uauy et.al. 2006) – a sequence which does not show UTRs. Black arrows mark start of transcript or peptide. NAC domains are based on Prosite annotation. TILLING mutations are annotated with wild-type/mutant alleles. For more information on TILLING mutations see Table 2.12 and Table 3.14. 3

Figure 2.1 Crossing scheme for NAM-2 TILLING lines. Read from top to bottom. Capital letters = wild type allele; lower case = TILLING loss-of-function allele; BC_1 = backcross 1; F_1 and F_2 = generation 1 and 2 after most recent cross. Red script shows the probability of each of the progeny shown. Months taken for crossing scheme in speed breeding shown on the left. 17

Figure 2.2 Example of KASP genotyping assay for the BC_1F_2 population of cross X61, with 336 plants segregating for NAM-A2, NAM-B2 and NAM-D2 TILLING mutations. A) Structure of KASP primers. In a wild-type sample, the WT primer and the COM primer amplify producing the reverse complement of the HEX tag sequence. This binds the HEX dye and fluorescence is detected. In a homozygous mutant, the MUT and COM primers amplify, leading to FAM fluorescence. B) KASP genotyping output for NAM-A2, NAM-B2 and NAM-D2 (top to bottom). HEX fluorescence on the y-axis and FAM fluorescence on the x-axis. Three clusters were called (Red = wild-type / Y:Y, Green = heterozygous / X:Y, Blue = homozygous / X:X). C) Summary table of number of plants per genotype. Genotypes listed in Figure 2.1 and triple heterozygotes were kept (yellow highlight). 18

Figure 2.3 Pipeline for seed bulking of NAM-2 homozygous mutant lines. Leaf tissue samples were taken from 2-3 week old seedlings and used for KASP genotyping,

which confirmed plant genotypes. Bagged ears from individual plants were harvested for glasshouse experiments, while unbagged ears were bulk harvested for a field trial 19

Figure 2.4 Leaf senescence scoring scale for field trials. Examples of percentage leaf yellowing in 10% intervals from 0% to 100% taken from wheat breeding lines scored in 2022 (not otherwise shown). Leaf senescence was scored in 5% intervals. Images cropped to show centre of 6m field plots. 31

Figure 2.5 Ear senescence scoring scale for field trials, Examples of percentage ear yellowing in 20% intervals from 0% to 100% taken from wheat breeding lines scored in 2020 (not otherwise shown). Ear senescence was scored in 10% intervals. Images show 6m field plots..... 31

Figure 2.6 Graphical representation of senescence metrics for field data. The x-axis is shown in Thermal time after heading. The leaf senescence time-course was inferred by linear interpolation between senescence scores (black dots connected by black lines). Duration of leaf senescence (Dur_Leaf_Sen) is the Thermal time between reaching 10% and 90% leaf senescence (red horizontal line). Area under curve (AUC) of leaf senescence (AUC_Leaf_Sen) is the area below the leaf senescence time-course (blue shading)..... 35

Figure 2.7 Experimental layout for NAM-2 Field trial. 1m^2 trial plots were laid out in a RCBD with each magazine/column as a block, containing two plots of Cadenza and one plot of each other genotype. The entire trial was surrounded by guard plots (Soissons) to avoid edge effects. 43

Figure 2.8 NAM-2 is upregulated in wheat flag leaves in a time-course of early senescence. Expression level in transcripts per million (tpm) in flag leaves from 3DAA to 26DAA. (A) NAM-2; (B) NAM-1. Re-analysed from (Borrill et al. 2019). 45

Figure 2.9 Multiple alignment of NAM-1 and NAM-2 used to select TILLING mutations in NAM-2. Multiple alignment of peptide sequences (using first of two potential start codons) was carried out in Clustal Omega. "" marks amino acid identity. "." and ":" mark amino acids with similar chemical properties. NAM-B1 is not shown because there is not a functional gene copy in the reference genome. Annotations: 1) NAC conserved subdomains based on NAM-A1 in (Uauy et al. 2006); 2) Recorded mutation sites with an effect on senescence in at least one experiment from Table 2.13; 3) Recorded mutation sites with no effect on senescence, or not tested; 4) Mutation sites in NAM-2 in the Cadenza TILLING population; 5) Mutation sites in NAM-2 selected in this thesis..... 49*

Figure 2.10 Air temperature for NAM-2 glasshouse experiments. NAM-2 lines were grown in the glasshouse in two experiments starting September 2022 and February 2023. Air temperature at wheat canopy height was measured with an EasyLog at 15 minute intervals. Mean glasshouse air temperature in day-time 8am – 8pm (red solid lines) and night-time 8pm – 8am (blue dotted lines)..... 67

*Figure 2.11 Leaf senescence timing of NAM-2 triple mutant lines and controls varies between trials and crosses. TILLING lines from two independent crosses with mutations in NAM-2 and wild-type segregant controls were grown in the glasshouse in 2022 and 2023. (A, C, E, G) Flag leaf chlorophyll content (SPAD) in weeks after heading +/- 2 days. Average SPAD value at each timepoint was compared by Wilcoxon test, *=p<0.05 / **=p<0.01 / **=p<0.001. (B, F) Representative plants of NAM-2 triple mutant and control at 55DAH and 48DAH. (C, H) Representative plants of NAM-2 triple mutant and control at 41DAH and 43DAH, alongside flag leaves of the same plants. (A, B) Cross X50 grown in 2022. (C, D) Cross X50 grown in 2023. (E, F) Cross X61 grown in 2022. (G, H) Cross X61 grown in 2023. ..... 69*

*Figure 2.12 Some NAM-2 mutants showed later onset of leaf senescence than controls among X61 in 2022 and X50 in 2023, but some NAM-2 mutants showed earlier senescence onset among X61 in 2023. (A, B) Heading date (DAS); (C, D) Days from heading to SPAD=30. (A, C) 2022 Experiment. (B, D) 2023 Experiment. (A-D) ANOVA with post-hoc Tukey test, formula ~ Row + Block + Cross*Genotype, letters show significance groups at p<0.05. In graphs for X50, the "aabb" genotype derived from X54.* 71

*Figure 2.13 NAM-2 genotype affects AUC of leaf senescence, dependent on cross and experiment, but has no impact on Duration of leaf senescence. (A, B) Area under curve (AUC) of leaf senescence; (C, D) Duration of leaf senescence. (A, C) 2022 Experiment. (B, D) 2023 Experiment. (A-D) ANOVA with post-hoc Tukey test, formula ~ Row + Block + Cross*Genotype, letters show significance groups at p<0.05. In graphs for X50, the "aabb" genotype derived from X54.* 73

*Figure 2.14 In 2023, NAM-2 triple mutants in cross X50 trend towards later peduncle senescence and 25% leaf yellowing, while triple mutants in cross X61 trend towards earlier 25% leaf yellowing. (A) 25% flag leaf yellowing in 2023 Experiment; (B) 100% peduncle yellowing in 2023 Experiment. (A-B) ANOVA with post-hoc Tukey test, formula ~ Row + Block + Cross*Genotype, letters show significance groups at p<0.05. NB: 25% flag leaf yellowing and 100% peduncle yellowing were not shown for 2022 Experiment as a high number of missing values made these data unreliable. In graphs for X50, the "aabb" genotype derived from X54.* 74

Figure 2.15 Tiller number varied between NAM-2 TILLING lines in 2022 but was consistent in 2023, while NAM-2 X50 "aabb" was significantly taller than other lines in 2022, likely due to its distinct pedigree from other X50 lines. (A, B) Main tiller number; (C, D) Height of primary tiller (mm). (A, C) 2022 Experiment. (B, D) 2023

*Experiment. (A-D) ANOVA with post-hoc Tukey test, formula ~ Row + Block + Cross*Genotype, letters show significance groups at p<0.05. In graphs for X50, the "aabb" genotype derived from X54..... 77*

*Figure 2.16 Flag leaf length was lower in 2023 than 2022, but consistent between genotypes and crosses, while flag leaf width was higher across NAM-2 X50 compared to NAM-2 X61 in 2023. (A, B) Flag leaf length (mm); (C) Flag leaf width (mm). (A) 2022 Experiment. (B, C) 2023 Experiment. (A-C) ANOVA with post-hoc Tukey test, formula ~ Row + Block + Cross*Genotype, letters show significance groups at p<0.05. In graphs for X50, the "aabb" genotype derived from X54..... 78*

*Figure 2.17 Grain number and grain mass did not differ across the majority of NAM-2 TILLING lines. (A, B) Grain number; (C, D) Grain mass (g). (A, C) 2022 Experiment. (B, D) 2023 Experiment. (A-D) ANOVA with post-hoc Tukey test, formula ~ Row + Block + Cross*Genotype, letters show significance groups at p<0.05. In graphs for X50, the "aabb" genotype derived from X54..... 82*

*Figure 2.18 Some NAM-2 mutants showed increased thousand kernel weight in X50, with no differences within X61. (A, B) Thousand kernel weight (g); (C, D) Average grain length (mm). (A, C) 2022 Experiment. (B, D) 2023 Experiment. (A-D) ANOVA with post-hoc Tukey test, formula ~ Row + Block + Cross*Genotype, letters show significance groups at p<0.05. In graphs for X50, the "aabb" genotype derived from X54..... 84*

*Figure 2.19 NAM-2 lines show some variability in grain width and area. (A, B) Average grain width (mm); (C, D) Average grain area (mm^2). (A, C) 2022 Experiment. (B, D) 2023 Experiment. (A-D) ANOVA with post-hoc Tukey test, formula ~ Row + Block + Cross*Genotype, letters show significance groups at p<0.05. In graphs for X50, the "aabb" genotype derived from X54..... 86*

*Figure 2.20 NAM-2 triple mutants showed increased grain protein content compared to controls in X61 in 2022, but not in other experiments. (A) Predicted grain protein content (%) in 2022; (B) Predicted grain protein content (%) in 2023. (A-D) ANOVA with post-hoc Tukey test, formula ~ Row + Block + Cross*Genotype, letters show significance groups at p<0.05. In graphs for X50, the "aabb" genotype derived from X54. Diamonds and bars represent mean and standard error. 87*

*Figure 2.21 Normalising for thousand grain weight accounts for differences in protein content between 2022 and 2023. (A) Predicted protein mass per thousand grains (g) in 2022; (B) Predicted protein mass per thousand grains (g) in 2023. (A-D) ANOVA with post-hoc Tukey test, formula ~ Row + Block + Cross*Genotype, letters show significance groups at p<0.05. In graphs for X50, the "aabb" genotype derived from X54. Diamonds and bars represent mean and standard error. 88*

Figure 2.22 Mean daily air temperature at JIC Church Farm weather station from 01/05/2023 to 31/07/2023. NAM-2 TILLING lines were grown in the field at JIC Church Farm in the 2023 season. Air temperature was averaged across a 24-hour period. Annotations mark the time interval of heading, and dates when all plots had reached 10% and 100% leaf senescence. 92

Figure 2.23 Thermal time to 70% leaf senescence does not show an obvious spatial pattern. Tile plot shows thermal time to 70% leaf senescence (°C days) of each $1m^2$ plot as arranged in the field. Each x-axis column represents one block. 93

*Figure 2.24 Seedling establishment significantly differed between NAM-2 TILLING lines, however this did not relate to the number of functional copies of NAM-2. (A) Percentage of $1m^2$ plot covered with plants in March; (B) Average height across plot (cm) in May. (A, B, C, D) Analysed by ANOVA with post-hoc Tukey test, formula ~ Cross*Genotype, p<0.05. In graphs for X50, the "aabb" genotype derived from X54.*

Diamonds and bars represent mean and standard error. Non-mutagenized Cadenza (right hand panel) not included in statistical analysis. 94

Figure 2.25 Poor seedling establishment correlated with late heading, earlier 30% leaf senescence relative to heading, and later peduncle senescence in absolute time. Seedling vigour in November was categorised: Good = many large seedlings, similar to guard plots (Soissons). OK = several medium seedlings. Poor = few small seedlings, empty gaps in plot. Seedling vigour plotted against (A) Percentage of $1m^2$ plot covered with plants in March; (B) Average height across plot (cm) in May; (C) Date of ear emergence; (D) Area under curve (AUC) of leaf senescence; (E) Duration of leaf senescence; (F) Thermal time to 30% leaf senescence (°C days); (G) Thermal time to 90% leaf senescence (°C days); (H) Number of senesced peduncles out of 10 on 17/07/2023. (A-H) Analysed by ANOVA with post-hoc Tukey test, formula ~ Vigour.2023-11-10, $p<0.05$..... 96

Figure 2.26 Representative field plots from NAM-2 field trial. Field plots from replicate 2 photographed from the same angle before, during and after leaf senescence. Dates on left hand side; cross and genotype above. Percentage leaf yellowing for each plot is shown above the photograph. 97

Figure 2.27 NAM-2 TILLING lines vary in heading (ear emergence) date in the field. In graphs for X50, the "aabb" genotype derived from X54. Diamonds and bars represent mean and standard error..... 98

Figure 2.28 NAM-2 triple mutant lines showed later leaf senescence than controls in cross X50 but not cross X61 in the field. Percentage leaf yellowing scored visually, for each $1m^2$ plot, against thermal time after heading (°C days)..... 99

Figure 2.29 NAM-2 triple mutant lines showed later peduncle senescence than controls in cross X50 but not cross X61 in the field. Number of senesced peduncles out of 10, for each 1m^2 plot, against thermal time after heading (°C days)..... 99

*Figure 2.30 NAM-2 X50 "aabb" showed earlier onset and longer duration of senescence, while AUC of leaf senescence varied between NAM-2 TILLING lines. (A) Area under curve (AUC) of leaf senescence; (B) Duration of leaf senescence; (C) Thermal time to 10% leaf senescence (°C days); (D) Thermal time to 30% leaf senescence (°C days). (A, B, C, D) Analysed by ANOVA with post-hoc Tukey test, formula ~ Cross*Genotype, p<0.05. In graphs for X50, the "aabb" genotype derived from X54. Diamonds and bars represent mean and standard error. 102*

*Figure 2.31 NAM-2 X50 triple mutants reached 50% 70% and 90% leaf senescence later than controls. (A) Thermal time to 50% leaf senescence (°C days); (B) Thermal time to 70% leaf senescence (°C days); (C) Thermal time to 90% leaf senescence (°C days); (D) Number of senesced peduncles out of 10 on 20/07/2023. (A, B, C, D) Analysed by ANOVA with post-hoc Tukey test, formula ~ Cross*Genotype, p<0.05. In graphs for X50, the "aabb" genotype derived from X54. Diamonds and bars represent mean and standard error..... 104*

Figure 3.1 Overview of NAC5-A1 and NAP-A1 overexpression lines. Hexaploid Fielder wheat was transformed with a construct to express NAC5-A1 or NAP-A1 from a rice actin promoter (top right). Single-copy T_0 lines with 1 construct copy and multi-copy T_0 lines with 4+ construct copies were selected with a copy number assay (red ovals). T_1 progeny were grown in glasshouse experiments (bottom right). From the T_1 lines, homozygous and null segregants were selected with a copy number assay (red ovals). T_2 progeny were grown in glasshouse experiments (bottom right).

Blue bars represent transgenic construct insertions. Sowing dates of glasshouse experiments are used as unique identifiers for each experiment. 117

Figure 3.2 Randomized complete block design for NAC5-1 NAP-1 overexpression T_2 (23/12/2021). (A) Each block consisted of one plant per genotype, arranged at random in an 8-cell tray. (B) Blocks were split across upper and lower shelves of two identical CER cabinets lit by panels of LED lights. 134

Figure 3.3 Randomized complete block design for NAC5-1 NAP-1 Kronos TILLING (01/12/2021). (A) Each block consisted of one plant per genotype for NAC5-1 or two plants per genotype for NAP-1, arranged at random in an 8-cell tray. (B) Blocks were shuffled laterally along the glasshouse bench every two weeks to balance exposure to glasshouse lights. 136

Figure 3.4 TraesCS4A02G219700 and its homoeologs are the orthologs of OsNAC5. Peptide sequences of the 15 top BLAST hits of OsNAC5 in Triticum aestivum and Oryza sativa ssp. japonica were aligned in Clustal Omega. A rooted tree was built with the Neighbour-Joining method. The node containing OsNAC5 is highlighted. Numbers show support values from 100 bootstrap replicates. Scale bar shows number of substitutions per site. 138

Figure 3.5 Peptide alignment of OsNAC5, TraesCS4A02G219700 and its homoeologs. Alignment in Clustal Omega, displayed with MView. Amino acid residues with identity to OsNAC5 are highlighted red. 139

Figure 3.6 TraesCS4A02G131000 and its homoeologs are the orthologs of OsNAP. Peptide sequences of the 15 top BLAST hits of OsNAP in Triticum aestivum and Oryza sativa ssp. japonica were aligned in Clustal Omega. A rooted tree was built with the Neighbour-Joining method. The node containing OsNAP is highlighted.

Numbers show support values from 100 bootstrap replicates. Scale bar shows number of substitutions per site. 141

Figure 3.7 Peptide alignment of OsNAP and ONAC103 with TraesCS4A02G131000, TraesCS2A02G101900, TraesCS2A02G102000 and their homoeologs. Alignment in Clustal Omega, displayed with MView. Amino acid residues with identity to OsNAP are highlighted red..... 143

Figure 3.8 NAC5-1 and NAP-1 are upregulated in wheat flag leaves in a time-course of early senescence. Expression level in transcripts per million (tpm) in flag leaves from 3DAA to 26DAA. (A) NAC5-1; (B) NAP-1; (C, D) Paralogs of NAP-1. Re-analysed from (Borrill et al. 2019). 146

*Figure 3.9 Average expression of NAC5-A1 varies between independent T_1 transgenic lines. Average relative transcript level of (A) 3*FLAG::NAC5-A construct normalized to 5.4; (B) NAC5-A1 normalized to 5.con. RNA was extracted from pooled leaf samples of 12 T_1 plants per transgenic line, at 3 weeks. Relative transcript level was analysed by RT-qPCR using ΔΔCt method with Actin as reference gene, mean ±SD (n=3 technical replicates). "na" marks samples that were not amplified..... 148*

*Figure 3.10 Lines 5.4, 8.2 and 8.3 contain individuals with higher expression of NAC5-A1 than controls. Relative transcript level by RT-qPCR of (A) 3*FLAG::NAC5-A1 construct; (B) NAC5-A1; (C) NAC5-A1, NAC5-B1 and NAC5-D1 combined. RNA was extracted from leaves of individual T_1 plants at 3 weeks. Relative transcript level calculated the Pfaffl method with primer efficiencies and Actin as reference gene, normalised against the average of the single copy category, average of 3 technical replicates (n=12 plants). "na" marks samples that were not amplified..... 150*

Figure 3.11 Multiple phenotypes varied with the light level in the glasshouse. Heading dates in NAC5-A1 T1 lines, directly under glasshouse lights (L) or further from lights (D). Heading date scored in days, where 1 = 1st January 2021. 151

Figure 3.12 NAC5-A1 T_1 transgenic lines 8.2 and 8.3 senesced earlier than control 5.con but did not differ from control 8.con. Boxplots of (A) Heading date; (B) 25% flag leaf yellowing; (C) 100% peduncle yellowing (first tiller, n=12). DAH=Days after Heading. Letters show significance groups (post-hoc Tukey test, p<0.05). (D) Relative chlorophyll content of flag leaves measured by SPAD spectrophotometer, mean ±SE (n=12). Only lines directly under glasshouse lights are shown (see Methods 3.2.5.2). 153

Figure 3.13 NAC5-A1 T_1 transgenic lines 8.2 and 8.3 do not differ in grain mass or number from control 8.con. Boxplots of (A) Grain number; (B) Grain mass (g). Letters show significance groups (post-hoc Tukey test, p<0.05)..... 154

*Figure 3.14 Most, but not all, NAC5-A1 T_1 lines show expected segregation for the 3*FLAG::NAC5-A transgenic construct. Copy number of NAC5-1 construct in individual T_1 plants. Taqman qPCR was run against the nptII marker gene in the construct and analysed by ΔΔCt method, normalised against a known single-copy gene and the sample with median expression level in the "single copy" cluster (highlighted yellow)..... 155*

Figure 3.15 Multiple phenotypes of NAC5-1 and NAP-1 T2 lines vary between CER shelves. Plots of all genotypes in NAC5-1 and NAP-1 CER experiments categorised by CER shelf for (A) Heading date in days after sowing (DAS), (B) Main tiller number, (C) Seed number, (D) Flag leaf chlorophyll content (SPAD) in weeks after heading +/- 1 day. 157

*Figure 3.16 Flag leaves senesce later in NAC5-A1 transgenic compared to control for line 5.4 on Shelf 2 only. Flag leaf chlorophyll content (SPAD) in weeks after heading +/- 1 day was compared between homozygous transgenic and null segregant controls in T2 transgenic lines 5.4, 8.23 and 8.9. Average SPAD value at each timepoint was compared by Wilcoxon test, *=p<0.05. NB: Averages were taken of 2-5 data points; timepoints with small sample sizes may result in apparent differences that are not statistically significant. 158*

*Figure 3.17 Senescence phenotypes of NAC5-1 overexpression line 5.4. (A) Heading date (DAS); (B) 25% flag leaf yellowing; (C) 100% peduncle yellowing; (D) Days from heading to SPAD=30; (E) Area under curve (AUC) of leaf senescence; (F) Duration of leaf senescence (Days). (A-F) ANOVA with post-hoc Tukey test, formula ~ Shelf * Line_name, letters show significance groups at p<0.05. NB: Boxplots represent 2-5 individuals; small sample sizes may result in apparent differences that are not statistically significant. 160*

*Figure 3.18 Grain traits did not differ between homozygous NAC5-A1 transgenics and null segregants in line 5.4. (A) Main tiller number; (B) Seed mass (g); (C) Seed number; (D) Thousand grain weight; (E) Average grain length. ANOVA with post-hoc Tukey test, formula ~ Shelf * Line_name, letters show significance groups at p<0.05. NB: Boxplots represent 2-5 individuals; small sample sizes may result in apparent differences that are not statistically significant. 161*

Figure 3.19 Correlations between senescence traits and other phenotypes for NAC5-A1 transgenics data. Pearson's correlation coefficient, r^2. TT_SPAD10 = Days from heading to SPAD = 10, TT_SPAD30 = Days from heading to SPAD = 30, TT_SPAD40 = Days from heading to SPAD = 40, Dur_Leaf_Sen = Days from SPAD = 40 to SPAD = 10, AUC_Leaf_Sen = Area under flag leaf senescence SPAD curve,

Heading_date = Heading date (Days after sowing), Leaf_senescence_DAH = Days from heading to 25% leaf senescence, Peduncle_senescence_DAH = Days from heading to 100% peduncle senescence, Tiller_1 = number of main tillers, Seed_num = grain number per plant, Weight = grain mass per plant, TGW = thousand grain weight, O_area = mean area of grain, O_width = mean width of grain, O_length = mean length of grain..... 163

Figure 3.20 Plants with later sowing date had fewer tillers and seeds. Several plants in the NAP-1 TILLING experiment were re-sown three weeks later due to failed germination in the first batch. Plots show all plants in NAP-1 TILLING experiment categorised by sowing date, for (A) Heading date (DAS); (B) Days from heading to SPAD=30; (C) Number of main tillers and (D) Seed number. 168

Figure 3.21 Plants directly under glasshouse lights senesced faster. Flag leaf chlorophyll content (Weeks after Heading ± 2 days) for all plants in NAC5-1 TILLING experiment categorised by distance from the centre of the bench, where glasshouse lights were situated..... 171

*Figure 3.22 NAC5-1 double mutants retain flag leaf chlorophyll for longer than controls. (A-C) Flag leaf chlorophyll content (SPAD) in weeks after heading +/- 1 day was compared between NAC5-1 TILLING mutants and wild type segregant controls (AABB, n = 16). Average SPAD value at each timepoint was compared by Wilcoxon test, *=p<0.05. Data from crosses X388 and X392 were combined. (A) Double mutants (aabb, n = 14), (B) NAC5-B1 single mutants (AAbb, n = 14), NAC5-A1 single mutants (aaBB, n = 24). (B) Representative plants for wild type (AABB) single (aaBB / AAbb) and double (aabb) NAC5-1 mutants at 41DAH. (C) Flag leaves at 41DAH of plants in B. (D) Representative plants at 51DAH; different individuals to B. 173*

Figure 3.23 NAC5-1 double mutants show a trend toward later onset and AUC of leaf senescence however it is not statistically significant. (A) Heading date (DAS); (B) 25% flag leaf yellowing; (C) 100% peduncle yellowing; (D) Days from heading to SPAD=30; (E) Area under curve (AUC) of leaf senescence; (F) Duration of leaf senescence (Days). (A-F) ANOVA with post-hoc Tukey test, formula ~ Light + Block + Genotype, letters show significance groups at p<0.05. Data from crosses X388 and X392 were combined (n=14-24). *175*

Figure 3.24 Grain number, grain protein content, tiller number, and height did not differ between NAC5-1 TILLING lines, although grain length was higher in NAC5-1 double mutants. (A) Main tiller number; (B) Height of primary tiller (mm), (C) Seed mass (g); (D) Seed number; (E) Thousand grain weight; (F) Average grain length; (F) Grain protein content (%, subset of plants with seed mass > 15g). Data from crosses X388 and X392 were combined (n=14-24). *178*

*Figure 3.25 Average expression of NAP-A1 varies between independent T_1 transgenic lines. Average relative transcript level of (A) 3*FLAG::NAP-A1 construct; (B) NAP-A1. RNA was extracted from pooled leaf samples of 12 T_1 plants per transgenic line, at 3 weeks. Relative transcript level was analysed by RT-qPCR using $\Delta\Delta$Ct method with Actin as reference gene, mean $\pm$SD (n=3 technical replicates). "na" marks samples that were not amplified.* *179*

*Figure 3.26 Lines 7.9, 10.1, 10.5 and 10.9 contain individuals with higher expression of NAP-A1 than controls. Relative transcript level by RT-qPCR of (A) 3*FLAG::NAP-A1 construct; (B) NAP-A1; (C) NAP-A1, NAP-B1 and NAP-D1 combined. RNA was extracted from leaves of individual T_1 plants at 3 weeks. Relative transcript level calculated by the Pfaffl method with primer efficiencies and Actin as reference gene,*

normalised against the average of the single-copy category, average of 3 technical replicates (n=12 plants). "na" marks samples that were not amplified..... 181

Figure 3.27 Heading date varies dramatically among both NAP-A1 T_1 transgenic lines and non-transformed controls. (A) Heading date; (B) 25% flag leaf yellowing in days after heading (DAH); (C) 100% peduncle yellowing (DAH); (D) Grain mass. ANOVA with post-hoc Tukey test, significance groups at p<0.05..... 183

Figure 3.28 Higher expression of NAP-A1 correlates with later heading. Heading date plotted against transcript level of NAP-A1 in seedlings for individual plants. Correlation coefficient r^2 = 0.468, p = 4.36e-05. 184

*Figure 3.29 NAP-A1 T_1 lines show expected segregation for the 3*FLAG::NAP-A1 transgenic construct. Copy number of NAP-1 construct in individual T_1 plants. Taqman qPCR was run against the nptII marker gene in the construct and analysed by ΔΔCt method, normalised against a known single-copy gene and the sample with median expression level in the "single copy" cluster (highlighted yellow)..... 185*

*Figure 3.30 Flag leaf chlorophyll through senescence does not differ between NAP-A1 transgenics and control. Flag leaf chlorophyll content (SPAD) in weeks after heading +/- 1 day was compared between homozygous transgenic and null segregant controls in T2 transgenic lines 10.5 and 10.9. Average SPAD value at each timepoint was compared by Wilcoxon test, *=p<0.05. NB: Averages were taken of 2-5 data points; timepoints with small sample sizes may result in apparent differences that are not statistically significant. 186*

Figure 3.31 Senescence phenotypes do not differ between NAP-A1 overexpression lines 10.5 and 10.9 and corresponding controls. (A) Heading date (DAS); (B) 25% flag leaf yellowing; (C) 100% peduncle yellowing; (D) Days from heading to SPAD=30; (E) Area under curve (AUC) of leaf senescence; (F) Duration of leaf

*senescence (Days). (A-F) ANOVA with post-hoc Tukey test, formula ~ Shelf * Line_name, letters show significance groups at p<0.05. NB: Boxplots represent 2-5 individuals; small sample sizes may result in apparent differences that are not statistically significant. 188*

*Figure 3.32 Grain traits did not differ between homozygous NAP-A1 transgenics and null segregants in lines 10.5 and 10.9. (A) Main tiller number; (B) Seed mass (g); (C) Seed number; (D) Thousand grain weight; (E) Average grain length. (A-E) ANOVA with post-hoc Tukey test, formula ~ Shelf * Line_name, letters show significance groups at p<0.05. NB: Boxplots represent 2-5 individuals; small sample sizes may result in apparent differences that are not statistically significant. 190*

*Figure 3.33 NAP-1 double mutants and controls show no difference in the timing of flag leaf senescence. (A) Flag leaf chlorophyll content (SPAD) in weeks after heading +/- 1 day was compared between NAP-1 TILLING mutants (aabb, n = 10) and wild type segregant controls (AABB, n = 12). Average SPAD value at each timepoint was compared by Wilcoxon test, *=p<0.05. (B) Representative plants for wild type (AABB) single (AAbb) and double (aabb) NAP-1 mutants at 40DAH. Single (aaBB) mutant plants were omitted as none shared the same heading date. (C) Representative plants at 51DAH; different individuals to B. 193*

Figure 3.34 Peduncles senesce later in NAP-A1 single mutants (aaBB), while other senescence phenotypes do not differ significantly between NAP-1 mutants and controls. (A) Heading date (DAS); (B) 25% flag leaf yellowing; (C) 100% peduncle yellowing; (D) Days from heading to SPAD=30; (E) Area under curve (AUC) of leaf senescence; (F) Duration of leaf senescence (Days). (A-F) ANOVA with post-hoc Tukey test, formula ~ Light + Block + Genotype, letters show significance groups at p<0.05. Data from cross X585 (n = 8-12). 194

Figure 3.35 Grain number, grain protein content, tiller number, and height did not differ between NAP-1 double mutants and controls. (A) Main tiller number; (B) Height of primary tiller (mm), (C) Seed mass (g); (D) Seed number; (E) Thousand grain weight; (F) Average grain length; (G) Grain protein content (%, subset of plants with seed mass > 15g). (A-G) ANOVA with post-hoc Tukey test, formula ~ Light + Block + Genotype, letters show significance groups at p<0.05. Data from cross X585 (n = 8-12). NB: Grain traits of NAP-1 single mutants were affected by later sowing of some plants after failed germination (Methods 3.2.5.5). 197

Figure 4.1 Mean daily air temperature from May to July 2021 used in calculating senescence metrics. Annotations mark the time interval of heading, and dates when all plots had reached 10% and 100% leaf senescence. Data from weather station at Andrewsfield, Essex (Met Office 2023). 227

Figure 4.2 Mean daily air temperature from May to July 2022 used in calculating senescence metrics. Annotations mark the time interval of heading, and dates when all plots had reached 10% and 100% leaf senescence. Data from weather station at Andrewsfield, Essex (Met Office 2023). 227

Figure 4.3 In 2021, loss-of-function of NAM-A1 and NAM-B1 delayed leaf and ear senescence. Percentage leaf and ear yellowing were scored in 6m plots twice weekly from 2nd to 23rd July. Mean + SE shown for each genotype (n = 14 – 26). Capitals functional NAM-1 alleles; lower case non-functional NAM-1 alleles. WT marks NILs with genotype matching the hexaploid cultivar background that has a non-functional allele of NAM-B1. (A) Percentage leaf senescence; (B) Percentage ear senescence. 230

Figure 4.4 Lines with functional NAM-A1 or NAM-B1 alleles reached 30% and 70% leaf senescence earlier and showed a shorter duration of leaf senescence in 2021.

*(A) Ear emergence in days after 1st May (0.5 values indicate borderline between two days); (B) Thermal time to 30% leaf senescence (°C days); (C) Thermal time to 70% leaf senescence (°C days); (D) Area under curve (AUC) of leaf senescence; (E) Duration of leaf senescence (°C days). (A) Replicate 1 (n = 7-13); (B-E) Replicates 1 and 2 (n = 14-26). Capitals functional NAM-1 alleles; lower case non-functional NAM-1 alleles. ANOVA with post-hoc Tukey test, formula ~ NAM-A1 * NAM-B1, letters show significance groups at p<0.05. ..... 231*

*Figure 4.5 Lines with functional NAM-A1 or NAM-B1 alleles reached 30% and 70% ear senescence earlier in 2021. (A) Thermal time to 30% ear senescence (°C days); (B) Thermal time to 70% ear senescence (°C days); (C) Area under curve (AUC) of ear senescence; (D) Duration of ear senescence (°C days). (A-D) Replicates 1 and 2 (n = 14-26). Capitals functional NAM-1 alleles; lower case non-functional NAM-1 alleles. ANOVA with post-hoc Tukey test, formula ~ NAM-A1 * NAM-B1, letters show significance groups at p<0.05..... 232*

*Figure 4.6 Yield decreased and protein content increased with functional NAM-B1, while protein content decreased and yield did not differ with mutation of NAM-A1 in 2021. (A) Yield (t/ha) – Replicates 1 and 2 (n = 14-26); (B) Grain protein content (GPC) – Replicate 1 (n = 7-13); (C) Protein yield – Replicate 1 (n = 7-13). Capitals functional NAM-1 alleles; lower case non-functional NAM-1 alleles. ANOVA with post-hoc Tukey test, formula ~ NAM-A1 * NAM-B1, letters show significance groups at p<0.05. ..... 233*

Figure 4.7 In 2022, loss-of-function of NAM-A1 and NAM-B1 delayed leaf and ear senescence. Percentage leaf and ear yellowing were scored in 6m plots weekly from 16th June and twice weekly from 28th June to 17th July. Mean + SE shown for each genotype (n = 14 – 26). Capitals functional NAM-1 alleles; lower case non-functional

NAM-1 alleles. WT marks NILs with genotype matching the hexaploid cultivar background that has a non-functional allele of NAM-B1. (A) Percentage leaf senescence; (B) Percentage ear senescence. *235*

*Figure 4.8 Lines with functional NAM-A1 or NAM-B1 alleles reached 30% and 70% leaf senescence earlier and NAM-A1 lines showed longer duration of leaf senescence in 2022. (A) Ear emergence in days after 1st May; (B) Thermal time to 30% leaf senescence (°C days); (C) Thermal time to 70% leaf senescence (°C days); (D) Area under curve (AUC) of leaf senescence; (E) Duration of leaf senescence (°C days). (A-E) Replicate 1 (n = 7-13). Capitals functional NAM-1 alleles; lower case non-functional NAM-1 alleles. ANOVA with post-hoc Tukey test, formula ~ NAM-A1 * NAM-B1, letters show significance groups at p<0.05.* *236*

*Figure 4.9 Lines with functional NAM-A1 or NAM-B1 alleles reached 30% and 70% ear senescence earlier and double mutants showed reduced peduncle senescence in 2022. (A) Thermal time to 30% ear senescence (°C days); (B) Thermal time to 70% ear senescence (°C days); (C) Area under curve (AUC) of ear senescence; (D) Duration of ear senescence (°C days); (E) Number of yellowed peduncles out of 10 on 12th July. (A-E) Replicate 1 (n = 7-13). Capitals functional NAM-1 alleles; lower case non-functional NAM-1 alleles. ANOVA with post-hoc Tukey test, formula ~ NAM-A1 * NAM-B1, letters show significance groups at p<0.05.* *237*

*Figure 4.10 Mutation of NAM-A1 leads to increased plant height. Plot height (cm) by genotype in 2022. Capitals functional NAM-1 alleles; lower case non-functional NAM-1 alleles. ANOVA with post-hoc Tukey test, formula ~ NAM-A1 * NAM-B1, letters show significance groups at p<0.05.* *238*

Figure 4.11 Pipeline to extract and filter single nucleotide polymorphisms (SNPs) in NAC transcription factors from RAGT Exome capture data. Of 705 SNPs, 99 SNPs

passed quality filters, were biallelic, and the alternative allele was reported in more than one variety. RC = Read count, ALT = alternative allele. Purple oval: Input/Output. Blue rectangle: Process. Pale green rectangle: Decision. Scripts for this pipeline are available on Github (Evans 2023). 240

*Figure 4.12 Haplotypes in NAM-A1 in exome capture dataset. Gene model for transcript TraesCS6A02G108300.1 shown with exons as black rectangles, 5' and 3' UTRs as white rectangles, introns as lines, transcription start site marked with a triangle, aligned left to right with respect to chromosome 6A. Positions of variants marked with U (UTR), I (Intron), S (Synonymous), M (Missense) or F (Frameshift). Haplotype table lists haplotypes in NAM-A1, with base pairs on forward strand of chromosome 6A. First column shows published haplotypes based on 6A_7709609_TG/G and 6A_77099397_G/A (Cormier et al. 2015); second column shows haplotypes based on all SNPs shown where h1 matches the reference sequence (Chinese Spring RefSeq v1.1), Table shows number of lines confirmed (n) number of lines imputed plus confirmed (n.i) and proportion of total lines with haplotypes assigned (p.i). * indicates variants with functioning KASP markers. Amino acid changes: 6A_7709609_TG/G, Q396RIPSKYPAX; 6A_77099397_G/A, A171V. 241*

Figure 4.13 Haplotypes in NAM-A2 in exome capture dataset. Gene model for transcript TraesCS2A02G201800.1 shown with exons as black rectangles, 5' and 3' UTRs as white rectangles, introns as lines, transcription start site marked with a triangle, aligned left to right with respect to chromosome 2A. Positions of variants marked with U (UTR), I (Intron), S (Synonymous), M (Missense) or F (Frameshift). Haplotype table lists haplotypes in NAM-A2, with base pairs on forward strand of chromosome 6A. Table shows haplotypes where h1 matches the reference

sequence (Chinese Spring RefSeq v1.1), number of lines confirmed (n) number of lines imputed plus confirmed (n.i) and proportion of total lines with haplotypes assigned (p.i). No NAM-A2 variants had functioning KASP markers. Amino acid changes: 2A_175467727_C/G, P40R; 2A_175468910_C/… , S330SLSSGPALX.243

Figure 4.14 Pipeline to create and run KASP markers for SNPs in NAC TFs. KASP markers were generated using Polymarker (Ramirez-Gonzalez, Uauy,Caccamo 2015). Markers were run first on crossing parents, to determine the likely allele frequencies in each country (see Figure 4.15). Markers which had a non-zero allele frequency in French crossing parents were run on a French panel with associated phenotypic data (see Figure 4.16). Purple oval: Input/Output. Blue rectangle: Process. Pale green rectangle: Decision. QC: Quality Control. Scripts for this pipeline are available on Github (Evans 2023).....246

Figure 4.15 Frequencies of SNP alleles in NAC transcription factors in crossing parents. KASP markers were run on wheat crossing parents. ALT Frequency indicates the proportion of the alternative allele not found in the reference sequence (Chinese Spring RefSeq v1.1). Exotic includes germplasm not derived from cultivars. KASP marker names include chromosome, position, reference and alternative alleles.....247

*Figure 4.16 Yield and grain protein content did not differ between alleles for tested markers in NAC5-1 and NAM-D2. "POI 2022" and "LLC 2022" represent field trials at different sites. Yield and GPC (grain protein content) are shown for each allele. Gene name and marker ID are shown on left hand side. In this figure, dots mark outliers more than 1.5 * interquartile range away from the 25% or 75% quartile, ...249*

Figure 4.17 NAM-A1d is the most common haplotype in European elite wheat germplasm. (A) Frequencies and (B) counts of NAM-A1 haplotypes. "NAM-A1a/c"

shows individuals that may have either a NAM-A1a or NAM-A1c haplotype. "Undefined" shows individuals with heterozygous or missing SNP calls. Hexaploid wheat (number of accessions in brackets) from Watkins core collection (102) (Gardiner et al. 2018), INRA core collection (367) and elite cultivars from Europe (334) (Cormier et al. 2015), elite cultivars from Russia (93) (Leonova et al. 2022), Exome capture data (286) (RAGT) and crossing parents (France, Germany, UK, Czech, Exotic, Other) (RAGT). Exotic includes germplasm not derived from cultivars. NB: Haplotype NAM-A1b was reported in one accession of the INRA core collection. 251

Figure 4.18 Haplotype NAM-A1a correlates with decreased thousand grain weight (TGW), earlier ear emergence and earlier senescence in the Watkins core collection. (A) Thousand grain weight (g); (B) Average grain area (mm^2); (C) Average grain length (mm); (D) Average grain width (mm); I Date of ear emergence; (F) Plot grain mass (g); (G) Date of ear emergence; (H) Flag leaf senescence on 22nd July, unknown scale; (I) Stem senescence on 22nd July, unknown scale. (A-F) 2011; (G-I) 2010. Other includes heterozygous/unknown SNP calls; no individuals carried haplotype NAM-A1b. (A-I) ANOVA with post-hoc Tukey test, formula ~ NAMA1_haplotype, letters show significance groups at p<0.05. Phenotypic data re-analysed from field trials at Church Farm, Norwich in 2010 and 2011, with permission (Designing Future Wheat 2018). 257

iii. List of tables

Table 1.1 NAC transcription factors associated with senescence in wheat (Triticum aestivum), barley (Hordeum vulgare) and rice (Oryza sativa). Accession IDs (wheat, RefSeq v1.1; barley, Genbank;, rice, RAPDB) and common gene names are shown.

Noted are gene expression during natural / age-induced leaf senescence, effect of transgenic overexpression (any type of promoter), effect of loss-of-function including induced mutation and RNAi, and whether there is any kind of association (positive or negative) with protein content. Blank cells are unknown. This was not a systematic review. [1] Not all homoeologs of hexaploid wheat were tested. [2] Genbank ID supplied for NAM-B1 as it is absent from RefSeq v1.1..... 0

Table 2.1 KASP primers designed for genotyping of TILLING mutations in NAM-A2, NAM-B2, and NAM-D2. All primers designed are included, whether or not they were used for genotyping in the crossing program. 12

Table 2.2 PCR conditions for KASP genotyping using PACE genotyping mix 21

Table 2.3 Wheat growth conditions. "Phenotyping" locations were used for senescence phenotyping experiments; "Speed breeding" locations were used for crossing and seed bulking. Light: 16L:8D indicates 16 hours light, 8 hours darkness. Water: automatic flood benching (Auto) or manual watering (Manual)..... 23

Table 2.4 Full list of variables collected in a typical glasshouse experiment (NAM-2 experiment sown 21/09/2022). In column "Source or method", ID variables provide a unique identifier for each plant. Independent variables are determined by the experimental design. Calculated variables are derived from other variables. For the remaining rows, this column lists the equipment required to measure the trait. 27

Table 2.5 Grain traits measured by Marvin seed analyser (Marvintech). 29

Table 2.6 Grain traits measured by Near Infrared Spectrometer (Perten DA7250).. 29

Table 2.7 R packages used for data analysis, with a brief description of the main application of each package in this thesis. 32

Table 2.8 Summary of experimental design in this chapter. Sowing dates are used as unique identifiers for each experiment. Growth conditions and measurements

which differed between experiments are included. Location corresponds to Table 2.3. All experiments were laid out in a randomized complete block design (RCBD). 38

Table 2.9 Plant material for NAM-2 glasshouse experiments 21/09/2022 and 15/02/2023. Cross ID refers to Table 2.5. Generation: BC = number of backcrosses, F = generations since last cross. Genotype: capitals indicate wild-type allele, small letters indicate TILLING mutant allele. Genotype 7 (aabbDD) was unavailable from cross X50, so seed carrying the same mutations from cross X54 was used instead. 39

Table 2.10 Plant material for NAM-2 Field trial. Cross ID refers to Table 2.5. Generation: BC = number of backcrosses, F = generations since last cross. Genotype: capitals indicate wild-type allele, small letters indicate TILLING mutant allele. Genotype 7 (aabbDD) was unavailable from cross X50, so seed carrying the same mutations from cross X54 was used instead. 41

Table 2.11 Full list of variables collected in NAM-2 field experiment (12/10/2022). EE = ear emergence (heading). In column "Source or method", ID variables provide a unique identifier for each plant. Independent variables are determined by the experimental design. Calculated variables are derived from other variables. For the remaining rows, this column lists the equipment required to measure the trait. 44

Table 2.12 TILLING mutations selected in NAM-A2, NAM-B2 and NAM-D2. Gene ID from IWGSC RefSeq v1.1. Consequence = effect on the amino acid sequence. PSSM score = indicates the likelihood of a missense SNP in this position of the NAC domain across all NAC TFs..... 50

Table 2.13 Impact on senescence of published induced mutations in NAM-1 and NAM-2. TILLING line from [1] (Slade et al. 2005) [2] (Krasileva et al. 2017) [3] described in (Chapman et al. 2021b). Amino acid change shows original amino acid /

*new amino acid, * represents stop codon. AA position in original peptide may not match up between genes, and is based on the first of two potential start codons. Sub-domain shows conserved subdomain of NAC domain (where blank, residues are not in a conserved subdomain). Reference shows first author of paper presenting this mutation (Distelfeld et al. 2012; Borrill et al. 2019; Harrington et al. 2019; Avni et al. 2014; Chapman et al. 2021b). Whether this mutation in NAM-1 or NAM-2 led to a delayed senescence phenotype is described. n.s. = non-significant. Gene IDs: NAM-A1 TraesCS6A02G108300; NAM-D1 TraesCS6D02G096300; NAM-A2 TraesCS2A02G201800; NAM-B2 TraesCS2B02G228900. ..... 51*

Table 2.14 KASP primer sets used to genotype TILLING SNPs in NAM-A2, NAM-B2 and NAM-D2. Each primer set consists of competing WT and MUT forward primers targeting wild-type and mutant alleles of a SNP, with a reverse COM primer common to both alleles. For wheat, COM primers may or may not target a homoeolog-specific SNP. Generations of crossing program in which the primer set was used are listed. Primer sequences can be found in Table 2.3. 57

Table 2.15 Crosses for NAM-2 TILLING lines. For each SNP, the TILLING line ID and SNP consequence are shown. 58

Table 2.16 Full pedigree of plants used in NAM-2 experiments part 1: Crosses up to generation of triple heterozygotes. For each generation is listed Generation name, Sowing date, plant ID, genotype, and cross ID. Genotype shows WT allele in capitals and TILLING allele in small letters. TILLING lines on left hand side refer to Table 2.1. Cross ID refers to Table 2.5; S marks selfed plants. All seeds used in experiments in this chapter share this pedigree. 59

Table 2.17 Full pedigree of plants used in NAM-2 experiments part 2: Selfing and selection of homozygotes from a segregating population. For each generation is

listed Generation name, shorthand, sowing date, plant ID and genotype. Genotype shows WT allele in capitals and TILLING allele in small letters. Cross ID refers to Table 2.5. Seeds sown in NAM-2 glasshouse experiments (21/09/2022 and 15/02/2023) were progeny of the listed plants in Gen 8. Seeds sown in NAM-2 field experiment derive from the same crosses, with the same pedigree up to Gen 7 and different individuals in Gen 8, except for X50_G8 and X61_G5, which only share pedigree up to Gen 4..... 60

Table 2.18 Genotype counts from NAM-2 BC_1F_2 populations of cross X50 (Gen 6) and cross X54 (Gen 5). KASP genotyping carried out with original non-homoeolog-specific primers, so some genotypes may not be correct. X:X marks homozygous alleles, X:Y marks heterozygous, Y:Y marks wild-type. Where any SNP could not be called the individual was categorised as unknown. Expected counts calculated based on Mendelian segregation with equal probability of "X" or "Y" allele. Bold, underlined genotypes were retained for phenotyping experiments..... 62

Table 2.19 Genotype counts from NAM-2 BC_1F_3 populations of cross X61 (Gen 7). KASP genotyping carried out with redesigned, homoeolog-specific primers. X:X marks homozygous alleles, X:Y marks heterozygous, Y:Y marks wild-type. Where any SNP could not be called the individual was categorised as unknown. Expected counts calculated based on Mendelian segregation with equal probability of "X" or "Y" allele.Bold, underlined genotypes were retained for phenotyping experiments.. 63

Table 2.20 Chi-squared test for segregation of SNP alleles in NAM-A2, NAM-B2 and NAM-D2. Results from Table 2.18 and Table 2.19 were binned according to the genotype of a single SNP. Generation ID refers to Table 2.17. X:X marks homozygous alleles, X:Y marks heterozygous, Y:Y marks wild-type. Where any SNP could not be called the individual was categorised as unknown. Chi-squared test

used expected counts calculated based on Mendelian segregation with equal probability of "X" or "Y" allele. 65

*Table 2.21 P-values from Analysis of Variance of NAM-2 glasshouse experiments. Variables were analysed with formula ~ Row + Block + Cross*Genotype. Degrees of freedom for each explanatory factor in brackets. Significant p-values (threshold 0.05) in bold. Grain protein content was analysed with formula ~ Cross*Genotype, as seed from two plants was pooled for each measurement. 90*

Table 3.1 Primers used for qPCR of NAC5-1 and NAP-1 transgenic lines. Primer pairs were designed to amplify transgenic construct only, the A homoeolog or all three homoeologs. ACT2 is the reference gene (Tenea et al. 2011). 118

Table 3.2 Primer efficiency results for NAC5-1 and NAP-1 qPCR primer pairs. Many primer pairs were tested, but only primer pairs selected for qPCR experiments are shown. These primer efficiency values were used in qPCR analysis. 120

Table 3.3 KASP primers used to genotype TILLING mutations in NAC5-1 and NAP-1. A pair of allele-specific WT and MUT primers and a homoeolog-specific COM primer are used for each KASP reaction. 122

Table 3.4 Primers for Taqman copy number assay, from Additional file 1 in (Milner et al. 2018). The transgenic construct contains nptII while GAMYB is the reference. Primers were provided by JIC Molecular Genetics platform. 124

Table 3.5 qPCR program for Taqman copy number assay. 124

Table 3.6 PCR program for cDNA synthesis. 126

Table 3.7 qPCR program for testing for overexpression of NAC5-A1 and NAP-A1. 127

Table 3.8 Summary of experimental design in this chapter. Sowing dates of glasshouse experiments are used as unique identifiers for each experiment. Growth

conditions and measurements which differed between experiments are included. Location corresponds to Table 2.3. Most experiments were laid out in a randomized complete block design (RCBD). 129

Table 3.9 Plant material for NAC5-A1 overexpression T_1 (16/11/2020). T_1 progeny of single-copy, multi-copy and non-transformed control plants from transformation batches 5 and 8 were grown in the glasshouse. 131

Table 3.10 Plant material for NAP-A1 overexpression T_1 (29/04/2021). T_1 progeny of single-copy, multi-copy and non-transformed control plants from transformation batches 7 and 10 were grown in the glasshouse. 132

Table 3.11 Plant material for NAC5-1 NAP-1 overexpression T_2 (23/12/2021).T_2 progeny of homozygous and null / wild-type segregating single-copy T_1 lines were grown, as were T_2 multi-copy lines. 133

Table 3.12 Plant material for NAC5-1 NAP-1 Kronos TILLING (01/12/2021). Cross ID refers to Table 3.15. Generation: BC = number of backcrosses, F = generations since last cross. Genotype: capitals indicate wild-type allele, small letters indicate TILLING mutant allele. 27 plants were resown later due to seeds which failed to germinate or died. 135

Table 3.13 Naming of wheat genes used in this thesis. These wheat triads will be referred to as TaNAC5-1 and TaNAP-1 or NAC5-1 and NAP-1 after their orthologs in rice, OsNAC5 and OsNAP. Alternative names coined for these wheat genes are also shown. 144

Table 3.14 TILLING mutations selected in NAC5-A1, NAC5-B1, NAP-A1 and NAP-B1. Gene ID from IWGSC RefSeq v1.1. Variant ID is the wheat line containing the mutation and the SNP position. Consequence shows effect on the amino acid sequence. Subdomain shows where in five conserved NAC subdomains the

*mutation sits. PSSM score indicates the likelihood of a missense SNP in this position of the NAC domain across all NAC TFs. *Variant IDs could not be found for NAC5-A1 or NAP-B1 in RefSeq v1.1 as mutations were initially identified in previous gene annotation (TGAC). 165*

Table 3.15 Sets of TILLING lines for NAC5-1 and NAP-1. Two sets of TILLING lines were created for NAC5-1, and one for NAP-1. Cross ID is used to designate each set of lines in this thesis. 166

*Table 3.16 Summary of KASP genotyping results for NAC5-1 Kronos TILLING lines (01/12/2021). Here, "Y" represents wild-type alleles and "X" represents mutant alleles. Expected genotypes are highlighted in green. *These lines appear to have a different genotype than expected. 170*

Table 3.17 Summary of KASP genotyping results for NAP-1 Kronos TILLING lines (01/12/2021). Here, "Y" represents wild-type alleles and "X" represents mutant alleles. Expected genotypes are highlighted in green. 170

Table 4.1 Haplotypes of SNPs 6A_77099397_G/A and 6A_77098609_TG/G in NAM-A1, adapted from (Cormier et al. 2015). Base pairs on forward strand of chromosome 6A (reverse complement of NAM-A1 transcript). Upper label is variant ID in this thesis; lower label is variant ID in (Cormier et al. 2015). 213

Table 4.2 NAM-A1 and NAM-B1 alleles used to generate near-isogenic lines in UK hexaploid wheat. NAM-B1 is absent from RefSeq v1.1 so Genbank ID is given (Uauy et al. 2006). 215

Table 4.3 Near isogenic lines (NILs) for NAM-A1 and NAM-B1 grown in field trials. WT marks the genotype of the recurrent parent (UK hexaploid winter wheat cultivar "RGT Bowen"). Capital letters indicate functional gene copies; small letters indicate loss-of-function. 215

Table 4.4 Chromosome locations of NAC transcription factor genes used to select variants from exome capture data. Gene IDs and chromosome locations from RefSeq v1.1 via Ensembl Plants (Appels et al. 2018; Yates et al. 2022). 217

Table 4.5 Transcripts selected for Variant Effect Predictor (VEP). Alternative transcripts not selected are annotated with the amino acid insertion compared to selected transcripts. 218

Table 4.6 KASP markers used to genotype variants in NAC transcription factors. Marker ID includes chromosome, position, reference (REF) and alternative (ALT) alleles. KASP markers which functioned successfully are shown. Fluorescent "VIC" and "FAM" tags have been omitted from REF and ALT primers respectively for brevity. Specific = COM primer specific to one homoeolog; Semispecific = COM primer targets 2 homoeologs; Nonspecific = COM primer targets 3 homoeologs. [1] This thesis; [2] (Cormier et al. 2015). 221

Table 4.7 Number of data points for yield (YLD) and protein content (GPC) for KASP markers run on French breeding lines. LLC/POI are trial location codes, R1 is replicate 1. Phenotypic data are presented for these trials and some of the markers. 223

Table 4.8 NAM-A1 haplotypes in sequenced genomes of Triticum species containing an "A" genome. NAM-A1 genes were identified by BLASTN search of the NAM-A1 genomic sequence from RefSeq v1.1 against each genome, and BLAST hits were multiple aligned. Triticum urartu had a distinct gene-level haplotype to all accessions from RAGT exome capture. Genotypes at Axiom 35K marker AX-94490150 also identified through BLASTN. Genome sequences from [1] (Appels et al. 2018); [2] (Walkowiak et al. 2020); [3](Maccaferri et al. 2019; Avni et al. 2017); [4] (Ling et al. 2018); [5] (10+ Consortium 2019); [6] (Avni et al. 2017). 253

iv. List of definitions/abbreviations

Abbreviation	Definition
AA	Amino Acid
ABA	Abscisic Acid
ALT	Alternative allele
ANOVA	Analysis Of Variance
ASN1	*Asparagine Synthetase 1*
AUC	Area Under Curve (of senescence time-course)
CER	Controlled Environment Room
ChIP-seq	Chromatin Immunoprecipitation sequencing
COM	Common KASP primer
CT	Cycle Threshold (in qPCR)
CUC2	*Cup-shaped Cotyledon 2*
DAA	Days After Anthesis
DAH	Days After Heading
DAP-seq	DNA Affinity Purification sequencing
DAS	Days After Sowing
ddH_2O	Double Distilled water
EE	Ear Emergence (equivalent to heading for field trials)
EMS	Ethyl Methylsulfonate

GDH	*Glutamate Dehydrogenase*
GID2	*Gibberellin-insensitive Dwarf 2*
GO	Gene Ontology
GPC	Grain Protein Content
Gpc-B1	*Grain Protein Content B1* (QTL containing the *NAM-B1* gene in wheat)
GS	*Glutamine synthase*
GW-2	*Grain Weight 2*
GWAS	Genome Wide Association Study
IWGSC RefSeq v1.1	International Wheat Genome Sequencing Consortium (The genome sequence and annotation in wheat used in this thesis)
KASP	Kompetitive Allele-Specific PCR
MeJA	Methyljasmonate
MSU	(A genome annotation in rice)
MUT	Mutant allele KASP primer
NAC	NAM, ATAF, CUC2 transcription factor family
NAM	*No Apical Meristem*
NAP	*NAC-like, Activated by AP3/PI*
NDVI	Normalised Difference Vegetation Index
NIL	Near Isogenic Line
NIR	Near Infrared Spectrometer

PCR	Polymerase Chain Reaction
PSSM	Position-Specific Scoring Matrix
QC	Quality Control
qPCR	Quantitative PCR
QTL	Quantitative Trait Locus
RAPDB	(A genome annotation in rice)
RC	Read count
RCBD	Randomized Complete Block Design
REF	Reference allele
RFLP	Restriction fragment length polymorphism
RNAi	RNA interference
RNA-seq	RNA sequencing
RSL	Recombinant substitution line
RT-qPCR	Reverse Transcription qPCR (using cDNA)
SA	Salicylic Acid
SD	Standard Deviation
SE	Standard Error
SIFT	Sorting Intolerant From Tolerant
SNAC	Stress-Inducible NAC (subclade of NAC transcription factors, also known as NAC-a)
SNP	Single Nucleotide Polymorphism

SPAD	Soil Plant Analysis Development (spectrometer used to measure estimated leaf chlorophyll content and the values obtained)
TF	Transcription Factor
TGAC	(A genome annotation in wheat)
TGW	Thousand Grain Weight
TILLING	Targeting Induced Local Lesions In Genomes
T_m	Melting Temperature (of a primer)
TT_SPAD30	Days from heading to SPAD=30
UK	United Kingdom
UTR	Untranslated Region
VCF	Variant Call Format
VEP	Variant Effect Predictor
WT	Wild Type plant line or Wild Type allele KASP primer
YLD	Yield

1 INTRODUCTION

1.1 Wheat production is key to global food security

Wheat is the fourth most produced crop in the world by mass, after sugarcane, maize and rice (FAO 2020). The increasing global population, set to reach 9.7 billion by 2050, drives escalating demand for staple crops such as wheat (United Nations 2022). Through improved wheat varieties and intensification of agriculture, wheat yields increased globally through the late 20th century (Venske et al. 2019). For instance, in the UK wheat yield increased by almost 3t/ha between the 1970s and 1990s – however in the last 20 years yields have plateaued (FAO 2020). Increasing wheat production is not the only challenge – the Sustainable Development Goals target improving crop production whilst maintaining ecosystems, adapting to climate change and improving soil quality (SDG target 2.4) (United Nations 2023). Novel approaches to understand and harness the genetics of wheat could contribute to improved wheat varieties for a changing world.

1.2 The polyploid genome of modern wheat

1.2.1 Origin of the hexaploid genome of bread wheat

The evolutionary history of bread wheat (*Triticum aestivum* ssp. *aestivum*) has profoundly shaped the genome of this global staple crop. About 0.5 million years ago, the diploid *Triticum urartu* (AA) and a wild grass related to *Aegilops speltoides* (BB) crossed to form a hybrid (Figure 1.1) (Haas, Schreiber,Mascher 2019). Whole genome duplication formed a fertile tetraploid, wild emmer (*Triticum turgidum* spp.

dicoccoides, AABB) (Haas, Schreiber,Mascher 2019). Tetraploid wheat was cultivated in the Fertile Crescent region and acquired domestication traits including a non-brittle rachis conferred by mutation of *Br-A1* and *Br-B1* (Avni et al. 2017). Domesticated free-threshing tetraploids (AABB) hybridized with *Aegilops tauschii* (DD) to form hexaploid bread wheat (*Triticum aestivum* ssp. *aestivum,* AABBDD) (Figure 1.1) (Haas, Schreiber,Mascher 2019). This second polyploidization occurred 11,700 years ago, followed by continued introgressions from tetraploid into hexaploid wheat (Zhao et al. 2023). Three subgenomes from distinct donors make the bread wheat genome allohexaploid (Figure 1.1).

These two polyploidization events resulted in genetic bottlenecks, decreasing the genetic diversity of hexaploid wheat (Venske et al. 2019). On the other hand, it is suggested that a polyploid genome may improve the resilience of bread wheat, enabling it to be cultivated in diverse environments (Dubcovsky and Dvorak 2007). In wheat, in common with crops such as banana, potato and sugarcane, subspecies with higher ploidy have overtaken lower ploidy subspecies as the most commonly grown crops, with hexaploid bread wheat comprising the majority of wheat production today (Akagi et al. 2022).

1.2.2 Implications of the hexaploid genome of bread wheat

Whole genome duplication is common in the plant kingdom, and over time, duplicated genes are lost (pseudogenized) or diverge in sequence and function (Wendel 2000). However, as a recent polyploid, bread wheat retains three copies of over 50% of genes (Appels et al. 2018). These three orthologous gene copies are known as homoeologs (Figure 1.1). For example, *Gene-A1, Gene-B1* and *Gene-D1* are homoeologs, and are part of the triad *Gene-1* (Figure 1.1). Wheat homoeologs

share on average 97.2% identity at the transcript level (Schreiber et al. 2012). 72% of triads have balanced gene expression of the three homoeologs in any one tissue, within which 83% are stable across tissues (Ramírez-González et al. 2018). These similarities indicate that many homoeologous triads may retain the same function, a state known as genetic redundancy. Thus, in studies of gene function in wheat it is necessary to consider all homoeologs of a gene.

Despite its importance in the human diet, until recently the study of bread wheat genetics was held back by its complex polyploid genome. The bread wheat genome is 17Gbp, approximately 40 times larger than the 400Mbp rice (*Oryza sativa*) genome, and 85% of the wheat genome consists of repetitive transposable elements (Appels et al. 2018). A chromosome scale assembly of the wheat genome was achieved in 2018, whereas the rice genome was sequenced in 2005 (Appels et al. 2018; Sasaki and International Rice Genome Sequencing 2005). Nevertheless, a recent proliferation of genome sequences, transcriptomes, genetic variation data and other genetic resources has opened doors to characterising genes and gene networks in wheat (Borrill, Harrington,Uauy 2019; Walkowiak et al. 2020).

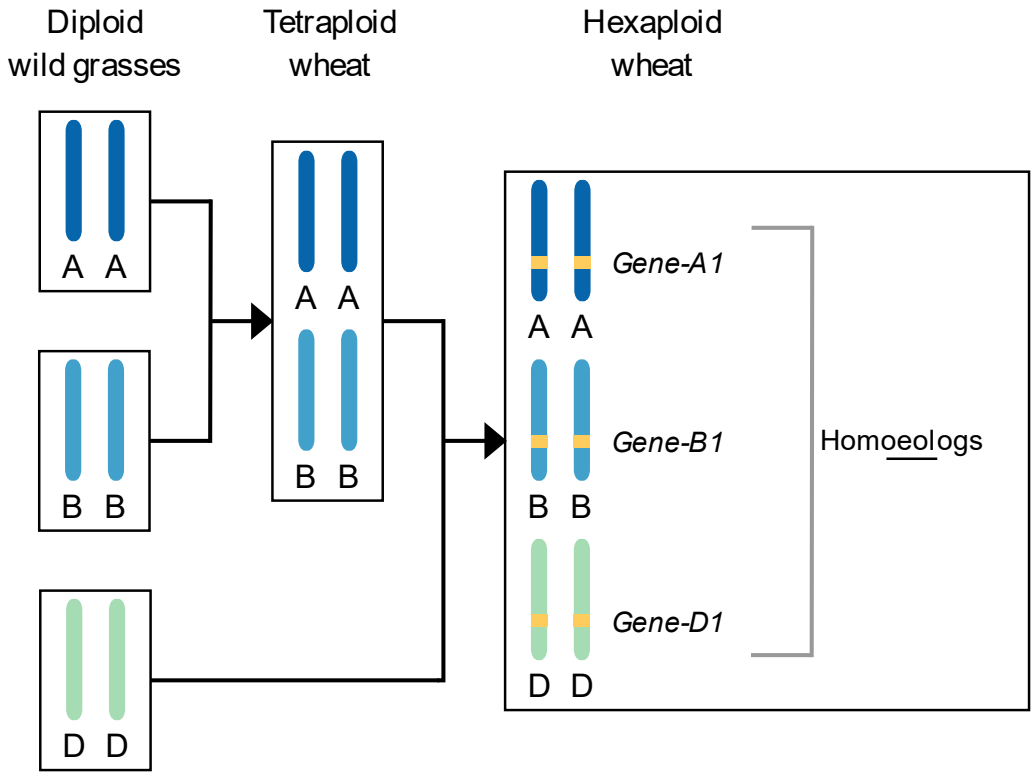


Figure 1.1 The allohexaploid genome of bread wheat (Triticum aestivum ssp. aestivum, AABBDD) derives from two successive hybridization and whole genome duplication events. Most genes in bread wheat have three copies on the A, B and D subgenomes, known as homoeologs.

1.3 Wheat grain protein content is important for human nutrition and bread quality

Wheat varieties with high grain protein content are important for both bread quality and human nutrition. Wheat provides not only 18% of calories but also 20% of protein in global diets (FAO 2020). In addition, high grain protein content is required for breadmaking (Cauvain 2012). In the UK, around 12 million loaves of bread are purchased every day, and 80% of flour is milled from wheat grown in the UK (UK

Flour Millers 2023). Thus, high protein bread-making varieties are a key part of UK wheat production (AHDB 2023a).

1.4 The challenge of improving wheat grain protein content

1.4.1 The trade-off between grain protein content and yield

It is a challenge to improve wheat grain protein content without reduction in yield because there is a trade-off between the two. Yield is negatively correlated with protein content between cultivars within the same environment (Zhao et al. 2015; Simmonds 1995; Bogard et al. 2010; Shorinola et al. 2022). The correlation coefficient has been reported as -0.7, with a range from -0.3 to -0.9 (Simmonds 1995; Bogard et al. 2010; Bokore et al. 2019). The trade-off can partially be explained by a dilution effect. If grain starch accumulation increases, while protein accumulation either remains the same or increases by a smaller amount, this leads to grains with higher yield and lower protein content. Due to this trade-off, selecting for increased protein content, with no selection for yield, is likely to result in a decrease in yield.

The trade-off between yield and protein content has a genetic basis. Across environments yield and protein can vary widely, but within a given environment and resource availability, cultivars are represented well by a negative linear regression (Simmonds 1995). Genome-wide association studies have identified quantitative trait loci with opposite effects on protein content and either yield or thousand grain weight (Thorwarth et al. 2019; Groos et al. 2003). Genetic mapping of biparental populations across multiple environments identified five QTL (Quantitative Trait Locus) regions with antagonistic effects on yield and protein content, compared to two regions

impacting protein content independently of yield (Bogard et al. 2013). This demonstrates that multiple pleiotropic genetic loci underpin the protein-yield trade-off.

1.4.2 The challenge

In intensified production systems, wheat crops with high yield and protein content are achieved by increasing nitrogen input. The UK is in the top ten countries for fertiliser application per area of cropland, with an average of 166kg/ha nitrogen applied (2010-2020) (FAO 2020). For wheat, an additional late application of nitrogen fertiliser is recommended to increase post-anthesis nitrogen uptake from soil, and achieve high grain protein content (AHDB 2023c). However, synthetic fertiliser application contributes 27% of emissions of greenhouse gas N_2O from agriculture, while manure left on pasture contributes 35% (2000-2019) (FAO 2020). In addition, nitrogenous fertiliser production requires high energy input, and nitrogen leaching, which is detrimental to aquatic environments, increases exponentially with increasing fertiliser application (Yang et al. 2017). A decrease, not an increase, in nitrogen inputs is needed to move closer to goals for sustainable agriculture (United Nations 2023).

In summary, wheat production needs to increase if it is to keep pace with the growing global population. Improving grain protein content could increase the baking quality and nutritional value of bread. However, there is a trade-off between yield and grain protein content, and nitrogen fertiliser is environmentally costly. Is it possible to improve wheat grain protein content without increasing nitrogen inputs, or compromising on yield?

1.5 What is senescence?

1.5.1 The process of plant senescence

Senescence in plants takes two main forms. Senescence is the final developmental stage in plants with an annual lifecycle, including wheat; the whole plant dies after a process known as monocarpic senescence (Davies and Gan 2012). Senescence also occurs in individual plant organs such as older leaves, or petals and sepals after flowering (Wojciechowska, Sobieszczuk-Nowicka,Bagniewska-Zadworna 2018). Fundamental to understanding plant senescence is that both organ senescence and monocarpic senescence have adaptive value, as they have evolved to enable resources to be reallocated to developing shoots or seeds (Leopold 1961). This resource reallocation occurs via gradual breakdown, or catabolism, of cell components in senescing source tissues, followed by remobilization of nutrients from source to sink tissues (Thomas and Ougham 2014).

Senescence timing is commonly assessed by measuring the gradual loss of leaf green colour. Extended leaf green colour may represent “functional stay-green”, through either a later onset (Type A) or a slower rate (Type B) of senescence (Thomas and Howarth 2000). Extended leaf green colour is also observed in mutants of chlorophyll degradation genes such as *SGR*, in which other senescence processes such as cellular catabolism and the decline in photosynthesis continue at the normal rate (Thomas and Ougham 2014). These mutants are labelled cosmetic or Type C stay-green (Thomas and Howarth 2000).

Inside a senescing leaf, catabolic enzymes are upregulated to break down proteins, starch, lipids, nucleic acids, and chlorophyll (Buchanan-Wollaston 1997). Organelles

are degraded in a controlled, gradual manner. The chloroplast is the first organelle to be degraded, accompanied by a decline in leaf photosynthesis. Leaves lose their green colour as chlorophyll is degraded into a non-light-responsive compound (Thomas and Ougham 2014). In wheat, chloroplasts in flag leaves lose their internal thylakoid structure from 16 days after anthesis (DAA) (Kong et al. 2016). The nucleus and mitochondria are maintained for longer, to regulate the cell and provide it with energy. Without photosynthesis, catabolism of starch into sugars and membrane lipids into oxo-acids like α-ketoglutarate fuels mitochondrial respiration (Buchanan-Wollaston 1997). Large vesicles engulf organelles for degradation in the vacuole, a process known as autophagy (Wang and Schippers 2019). Condensing of the chromatin, DNA laddering and controlled collapse of the vacuole mark the last stages of leaf senescence (Lim, Kim,Nam 2007).

1.5.2 Nitrogen is remobilized from leaves to grain during senescence

Wheat grain protein content depends on senescence: 65-90% of grain nitrogen is remobilized from senescing leaves, while the remainder comes from post-anthesis root uptake (Bogard et al. 2010; Kichey et al. 2007). Nitrogen is generally the limiting element for wheat grain protein production, and comprises 17.5% of wheat grain protein by mass (AHDB 2023c). How is nitrogen remobilized from leaves to grain in wheat?

Nitrogen remobilization begins when protease enzymes break down proteins in the leaf to amino acids. In wheat flag leaves, proteases are upregulated during senescence including aspartic proteases, serine proteases, subtilin-like proteases and cysteine proteases, and similar results were found in microarray data from barley (Gregersen and Holm 2007; Parrott et al. 2007; Roberts et al. 2011). About 75% of

leaf proteins are present in the chloroplast; Rubisco, the key CO_2 fixation enzyme, constitutes 1/3 of leaf proteins (Roberts et al. 2012). Proteases within the chloroplast begin degradation of Rubisco (Distelfeld, Avni,Fischer 2014). Chloroplast proteins including Rubisco are transported to lytic vacuoles by autophagy, where they are catabolised by senescence-specific proteases (Buchanan-Wollaston 1997; Distelfeld, Avni,Fischer 2014). Proteases were upregulated in near isogenic barley lines with high protein content, with chloroplastic proteases upregulated at 14-21DAA and lytic vacuole cysteine proteases and serine carboxypeptidases at 21DAA (Jukanti et al. 2008). QTLs for carboxypeptidase activity in grain filling co-locate with QTLs for nitrogen content in barley (Yang et al. 2004). This demonstrates that leaf proteolysis is important for grain protein content in cereals.

A subset of amino acids are used for long-distance transport of reduced nitrogen in plants: glutamine, glutamate, aspartate, threonine, serine, arginine and asparagine (Distelfeld, Avni,Fischer 2014). Glutamine comprises half of the amino acids in the phloem sap of the peduncle in wheat (Distelfeld, Avni,Fischer 2014). Glutamine for export is synthesised by GS1 in the cytoplasm of cells in the vascular bundle (Kichey et al. 2005). In *Arabidopsis thaliana* and in wheat, cytosolic *GS1* is upregulated during senescence, but plastidial *GS2* is downregulated (Buchanan-Wollaston 1997; Andleeb, Knight,Borrill 2023). GS1 synthesises glutamine from ammonia and glutamate, which in turn comes from transamination of α-ketoglutarate, a product of lipid catabolism (Buchanan-Wollaston 1997).

Glutamine and other amino acids are exported from the chloroplast and vacuole of leaf cells to the cytoplasm by active transport, released to the apoplast, then imported to the phloem (Distelfeld, Avni,Fischer 2014; Okumoto and Pilot 2011).

Mineral nutrients such as iron and zinc are imported to the phloem with chelating agents such as nicotianamines (Ricachenevsky, Menguer,Sperotto 2013). The phloem flows to the roots and sink tissues, including grains (Distelfeld, Avni,Fischer 2014). In wheat, maternal and grain tissues are not physically connected, therefore amino acids are released from maternal tissues to the apoplast, probably by passive transporters, and must be actively taken up through the aleurone layer to the endosperm (Okumoto and Pilot 2011). It is possible that nutrients from the leaves are transported indirectly to the grain via the glumes, which senesce later than the flag leaf (Kong et al. 2015). In wheat, most of the amino acids imported to the endosperm are used to synthesize storage proteins – glutenins and gliadins (Cauvain 2012).

1.5.3 Senescence timing is modulated by both developmental age and environmental stress

The timing of leaf senescence is primarily determined by the developmental age of the leaf. An *Arabidopsis* leaf passes through three phases: a leaf in early growth phase is unable to senesce; a mature leaf is competent to senesce in response to environmental stress signals; and in the third phase a leaf begins to senesce in the absence of other signals (Schippers 2015). In wheat, flowering and seed set promote monocarpic senescence of the whole plant (Davies and Gan 2012).

One way in which developmental age mediates senescence is through sugar signalling. Leaf sugar contents peak in mature leaves or at the early stages of leaf senescence (Kim 2019). Steam-girdling of leaves to prevent sugar export accelerates senescence (Kim 2019). Overexpression of hexokinase – a sensor for glucose – promotes earlier leaf senescence, as does overexpression of trehalose-6-phosphate synthase to increase the level of trehalose-6-phosphate, a signalling molecule which

is a proxy for sucrose levels (Kim 2019). Phytohormones also mediate age-induced senescence, via gradually increasing concentrations of ethylene, abscisic acid (ABA), methyljasmonate (MeJA) and salicylic acid (SA) with leaf age (Schippers 2015). Application of SA or MeJA promotes early leaf senescence, while mutation in the ethylene signalling pathway delays senescence (Buchanan-Wollaston 1997; Beltrano et al. 1998; Lim, Kim,Nam 2007). Age-induced senescence is initiated by a convergence of multiple signalling mechanisms.

In wheat, where monocarpic senescence coincides with grain filling, nutrient remobilization feeds back to affect the rate of senescence. Half-defoliated plants with a lower source-sink ratio show faster leaf senescence, while half-degrained plants with a higher source-sink ratio show slower leaf senescence (Lv et al. 2020b). This has the impact of adapting the rate of nutrient remobilization to supply sink demand. As the initial phase of nitrogen remobilization can begin as early as anthesis, it can influence senescence timing from before the onset of visible leaf yellowing (Kong et al. 2016).

Abiotic and biotic stress can both induce premature leaf senescence and modulate the timing of monocarpic senescence. Detached leaves in darkness senesce rapidly. Lack of light is detected by phytochrome B, which initiates a signalling cascade promoting senescence via *PIF4* and *PIF5* (Schippers 2015). Cytokinin, which inhibits the onset of senescence, decreases in concentration (Distelfeld, Avni,Fischer 2014). Darkness also leads to sugar starvation, which can trigger senescence via the *SnRK* pathway (Kim 2019). Drought stress promotes earlier senescence via ABA, as ABA application alters the expression of multiple senescence-associated genes (Lim, Kim,Nam 2007). Pathogens and wounding may accelerate plant senescence via SA

and MeJA (Lim, Kim,Nam 2007). Finally, reactive oxygen species accelerate senescence; these compounds are generated by oxidative damage including during senescence itself and by the pollutant ozone (O_3) (Bhattacharjee 2005; Broberg et al. 2021). Thus, environmental stress-induced senescence occurs through distinct but overlapping pathways to age-induced senescence. The following sections are primarily focused on age-induced, monocarpic senescence.

1.6 Wheat leaf senescence is linked to both grain yield and grain protein content

1.6.1 The link between senescence, yield and grain protein content

The timing of senescence onset is proposed to mediate the trade-off between protein content and yield by determining the transition from photosynthesis to nitrogen remobilization (Gregersen, Holm,Krupinska 2008; Thomas and Ougham 2014). Increased grain yield with delayed leaf senescence can be explained as an extended duration of leaf photosynthesis (Figure 1.2). Leaf photosynthetic capacity decreases gradually through senescence, and expression of genes encoding photosystem components and Rubisco are downregulated (Buchanan-Wollaston 1997). Extended leaf photosynthesis increases the “source” carbohydrate availability for grain filling. Increased grain protein content with earlier leaf senescence can be explained as an extended duration of nitrogen remobilization (Figure 1.2). The earlier the onset of protein degradation in the leaves, the earlier amino acids can be transported from leaves to grain. As the majority of leaf proteins are found in the chloroplast, it is likely that leaf protein degradation cannot be decoupled from decline of photosynthesis

(Roberts et al. 2012). In this way the negative correlation between grain protein content and yield can be maintained (Figure 1.2).

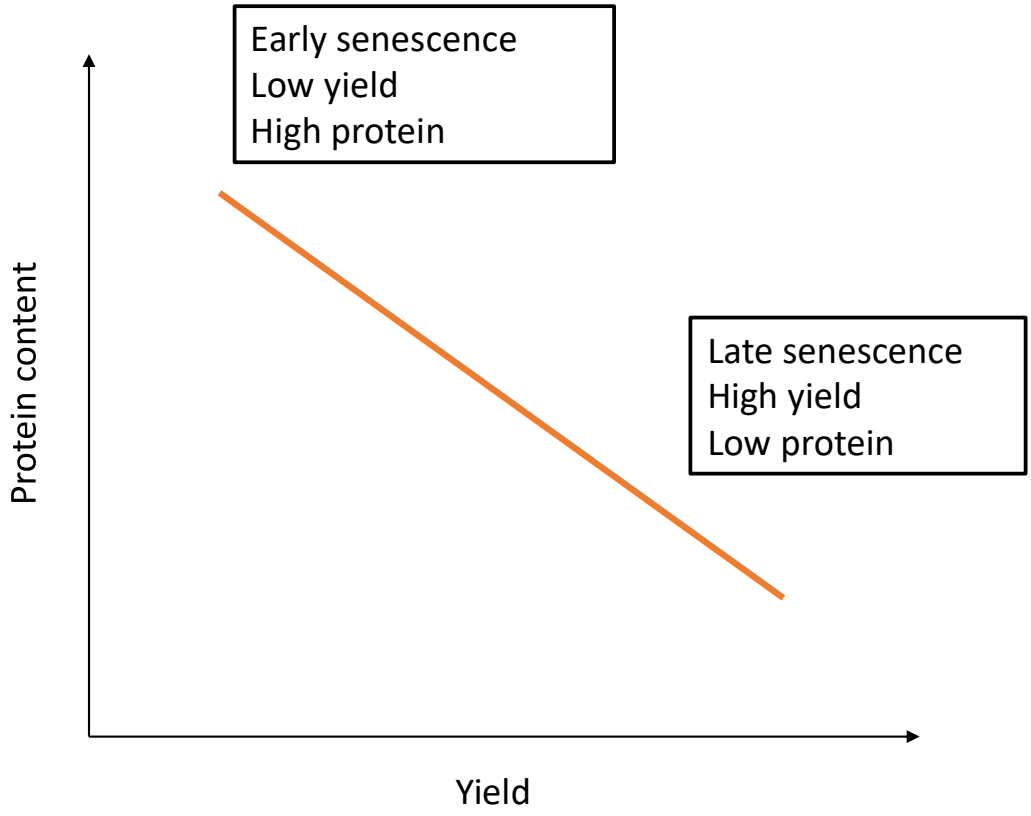


Figure 1.2 Conceptual diagram of the connection between senescence and the trade-off between protein content and yield.

Delayed leaf senescence frequently correlates with increased grain yield in cereal crops (Kichey et al. 2007; Gregersen, Holm,Krupinska 2008). A wheat line with earlier senescence showed decreased thousand kernel weight (Derkx et al. 2012). In maize, a cultivar with earlier leaf senescence had higher grain protein content (Gong et al. 2020).The *Gpc-B1* locus, which increases grain protein content, is also associated with earlier leaf senescence, and sometimes decreased grain mass and thousand kernel weight in wheat (Uauy, Brevis,Dubcovsky 2006; Bogard et al. 2010). Similar findings were reported in near isogenic lines differing in *HvNAM-1* in barley

(Jukanti and Fischer 2008). These correlations provide evidence for the connection between senescence, grain protein content and yield.

A study of a nested association mapping population identified 68 QTL regions (Quantitative Trait Loci) for senescence traits (Christopher et al. 2021). Of these, three collocated with yield: two on chromosome 4A were associated with maximum leaf greenness and yield, while one on chromosome 7D was associated with multiple senescence traits and yield (Christopher et al. 2021). A Genome Wide Association Study (GWAS) for days to ripening based on national trials of UK winter wheat varieties identified a QTL on chromosome 6A, which contains the senescence regulator *NAM-A1* (Shorinola et al. 2022). An early leaf senescence locus *Els2* from a wheat mutant line has been fine-mapped to a region on chromosome 2BL, while a QTL for early leaf senescence from a mutant population in Kronos has been mapped to a 4.3Mb region on chromosome 3A using bulk segregant analysis (Harrington et al. 2019a; Wang et al. 2020). This highlights that senescence timing is a complex trait underpinned by multiple loci.

1.6.2 The impact of senescence on yield and protein content depends on the environment

Delayed leaf senescence may not correlate with grain yield when yield is limited by other factors. Prolonged photosynthetic capacity may not translate to sugar production – increased source – if the rate of photosynthesis is limited by light or water availability. Wheat yield may be limited by the overall sink capacity, such as number of spikes and florets per spike, which are determined before anthesis (Distelfeld, Avni,Fischer 2014). Finally, yield may be limited by the efficiency of remobilization of sugars from leaves to grain or assimilation of starch within the grain,

which in turn limits thousand kernel weight. In one experiment in wheat, decreasing the source availability by removing all leaves but the flag leaf had no effect on grain mass per grain, therefore grain mass per grain was not limited by source availability (Lv et al. 2020b). Reducing sink demand by removing half the grains from the spike increased grain mass per grain, indicating that grain mass per grain was limited by the rate of remobilization from leaves to spike (Lv et al. 2020b).

Earlier leaf senescence may not correlate with increased protein content under high-nitrogen conditions where post-anthesis nitrogen uptake from roots makes a higher contribution to protein content (Kong et al. 2016). Nitrogen remobilization explained some of the variation in grain nitrogen concentration in European wheat cultivars under low, but not high, nitrogen conditions (Gaju et al. 2014). Variation among one panel of wheat cultivars for grain protein deviation (increased protein content relative to the yield-protein regression line) was mainly explained by variation in post-anthesis nitrogen uptake, suggesting that post-anthesis uptake may not be linked to the protein-yield trade-off (Bogard et al. 2011).

1.6.3 The opportunity to improve nitrogen remobilization

Nevertheless, nitrogen remobilization contributes at least twice as much grain nitrogen as post-anthesis nitrogen uptake under standard conditions (Kichey et al. 2007; Bogard et al. 2010). Nitrogen remobilization efficiency is defined as the proportion of above ground crop nitrogen at anthesis which is not recovered in the crop at harvest (Kong et al. 2016; Gaju et al. 2014). In maize, a cultivar with earlier leaf senescence and higher grain protein content displayed more efficient nitrogen remobilization from leaves to grain, measured through the partitioning of ^{15}N applied at stem elongation (Gong et al. 2020). By accelerating senescence and increasing

nitrogen remobilization efficiency, wheat grain protein content could be increased without additional nitrogen input.

1.7 Transcription factors regulate senescence in plants

1.7.1 The role of transcription factors in plant senescence

Senescence would not be possible without transcription factors. Transcription factors integrate the signals of developmental age and environmental stress to initiate senescence by regulating gene expression (Schippers 2015). Transcription factors coordinate the upregulation of catabolic enzymes, transporters required for nitrogen remobilization and other senescence-associated genes; and downregulation of photosynthetic apparatus and biosynthetic enzymes. In *Arabidopsis,* the onset of leaf senescence is regulated by transcription factors including NAC (e.g. *ORE1*), WRKY (e.g. *WRKY53*) and TCP (e.g. *TCP4*) family transcription factors (Schippers 2015). These transcription factors form a complex network of interactions that changes through the course of senescence (Kim et al. 2018).

1.7.2 The NAC family of transcription factors in senescence

The plant-specific NAC (*NAM, ATAF, CUC3*) family of transcription factors plays a prominent role in senescence regulation. In *Arabidopsis,* over 30 – about a third – of the NAC transcription factors are upregulated in senescing leaves (Kim, Nam,Lim 2016). In dicots *Arabidopsis* and *Populus tricarpa,* known senescence associated NAC transcription factors are mostly found in the subclades NAC-a (SNAC) and NAC-d (NAM/CUC3), with some in NAC-b (TIP) and a few in other subclades (Podzimska-Sroka et al. 2015; Nakashima et al. 2012; Wang et al. 2021a). *ORE1* and *NAP* are examples of *Arabidopsis* NAC transcription factors that integrate

multiple signals to regulate senescence. *ORE1* is inhibited by microRNA miR164, then as miR164 decreases in abundance with leaf age, *ORE1* is activated by ethylene via *EIN3* (Schippers 2015). *NAP* expression is increased by both ethylene and ABA, then creates a feedback loop to accelerate senescence by upregulating ABA biosynthesis genes (Schippers 2015). Both *ORE1* and *NAP* upregulate transcription of senescence-associated genes to promote the onset of leaf senescence (Schippers 2015).

NACs are one of the largest families of transcription factors, and display diverse functions in plant development, pathogen defence, abiotic stress responses, phytohormone responses and senescence (Olsen et al. 2005). Most NAC transcription factors have a conserved N-terminal NAC domain, and an intrinsically disordered C-terminal domain (Olsen et al. 2005). The NAC domain is required for both protein dimerization and DNA binding, with subdomains i and ii at the dimerization region and subdomains iii, iv and v at the protein-DNA interface based on crystal structures (Ernst et al. 2004; Welner et al. 2012). In wheat, TaNAM-1 dimerization involves subdomains i and iii of the NAC domain, as missense mutations in these subdomains can abolish heterodimerization of TaNAM-A1 and TaNAM-B1 proteins (Harrington et al. 2019b). Transcription factors in the NAC-a subclade, including *ANAC019*, *ATAF1*, rice *OsNAC5* and wheat *TaNAM-A1* bind to a CACG consensus motif (Kim, Nam,Lim 2016; Takasaki et al. 2010; Mao et al. 2020). NAC transcription factors are generally activators, rather than repressors, of transcription (Olsen et al. 2005). The C-terminal domain of barley NAC transcription factor HvNAC005 is sufficient to activate transcription (Christiansen et al. 2016). ANAC092 binds a protein called GLK through its C-terminal domain, an interaction

which reduces GLK activity in senescence (Kim, Nam,Lim 2016). *ATAF1*, another NAC, promotes *ANAC092* transcription (Kim, Nam,Lim 2016). In summary, NAC transcription factors can form homodimers, heterodimers, and protein-protein interactions; activate transcription; and provide multiple layers of regulation.

Wheat contains 453 NAC transcription factors belonging to 146 homoeologous triads (Borrill, Harrington,Uauy 2017). A coexpression analysis identified two expression modules with enrichment of NAC transcription factors uniquely from NAC-a and NAC-d subclades (which contained many senescence-associated transcription factors in *Arabidopsis*) (Borrill, Harrington,Uauy 2017; Podzimska-Sroka et al. 2015). These modules were associated with photosynthesis, protein export from nucleus and response to water (Borrill, Harrington,Uauy 2017). What is known about the role of NAC transcription factors in senescence in wheat?

1.7.3 Advancing understanding of NAC transcription factors regulating senescence in wheat

Although many NAC transcription factors involved in senescence have been identified in *Arabidopsis* and rice, it cannot be assumed that orthologous genes in wheat perform the same functions. The NAC transcription factor family underwent distinct gene expansions in monocot and dicot lineages (Zhu et al. 2012). Among NAC transcription factors, the orthologs rice *SNAC1* and barley *HvSNAC1* have different mutant phenotypes (Podzimska-Sroka et al. 2015), and *NAM-1* is involved in leaf senescence in wheat, but anther development in rice (Distelfeld et al. 2012). Hence, to understand the regulation of senescence in wheat, it is necessary to characterise transcription factor function in wheat.

To investigate the regulation of leaf senescence directly in wheat, an RNA-seq time course of early flag leaf senescence was carried out (Borrill et al. 2019). The senescence time-course was marked by two temporal waves of transcriptomic changes, with the first mainly downregulated and the second mainly upregulated genes (Borrill et al. 2019). NAC, CCAAT_HAP1 and RWP-RK transcription factor families were significantly enriched among genes upregulated during flag leaf senescence (Borrill et al. 2019). 32% of the NAC family was upregulated during the time-course of senescence from 10DAA onwards (Borrill et al. 2019). In five out of six cases including *ORE1*, *Arabidopsis* senescence-associated NACs and their wheat orthologs differed in expression pattern through senescence (Borrill et al. 2019). Only 60% of rice genes had the same expression pattern as their ortholog in wheat (Borrill et al. 2019). This reiterates the importance of NAC transcription factors in regulating wheat senescence, and the need to characterise senescence-regulating transcription factors in wheat.

1.8 The role of NAC transcription factors in regulating senescence in wheat

1.8.1 Senescence-associated NAC transcription factors in wheat, barley and rice

Several NAC transcription factors are upregulated during leaf senescence or have been shown to promote leaf senescence in wheat, barley and rice (Table 1.1). A few of these NAC transcription factors are also associated in some way with grain protein content (Table 1.1). *TaNAM-B1*, the causative gene behind the *Gpc-B1* locus, promotes earlier senescence, improves nitrogen remobilization and increases grain

protein content in wheat (Uauy et al. 2006; Waters et al. 2009; Avni et al. 2014). *TaNAM-1* and its paralog *TaNAM-2* are introduced in more detail in Chapter 2. Out of eight NAC transcription factors in rice, *OsNAC5* and *OsNAP* were both upregulated in senescence and associated with grain protein content (Table 1.1) (Sperotto et al. 2009; Sun et al. 2015; Zhou et al. 2013; Liang et al. 2014). Hence *OsNAC5, OsNAP* and their wheat orthologs *TaNAC5-1* and *TaNAP-1* are candidates for regulating senescence and nitrogen remobilization, and are introduced in more detail in Chapter 3. Barley *HvNAC026* and *HvNAC001* also have potential to be involved in nitrogen remobilization, because they were upregulated in standard but not high nitrogen conditions (compared to *HvNAC013,* upregulated in both standard and high nitrogen) (Hollmann, Gregersen,Krupinska 2014).

In contrast, other senescence-regulating NAC transcription factors were also associated with drought tolerance. Loss-of-function mutants of *OsNAC2* showed delayed senescence and increased yield under standard conditions, while overexpression increased tolerance to seedling drought stress (Mao et al. 2017; Jiang et al. 2019). *ONAC054* and *ONAC096* promote earlier senescence, as loss-of-function lines have delayed senescence, and they are upregulated under drought stress (Sun et al. 2015; Sakuraba et al. 2020; Kang et al. 2019). *TaNAC69-3* is upregulated under drought stress and senescence (Xue et al. 2006; Borrill et al. 2019). Given that drought stress accelerates senescence, it is possible that these genes are involved in regulating drought-induced senescence (Lim, Kim,Nam 2007).

Many of these NAC transcription factors upregulated during senescence share common features. ABA, which increases in concentration under both senescence and abiotic stress, upregulates the expression of *TaNAC69-3, HvNAC005,*

HvNAC027, ONAC054, OsNAP, ONAC096, and *OsNAC5* (Sun et al. 2015; Zhang et al. 2021a; Christiansen, Holm,Gregersen 2011; Sakuraba et al. 2020; Liang et al. 2014). *OsNAC5* overexpression improves drought tolerance, and *TaNAM-A1* is upregulated under drought stress, indicating that it is possible for a transcription factor to regulate drought stress response as well as nitrogen remobilization in senescence (Jeong et al. 2013; Mao et al. 2020). *TaNAM-1, TaNAM-2* and *TaNAC3-1* share predicted downstream targets (Borrill et al. 2019; Harrington 2019). None of these transcription factors can be ruled out from having a role in nitrogen remobilization and grain protein content.

Few NAC transcription factors negatively regulate senescence timing. *TaNAC-S* is a negative regulator of leaf senescence; overexpression of *TaNAC-S* delayed leaf senescence (Table 1.1) (Zhao et al. 2015). Interestingly, *TaNAC-S* overexpression lines also had higher grain nitrogen concentration at a given yield (Zhao et al. 2015). Whilst this is converse to the concept that later senescence reduces nitrogen remobilization, it could be explained by increased post-anthesis nitrogen uptake (Bogard et al. 2010). *OsNAC106* delays senescence when overexpressed, with increased yield, whilst a stop codon mutation in *OsNAC109* led to premature senescence and increased production of reactive oxygen species (Sakuraba et al. 2015; Li et al. 2021).

In summary, many positive regulators of senescence and few negative regulators of senescence have been identified among NAC transcription factors in wheat, barley and rice. Some of these transcription factors were associated with grain protein content while others were associated with drought response. To investigate the regulation of nitrogen remobilization during senescence, NAC transcription factors

with evidence linking them to both senescence and grain protein content – *TaNAM-2* and the wheat orthologs of *OsNAC5* and *OsNAP* – were selected for further characterisation in this thesis.

Table 1.1 NAC transcription factors associated with senescence in wheat (Triticum aestivum), barley (Hordeum vulgare) and rice (Oryza sativa). Accession IDs (wheat, RefSeq v1.1; barley, Genbank;, rice, RAPDB) and common gene names are shown. Noted are gene expression during natural / age-induced leaf senescence, effect of transgenic overexpression (any type of promoter), effect of loss-of-function including induced mutation and RNAi, and whether there is any kind of association (positive or negative) with protein content. Blank cells are unknown. This was not a systematic review. [1] Not all homoeologs of hexaploid wheat were tested. [2] Genbank ID supplied for NAM-B1 as it is absent from RefSeq v1.1.

Accession IDs	**Gene name**	**Species**	**Expression in leaf senescence**	**Overexpression effect on leaf senescence timing**	**Loss-of-function effect on leaf senescence timing**	**Associated with grain protein content**	**Reference**
TraesCS2A02G201800 TraesCS2B02G228900 TraesCS2D02G214100	*TaNAM-2*	*Triticum aestivum*	Upregulated		Later [1]		(Borrill et al. 2019)
TraesCS5A02G143200 TraesCS5B02G142100 TraesCS5D02G148800	*NAC69-3 NAC69-1*	*Triticum aestivum*	Upregulated				(Borrill et al. 2019)
TraesCS6A02G108300 DQ869673 [2] TraesCS6D02G096300	*TaNAM-1*	*Triticum aestivum*	Upregulated	No effect [1]	Later	Yes [1]	(Uauy et al. 2006) (Avni et al. 2014) (Harrington 2019)

TraesCS7A02G305200 TraesCS7B02G205600 TraesCS7D02G302000	*TaNAC-S*	*Triticum aestivum*	Downregulated [1]	Later [1]		Yes [1]	(Zhao et al. 2015)
TraesCS2A02G101400 TraesCS2B02G118500 TraesCS2D02G100900	*TaNAC3-1*	*Triticum aestivum*	Upregulated		Later [1]		(Harrington 2019)
AK249749	*HvNAC007*	*Hordeum vulgare*	Upregulated				(Christiansen, Holm,Gregersen 2011)
AK251058	*HvNAC005*	*Hordeum vulgare*	Upregulated	Earlier			(Christiansen et al. 2016) (Hollmann, Gregersen,Krupinska 2014)
AK368213	*HvNAC027*	*Hordeum vulgare*	Upregulated				(Christiansen, Holm,Gregersen 2011) (Christiansen and Gregersen 2014)

AY672069	*HvNAC031 HSINAC*	*Hordeum vulgare*	Upregulated		(Christiansen, Holm,Gregersen 2011)
EU908210	*HvNAC029 HvNAM-1*	*Hordeum vulgare*	Upregulated	Yes	(Christiansen, Holm,Gregersen 2011) (Christiansen and Gregersen 2014)
EX573211	*HvNAC001*	*Hordeum vulgare*	Upregulated		(Hollmann, Gregersen,Krupinska 2014) (Christiansen and Gregersen 2014)
FR821737	*HvNAC008 HvSF6*	*Hordeum vulgare*	Upregulated		(Christiansen, Holm,Gregersen 2011)
TC163636	*HvNAC013*	*Hordeum vulgare*	Upregulated		(Hollmann, Gregersen,Krupinska 2014) (Christiansen and Gregersen 2014)

TC164854	*HvNAC026*	*Hordeum vulgare*	Upregulated				(Hollmann, Gregersen,Krupinska 2014) (Christiansen and Gregersen 2014)
Os03g0119966	*ONAC054*	*Oryza sativa*			Later		(Sakuraba et al. 2020)
Os03g0327800	*OsNAPPS1 ONAC058*	*Oryza sativa*	Upregulated	Earlier	Later	Yes	(Liang et al. 2014) (Zhou et al. 2013)
Os04g0460600	*OsNAC2 ONAC004*	*Oryza sativa*		Earlier	Later		(Mao et al. 2017)
Os06g0675600	*ONAC011*	*Oryza sativa*		Earlier	Later		(El Mannai et al. 2017)
Os07g0138200	*ONAC096*	*Oryza sativa*	Upregulated		Later		(Kang et al. 2019)
Os08g0433500	*OsNAC106*	*Oryza sativa*	Upregulated then downregulated	Later			(Sakuraba et al. 2015)

Os09g0552800	*OsNAC109*	*Oryza sativa*		Earlier		(Li et al. 2021)
Os11g0184900	*OsNAC5 ONAC009*	*Oryza sativa*	Upregulated		Yes	(Sperotto et al. 2009) (Sun et al. 2015) (Sharma et al. 2019)

1.8.2 NAC transcription factors in this thesis

Four wheat NAC transcription factors are the primary focus of this thesis: *NAM-1,* on chromosome 6; *NAM-2,* on chromosome 2; *NAC5-1,* on chromosome 4; and *NAP-1,* also on chromosome 4 (Figure 1.3). These four NAC transcription factors are all part of the NAC-a (SNAC) subclade (Podzimska-Sroka et al. 2015; Nakashima et al. 2012). In hexaploid bread wheat, each of these transcription factors consists of a triad of homoeologous gene copies on the A, B and D subgenomes (Figure 1.1, Figure 1.4). A partial exception to this is *NAM-B1,* for which the majority of hexaploid bread wheat accessions do not contain a functional gene copy, including the Chinese Spring reference sequence IWGSC RefSeq v1.1 (Appels et al. 2018; Uauy et al. 2006; Hagenblad et al. 2012; Lee et al. 2017). Context for this is explained in Chapter 2. Therefore, the coding sequence of *NAM-B1* amplified from wild emmer wheat is displayed (Figure 1.4) (Uauy et al. 2006). *NAM-1, NAM-2* and *NAP-1* transcripts consist of three exons, with *NAM-A1, NAM-A2* and *NAM-B2* annotated with two transcripts, alternatively spliced between the second and third exons (Figure 1.4). *NAC5-1* consists of two exons. Each of these NAC transcription factors contains the conserved NAC domain in the N-terminal part of the peptide (Figure 1.4).

1.8.1 Technologies for wheat gene characterisation in this thesis

This thesis employed TILLING (Targeting Induced Local Lesions In Genomes) population resources and transgenic overexpression to characterise NAC transcription factors in wheat (Krasileva et al. 2017). TILLING mutant lines are generated by applying the mutagen ethyl methylsulfonate (EMS), which causes single nucleotide changes, specifically C>T or G>A transitions (McCallum et al. 2000). TILLING technology has been successfully applied to characterise gene

function in wheat (Slade et al. 2005; Simmonds et al. 2016). In this thesis TILLING populations in hexaploid Cadenza and tetraploid Kronos were utilised, because exome capture sequencing data enabled mutations in genes of interest to be identified rapidly (Krasileva et al. 2017). Although gene editing could also knock out three homoeologs of a gene, TILLING lines are simpler, cheaper, and free from regulatory restrictions (Uauy, Wulff,Dubcovsky 2017). Caveats of using TILLING mutants are that missense mutations may or may not abolish protein function, and each line carries a high background mutation load (Uauy, Wulff,Dubcovsky 2017). To characterise loss-of-function of *NAM-2* in Chapter 2, the hexaploid Cadenza population was selected as this enabled investigation of all three homoeologs, and field trials in the UK climate. To characterise loss-of-function of *NAC5-1* and *NAP-1* in Chapter 3*,* the tetraploid Kronos population was selected as fewer crosses are required to generate a complete knockout. The location and consequences of these mutations in on the transcript and peptide sequences are summarised here (Figure 1.4).

In Chapter 3, wheat was transformed to overexpress *NAC5-1* and *NAP-1,* as transformation has reached practical efficiencies in wheat (Hayta et al. 2019).

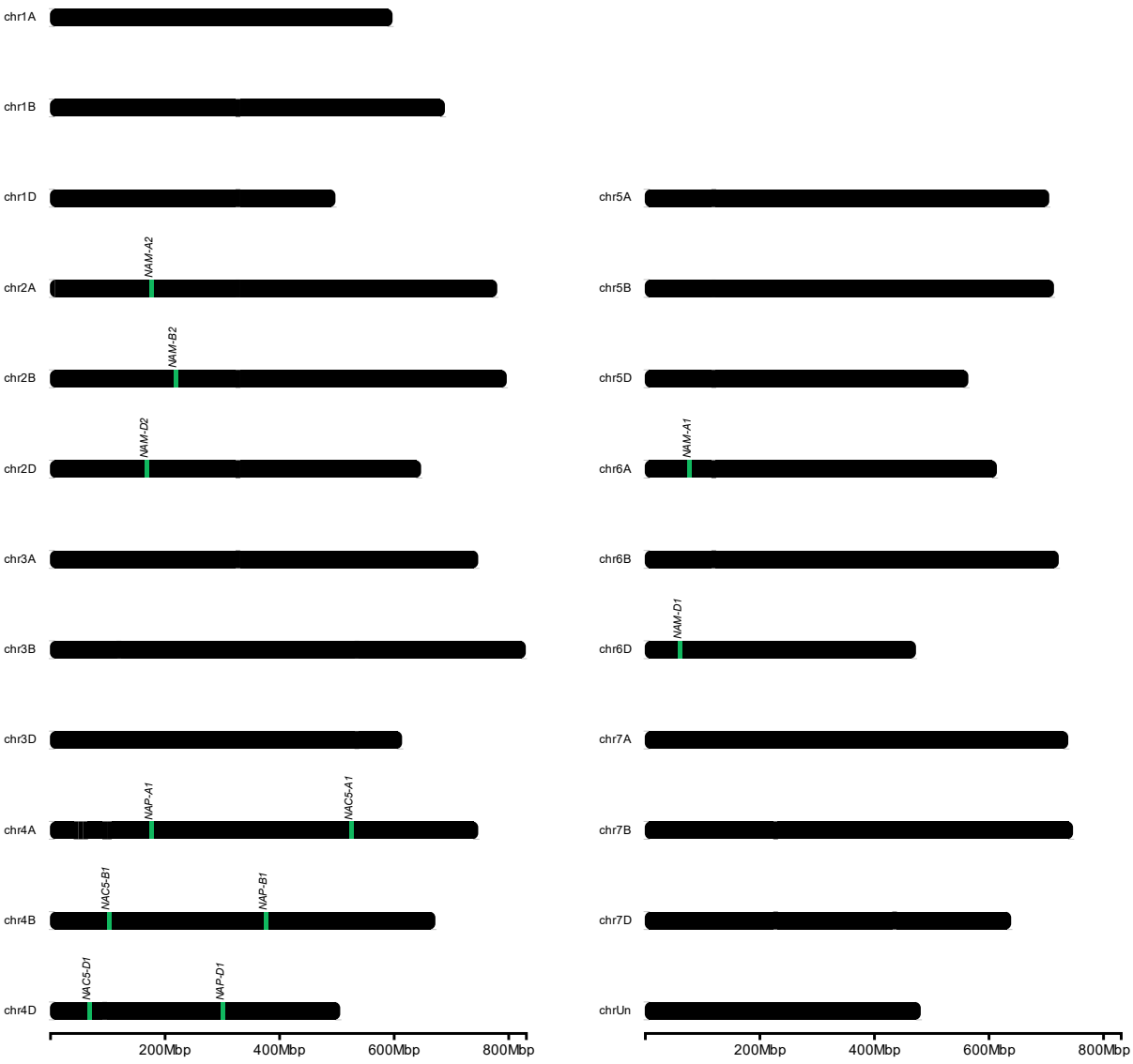


Figure 1.3 Location of NAM-1, NAM-2, NAC5-1 and NAP-1 homoeologs in the bread wheat reference genome, Chinese Spring RefSeq v1.1 (Appels et al. 2018). NAM-B1 is not shown as the reference genome does not contain a functional gene copy. Figure generated with R package chromoMap (Anand and Rodriguez Lopez 2022).

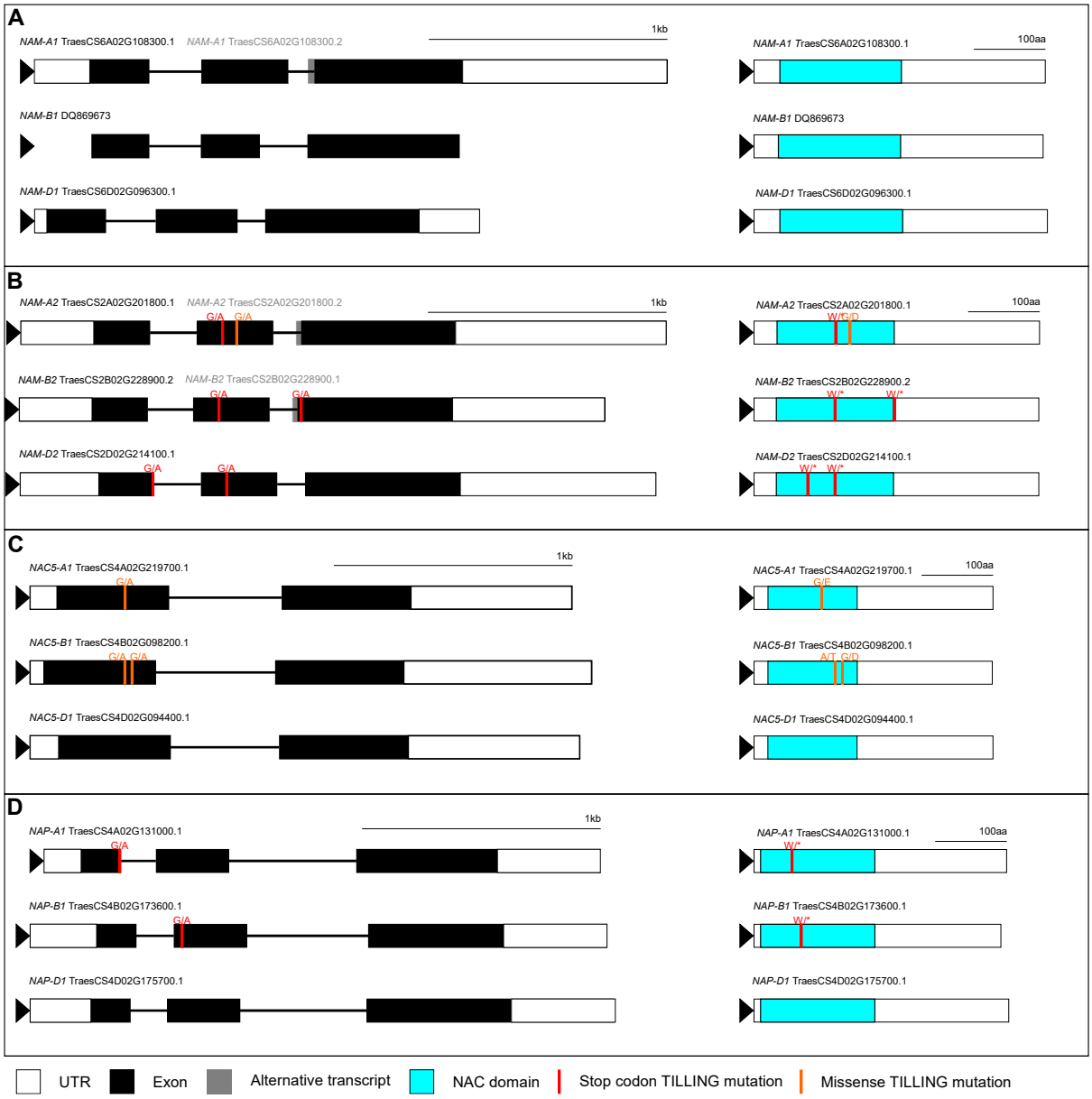


Figure 1.4 Schematics of NAM-1, NAM-2, NAC5-1 and NAP-1 transcripts and peptide sequences. Transcripts taken from the bread wheat reference genome (IWGSC Refseq v1.1) (Appels et al. 2018); except for NAM-B1 which is from Genbank DQ869673 (Uauy et al. 2006) – a sequence which does not show UTRs. Black arrows mark start of transcript or peptide. NAC domains are based on Prosite annotation. TILLING mutations are annotated with wild-type/mutant alleles. For more information on TILLING mutations see Table 2.12 and Table 3.14.

1.8.2 Senescence-regulating transcription factors as targets for improving senescence timing

In summary, leaf senescence is a complex developmental stage involving catabolism, nitrogen remobilization, termination of photosynthesis and eventual cell death. Transcription factors initiate the widespread transcriptomic changes needed to implement the multitude of processes of leaf senescence. NAC transcription factors which positively regulate the timing of age-induced senescence have been identified in *Arabidopsis,* rice, barley, and wheat. In wheat, earlier senescence correlates with decreased yield or kernel weight, and increased grain protein content. NAC transcription factors regulating senescence in wheat could be promising targets to alter the timing of senescence and optimise the balance between protein content and yield.

1.9 Objectives

The objective of this thesis is to advance knowledge of the transcriptional regulation of senescence timing in wheat. This will contribute to uncovering the network of transcription factors regulating leaf senescence in wheat, which is not yet fully understood. Transcription factors promoting senescence may also increase grain protein content, through improving nitrogen remobilization efficiency, and/or decrease yield. Therefore, identifying senescence-regulating transcription factors is an alternative angle to understand the protein-yield trade-off and tackle the challenge of increasing wheat grain protein content.

To achieve this, the role of specific NAC transcription factors in senescence timing will be characterised.

- Chapter 2 will test the hypothesis that *NAM-2* promotes earlier senescence and increased protein content in hexaploid bread wheat.
- Chapter 3 will test the hypothesis that the wheat orthologs of *OsNAC5* and *OsNAP* promote earlier senescence in wheat.
- Chapter 4 will test the hypothesis that senescence-regulating NAC transcription factors can be targeted to improve grain protein content in a UK wheat breeding context.

2 DOES *NAM-2* AFFECT THE TIMING OF SENESCENCE OR GRAIN PROTEIN CONTENT?

2.1 Introduction

During wheat grain filling, nutrients are remobilized from senescing leaves to the developing grain (Distelfeld, Avni,Fischer 2014). Therefore, the timing of leaf senescence is linked to grain protein and micronutrient content (Kong et al. 2016). NAC transcription factors are known to form a key part of the network regulating leaf senescence in *Arabidopsis thaliana* and rice (Schippers 2015; Podzimska-Sroka et al. 2015). The wheat NAC transcription factor *NAM-1* exemplifies these principles, as explained in the following sections.

2.1.1 Discovery of *NAM-1* de novo in wheat

An accession of wild emmer wheat (*Triticum turgidum spp. dicoccoides*) with high grain protein content was identified in 1978 (Avivi 1978). Chromosome 6B was identified as the genetic basis of the high protein content using a chromosome substitution line containing chromosome 6B from wild emmer (DIC-6B) in tetraploid wheat Langdon (Cantrell and Joppa 1991). From this chromosome substitution line, homozygous recombinant substitution lines (RSLs) with recombination in chromosome 6B were developed to map a locus now known as *Grain Protein Content B1* (*Gpc-B1*) to an interval around 5.9cM (centiMorgans) with RFLP (restriction fragment length polymorphism) markers (Joppa et al. 1997; Chee et al. 2001). The *Gpc-B1* locus was further refined to 2.7cM by development of novel

RFLP markers within this interval, and a larger panel of RSLs (Olmos et al. 2003). A physical map of the locus was built via comparison with the colinear segment of the rice genome, enabling molecular markers to be developed to build a high-resolution genetic map, and fine-map a 7.4kb region containing a single gene (Distelfeld et al. 2006; Uauy, Brevis,Dubcovsky 2006; Uauy et al. 2006). Meanwhile, the genes *No Apical Meristem* (*NAM*) of *Petunia* and *Cup-Shaped Cotyledon 2 (CUC2)* of *Arabidopsis* were cloned, which give their names to the NAC (*NAM, ATAF1, CUC2*) transcription factor family (Souer et al. 1996; Aida et al. 1997).

The gene responsible for the high grain protein content of the *Gpc-B1* locus was named *NAM-B1* after its similarity to *NAM* (Genbank ID DQ869673) (Uauy et al. 2006).Lines with introgression of the *Gpc-B1* locus from wild emmer had higher grain protein, iron, zinc, and manganese content, and earlier senescence, while RNAi lines targeting *NAM-1* had lower grain protein content (GPC) (Uauy, Brevis,Dubcovsky 2006; Distelfeld et al. 2007). Mutation of *NAM-A1* (TraesCS6A02G108300) and *NAM-D1* (TraesCS6D02G096300) in hexaploid wheat already lacking functional *NAM-B1* reduced GPC by 10-21% in field trials across two years and three sites (Avni et al. 2014). Similarly, mutation of *NAM-A1,* in tetraploid wheat already lacking functional *NAM-B1,* decreased GPC by 13-19% and reduced iron and zinc content in field trials in 3 sites (Pearce et al. 2014). These *nam-a1* mutant lines displayed up to 27 days delay in senescence (Pearce et al. 2014).

2.1.2 Evolution of *NAM-1* and *NAM-2*

The *NAM-1* triad is found within a subclade of NAC transcription factors known as NAC-a or stress-inducible NAC (SNAC) (Nakashima et al. 2012; Podzimska-Sroka et al. 2015). In *Arabidopsis, AtNAM / NARS2* (At1g52880) and *AtNAC2 /NARS1* (At3g15510) are most closely related to *NAM-1* based on a phylogeny of the

conserved NAC domains (Distelfeld et al. 2012). Both of these genes are involved in embryonic development: *nam* mutants have no apical meristem, cotyledon fusions, and aberrant floral development, while *nam/nac2* double mutants in have abnormally shaped seeds and arrested embryo development (Olsen et al. 2005; Kunieda et al. 2008). Within monocots, the ortholog of *NAM-1* in rice is *ONAC010* (Os07g37920) (Distelfeld et al. 2012). *ONAC010* increases slightly in expression during senescence, but far less than *NAM-1*, and RNAi lines had no senescence phenotype (Distelfeld et al. 2012). In contrast, *ONAC010* is upregulated in stamens at flowering, and RNAi lines were male sterile, had fewer pollen grains, and anthers failed to split to release pollen (Distelfeld et al. 2012). Notably, of the four C-terminal motifs present in *NAM-1*, *ONAC010* has two of the motifs, while *AtNAM* and *AtNAC2* only have one of the motifs (Christiansen et al. 2016). Thus, *NAM-1* has diverged in both structure and function from *ONAC010* and has evolved the function of regulating senescence since the last common ancestor of wheat and rice.

Through a gene duplication within the *Triticeae, NAM-1* has a paralog, *NAM-2*, in wheat (TraesCS2A02G201800; TraesCS2B02G228900; TraesCS2D02G214100). Similarly, barley contains the paralogous genes *HvNAM-1/HvNAC029* (EU368851/EU908210) and *HvNAM-2* (Distelfeld et al. 2008; Christiansen, Holm,Gregersen 2011). *HvNAM-1* is upregulated in early flag leaf senescence, and in ears and grain of barley (Christiansen, Holm,Gregersen 2011; Christiansen and Gregersen 2014). Near isogenic lines lacking *HvNAM-1* showed delayed senescence and reduced protein content (Jukanti and Fischer 2008). Allelic variation in *HvNAM-1* between barley accessions correlated with altered GPC in two studies, while *Hordeum bulbosum*, which has a non-functional allele of *NAM-1*, has low GPC (Wang et al. 2015; Jamar et al. 2010; Christiansen and Gregersen 2014). A genome

wide association study (GWAS) recovered a single nucleotide polymorphism (SNP) in an intron of *HvNAM-2* associated with grain protein content (Cai et al. 2013). These results indicate that *HvNAM-1* and putatively *HvNAM-2* share a role in regulating grain protein content and senescence conserved with wheat *NAM-1*.

Three alleles of *NAM-B1* featured in the evolution and domestication of wheat. In wild emmer (*Triticum turgidum* spp. *dicoccoides*, AABB), 16 out of 18 accessions contained the full-length *NAM-B1* while one had a +1bp insertion at the fourth amino acid, disrupting the reading frame, and one was heterozygous (Lundstrom, Leino,Hagenblad 2017). Domesticated emmer accessions (*T. turgidum* spp. *dicoccum*, AABB) were polymorphic for the full-length allele, the +1bp allele and a deletion allele with a deletion of over 100kb (Lundstrom, Leino,Hagenblad 2017). This indicates that the +1bp allele originated in wild emmer, while the deletion allele originated in domesticated emmer. Current evidence indicates that durum wheat (*T. turgidum* spp. *durum,* AABB) is fixed for loss-of-function of *NAM-B1*, with most accessions – including Langdon, the recurrent parent used to map *NAM-B1* – containing the +1bp allele, which carries a selective sweep signature (Lundstrom, Leino,Hagenblad 2017; Uauy et al. 2006).

It was initially believed that loss-of-function of *NAM-B1* was also fixed in bread wheat (*T. aestivum* ssp. *aestivum*), with around 70% of lines carrying the deletion allele, and 30% of lines the +1bp allele (Hagenblad et al. 2012). However, spring bread wheat landraces and cultivars from Norway, Sweden and Finland were found to carry functional *NAM-B1*, in addition to historical bread and spelt (*T. aestivum* ssp. *spelta,* AABBDD) landraces from the 19th century (Asplund, Hagenblad,Leino 2010; Hagenblad et al. 2012). Even so, the functional *NAM-B1* allele remains rare in cultivated bread wheat: it was absent from a panel of 218 Chinese wheat cultivars

(Chen et al. 2017). As some domesticated wheats, such as domesticated emmer, contain functional *NAM-B1*, and recent literature favours a single domestication event for polyploid wheat, *NAM-B1* does not appear to be a domestication gene (Lundstrom, Leino,Hagenblad 2017; Zhao et al. 2023). Loss-of-function alleles of *NAM-B1* were strongly selected and almost fixed in durum wheat and bread wheat, indicating that *NAM-B1* is a diversification gene in the evolution of polyploid wheat (Lundstrom, Leino,Hagenblad 2017; Hagenblad et al. 2012; Chen et al. 2017).

Selection for increased kernel weight may have driven the spread of the +1bp and deletion alleles of *NAM-B1* (Lundstrom, Leino,Hagenblad 2017). Introgression of the *Gpc-B1* locus decreased kernel weight in multiple studies (Uauy, Brevis,Dubcovsky 2006; Brevis and Dubcovsky 2010; Bokore et al. 2019). Retention of functional *NAM-B1* in Nordic landraces could be explained by higher selection for early maturity in this high-latitude region: Nordic cultivars with functional *NAM-B1* show early anthesis and senescence, but no improvement in protein content, compared to other Nordic cultivars (Hagenblad et al. 2012; Asplund et al. 2013). In addition to alleles of *NAM-B1,* allelic variation in *NAM-A1* has been identified in bread wheat populations, and is introduced in Chapter 4 (Cormier et al. 2015).

2.1.3 *NAM-1* increases grain protein by promoting the onset of senescence and nitrogen remobilization.

What is the mechanism by which *NAM-1* increases grain protein content? *Gpc-B1* introgression lines show a lower nitrogen content in straw at harvest (Kade et al. 2005; Brevis and Dubcovsky 2010). Lower nitrogen in straw suggests that *NAM-B1* promotes nitrogen remobilization from stem to ear. RNAi lines were generated to reduce expression of *NAM-A1*, *NAM-D1, NAM-B2* and *NAM-D2* (Uauy et al. 2006). *NAM* RNAi lines had lower grain nitrogen content, while only 29% of flag leaf

nitrogen was remobilized out of leaves, compared to 45% in control lines (Waters et al. 2009). Similarly, grain iron and zinc contents were reduced (Waters et al. 2009). The RNAi lines showed delayed flag leaf senescence, as did TILLING (Targeting Induced Local Lesions In Genomes) lines with mutations in *NAM-A1* and *NAM-D1* (Avni et al. 2014).TILLING lines also contained increased flag leaf nitrogen at 50DAA (Days After Anthesis) and peduncle nitrogen at harvest (Avni et al. 2014). These results indicate that reduced *NAM* expression impairs nitrogen and micronutrient remobilization from the leaves to the grain during senescence (Waters et al. 2009).

Does *NAM-1* contribute to the trade-off between wheat grain protein content and yield? This negative genetic correlation implies that pleiotropic genetic loci exist which result in increased protein content with decreased yield (Bogard et al. 2011). In some experiments, *Gpc-B1* introgression lines showed a reduction in yield, however yield did not differ between *Gpc-B1* alleles in 77% of comparisons from 25 field studies (Uauy, Brevis,Dubcovsky 2006; Tabbita, Pearce,Barneix 2017). In *NAM* RNAi lines, total sugar production in leaves increased due to 10 days prolonged photosynthesis (Borrill et al. 2015). However, this did not translate to higher grain weight as the sugars were not transported to the grain, but an equivalent of 13% of the additional sugar remained in the stem, suggesting that sink capacity is also necessary for increased grain mass (Borrill et al. 2015). Together, this suggests that while *NAM-1* promotes earlier senescence, this may or may not translate to reduced yield dependent on environmental conditions and genetic constraints.

NAM-1 and *NAM-2* may also be involved in the abiotic stress response. Transcript levels of *NAM-B2* increased 13-fold after 48 hours salt stress, and slightly after 2 days osmotic stress in winter durum wheat (Baloglu et al. 2012). *NAM-1* and *NAM-2* are upregulated transiently in roots 1 hour after seedling drought stress, and to a

greater extent in shoots 3-6 hours after drought stress (using non-homoeolog-specific primers) (Mao et al. 2020). Increased expression of *NAM-1* and *NAM-2* under abiotic stresses could be in response to ABA signalling, as there are multiple ABA response elements in the promoters (Mao et al. 2020). Constitutive overexpression of *NAM-A1* in *Arabidopsis thaliana* and wheat resulted in higher lateral root formation and root dry mass, and higher drought tolerance (*Arabidopsis:* 14d drought in grown plants; wheat: 30d drought in seedlings) (Mao et al. 2020).

2.1.4 Further characterising the role of *NAM-2* in leaf senescence.

In summary, *NAM-A1, NAM-B1* and *NAM-D1* promote increased grain protein content and earlier senescence (Uauy et al. 2006; Avni et al. 2014). *NAM-1* increases protein content by upregulating genes involved in amino acid transport, which accelerates nitrogen remobilization from senescing flag leaves to developing grain (Pearce et al. 2014; Waters et al. 2009).

Does *NAM-2*, the paralog of *NAM-1,* also promote earlier senescence, nitrogen remobilization and grain protein content? *NAM-2* homoeologs are expressed in early flag leaf senescence and appear as hub genes in a network of transcription factors in senescence, making them candidate senescence regulators independently of their homology to *NAM-1* (Borrill et al. 2019). Mutation of *NAM-B2* showed no effect in tetraploid wheat in a *nam-b1* background, and no effect or borderline delayed senescence in a *nam-a1/nam-b1* background (Distelfeld et al. 2012; Pearce et al. 2014; Borrill et al. 2019). Mutation of *NAM-A2* delayed peduncle senescence, while mutation of both *NAM-A2* and *NAM-B2* delayed flag leaf and peduncle senescence in a tetraploid *nam-b1* background (Borrill et al. 2019). This suggests that *NAM-A2* promotes earlier senescence, and *NAM-B2* may act redundantly to promote senescence, as loss-of-function of *NAM-B2* only has any phenotypic effect when

other *NAM* genes are also mutated. However, it has not been reported whether *NAM-D2* impacts senescence.

Evidence for a link between *NAM-2* and wheat grain protein content is sparser. In barley, a SNP in *HvNAM-2* correlated with grain protein content (Cai et al. 2013). In wheat, RNAi lines targeting *NAM-B2*, *NAM-D2* and all homoeologs of *NAM-1* showed more than 30% reduction in GPC, compared to 10-21% reduction in GPC in TILLING mutant lines for all homoeologs of *NAM-1* (Uauy et al. 2006; Avni et al. 2014). This implies that *NAM-B2* and *NAM-D2* may contribute to increasing grain protein content, however this comparison is inadequate given different germplasm and experimental conditions. In addition, the RNAi lines do not represent a full knock-down of *NAM-2,* as *NAM-A2* expression is unaffected (Andleeb et al. 2022). Hence, research is needed to test the effect of *NAM-2* on wheat grain protein content.

2.1.5 Objectives

In this chapter, the following questions will be addressed.

1. How does loss-of-function of *NAM-A2, NAM-B2* and *NAM-D2* affect the timing of senescence in hexaploid wheat?
2. How does loss-of-function of *NAM-2* affect grain protein content in hexaploid wheat?

To characterise the function of *NAM-2* in senescence, an approach was taken inspired by a roadmap for gene characterisation in wheat (Adamski et al. 2020). Mutations likely to lead to loss-of-function of *NAM-A2, NAM-B2* and *NAM-D2* were selected from the hexaploid Cadenza TILLING population (Krasileva et al. 2017). Triple mutant lines for *NAM-2* were generated by crossing, using a speed breeding

technique (Watson et al. 2018). The timing of flag leaf senescence was assessed in *NAM-2* mutant lines in two glasshouse experiments and one field trial, while wheat grain protein content was assessed in glasshouse experiments.

2.2 Methods

2.2.1 Gene expression data

To assess the pattern of NAC transcription factor expression during flag leaf senescence, transcript levels of NAC genes in wheat flag leaves from 3DAA (Days After Anthesis) to 26DAA were re-analysed from RNA-seq data (Borrill et al. 2019). Gene IDs were input into the Wheat Expression Browser and raw data in transcripts per million (tpm) were extracted (Borrill, Ramirez-Gonzalez,Uauy 2016). Transcript level of each homoeolog from the flag leaf senescence time-course was plotted.

2.2.2 Development of *NAM-2* TILLING mutant lines

2.2.2.1 Selection of TILLING mutations

To generate wheat lines with probable loss-of-function of a NAC transcription factor in wheat, single nucleotide polymorphisms (SNPs) were assessed from the exome-capture sequenced TILLING (Targeting Induced Local Lesions In Genomes) population in either hexaploid Cadenza (for *NAM-2*) or tetraploid Kronos (for *NAC5-1* and *NAP-1*) wheat (Krasileva et al. 2017; McCallum et al. 2000). To maximise the probability of disrupting NAC protein function, SNPs were selected: a) with a stop codon before the end of the NAC domain, or b) with a conserved missense mutation within the NAC domain. NAC subdomains were annotated following annotation of *NAM-A1* and *NAM-B1* (Uauy et al. 2006). Sequence conservation was assessed by the position-specific scoring matrix (PSSM) for the NAC domain, using NCBI PSSM

viewer (no longer available) (NCBI 2020). To further assess the possible functional impact of SNPs in *NAM-2*, previously tested induced mutations in *NAM-1* and *NAM-2* were collected from the literature (Distelfeld et al. 2012; Avni et al. 2014; Borrill et al. 2019; Harrington et al. 2019b). Wheat lines carrying TILLING mutations were ordered from the Germplasm Resources Unit (Germplasm Resources Unit 2019).

2.2.2.2 Design of KASP primers to genotype TILLING lines

To track SNPs in TILLING lines, primers for KASP genotyping (LGC Genomics) were obtained using two methods: Polymarker and manual design (*Table 2.1*).

Predesigned KASP primers associated with the TILLING population were accessed from Ensembl Plants (Yates et al. 2022). These KASP primers were designed with the automated Polymarker tool using method as described at Wheat Training (Ramirez-Gonzalez, Uauy,Caccamo 2015; Wheat Training 2023). A HEX/VIC tag was added to the wild-type allele (WT) primer and a FAM tag to the mutant allele (MUT) primer.

To design KASP primers manually, *NAM-A2, NAM-B2* and *NAM-D2* genomic sequences were aligned, and primers were designed manually in Benchling software (Benchling 2021), to match the following criteria:

1. WT and MUT primers contain the wild-type and mutant SNP alleles at the 3’ end of the primer
2. COM primers contain a homoeolog-specific base pair at the 3' end of the primer
3. Product size less than 350bp, ideally 50 – 150bp
4. T_m 55-62°C
5. GC content closer to 50% of choices available

A HEX/VIC tag was added to the WT primer and a FAM tag to the MUT primer.

Table 2.1 KASP primers designed for genotyping of TILLING mutations in NAM-A2, NAM-B2, and NAM-D2. All primers designed are included, whether or not they were used for genotyping in the crossing program.

Primer	Sequence	Description	Primer design method
CE1773-WT	GAAGGTCGGAGTCAACGGATTcgagcgccttcttgacgC	WT primer for TraesCS2A02G201800 (NAM-A2) in Cadenza1773	Polymarker
CE1773-MUT	GAAGGTGACCAAGTTCATGCTcgagcgccttcttgacgT	MUT primer for TraesCS2A02G201800 (NAM-A2) in Cadenza1773	Polymarker
CE1773-COM	CAAACCTATCCTGGCCTCC	COM Semi-specific primer for TraesCS2A02G201800 (NAM-A2) in Cadenza1773	Polymarker
CE1656-WT	GAAGGTCGGAGTCAACGGATTgccacgtcggggtactgG	WT primer for TraesCS2A02G201800 (NAM-A2) in Cadenza1656	Polymarker
CE1656-MUT	GAAGGTGACCAAGTTCATGCTgccacgtcggggtactgA	MUT primer for TraesCS2A02G201800 (NAM-A2) in Cadenza1656	Polymarker
CE1656-COM	GGCCAGGATAGGTTTGTCC	COM Semi-specific primer for TraesCS2A02G201800 (NAM-A2) in Cadenza1656	Polymarker
CE1436-WT	GAAGGTCGGAGTCAACGGATTgctacgtcggggtactgG	WT primer for TraesCS2B02G228900 (NAM-B2) in Cadenza1436	Polymarker
CE1436-MUT	GAAGGTGACCAAGTTCATGCTgctacgtcggggtactgA	MUT primer for TraesCS2B02G228900 (NAM-B2) in Cadenza1436	Polymarker
CE1436-COM	AGGCCAGGATAGGTTTGTCC	COM Semi-specific primer for TraesCS2B02G228900 (NAM-B2) in Cadenza1436	Polymarker
CE0895-WT	GAAGGTCGGAGTCAACGGATTctcatcagttggacgactgG	WT primer for TraesCS2B02G228900 (NAM-B2) in Cadenza0895	Polymarker

CE0895-MUT	GAAGGTGACCAAGTTCATGCTctcatcagttggacgactgA	MUT primer for TraesCS2B02G228900 (NAM-B2) in Cadenza0895	Polymarker
CE0895-COM	CGGCCTTGTTGATCTTCTTGTAT	COM Semi-specific primer for TraesCS2B02G228900 (NAM-B2) in Cadenza0895	Polymarker
CE0237-WT	GAAGGTCGGAGTCAACGGATTctctacaagttcgacccatgG	WT primer for TraesCS2D02G214100 (NAM-D2) in Cadenza0237	Polymarker
CE0237-MUT	GAAGGTGACCAAGTTCATGCTctctacaagttcgacccatgA	MUT primer for TraesCS2D02G214100 (NAM-D2) in Cadenza0237	Polymarker
CE0237-COM	AAGCACGACGAGGTGAGATA	COM Semi-specific primer for TraesCS2D02G214100 (NAM-D2) in Cadenza0237	Polymarker
CE0231-WT	GAAGGTCGGAGTCAACGGATTgcgacgtcggggtactgG	WT primer for TraesCS2D02G214100 (NAM-D2) in Cadenza0231	Manual
CE0231-MUT	GAAGGTGACCAAGTTCATGCTgcgacgtcggggtactgA	MUT primer for TraesCS2D02G214100 (NAM-D2) in Cadenza0231	Manual
CE0231-COM	CGCCTTCTTGACGCCGAC	COM Semi-specific primer for TraesCS2D02G214100 (NAM-D2) in Cadenza0231	Manual
CE0895-WT-2	GAAGGTCGGAGTCAACGGATTatatgcggcacagcacC	WT primer for TraesCS2D02G214100 (NAM-B2) in Cadenza0895	Manual
CE0895-MUT-2	GAAGGTGACCAAGTTCATGCTatatgcggcacagcacT	MUT primer for KASP genotyping of TraesCS2D02G214100 (NAM-B2) in Cadenza0895	Manual
CE0895-COM-2	GCTTAGGGTATTGTGGTTGATGAAT	COM Specific primer for KASP genotyping of TraesCS2D02G214100 (NAM-B2) in Cadenza0895	Manual
CE0895-COM-3	TGCCCGCCGTGGCATAAA	COM Specific primer for KASP genotyping of TraesCS2D02G214100 (NAM-B2) in Cadenza0895	Manual

CE1656-COM-2	CCCAACAGGGCGGCC	COM Specific primer for TraesCS2A02G201800 (NAM-A2) in Cadenza1656	Manual
CE1656-COM-4	CCGCGCGATCGATCGAT	COM Specific primer for TraesCS2A02G201800 (NAM-A2) in Cadenza1656	Manual
CE1656-COM-3	ACACATGTATGTAGATGGTTTATGTG	COM Specific primer for TraesCS2A02G201800 (NAM-A2) in Cadenza1656	Manual
CE0231-COM-3	CCCAACAGGGCGGCG	COM Specific primer for TraesCS2D02G214100 (NAM-D2) in Cadenza0231	Manual
CE0231-COM-2	AGGCCATGATAGGCTTGTCG	COM Specific primer for TraesCS2D02G214100 (NAM-D2) in Cadenza0231	Manual
CE1436-COM-2	GAGAAGGCGACCTTCGGT	COM Specific primer for TraesCS2B02G228900 (NAM-B2) in Cadenza1436	Manual
CE1436-COM-3	CCCAACAGGGCGGCT	COM Specific primer for TraesCS2B02G228900 (NAM-B2) in Cadenza1436	Manual
CE1436-COM-4	GTACCCTGAGAGAGGCAGA	COM Specific primer for TraesCS2B02G228900 (NAM-B2) in Cadenza1436	Manual
CE1436-COM-5	CCCTAAGCTCGAGAGTAATTAAAC	COM Specific primer for TraesCS2B02G228900 (NAM-B2) in Cadenza1436	Manual
CE1656-MUT-3	GAAGGTGACCAAGTTCATGCTgtgccggtggccttT	MUT primer for TraesCS2A02G201800 (NAM-A2) in Cadenza1656	Manual

CE1656-WT-3	GAAGGTCGGAGTCAACGGATTgtgccggtggccttC	WT primer for TraesCS2A02G201800 (NAM-A2) in Cadenza1656	Manual
CE1773-COM-2	ggcacGgacaaAcctatcC	COM Semi-specific primer for KASP genotyping of TraesCS2A02G201800 (NAM-A2) in Cadenza1773	Manual
CE1773-WT-3	GAAGGTCGGAGTCAACGGATTgccgggagaaggtcgG	WT primer for KASP genotyping of TraesCS2A02G201800 (NAM-A2) in Cadenza1773	Manual
CE1773-MUT-3	GAAGGTGACCAAGTTCATGCTgccgggagaaggtcgA	MUT primer for KASP genotyping of TraesCS2A02G201800 (NAM-A2) in Cadenza1773	Manual
CE1773-COM-3	ACTCGTGCATGATCCAGTTG	COM Non-specific primer for KASP genotyping of TraesCS2A02G201800 (NAM-A2) in Cadenza1773	Manual

2.2.2.3 Crossing scheme for *NAM-2* TILLING lines

To generate lines with mutations in all three copies of *NAM-2*, TILLING lines were crossed together, using KASP genotyping to confirm genotypes at each generation (*Figure 2.1*). These plants were grown under speed breeding conditions (Watson et al. 2018). Plant maintenance, crossing, harvest and threshing were assisted on occasion by Philippa Borrill, Muhammad Ali, Emilie Knight, Sophie Mogg and Sam Burrows.

Firstly, all TILLING lines were back-crossed to Cadenza to reduce background mutation load (Uauy, Wulff,Dubcovsky 2017). Heterozygous *nam-a2* and *nam-d2* mutants were crossed together, yielding heterozygous *nam-a2/nam-d2* double mutants with a mendelian segregation probability of ¼ (*Figure 2.1*). *nam-a2/nam-d2* double mutants were crossed with homozygous *nam-b2* single mutants to generate triple heterozygous BC_1F_1 plants. BC_1F_1 plants were selfed, and segregating populations of BC_1F_2 seedlings were grown and genotyped (*Figure 2.2*). Homozygous genotypes and triple heterozygotes were kept. Where necessary, triple heterozygous BC_1F_2 plants were selfed to generate additional segregating populations.

To bulk seed, progeny of confirmed single, double and triple mutant plants as well as wild-type segregants were grown in glasshouse conditions, with 8 plants per genotype . Two plants per genotype were bagged, harvested individually, and provided seed for both *NAM-2* glasshouse experiments (Figure 2.3). Six plants per genotype were not bagged, harvested in bulk, and provided seed for the *NAM-2* field trial (Figure 2.3).

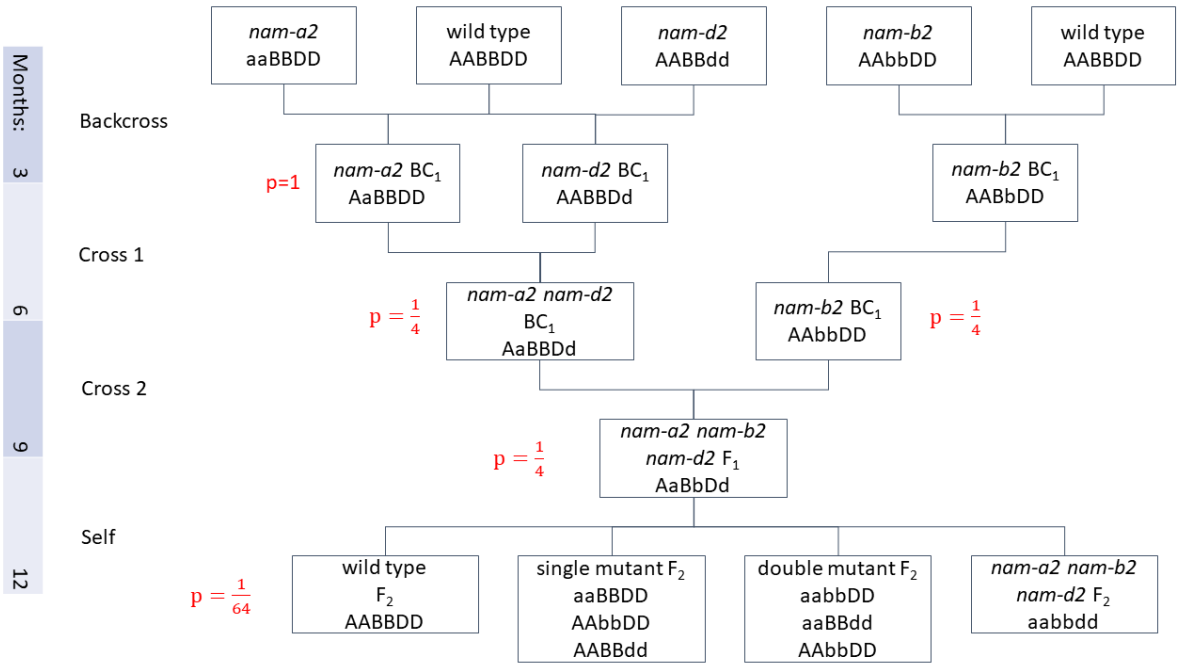


Figure 2.1 Crossing scheme for NAM-2 TILLING lines. Read from top to bottom. Capital letters = wild type allele; lower case = TILLING loss-of-function allele; BC_1 = backcross 1; F_1 and F_2 = generation 1 and 2 after most recent cross. Red script shows the probability of each of the progeny shown. Months taken for crossing scheme in speed breeding shown on the left.

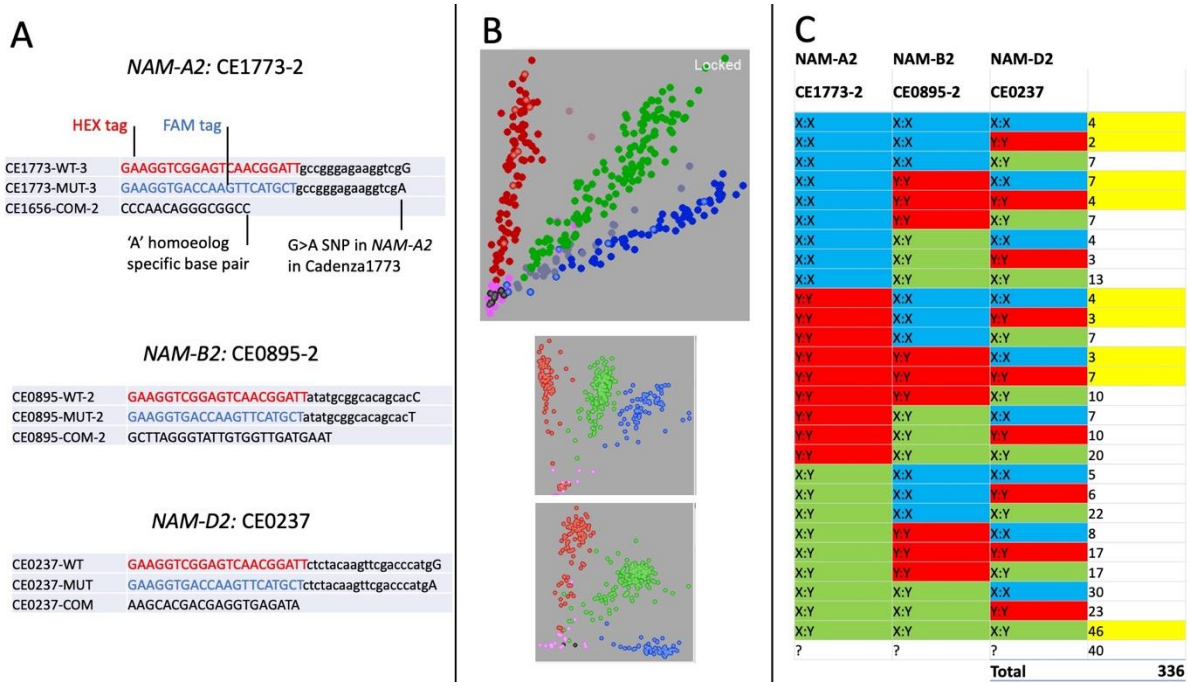


Figure 2.2 Example of KASP genotyping assay for the BC_1F_2 population of cross X61, with 336 plants segregating for NAM-A2, NAM-B2 and NAM-D2 TILLING mutations. A) Structure of KASP primers. In a wild-type sample, the WT primer and the COM primer amplify producing the reverse complement of the HEX tag sequence. This binds the HEX dye and fluorescence is detected. In a homozygous mutant, the MUT and COM primers amplify, leading to FAM fluorescence. B) KASP genotyping output for NAM-A2, NAM-B2 and NAM-D2 (top to bottom). HEX fluorescence on the y-axis and FAM fluorescence on the x-axis. Three clusters were called (Red = wild-type / Y:Y, Green = heterozygous / X:Y, Blue = homozygous / X:X). C) Summary table of number of plants per genotype. Genotypes listed in Figure 2.1 and triple heterozygotes were kept (yellow highlight).

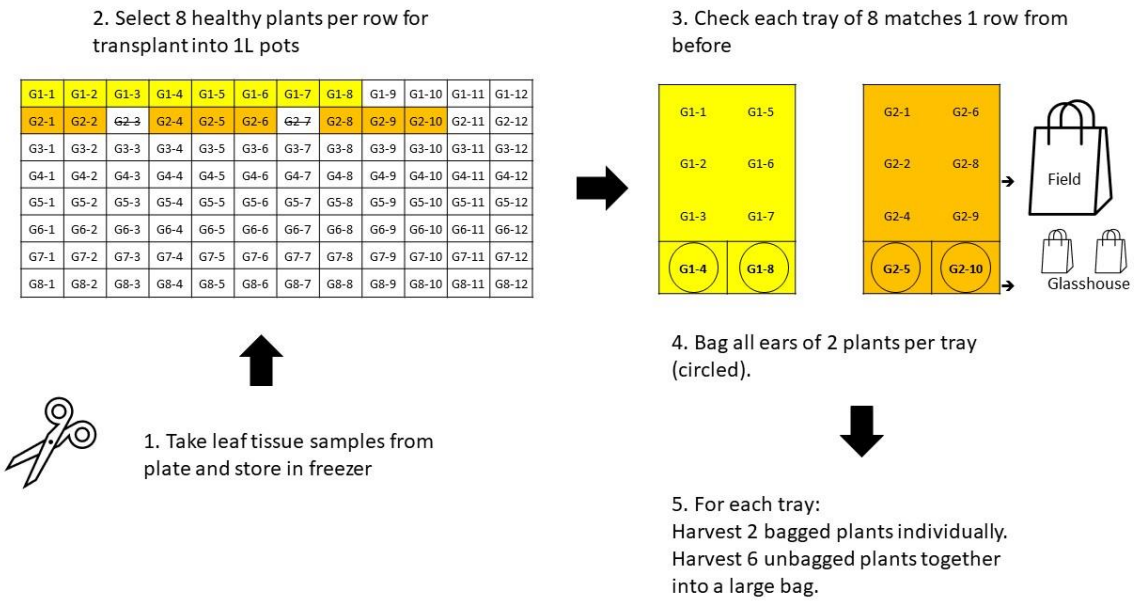


Figure 2.3 Pipeline for seed bulking of NAM-2 homozygous mutant lines. Leaf tissue samples were taken from 2-3 week old seedlings and used for KASP genotyping, which confirmed plant genotypes. Bagged ears from individual plants were harvested for glasshouse experiments, while unbagged ears were bulk harvested for a field trial

2.2.3 Working with TILLING lines

2.2.3.1 DNA extraction

For DNA extraction, 50-100mg samples of leaf tissue from 2–3-week-old wheat seedlings were collected into a deep, round-bottomed 96-well plate (ABGene or Thermofisher). DNA extraction buffer was prepared as follows:

100ml 1M Tris-HCl pH 7.5
100ml 0.5M EDTA pH 8.0
125ml 10% SDS
675ml ddH_2O

500µl DNA extraction buffer at 65°C was added to each well of the 96-well plate. Ball-bearings were added using a bead dispenser (Qiagen). Sealed plates were agitated in a TissueLyser II (Qiagen) for 1 min at 3,000rpm or a Genogrinder 2010

(SPEX) for 2 min at 1750rpm, in two bursts. Plates were spun briefly then incubated at 65°C for 1 hour then room temperature for 15 minutes. After adding 250µl 6M ammonium acetate, plates were shaken and incubated at 4°C for 15 minutes. Plates were spun for 15min at 4,000rpm. In a new plate, 600µl supernatant and 360µl isopropanol at -20°C were mixed and incubated at -20°C for 5 minutes. Plates were spun for 15min at 5,000rpm and the supernatant was discarded. Plates were washed with 500µl 70% ethanol, then spun for 15min at 5,000rpm and the supernatant was discarded. DNA pellets were dried at 65°C for 20min, then resuspended in 100µl ddH_2O.

2.2.3.2 KASP genotyping

For KASP (Kompetitive Allele-Specific PCR, LGC Genomics), DNA was extracted from leaves of 2-3-week-old wheat plants. Each well of a 384-well plate was filled as follows:

2.5µl DNA diluted 1:10
2.425µl PACE genotyping mix
0.075µl Primer mix (12ng/µl WT, 12ng/µl MUT, 30ng/µl COM)

PCR was run with 10 touchdown cycles followed by 30 cycles of two-step PCR (*Table 2.2*). A PheraStar plate reader recorded the fluorescence of 'HEX' and 'FAM' labels. Genotypes were called into up to three clusters: wild-type (high HEX), homozygous (high FAM) and heterozygous (intermediate) using KlusterCaller software.

Table 2.2 PCR conditions for KASP genotyping using PACE genotyping mix

programme	Temperature (°C)	Time	Cycles
pre increase	30	1min	1
	94	15min	
Touchdown	94	20sec	10
	65-57, decreasing 0.8°C per cycle	60sec	
Amplification	94	20sec	30
	57	60sec	
cooling to	30	1min	1

2.2.3.3 Crossing

To cross two wheat plants, an ear ¼ to ½ emerged from the sheath was selected as parent 1, and an ear fully emerged (headed) as parent 2. The ear from parent 1 was emasculated by trimming tips of lemma and glumes, removing all three green anthers from each floret, discarding rudimentary florets, and covering the ear with a bag. 2-3 days later (under speed breeding), each floret was pollinated using anthers from parent 2. Yellow anthers at the base of the floret, which start to burst with fresh pollen, pollinate the most effectively. Crosses were recorded both on a label attached to the ear, and in a notebook.

2.2.4 Plant growth

2.2.4.1 Seed germination

Seeds were germinated in petri dishes on damp filter paper and kept in the dark at 4˚C for 2-3 days then at 25˚C for 2 days. Seedlings were planted in trays of damp compost, with roots beneath the compost and coleoptile above the surface.

2.2.4.2 Plant growth conditions

Wheat plants were grown in several locations and conditions, summarised below (*Table 2.3*).

To compress the generation time for crossing and seed bulking, wheat plants were grown under speed breeding conditions with 22h light and 2h dark, at 22˚C day / 17˚C night (Watson et al. 2018) (*Table 2.3*). Seedlings were transplanted after 2 weeks into individual pots. For speed breeding in a controlled environment room (CER), adult plants were watered with 150ml water per plant 2-3 times per week and fertilised twice with high nitrogen fertiliser, at the tillering stage and just before heading. For speed breeding in the glasshouse, plants were watered by automatic bench flooding, and fertiliser and fungicides were applied according to standard practice (*Table 2.3*). Adult plants were loosely tied to stakes from stem elongation stage to support tillers. Ears were covered with bags at heading (½ to fully emerged from the flag leaf sheath) to ensure self-pollination. Seeds were harvested after 10 weeks and left at 30˚C until dry. Alternatively, water was withheld in late senescence to accelerate seed drying before harvest.

For senescence phenotyping experiments, plants were grown in 16h light and 8h dark in either a glasshouse with supplementary lighting, run at minimum 20˚C day/ 18˚C night; or a CER (Hettich) with homogeneous LED lighting panels set at 300μmol light intensity, with 70% humidity, and 20˚C day/ 15˚C night (*Table 2.3*). Seedlings were transplanted after 3 weeks into individual pots. Plants were watered by automatic bench flooding. Fertiliser and fungicides were applied according to standard practice. Adult plants were supported with stakes and ears were bagged in some experiments. Seeds were harvested at maturity.

Table 2.3 Wheat growth conditions. "Phenotyping" locations were used for senescence phenotyping experiments; "Speed breeding" locations were used for crossing and seed bulking. Light: 16L:8D indicates 16 hours light, 8 hours darkness. Water: automatic flood benching (Auto) or manual watering (Manual).

Purpose	Location	Light	Water	Temperature	Seedlings trays / compost	Adult plants pots / compost	Other
Phenotyping	Glasshouse UoB	16L:8D Supplementary	Auto	20˚C day/ 18˚C night minimum	24 cell trays / 3:1 compost:perlite	11cm pots / 3:1 compost:perlite	Standard practice fertiliser and fungicides
Phenotyping	Glasshouse JIC	16L:8D Supplementary	Auto	20˚C day/ 18˚C night minimum	96 cell trays / John Innes F2 Starter + grit OR John Innes Cereal Mix	1L pots / John Innes Cereal Mix	Standard practice fertiliser and fungicides
Phenotyping	CER JIC	16L:8D LED 300umol light intensity	Auto	20˚C day/ 15˚C night	96 cell trays / John Innes F2 Starter + grit	9cm pots / John Innes Cereal Mix	70% humidity Fungicide against mildew applied 3-4 times
Speed breeding	Speed breeding glasshouse JIC	22L:2D Supplementary	Auto	22˚C day/ 17˚C night minimum	96 cell trays / John Innes F2 Starter + grit	1L pots / John Innes Cereal Mix	Standard practice fertiliser and fungicides
Speed breeding	Speed breeding CER UoB	22L:2D LED	Manual	22˚C day/ 17˚C night	24 cell trays / 3:1 compost:perlite	11cm pots / 3:1 compost:perlite	70% humidity Fertiliser applied twice, no fungicides

2.2.4.3 Threshing

Harvested dry ears were threshed by one of two methods. For crossing and phenotyping, where it was crucial to avoid seed loss, ears were threshed by hand. Ears were rolled in a cricket bat handle to release the seeds. A vacuum pump removed the chaff through a vent in an enclosed workstation. For larger quantities of seed, ears were threshed with a threshing machine (Haldrup).

2.2.5 Phenotyping for glasshouse and CER experiments

2.2.5.1 Phenotyping heading

The period of leaf senescence and grain filling occurs between anthesis (fertilization) and maturity. Heading occurs 2-3 days before anthesis and is used as a proxy for anthesis. Heading was scored for the first tiller of each plant. Heading was assigned to ears just emerged from the flag leaf sheath, while ears with 1-3cm peduncle visible were assigned to the previous day. Ears were covered with bags at heading to ensure self-pollination.

2.2.5.2 Phenotyping senescence with a SPAD meter

Leaf chlorophyll content was assessed with a SPAD spectrometer (SPAD502, Konica Minolta). The SPAD meter was calibrated against a reference plate before starting each experiment. SPAD meter readings were taken on the flag leaf of the first tiller of each plant. The clip was held on eight points on the leaf surface, at the centre and edge of four evenly-space points along the leaf length. The average of the eight measurements was recorded. Multiple measurements per leaf are needed as SPAD values vary along the leaf length, even at heading stage (Yuan et al. 2016). SPAD readings were made at heading, then weekly through senescence, until either a defined time was reached, or SPAD decreased below 10 showing that the leaf was

fully senesced. In some experiments SPAD readings were taken twice weekly in the rapid phase of senescence.

2.2.5.3 Scoring senescence by eye in the glasshouse

Leaf senescence and peduncle senescence were scored for the first tiller of each plant. Leaf senescence was scored on the date of 25% leaf yellowing, where a quarter of the leaf is yellow, or overall leaf colour has moved a quarter of the way from green to yellow. The flag leaf was always scored; in some cases the second leaf below the flag leaf was also scored. Peduncle senescence was scored on the date of 100% peduncle yellowing, where the stem between flag leaf and ear is yellow around the full circumference.

2.2.5.4 Phenotyping other traits

Agronomic traits such as plant height, tiller number and flag leaf length were also measured in phenotyping experiments (*Table 2.4*). Unusual phenotypes and potential confounding factors such as leaf chlorosis, infection, and snapped ears were noted.

Grain mass, grain number, kernel weight and grain dimensions were measured with a Marvin seed analyser (Marvintech) (*Table 2.5*). Grain mass data were presented as g/plant as measured, given that moisture content was only measured in a subset of experiments. Grain protein content and moisture content were measured with a Near Infrared Spectrometer (NIR, Perten DA7250) calibrated with manufacturer-supplied wheat grain data (*Table 2.6*). Protein content was normalised for moisture content.

For some experiments the air temperature at plant canopy height was measured at 15min intervals using an EasyLog (Lascar Electronics). Photographs of plants and leaves were taken by the JIC Photography Platform.

Table 2.4 Full list of variables collected in a typical glasshouse experiment (NAM-2 experiment sown 21/09/2022). In column "Source or method", ID variables provide a unique identifier for each plant. Independent variables are determined by the experimental design. Calculated variables are derived from other variables. For the remaining rows, this column lists the equipment required to measure the trait.

Column	Type	Source or method	Description
Index	integer	ID	Number written at top of label, 905 = Block 9, Position 5
Block	integer	independent variable	Block in randomised complete block design (primary blocking variable)
Position	integer	independent variable	Position within Block (randomised)
Row	integer	independent variable	Row from middle to edge of bench (secondary blocking variable)
Line_name	character	independent variable	Line name of plant material
Plant_num	integer	ID	Number of plant (unique)
Rep		independent variable	Replicate of plant within genotype (1 to 10)
Sample		ID	Line_name-Plant_num, for compatibility with KASP & other data
SPAD_2022-10-28	number (1 dp)	SPAD meter	SPAD score of newest fully expanded leaf of 1st tiller - to quantify chlorosis phenotype in X61
Heading_date	date	Eye	Date of heading - ear fully emerged from flag leaf sheath
SPAD_heading	number (1 dp)	SPAD meter	SPAD score at heading of flag leaf of 1st tiller - average of 8 readings
Leaf_senescence	date	Eye	Date of 25% leaf yellowing (flag leaf of 1st tiller)

Leaf_senescence_2nd	date	Eye	Date of 25% leaf yellowing (2nd leaf down from flag leaf)
Peduncle_senescence	date	Eye	Date of 100% peduncle yellowing
Weekday	integer	Calculated	Numerical day of week of heading (1 = Monday, 7 = Sunday)
Days	integer	Calculated	Days from heading to Date_1
Scoring_day	character	Calculated	Which day to score SPAD for this plant, MON or FRI
Date_1	date	Calculated	Mon/Fri at 5-8 DAH. First day after heading to score SPAD.
SPAD_2022-11-28	number (1 dp)	SPAD meter	SPAD score at 2022-11-28 of flag leaf of 1st tiller - average of 8 readings. Repeated across many dates.
Flag_leaf_length	number (to 5mm)	Ruler	Length of flag leaf of 1st tiller (mm)
Height	number (to 5mm)	Meter rule	Height of 1st tiller at maturity (mm)
Tiller_1	integer	Eye	Number of main tillers at maturity
Tiller_2	integer	Eye	Number of back tillers at maturity. Back tillers are less than ½ height of main tillers, later and have smaller ears.
Snapped_pre_peduncle_sen	TRUE or FALSE	Eye	Was first tiller snapped before 100% peduncle senescence?
Comment	character	Eye	Anything unusual worth noting
Photo	character	Camera	Each letter marks a set of plants with matching heading date & ideally healthy, to be photographed together

Table 2.5 Grain traits measured by Marvin seed analyser (Marvintech).

Column	Type	Source or method	Description
Seed_num	integer	Marvin	Number of seeds
Weight	number	Marvin	Total grain weight (g)
TGW	number	Marvin	Thousand grain weight, = Weight / Seed_num * 1000 (g)
O_area	number	Marvin	Average (probably mean) area per seed (mm^2)
O_width	number	Marvin	Average (probably mean) width per seed (mm)
O_length	number	Marvin	Average (probably mean) length per seed (mm)
Date_Marvin	date	Marvin	Date of Marvin measurement
Machine	text	Marvin	Name of Marvin machine used

Table 2.6 Grain traits measured by Near Infrared Spectrometer (Perten DA7250).

Column	Type	Source or method	Description
Date_NIR	date	NIR	Date of NIR measurement
Predicted Protein Dry basis %	percent	NIR	Predicted Protein Dry basis (%)
Predicted Moisture Content %	percent	NIR	Predicted Moisture Content (%)

Sample Tray	text	NIR	Small Plastic Cup, rotating: default for 15-25g seed

2.2.6 Phenotyping for field experiments

2.2.6.1 Phenotyping heading

To score heading in field plots, the date of heading was set when ears had fully emerged from the flag leaf in 50% of the plot.

2.2.6.2 Phenotyping senescence

Leaf senescence was scored as percentage of leaf area yellow or brown for visible leaves in each plot, in 5% intervals (*Figure 2.4*). This score reflects yellowing of flag leaves, and to a lesser extent lower leaves. Ear senescence was scored as percentage ear yellowing, in 10% intervals (*Figure 2.5*). Leaf and ear senescence were scored twice weekly until either a defined time was reached, or senescence reached 100%. Peduncle senescence was scored by taking 10 peduncles at random from the centre of the plot and counting the number of completely yellow peduncles.

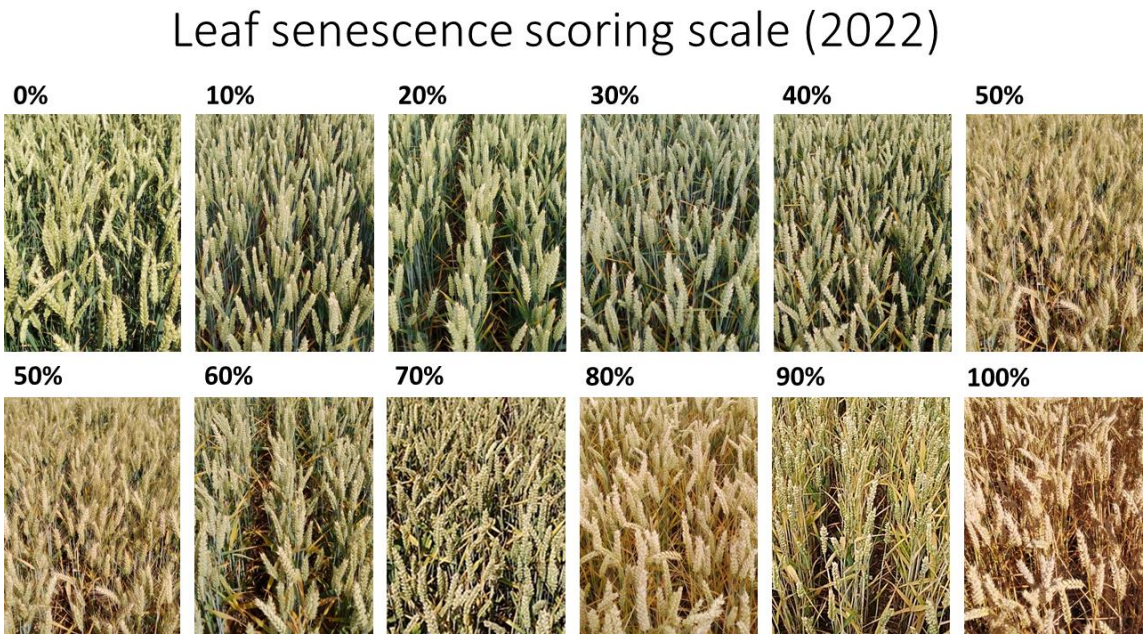


Figure 2.4 Leaf senescence scoring scale for field trials. Examples of percentage leaf yellowing in 10% intervals from 0% to 100% taken from wheat breeding lines scored in 2022 (not otherwise shown). Leaf senescence was scored in 5% intervals. Images cropped to show centre of 6m field plots.

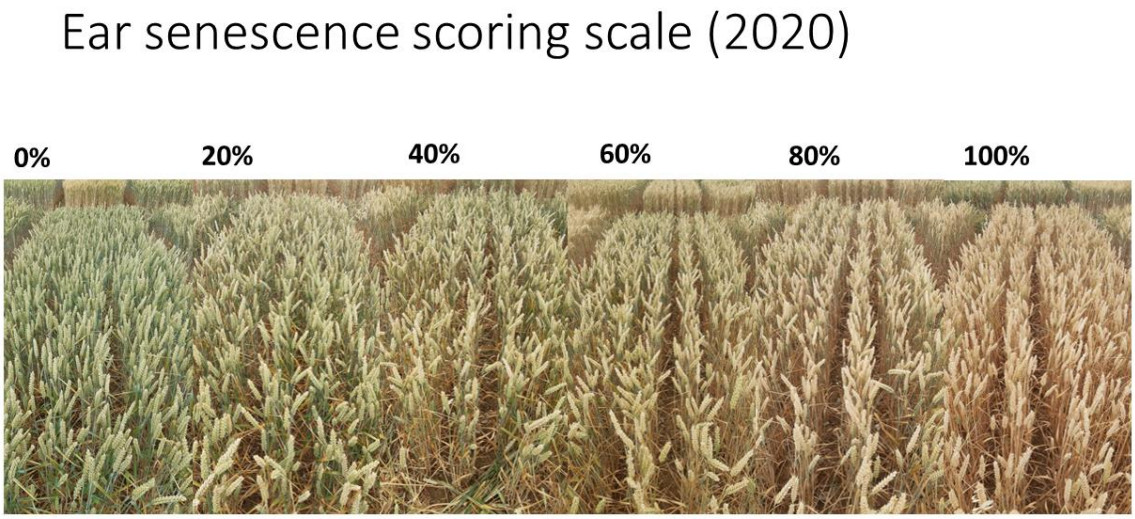


Figure 2.5 Ear senescence scoring scale for field trials, Examples of percentage ear yellowing in 20% intervals from 0% to 100% taken from wheat breeding lines scored in 2020 (not otherwise shown). Ear senescence was scored in 10% intervals. Images show 6m field plots.

2.2.7 Data analysis

Unless stated otherwise, data analysis was carried out in R software. Most graphs were plotted with ggplot2, and other packages were used for data analysis (*Table 2.7*). R Studio was used as a graphical interface, and Git was used for version control. All scripts are available on Github (Evans 2023).

Table 2.7 R packages used for data analysis, with a brief description of the main application of each package in this thesis.

R package	Version	Uses of R package in this thesis
agricolae	1.3-5	Prepare randomized complete block designs
arm	1.12-2	display() function used with ANOVA
base	4.0.4	The R Base Package
car	3.0-12	ANOVA
emmeans	1.7.0	Post-hoc tests, e.g. Tukey test, and estimated means
GGally	2.1.2	Plot correlation plots
ggplot2	3.3.5	Plot graphs
ggpubr	0.4.0	Arrange multi-panel figures and run Wilcoxon tests
lubridate	1.8.0	Handle date and datetime variables
MESS	0.5.7	auc() function for area under curve
multcomp	1.4-20	cld() function for compact letter display
RColorBrewer	1.1-2	Colour palettes for figures
readr	2.0.2	Read in data
readxl	1.3.1	Read in data
stringr	1.4.0	Handle text
svglite	2.1.0	Save figures in .svg format
tidyverse	1.3.1	Manipulate data tables

2.2.7.1 Calculating senescence metrics in the field

To present condensed, biologically meaningful indicators of senescence for field experiments, senescence metrics were calculated from time-courses of percentage leaf and ear senescence. Metrics for percentage senescence are adapted from (Chapman et al. 2021a).

To account for both differences in heading date between plots and differences in temperature over time and between trials, senescence scoring dates were converted to thermal time after heading. Thermal time is often used as a scale for wheat development, as wheat progresses through development more rapidly at higher temperatures (AHDB 2023c). Percentage leaf and ear senescence data were rearranged into a long format table with one row per percentage senescence score. Mean daily temperature was calculated as an average across 24 hours from 00:00, using hourly weather station temperature readings. For the *NAM-2* field trial at Church Farm, Bawburgh, Norfolk, the weather station was onsite. For field trials at RAGT Seeds Ltd., Ickleton, Essex, data from a weather station 18.3 miles distant at Andrewsfield, Essex was used (Met Office 2023). Thermal time (°C days) after heading (ear emergence) was calculated as cumulative mean daily temperature from 1 day after heading to scoring date for each plot.

Thermal time to reach a specific leaf senescence score (10%, 30%, 50%, 70% and 90%) was calculated by linear interpolation using stats::approx(), equivalent to drawing straight lines between successive leaf senescence scores.Duration of leaf senescence was defined as thermal time from 10% leaf senescence to 90% leaf senescence (*Figure 2.6*). Rate of leaf senescence was also calculated as the gradient between 10% and 90% leaf senescence, but in analysis, duration rather than rate was used as it conformed better to linear model assumptions. Thermal time

to 30% leaf senescence was used as the definition for onset of leaf senescence. While previously, 10% leaf senescence has been used as a threshold for senescence onset, 30% was selected here for closer comparison with glasshouse data (Chapman et al. 2021a). Area under curve (AUC) of leaf senescence was calculated with MESS::auc(), and defined as the area bounded by the leaf senescence “curve” formed by linear interpolation, the horizontal line y=0, and the vertical line x = auc_limit, where auc_limit is the minimum thermal time after heading of the last senescence score (*Figure 2.6*). Scripts for calculation of senescence metrics are available on Github (Evans 2023).

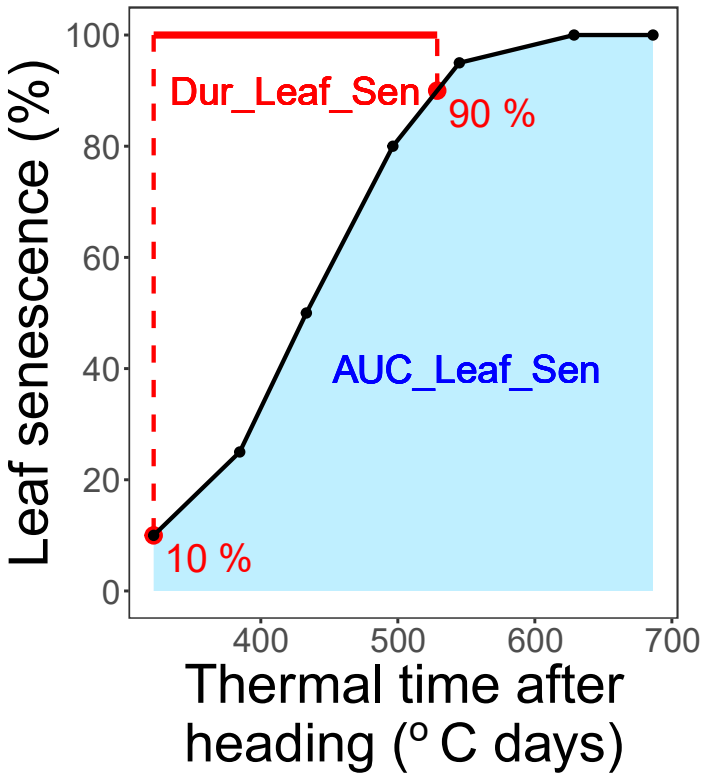


Figure 2.6 Graphical representation of senescence metrics for field data. The x-axis is shown in Thermal time after heading. The leaf senescence time-course was inferred by linear interpolation between senescence scores (black dots connected by black lines). Duration of leaf senescence (Dur_Leaf_Sen) is the Thermal time between reaching 10% and 90% leaf senescence (red horizontal line). Area under curve (AUC) of leaf senescence (AUC_Leaf_Sen) is the area below the leaf senescence time-course (blue shading).

2.2.7.2 Calculating senescence metrics in the glasshouse

To present condensed indicators of senescence for glasshouse and CER experiments, senescence metrics were calculated using time-courses of SPAD measurements, using methods adapted from those used for field data.

To account for differences in heading date between plots, SPAD scoring dates were converted to days after heading. Time in days after heading was calculated as the number of days from heading to scoring date for each plant.

Days from heading to a specific SPAD value (40, 30, 10) was calculated by linear interpolation using stats::approx(). Onset of leaf senescence was defined as days to a SPAD value of 30. Duration of leaf senescence was defined as days from SPAD of 40 to SPAD of 10. Area under curve (AUC) of leaf senescence was calculated with MESS::auc(), and defined as the area bounded by the SPAD “curve” formed by linear interpolation, the horizontal line y=0, and the vertical line x = Heading_date. Days from heading was used instead of thermal time, because temperature data was not available for every glasshouse experiment, and temperatures were expected to be more uniform in the glasshouse.

Caution: while in field data a high AUC denotes early senescence, in glasshouse data a high AUC denotes late senescence. Scripts for calculation of senescence metrics are available on Github (Evans 2023).

2.2.7.3 Statistical analysis

For statistical analysis of phenotyping experiments, most phenotypic traits were analysed in R software using a linear model with the base formula:

lm(Trait ~ Block + Genotype)

In some experiments, secondary blocking factors were also included as fixed effects. This is noted in Experimental Design sections and where relevant, the rationale for adjusting the analysis model is explained in Results sections. A type II analysis of variance (ANOVA) was carried out using this model and the package car. Post-hoc pairwise comparisons were implemented using the Tukey method and packages emmeans and multcomp, with a threshold of $p<0.05$. As raw SPAD values are not normally distributed, SPAD values were compared by a non-parametric Wilcoxon

test with a threshold of $p<0.05$. Scripts used for statistical analysis are available on Github (Evans 2023).

Boxplots were generated in ggplot2, with summary statistics derived from function boxplot.stats(). In each boxplot, a horizontal line shows the median, a filled box shows 25% and 75% quantiles, and whiskers extend to the most extreme datapoint which is no more than 1.5 * interquartile range (= range contained within filled box) away from the box. Boxplots are overlaid with all individual datapoints. On some boxplots, only outlier points are shown (more than 1.5* interquartile range away from the box).

2.2.8 Experimental Design

2.2.8.1 Summary of experimental design

The dates, location of plants grown and number of replicates for each experiment in this chapter are detailed below (*Table 2.8*). SPAD readings were taken for glasshouse experiments, while leaf yellowing was scored visually for field experiments (*Table 2.8*). Grain mass, grain number and protein content were measured in only some experiments due to constraints on time (*Table 2.8*). Further detail follows on the design of each experiment.

Table 2.8 Summary of experimental design in this chapter. *Sowing dates are used as unique identifiers for each experiment. Growth conditions and measurements which differed between experiments are included. Location corresponds to Table 2.3. All experiments were laid out in a randomized complete block design (RCBD).*

Experiment sowing date	**Harvest date**	**Plant material**	**Location**	**Experimental layout**	**Type of senescence phenotyping**	**Timing of senescence phenotyping**	**Grain mass and number measured**	**GPC measured**
21/09/2022	19/01/2023	*NAM-2* Cadenza TILLING	Glasshouse JIC	RCBD plus 10 reps per genotype	SPAD meter	At Heading; Weekly 5-8DAH to SPAD=0; twice weekly in rapid phase of senescence	Yes	Yes
15/02/2023	13/06/2023	*NAM-2* Cadenza TILLING	Glasshouse JIC	RCBD plus 10 reps per genotype	SPAD meter	At Heading; Weekly 5-8DAH to SPAD=0; twice weekly in rapid phase of senescence	Yes	Yes
12/10/2022	21/08/2023	*NAM-2* Cadenza TILLING	Field, Church Farm	RCBD 4* 1m plots per genotype	Visual scoring of leaf senescence	Twice weekly from 14 days after earliest heading to 100% senescence	No	No

2.2.8.2 NAM-2 Glasshouse experiments (21/09/2022 and 15/02/2023)

To test the effect of mutations in *NAM-2* on senescence, *NAM-2* TILLING lines were grown in the glasshouse in two experiments sown on 21/09/2022 and 15/02/2023. Both experiments used two sets of single, double, and triple mutants and controls derived from the segregating populations of cross X50 and cross X61 (*Table 2.9*, Methods 2.2.2.3). Bulked seed from the BC_1F_4 or BC_1F_5 generation was used. For both experiments, genotypes of all plants were confirmed by KASP genotyping (Methods 2.2.2.2).

Plants were arranged in two randomized complete block designs with 10 blocks of 8 genotypes, one for each of X50 and X61. Blocks were shuffled along the length of the bench every two weeks for more even light exposure. Rows across the depth of the bench were added as a second blocking variable by setting the first 8 blocks into a “Latin Square” design, with an equal number of plants per row as well as per block for each genotype. Marvin and NIR measurements were carried out by Jack Eagle and Rosa Whittingham.

Table 2.9 Plant material for NAM-2 glasshouse experiments 21/09/2022 and 15/02/2023. Cross ID refers to Table 2.15. Generation: BC = number of backcrosses, F = generations since last cross. Genotype: capitals indicate wild-type allele, small letters indicate TILLING mutant allele. Genotype 7 (aabbDD) was unavailable from cross X50, so seed carrying the same mutations from cross X54 was used instead.

Gene name	Line name	Cross	Generation	Genotype	Plants per line
NAM-2	NAM2-X50-G1	X50	BC_1F_4	AABBDD	10
NAM-2	NAM2-X50-G2	X50	BC_1F_5	AABBdd	10
NAM-2	NAM2-X50-G3	X50	BC_1F_5	AAbbDD	10

NAM-2	NAM2-X50-G4	X50	BC_1F_5	Aabbdd	10
NAM-2	NAM2-X50-G5	X50	BC_1F_5	aaBBDD	10
NAM-2	NAM2-X50-G6	X50	BC_1F_5	aaBBdd	10
NAM-2	NAM2-X54-G7	X54	BC_1F_5	aabbDD	10
NAM-2	NAM2-X50-G8	X50	BC_1F_4	aabbdd	10
NAM-2	NAM2-X61-G1	X61	BC_1F_5	AABBDD	10
NAM-2	NAM2-X61-G2	X61	BC_1F_5	AABBdd	10
NAM-2	NAM2-X61-G3	X61	BC_1F_5	AabbDD	10
NAM-2	NAM2-X61-G4	X61	BC_1F_5	Aabbdd	10
NAM-2	NAM2-X61-G5	X61	BC_1F_5	aaBBDD	10
NAM-2	NAM2-X61-G6	X61	BC_1F_5	aaBBdd	10
NAM-2	NAM2-X61-G7	X61	BC_1F_5	aabbDD	10
NAM-2	NAM2-X61-G8	X61	BC_1F_5	aabbdd	10

Data was analysed separately for each of the two experiments using the following formula:

lm(Trait ~ Row + Block + Cross*Genotype)

For GPC, seed from two individuals was pooled for each measurement, selected at random, in order to exceed 15g seed in all measurements. GPC was analysed using the following formula:

lm(Trait ~ Cross*Genotype)

To calculate “Protein mass per thousand grain” for these pooled measurements the following formula was used. “i” and “j” represent two plants, $GPC_{(i+j)}$ was a pooled measurement of the seeds of both plants.

$$\text{Protein mass per thousand grain} = GPC_{(i+j)} * (Grain_mass_i + Grain_mass_j) / (Grain_number_i + Grain_number_j) * 1000/100$$

2.2.8.3 NAM-2 Field trial

To test the effect of mutations in *NAM-2* under field conditions, *NAM-2* TILLING lines from crosses X50 and X61 (in a Cadenza background) as well as non-mutagenized Cadenza were grown in 1m*1.3m plots in a field trial at JIC Church Farm, Bawburgh, Norfolk, in 2023 (*Table 2.10*). Bulked, non-bagged grain was dressed with Redigo Pro and equally distributed between drilling cups by volume. Plots were arranged in a randomized complete block design surrounded by guard plots (*Figure 2.7*). Plots were drilled on 12/10/22 and harvested on 21/08/23. Plots were treated with a total of 218kg/ha N, 50kg/ha SO_3, 75kg/ha K_2O, and 92kg/ha P_2O between 20/02/23 and 19/04/23, with herbicide, insecticide and fungicide treatments throughout the growing season. Plots were drilled, treated and harvested by the JIC Field Experimentation team.

Table 2.10 Plant material for NAM-2 Field trial. Cross ID refers to Table 2.15. Generation: BC = number of backcrosses, F = generations since last cross. Genotype: capitals indicate wild-type allele, small letters indicate TILLING mutant allele. Genotype 7 (aabbDD) was unavailable from cross X50, so seed carrying the same mutations from cross X54 was used instead.

Gene name	Line name	Cross	Generation	Genotype	Field plots per line
	Cadenza			AABBDD	8
NAM-2	NAM2-X50-G1	X50	BC_1F_4	AABBDD	4
NAM-2	NAM2-X50-G2	X50	BC_1F_5	AABBdd	4

NAM-2	NAM2-X50-G3	X50	BC_1F_5	AAbbDD	4
NAM-2	NAM2-X50-G4	X50	BC_1F_5	AAbbdd	4
NAM-2	NAM2-X50-G5	X50	BC_1F_5	aaBBDD	4
NAM-2	NAM2-X50-G6	X50	BC_1F_5	aaBBdd	4
NAM-2	NAM2-X54-G7	X54	BC_1F_5	aabbDD	4
NAM-2	NAM2-X50-G8	X50	BC_1F_4	aabbdd	4
NAM-2	NAM2-X61-G1	X61	BC_1F_5	AABBDD	4
NAM-2	NAM2-X61-G2	X61	BC_1F_5	AABBdd	4
NAM-2	NAM2-X61-G3	X61	BC_1F_5	AAbbDD	4
NAM-2	NAM2-X61-G4	X61	BC_1F_5	AAbbdd	4
NAM-2	NAM2-X61-G5	X61	BC_1F_5	aaBBDD	4
NAM-2	NAM2-X61-G6	X61	BC_1F_5	aaBBdd	4
NAM-2	NAM2-X61-G7	X61	BC_1F_5	aabbDD	4
NAM-2	NAM2-X61-G8	X61	BC_1F_5	aabbdd	4

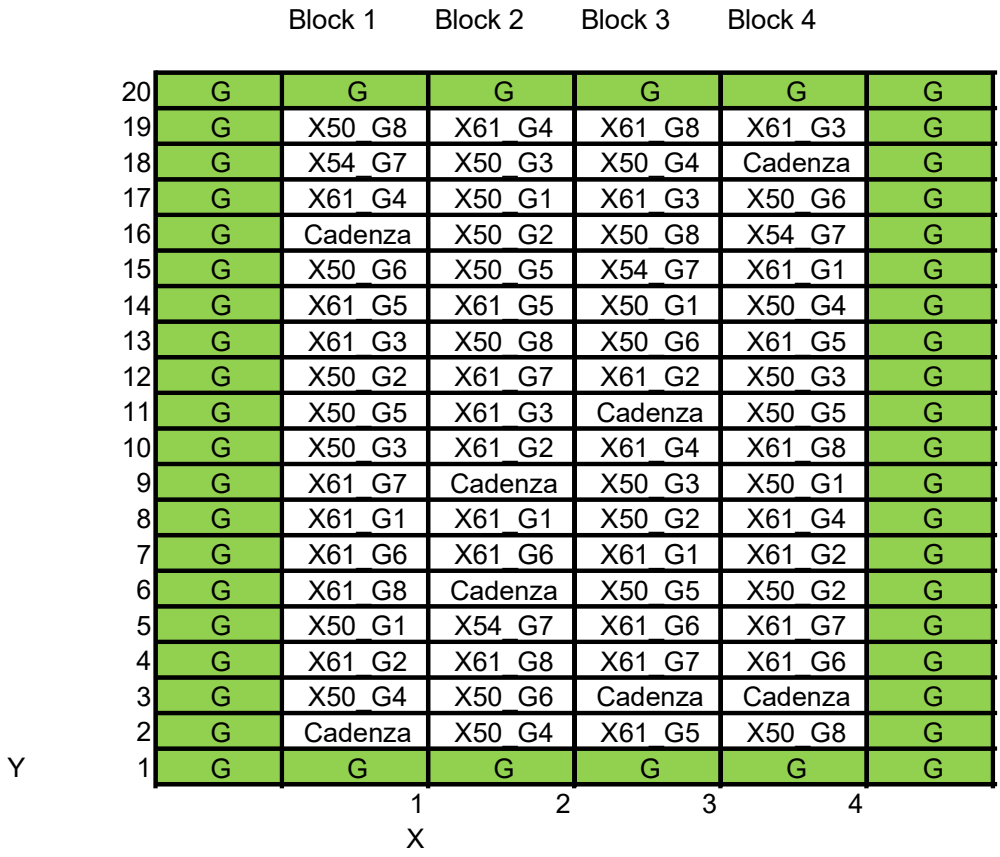


Figure 2.7 Experimental layout for NAM-2 Field trial. 1m^2 trial plots were laid out in a RCBD with each magazine/column as a block, containing two plots of Cadenza and one plot of each other genotype. The entire trial was surrounded by guard plots (Soissons) to avoid edge effects.

In the *NAM-2* field experiment, leaf senescence was scored twice weekly from 14 days after the earliest heading, and peduncle senescence was also scored on five occasions (Table 2.11). Vigour, Cover, Height and Septoria were also scored as simple ways to record additional phenotypic differences observed between plots in the trial (Table 2.11). Field data were analysed with the following formula:

lm(Trait ~ Cross*Genotype)

Table 2.11 Full list of variables collected in NAM-2 field experiment (12/10/2022). EE = ear emergence (heading). In column "Source or method", ID variables provide a unique identifier for each plant. Independent variables are determined by the experimental design. Calculated variables are derived from other variables. For the remaining rows, this column lists the equipment required to measure the trait.

Column	Type	Source or method	Description
Index	integer	ID	Number written at top of label.
Block	integer	independent variable	Block in randomised complete block design (primary blocking variable)
Line_name	character	independent variable	Line name of plant material
X	integer	independent variable	X-axis position of plot
Y	integer	independent variable	Y-axis position of plot
Vigour.2022-11-10	factor	Eye	Vigour on 10th November. Good = many large seedlings, similar to Guard plots. OK = several medium seedlings. Poor = few small seedlings, empty gaps in plot
Cover.2023-03-06	percentage	Eye	Percentage of 1m2 plot covered with plants on 6th March. 100% = as much cover as guard plots
EE	date	Eye	Ear fully emerged from flag leaf on half of plants in plot
Height.2023-05-05	number (to 1cm)	Meter rule	Average height across plot (cm) on 5th May.
Septoria	factor	Eye	0 = no septoria; 1 = hard to spot; 2 = obvious on lower leaves but absent/rare on flag leaves; 3 = obvious on lower leaves and flag leaves. NB: this is not an official scoring scale.
Leaf_senescence	percentage	Eye	Percentage leaf area senesced (yellow/brown) vs not senesced (green), an average of visible leaves in plot.
Peduncle_senescence	integer	Eye	Take 10 peduncles (stem below ear) at random from near centre of plot. Count

			number of senesced (yellow / brown) peduncles.
Comment	character	Eye	Anything unusual worth noting

2.3 Results

2.3.1 Expression pattern of *NAM-2* during flag leaf senescence

The expression pattern of *NAM-2* during early flag leaf senescence was assessed using published RNA-seq data (Borrill et al. 2019). *NAM-A2, NAM-B2* and *NAM-D2* expression gradually increases from 3DAA (Days After Anthesis) to 26DAA (Figure 2.8A). *NAM-A1* and *NAM-D1*, the paralogs of *NAM-2,* also increase in expression in early senescence, with a rapid increase from 3DAA to 15DAA followed by a plateau in expression, with *NAM-A1* decreasing in expression from 21DAA to 26DAA (Figure 2.8B). *NAM-A2* and *NAM-B2* reach a maximal expression level of around 10tpm, higher than *NAM-D2* but lower than *NAM-1* (Figure 2.8A, B).

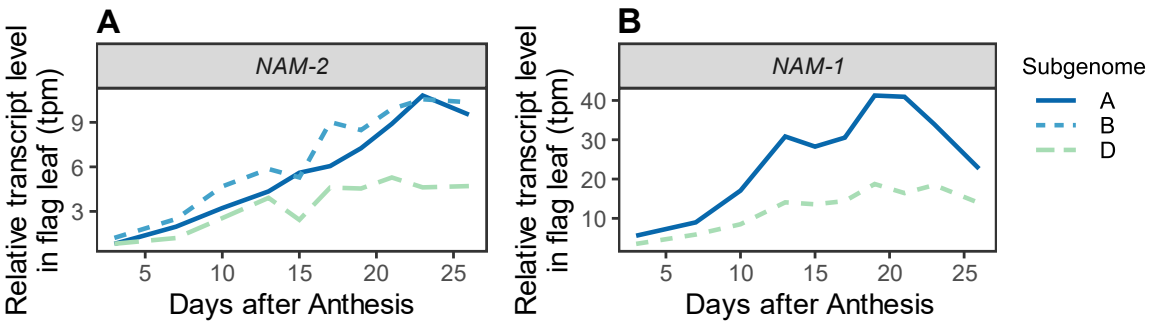


Figure 2.8 NAM-2 is upregulated in wheat flag leaves in a time-course of early senescence. Expression level in transcripts per million (tpm) in flag leaves from 3DAA to 26DAA. (A) NAM-2; (B) NAM-1. Re-analysed from (Borrill et al. 2019).

2.3.2 Development of *NAM-2* TILLING lines

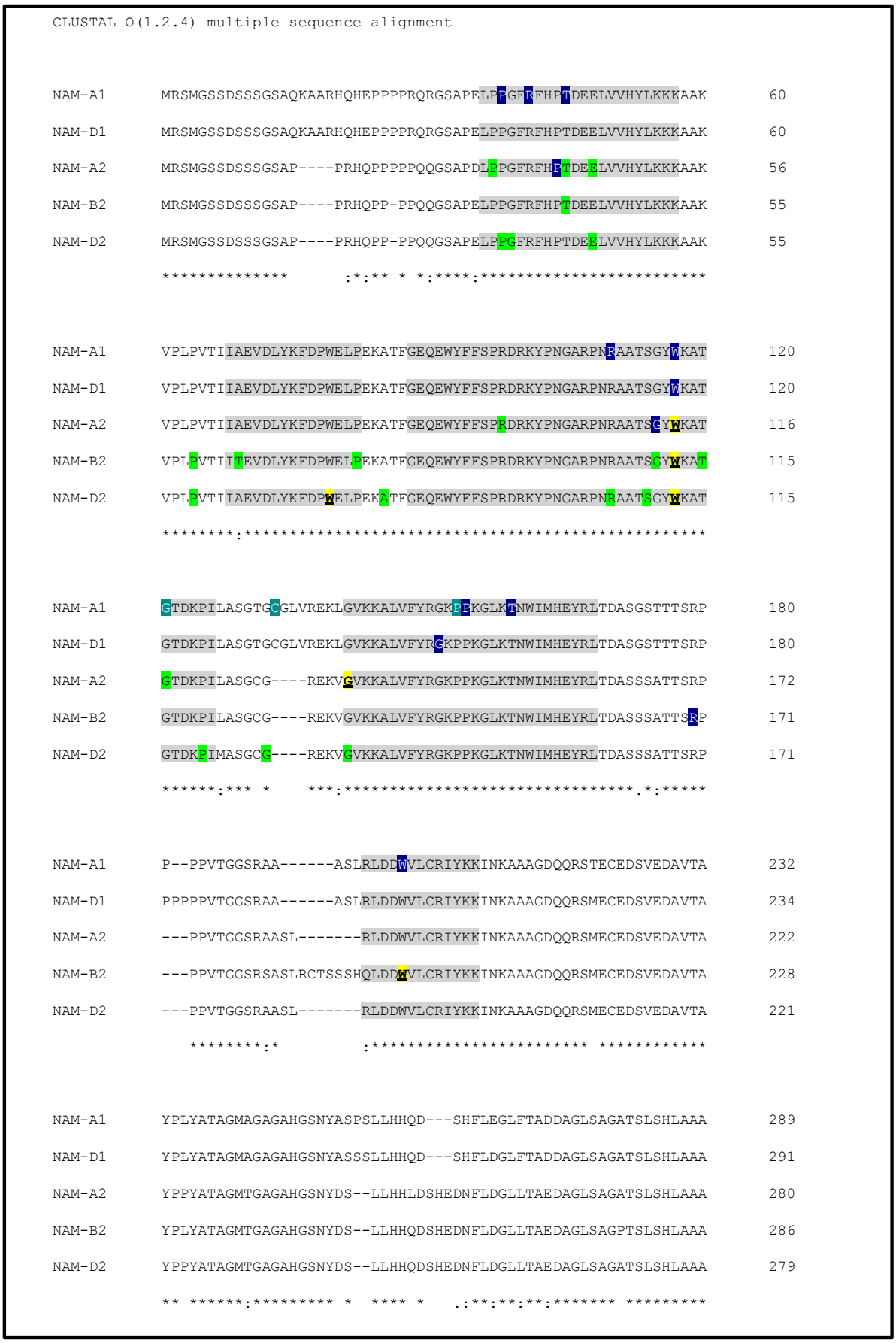
2.3.2.1 Selection of TILLING mutations in *NAM-2*

To generate wheat with loss-of-function of *NAM-2*, single nucleotide polymorphisms (SNPs) in *NAM-A2*, *NAM-B2* and *NAM-D2* were selected from the hexaploid wheat Cadenza TILLING (Targeting Induced Local Lesions In Genomes) population (Methods 2.2.2) (McCallum et al. 2000; Krasileva et al. 2017). Hexaploid Cadenza was selected in order to investigate all three homoeologs of *NAM-2,* and for the capability to run a field trial in the UK climate.

A G>A mutation converting a tryptophan residue to a stop codon (TGG>TGA) in NAC subdomain iii was selected from the Cadenza TILLING population for *NAM-A2*, *NAM-B2* and *NAM-D2* (*Table 2.12*). Alignment of all homoeologs of *NAM-1* and *NAM-2* with Clustal Omega 1.2.2 confirmed that these stop codon mutations are at the same position as each other, and as previously studied stop codon mutations in *NAM-A1, NAM-D1* and *NAM-B2* (, *Table 2.13*). In *NAM-A1* and *NAM-D1*, this stop codon in subdomain iii led to a delay in leaf senescence, supporting the hypothesis that this stop codon would disrupt *NAM-2* protein function (Distelfeld et al. 2012; Avni et al. 2014). In *NAM-B2,* this stop codon mutation did not affect leaf senescence in a wild-type background, and led to a borderline non-significant delay in leaf senescence in a *nam-a1* background (Distelfeld et al. 2012).

In *NAM-A2*, a missense mutation between subdomains iii and iv was selected (*Table 2.12*). Despite being outside the conserved subdomains, this mutation was selected because it had a highly negative PSSM score of -6, and in tetraploid Kronos, an identical mutation in *NAM-A2* led to a delay in peduncle senescence (*Table 2.13*) (Borrill et al. 2019). In *NAM-B2*, a stop codon mutation in subdomain v was selected

(*Table 2.12*). Alignment confirmed that a stop codon in the same position in *NAM-A1* was previously studied, and led to a delay in leaf senescence (Avni et al. 2014) (*Table 2.13*). In *NAM-D2*, a stop codon mutation in subdomain ii was selected (*Table 2.12*).


CLUSTAL O(1.2.4) multiple sequence alignment
NAM-A1 MRSMGSSDSSSGSAQKAARHQHEPPPPRQRGSAPELPEGFRFHPTDEELVVHYLKKKAAK 60
NAM-D1 MRSMGSSDSSSGSAQKAARHQHEPPPPRQRGSAPELPPGFRFHPTDEELVVHYLKKKAAK 60
NAM-A2 MRSMGSSDSSSGSAP----PRHQPPPPPQQGSAPDLPPGFRFHPTDEELVVHYLKKKAAK 56
NAM-B2 MRSMGSSDSSSGSAP----PRHQPP-PPQQGSAPELPPGFRFHPTDEELVVHYLKKKAAK 55
NAM-D2 MRSMGSSDSSSGSAP----PRHQPP-PPQQGSAPELPPGFRFHPTDEELVVHYLKKKAAK 55
NAM-A1 VPLPVTIIAEVDLYKFDPWELPEKATFGEQEWYFFSPRDRKYPNGARPNRAATSGYWKAT 120
NAM-D1 VPLPVTIIAEVDLYKFDPWELPEKATFGEQEWYFFSPRDRKYPNGARPNRAATSGYWKAT 120
NAM-A2 VPLPVTIIAEVDLYKFDPWELPEKATFGEQEWYFFSPRDRKYPNGARPNRAATSGYWKAT 116
NAM-B2 VPLPVTIITEVDLYKFDPWELPEKATFGEQEWYFFSPRDRKYPNGARPNRAATSGYWKAT 115
NAM-D2 VPLPVTIIAEVDLYKFDPWELPEKATFGEQEWYFFSPRDRKYPNGARPNRAATSGYWKAT 115
NAM-A1 GTDKPILASGTGCGLVREKLGVKKALVFYRGKPPKGLKTNWIMHEYRLTDASGSTTTSRP 180
NAM-D1 GTDKPILASGTGCGLVREKLGVKKALVFYRGKPPKGLKTNWIMHEYRLTDASGSTTTSRP 180
NAM-A2 GTDKPILASGCG----REKVGVKKALVFYRGKPPKGLKTNWIMHEYRLTDASSATTSRP 172
NAM-B2 GTDKPILASGCG----REKVGVKKALVFYRGKPPKGLKTNWIMHEYRLTDASSATTSRP 171
NAM-D2 GTDKPIMASGCG----REKVGVKKALVFYRGKPPKGLKTNWIMHEYRLTDASSATTSRP 171
NAM-A1 P--PPVTGGSRAA------ASLRLDDWVLCRIYKKINKAAAGDQQRSTECEDSVEDAVTA 232
NAM-D1 PPPPPVTGGSRAA------ASLRLDDWVLCRIYKKINKAAAGDQQRSMECEDSVEDAVTA 234
NAM-A2 ---PPVTGGSRAASL-------RLDDWVLCRIYKKINKAAAGDQQRSMECEDSVEDAVTA 222
NAM-B2 ---PPVTGGSRSASLRCTSSSHQLDDWVLCRIYKKINKAAAGDQQRSMECEDSVEDAVTA 228
NAM-D2 ---PPVTGGSRAASL-------RLDDWVLCRIYKKINKAAAGDQQRSMECEDSVEDAVTA 221
NAM-A1 YPLYATAGMAGAGAHGSNYASPSLLHHQD---SHFLEGLFTADDAGLSAGATSLSHLAAA 289
NAM-D1 YPLYATAGMAGAGAHGSNYASSSLLHHQD---SHFLDGLFTADDAGLSAGATSLSHLAAA 291
NAM-A2 YPPYATAGMTGAGAHGSNYDS--LLHHLDSHEDNFLDGLLTAEDAGLSAGATSLSHLAAA 280
NAM-B2 YPLYATAGMTGAGAHGSNYDS--LLHHQDSHEDNFLDGLLTAEDAGLSAGPTSLSHLAAA 286
NAM-D2 YPPYATAGMTGAGAHGSNYDS--LLHHQDSHEDNFLDGLLTAEDAGLSAGATSLSHLAAA 279

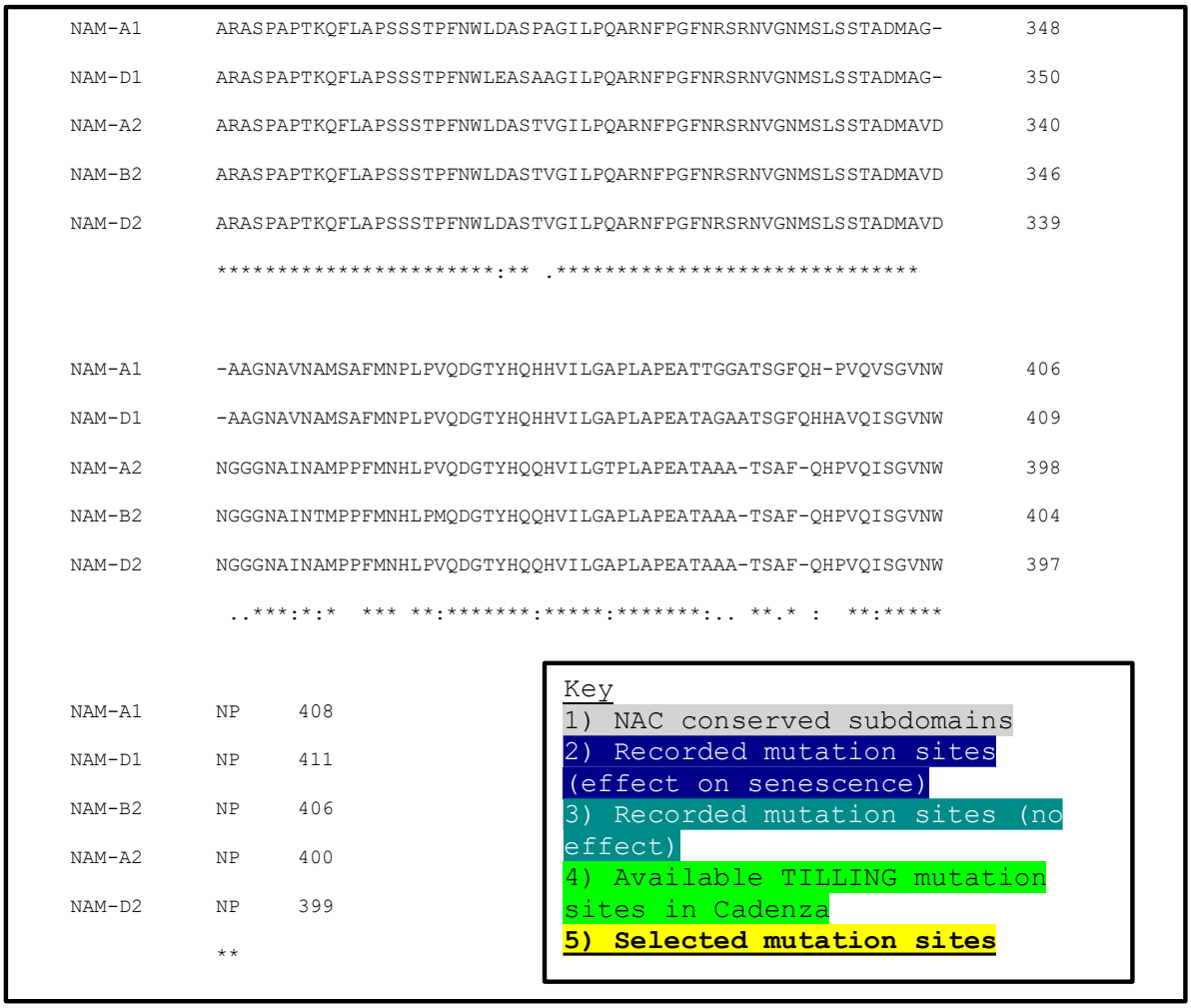


Figure 2.9 Multiple alignment of NAM-1 and NAM-2 used to select TILLING mutations in NAM-2. Multiple alignment of peptide sequences (using first of two potential start codons) was carried out in Clustal Omega. "" marks amino acid identity. "." and ":" mark amino acids with similar chemical properties. NAM-B1 is not shown because there is not a functional gene copy in the reference genome. Annotations: 1) NAC conserved subdomains based on NAM-A1 in (Uauy et al. 2006); 2) Recorded mutation sites with an effect on senescence in at least one experiment from Table 2.13; 3) Recorded mutation sites with no effect on senescence, or not tested; 4) Mutation sites in NAM-2 in the Cadenza TILLING population; 5) Mutation sites in NAM-2 selected in this thesis.*

Table 2.12 TILLING mutations selected in NAM-A2, NAM-B2 and NAM-D2. Gene ID from IWGSC RefSeq v1.1. Consequence = effect on the amino acid sequence. PSSM score = indicates the likelihood of a missense SNP in this position of the NAC domain across all NAC TFs.

Gene	Gene ID	Variant ID	Alleles	Conse-quence	Amino acids	Amino acid position	Subdomain	PSSM score
NAM-A2	TraesCS2A02G201800	Cadenza1656. Chr2A.175468143	G/A	stop gained	W/*	113	iii	
NAM-A2	TraesCS2A02G201800	Cadenza1773. Chr2A.175468202	G/A	missense variant	G/D	133		-6
NAM-B2	TraesCS2B02G228900	Cadenza1436. Chr2B.223154643	G/A	stop gained	W/*	112	iii	
NAM-B2	TraesCS2B02G228900	Cadenza0895. Chr2B.223154988	G/A	stop gained	W/*	195	v	
NAM-D2	TraesCS2D02G214100	Cadenza0237. Chr2D.175331412	G/A	stop gained	W/*	74	ii	
NAM-D2	TraesCS2D02G214100	Cadenza0231. Chr2D.175331721	G/A	stop gained	W/*	112	iii	

*Table 2.13 Impact on senescence of published induced mutations in NAM-1 and NAM-2. TILLING line from [1] (Slade et al. 2005) [2] (Krasileva et al. 2017) [3] described in (Chapman et al. 2021b). Amino acid change shows original amino acid / new amino acid, * represents stop codon. AA position in original peptide may not match up between genes, and is based on the first of two potential start codons. Sub-domain shows conserved subdomain of NAC domain (where blank, residues are not in a conserved subdomain). Reference shows first author of paper presenting this mutation (Distelfeld et al. 2012; Borrill et al. 2019; Harrington et al. 2019b; Avni et al. 2014; Chapman et al. 2021b). Whether this mutation in NAM-1 or NAM-2 led to a delayed senescence phenotype is described. n.s. = non-significant. Gene IDs: NAM-A1 TraesCS6A02G108300; NAM-D1 TraesCS6D02G096300; NAM-A2 TraesCS2A02G201800; NAM-B2 TraesCS2B02G228900.*

Gene	**Genetic background**	**TILLING line**	**Amino acid change**	**AA position in original peptide**	**Sub-domain**	**Reference**	**Delayed senescence?**
NAM-A1	Kronos	K1107 [2]	11aa deletion	splice acceptor variant, intron 2	v	Harrington	Yes – peduncle only
NAM-A1	Kronos	K3661 [2]	P/S	38	i	Harrington	Yes – leaf and peduncle
NAM-A1	Kronos	K2615 [2]	R/Q	41	i	Harrington	Yes – peduncle only

NAM-A1	Kronos	K2734 [2]	T/M	45	i	Harrington	Yes – leaf and peduncle
NAM-A1	Kronos	K2711 [2]	R/W	110	iii	Harrington	Yes – leaf and peduncle
NAM-A1	Kronos	[1]	W/*	117	iii	Distelfeld	Yes
NAM-A1	Kronos	K3741 [2]	G/D	121	iii	Harrington	not tested
NAM-A1	Kronos	K2551 [2]	C/Y	133		Harrington	No (non-conserved residue)
NAM-A1	Kronos	K3186 [2]	P	153	iv	Harrington	No (synonymous)
NAM-A1	Kronos	K2060 [2]	P/L	154	iv	Harrington	Yes – leaf and peduncle in first experiment, no in second experiment
NAM-A1	Express	[1]	W/*	199	v	Avni	Yes
NAM-A1	Paragon	[3]	T/I	159	iv	Chapman	Yes – leaf and peduncle
NAM-A2	Kronos	K3240 [2]	P/S	40	i	Borrill	Yes

NAM-A2	Kronos	K0282 [2]	G/R	111	iii	Borrill	Yes
NAM-A2	Kronos	K0427 [2]	G/D	133		Borrill	Yes
NAM-B2	Kronos	[1]	W/*	112	iii	Distelfeld	No (alone), borderline effect n.s. (with *nam-a1*)
NAM-B2	Kronos	K4452 [2]	R/*	170		Borrill	No (alone), yes (with *nam-a2*)
NAM-D1	Express	[1]	W/*	117	iii	Avni	Yes
NAM-D1	Paragon	[3]	G/E	151	iv	Chapman	Yes – leaf and peduncle

2.3.2.2 KASP primer design for *NAM-2* lines

In each generation, the alleles of these SNPs were genotyped using KASP (Kompetitive Allele-Specific PCR) with homoeolog-specific primers. None of the common (COM) primers designed via Polymarker were fully homoeolog-specific. This is likely because no homoeolog-specific primers passed strict criteria for other primer properties, such as GC content, implemented in Polymarker (Ramirez-Gonzalez, Uauy,Caccamo 2015). Whilst these non-specific COM primers were used initially, primers for five out of six SNPs were replaced with homoeolog-specific primers, designed manually, at later points in the crossing program (*Table 2.14*).

Non-specific primers lead to two problems. Where there is a SNP segregating in the A homoeolog, while B and D homoeologs contain the wild-type allele, a non-specific KASP primer can distinguish alleles in the A homoeolog, however the distance between clusters is reduced because of extraneous wild-type fluorescent signal from the B and D homoeologs in all samples. Where clusters overlap, some genotypes cannot be called. Primer sets for Cad1773 and Cad1895 were replaced with homoeolog-specific primers to improve cluster calling (*Table 2.14*). Cad1656, Cad1436 and Cad0231 all contained a G>A SNP at the same position in the coding sequence. Thus, when these lines were crossed together, fluorescence results from non-specific KASP primers were affected by the allele in two or three homoeologs, making it difficult to call genotypes. For this reason, these three primer sets were replaced with homoeolog-specific primers (*Table 2.14*).

Homoeolog-specific primers were designed manually, and at least two possible primer sets per SNP were validated by genotyping samples with known wild-type and homozygous genotypes. The homoeolog-specific primer set with the greatest distance between wild-type and homozygous clusters in KlusterCaller was selected.

2.3.2.3 Generation of *NAM-2* triple mutant lines

To generate *NAM-2* triple mutant lines, TILLING lines were grown under speed breeding conditions (Watson et al. 2018). To reduce background mutation load, each TILLING line was backcrossed once (Uauy, Wulff,Dubcovsky 2017). To ensure that phenotypes could not be attributed to mutations in genes other than *NAM*-2, two independent crosses were made. The stop codon mutations in subdomain iii of *NAM-A2, NAM-B2* and *NAM-D2* were combined in cross X50 and cross X54 (*Table 2.12*,*Table 2.15*). Crosses X50 and X54 contain the same mutations deriving from the same *nam-a2* and *nam-d2* BC_1 single mutant plants, with different *nam-b2* BC_1 single mutant plants (*Table 2.16*). The segregating BC_1F_2 population contained 104 seedlings of X50 and 29 of X54, of which six out of eight homozygous genotypes were present in X50 (Table 2.18). For X50, the frequencies of mutant alleles in *NAM-A2, NAM-B2* and *NAM-D2* were consistent with Mendelian segregation (Chisquared test, p> 0.05) (Table 2.20). For X54, the genotypes for *NAM-B2* were significantly different from expectation (Table 2.20). This reflects the difficulty of genotype calling with the non-specific primers that were initially used. After primers were redesigned, all individuals that were kept from the X50 and X54 populations were re-genotyped with homoeolog-specific primers. Six homozygous genotypes were obtained from X50 at BC_1F_2, the *nam-d2* single mutant from X50 at BC_1F_3, and the *nam-a2/nam-b2* double mutant from X54 (*Table 2.17*).

The missense mutation in *NAM-A2* and alternative stop codons in *NAM-B2* and *NAM-D2* were combined in cross X61 (*Table 2.12*,*Table 2.15*). For cross X61, only one triple heterozygote was recovered at BC_1F_1, so triple heterozygotes at BC_1F_2 were selfed for a segregating population at BC_1F_3 (*Table 2.17*). Homoeolog-specific primers were used to genotype this population. This population consisted of 336

seedlings, from which at least 2 plants were recovered for all eight homozygous genotypes (Table 2.19). For X61, the frequencies of mutant alleles in *NAM-A2, NAM-B2* and *NAM-D2* were consistent with Mendelian segregation (Chisquared test, p>0.05) (Table 2.20). For both crosses, homozygous triple mutants, as well as single and double mutants and wild-type, were harvested and seed bulked for phenotyping experiments (*Table 2.17*).

Table 2.14 KASP primer sets used to genotype TILLING SNPs in NAM-A2, NAM-B2 and NAM-D2. Each primer set consists of competing WT and MUT forward primers targeting wild-type and mutant alleles of a SNP, with a reverse COM primer common to both alleles. For wheat, COM primers may or may not target a homoeolog-specific SNP. Generations of crossing program in which the primer set was used are listed. Primer sequences can be found in Table 2.1.

Gene	TILLING line	WT	MUT	COM	Product size	Fully homoeolog specific	Primer design method	Generations genotyped with these primers
NAM-A2	Cad1656	CE1656-WT	CE1656-MUT	CE1656-COM	72	No	Polymarker	Gen 1 to Gen 6
NAM-A2	Cad1656	CE1656-WT-3	CE1656-MUT-3	CE1656-COM-2	65	Yes	Manual	Gen 7, Gen 8, regenotyping of Gen 5, Gen 6
NAM-B2	Cad1436	CE1436-WT	CE1436-MUT	CE1436-COM	73	No	Polymarker	Gen 1 to Gen 6
NAM-B2	Cad1436	CE1656-WT-3	CE1656-MUT-3	CE1436-COM-3	65	Yes	Manual	Gen 7, Gen 8, regenotyping of Gen 5, Gen 6
NAM-D2	Cad0231	CE0231-WT	CE0231-MUT	CE0231-COM	111	No	Polymarker	Gen 1 to Gen 6
NAM-D2	Cad0231	CE0231-WT	CE0231-MUT	CE0231-COM-2	73	Yes	Manual	Gen 7, Gen 8, regenotyping of Gen 5, Gen 6
NAM-A2	Cad1773	CE1773-WT	CE1773-MUT	CE1773-COM	80	No	Polymarker	Gen 1 to Gen 7
NAM-A2	Cad1773	CE1773-WT	CE1773-MUT	CE1656-COM-2	127	Yes	Manual	Gen 8, regenotyping of Gen 5, Gen 6, Gen 7
NAM-B2	Cad0895	CE0895-WT	CE0895-MUT	CE0895-COM	57	No	Polymarker	Gen 1
NAM-B2	Cad0895	CE0895-WT-2	CE0895-MUT-2	CE0895-COM-2	103	Yes	Manual	Gen 2 to Gen 8
NAM-D2	Cad0237	CE0237-WT	CE0237-MUT	CE0237-COM	58	No	Polymarker	Gen 1 to Gen 8

Table 2.15 Crosses for NAM-2 TILLING lines. For each SNP, the TILLING line ID and SNP consequence are shown.

Cross ID	***NAM-A2***		***NAM-B2***		***NAM-D2***	
X50	Cad1656	stop codon	Cad1436	stop codon	Cad0231	stop codon
X54	Cad1656	stop codon	Cad1436	stop codon	Cad0231	stop codon
X61	Cad1773	missense	Cad0895	stop codon	Cad0237	stop codon

Table 2.16 Full pedigree of plants used in NAM-2 experiments part 1: Crosses up to generation of triple heterozygotes. For each generation is listed Generation name, Sowing date, plant ID, genotype, and cross ID. Genotype shows WT allele in capitals and TILLING allele in small letters. TILLING lines on left hand side refer to Table 2.12. Cross ID refers to Table 2.15; S marks selfed plants. All seeds used in experiments in this chapter share this pedigree.

TILLING line		**Gen 1**			**Gen 2**			**Gen 3**		
		20/07/2020			12/10/2020			12/01/2021		
Plant ID	Genotype	Plant ID	Genotype	Cross	Plant ID	Genotype	Cross	Plant ID	Genotype	Cross
Cadenza		CadWT-4	AABBDD	**X14**	Cad1436-BC1-?	AABbDD	S	Cad1436-BC1-38	AAbbDD	**X50**
Cadenza1436	AABbDD	Cad1436-1	AAbbDD	**X14**						
Cadenza1656	AaBBDD	Cad1656-21	aaBBDD	**X17**	Cad1656-BC1-3	AaBBDD	**X31**	NAM2-AD-6	AaBBDd	**X50**
Cadenza		CadWT-14	AABBDD	**X17**				NAM2-AD-7	AaBBDd	**X54**
Cadenza0231	AABBdd	Cad0231-17	AABBdd	**X6**	Cad0231-BC1-2	AABBDd	**X31**			
Cadenza		CadWT-21	AABBDD	**X6**						
Cadenza		CadWT-4	AABBDD	**X14**	Cad1436-BC1-?	AABbDD	S	Cad1436-BC1-41	AAbbDD	**X54**
Cadenza1436	AABbDD	Cad1436-1	AAbbDD	**X14**						
Cadenza1773	AaBBDD	Cad1773-20	aaBBDD	**X22**	Cad1773-BC1-11	AaBBDD	**X44**	NAM2-AD-20	AaBBDd	**X61**
Cadenza		CadWT-15	AABBDD	**X22**						
Cadenza0237	AABBdd	Cad0237-10	AABBdd	**X7**	Cad0237-BC1-3	AABBDd	**X44**			
Cadenza		CadWT-14	AABBDD	**X7**						
Cadenza0895	AAbbDD	Cad0895-18	AAbbDD	**X2**	Cad0895-BC1-?	AABbDD	S	Cad0895-BC1-34	AAbbDD	**X61**
Cadenza		CadWT-22	AABBDD	**X2**						

Table 2.17 Full pedigree of plants used in NAM-2 experiments part 2: Selfing and selection of homozygotes from a segregating population. For each generation is listed Generation name, shorthand, sowing date, plant ID and genotype. Genotype shows WT allele in capitals and TILLING allele in small letters. Cross ID refers to Table 2.15. Seeds sown in NAM-2 glasshouse experiments (21/09/2022 and 15/02/2023) were progeny of the listed plants in Gen 8. Seeds sown in NAM-2 field experiment derive from the same crosses, with the same pedigree up to Gen 7 and different individuals in Gen 8, except for X50_G8 and X61_G5, which only share pedigree up to Gen 4.

	Gen 4		**Gen 5**		**Gen 6**		**Gen 7**		**Gen 8**	
	BC_1F_1		BC_1F_2		BC_1F_2		BC_1F_3		BC_1F_3/BC_1F_4	
	16/04/2021		21/07/2021		04/08/2021		26/11/2021		22/04/2022	
Cross	Plant ID	Genotype	Plant ID	Genotype	Plant ID	Genotype	Plant ID	Genotype	Plant ID	Genotype
X50	X50-2	AaBbDd			X50-2-18	aabbdd			NAM2-X50-G8-15	aabbdd
X50	X50-2	AaBbDd			X50-2-18	aabbdd			NAM2-X50-G8-16	aabbdd
X50	X50-2	AaBbDd			X50-2-23	AAbbdd	X50-2-23-2	AAbbdd	NAM2-X50-G4-3	AAbbdd
X50	X50-2	AaBbDd			X50-2-23	AAbbdd	X50-2-23-2	AAbbdd	NAM2-X50-G4-9	AAbbdd
X50	X50-2	AaBbDd			X50-2-5	aaBBdd	X50-2-5-1	aaBBdd	NAM2-X50-G6-2	aaBBdd
X50	X50-2	AaBbDd			X50-2-5	aaBBdd	X50-2-5-1	aaBBdd	NAM2-X50-G6-9	aaBBdd
X50	X50-2	AaBbDd			X50-2-7	AABBDD			NAM2-X50-G1-1	AABBDD
X50	X50-2	AaBbDd			X50-2-7	AABBDD			NAM2-X50-G1-10	AABBDD
X50	X50-5	AaBbDd			X50-5-29	AaBbDd	X50-5-29-6	AABBdd	NAM2-X50-G2-5	AABBdd
X50	X50-5	AaBbDd			X50-5-29	AaBbDd	X50-5-29-6	AABBdd	NAM2-X50-G2-7	AABBdd
X50	X50-5	AaBbDd			X50-5-38	AAbbDD	X50-5-38-4	AAbbDD	NAM2-X50-G3-2	AAbbDD
X50	X50-5	AaBbDd			X50-5-38	AAbbDD	X50-5-38-4	AAbbDD	NAM2-X50-G3-5	AAbbDD
X50	X50-5	AaBbDd			X50-5-73	aaBBDD	X50-5-73-1	aaBBDD	NAM2-X50-G5-10	aaBBDD
X50	X50-5	AaBbDd			X50-5-73	aaBBDD	X50-5-73-1	aaBBDD	NAM2-X50-G5-11	aaBBDD

X54	X54-11	AaBbDd	X54-11-59	aabbDD					NAM2-X54-G7-18	aabbDD
X54	X54-11	AaBbDd	X54-11-59	aabbDD					NAM2-X54-G7-19	aabbDD
X61	X61-6	AaBbDd			X61-6-15	AaBbDd	X61-25	AABBdd	NAM2-X61-G2-2	AABBdd
X61	X61-6	AaBbDd			X61-6-15	AaBbDd	X61-25	AABBdd	NAM2-X61-G2-4	AABBdd
X61	X61-6	AaBbDd			X61-6-15	AaBbDd	X61-30	AAbbDD	NAM2-X61-G3-4	AAbbDD
X61	X61-6	AaBbDd			X61-6-15	AaBbDd	X61-30	AAbbDD	NAM2-X61-G3-6	AAbbDD
X61	X61-6	AaBbDd			X61-6-15	AaBbDd	X61-51	AAbbdd	NAM2-X61-G4-3	AAbbdd
X61	X61-6	AaBbDd			X61-6-15	AaBbDd	X61-51	AAbbdd	NAM2-X61-G4-8	AAbbdd
X61	X61-6	AaBbDd			X61-6-15	AaBbDd	X61-61	aaBBdd	NAM2-X61-G6-2	aaBBdd
X61	X61-6	AaBbDd			X61-6-15	AaBbDd	X61-61	aaBBdd	NAM2-X61-G6-8	aaBBdd
X61	X61-6	AaBbDd			X61-6-15	AaBbDd	X61-77	aabbdd	NAM2-X61-G8-5	aabbdd
X61	X61-6	AaBbDd			X61-6-15	AaBbDd	X61-77	aabbdd	NAM2-X61-G8-6	aabbdd
X61	X61-6	AaBbDd			X61-6-22	AaBbDd	X61-134	AABBDD	NAM2-X61-G1-3	AABBDD
X61	X61-6	AaBbDd			X61-6-22	AaBbDd	X61-134	AABBDD	NAM2-X61-G1-4	AABBDD
X61	X61-6	AaBbDd			X61-6-22	AaBbDd	X61-98	aaBBDD	NAM2-X61-G5-4	aaBBDD
X61	X61-6	AaBbDd			X61-6-22	AaBbDd	X61-98	aaBBDD	NAM2-X61-G5-9	aaBBDD
X61	X61-6	AaBbDd			X61-6-41	AaBbDd	X61-266	aabbDD	NAM2-X61-G7-1	aabbDD
X61	X61-6	AaBbDd			X61-6-41	AaBbDd	X61-266	aabbDD	NAM2-X61-G7-2	aabbDD

Table 2.18 Genotype counts from NAM-2 BC_1F_2 populations of cross X50 (Gen 6) and cross X54 (Gen 5). KASP genotyping carried out with original non-homoeolog-specific primers, so some genotypes may not be correct. X:X marks homozygous alleles, X:Y marks heterozygous, Y:Y marks wild-type. Where any SNP could not be called the individual was categorised as unknown. Expected counts calculated based on Mendelian segregation with equal probability of "X" or "Y" allele. Bold, underlined genotypes were retained for phenotyping experiments.

NAM-A2	NAM-B2	NAM-D2	X50 (Gen 6)		X54 (Gen 5)		
CE1656	CE1436	CE0231	Observed	Expected number	Observed	Expected number	Expected proportion out of 64
X:X	X:X	X:X	**1**	1.34	**2**	0.28	1
X:X	X:X	Y:Y	**0**	1.34	**2**	0.28	1
X:X	X:X	X:Y	3	2.69	1	0.56	2
X:X	Y:Y	X:X	**1**	1.34	**0**	0.28	1
X:X	Y:Y	Y:Y	**1**	1.34	**0**	0.28	1
X:X	Y:Y	X:Y	3	2.69	0	0.56	2
X:X	X:Y	X:X	2	2.69	0	0.56	2
X:X	X:Y	Y:Y	3	2.69	0	0.56	2
X:X	X:Y	X:Y	4	5.38	1	1.13	4
Y:Y	X:X	X:X	**1**	1.34	**0**	0.28	1
Y:Y	X:X	Y:Y	**1**	1.34	**6**	0.28	1
Y:Y	X:X	X:Y	2	2.69	0	0.56	2
Y:Y	Y:Y	X:X	**0**	1.34	**0**	0.28	1
Y:Y	Y:Y	Y:Y	**4**	1.34	**0**	0.28	1
Y:Y	Y:Y	X:Y	4	2.69	0	0.56	2
Y:Y	X:Y	X:X	1	2.69	2	0.56	2
Y:Y	X:Y	Y:Y	1	2.69	1	0.56	2
Y:Y	X:Y	X:Y	7	5.38	0	1.13	4
X:Y	X:X	X:X	2	2.69	1	0.56	2

X:Y	X:X	Y:Y	3	2.69	0	0.56	2
X:Y	X:X	X:Y	4	5.38	1	1.13	4
X:Y	Y:Y	X:X	2	2.69	0	0.56	2
X:Y	Y:Y	Y:Y	4	2.69	0	0.56	2
X:Y	Y:Y	X:Y	6	5.38	0	1.13	4
X:Y	X:Y	X:X	6	5.38	0	1.13	4
X:Y	X:Y	Y:Y	6	5.38	0	1.13	4
X:Y	X:Y	X:Y	14	10.75	1	2.25	8
		Unknown	18		11		
		Total	104		29		

Table 2.19 Genotype counts from NAM-2 BC_1F_3 populations of cross X61 (Gen 7). KASP genotyping carried out with redesigned, homoeolog-specific primers. X:X marks homozygous alleles, X:Y marks heterozygous, Y:Y marks wild-type. Where any SNP could not be called the individual was categorised as unknown. Expected counts calculated based on Mendelian segregation with equal probability of "X" or "Y" allele.Bold, underlined genotypes were retained for phenotyping experiments.

NAM-A2	NAM-B2	NAM-D2	X61		
CE1773-2	CE0895-2	CE0237	Observed genotype calls	Expected number	Expected proportion out of 64
X:X	X:X	X:X	**6**	4.4	1
X:X	X:X	Y:Y	**3**	4.4	1
X:X	X:X	X:Y	11	8.7	2
X:X	Y:Y	X:X	**9**	4.4	1
X:X	Y:Y	Y:Y	**6**	4.4	1
X:X	Y:Y	X:Y	4	8.7	2

X:X	X:Y	X:X	9	8.7	2
X:X	X:Y	Y:Y	4	8.7	2
X:X	X:Y	X:Y	16	17.4	4
Y:Y	X:X	X:X	**4**	4.4	1
Y:Y	X:X	Y:Y	**3**	4.4	1
Y:Y	X:X	X:Y	8	8.7	2
Y:Y	Y:Y	X:X	**3**	4.4	1
Y:Y	Y:Y	Y:Y	**7**	4.4	1
Y:Y	Y:Y	X:Y	10	8.7	2
Y:Y	X:Y	X:X	8	8.7	2
Y:Y	X:Y	Y:Y	10	8.7	2
Y:Y	X:Y	X:Y	21	17.4	4
X:Y	X:X	X:X	3	8.7	2
X:Y	X:X	Y:Y	5	8.7	2
X:Y	X:X	X:Y	15	17.4	4
X:Y	Y:Y	X:X	5	8.7	2
X:Y	Y:Y	Y:Y	14	8.7	2
X:Y	Y:Y	X:Y	15	17.4	4
X:Y	X:Y	X:X	22	17.4	4
X:Y	X:Y	Y:Y	20	17.4	4
X:Y	X:Y	X:Y	38	34.9	8
		Unknown	57		
		Total	**336**		

Table 2.20 Chi-squared test for segregation of SNP alleles in NAM-A2, NAM-B2 and NAM-D2. Results from Table 2.18 and Table 2.19 were binned according to the genotype of a single SNP. Generation ID refers to Table 2.17. X:X marks homozygous alleles, X:Y marks heterozygous, Y:Y marks wild-type. Where any SNP could not be called the individual was categorised as unknown. Chi-squared test used expected counts calculated based on Mendelian segregation with equal probability of "X" or "Y" allele.

Cross	Generation	Generation ID	Gene	Primer	X:X	X:Y	Y:Y	Total	Chisquared p-value
X61	BC_1F_3	Gen 7	*NAM-A2*	CE1773-2	68	137	74	279	0.840435453
X61	BC_1F_3	Gen 7	*NAM-B2*	CE0895-2	58	148	73	279	0.265969734
X61	BC_1F_3	Gen 7	*NAM-D2*	CE0237	69	138	72	279	0.952764903
X50	BC_1F_2	Gen 6	*NAM-A2*	CE1656	18	47	21	86	0.620801319
X50	BC_1F_2	Gen 6	*NAM-B2*	CE1436	17	44	25	86	0.464199037
X50	BC_1F_2	Gen 6	*NAM-D2*	CE0231	16	47	23	86	0.389901762
X54	BC_1F_2	Gen 5	*NAM-A2*	CE1656	6	3	9	18	0.011108997
X54	BC_1F_2	Gen 5	*NAM-B2*	CE1436	13	5	0	18	1.41377E-05
X54	BC_1F_2	Gen 5	*NAM-D2*	CE0231	5	4	9	18	0.025561533

2.3.3 *NAM-2* TILLING lines show inconsistent senescence phenotypes in the glasshouse

To test whether loss-of-function of *NAM-2* affects senescence timing, grain mass or protein content, *NAM-2* TILLING lines were grown in the glasshouse (Methods 2.2.8.2). As the experiments in 2022 and 2023 involved the same plant material and experimental design, results of both experiments are shown in parallel (Methods 2.2.8.2).

These experiments were carried out in a glasshouse with supplementary heating and lighting, but with limited capacity for cooling. The mean day-time air temperature at plant canopy height was significantly higher and more variable in the February to June 2023 experiment (15/02/2023) than in the September 2022 to February 2023 experiment (21/09/2022) (*Figure 2.10*). In the 2023 experiment, a mean temperature exceeding 30°C was recorded on 11th June (*Figure 2.10*).

Overall, mutation of all copies of *NAM-2* did not have a consistent impact on senescence timing. For cross X50 in 2022, the *NAM-2* triple mutant retained slightly higher flag leaf chlorophyll content at 7 weeks after heading compared to the control, but otherwise showed similar chlorophyll content (*Figure 2.11*A, B). In 2023, the *NAM-2* triple mutant retained significantly higher flag leaf chlorophyll content between 4 and 7 weeks after heading, and plants appeared greener (*Figure 2.11*C, D). For cross X61 in 2022, *NAM-2* triple mutants senesced later, with higher flag leaf chlorophyll content at 7-8 weeks after heading (*Figure 2.11*E, F). Conversely in 2023, *NAM-2* triple mutants senesced earlier, with reduced flag leaf chlorophyll content at 6-8 weeks after heading (*Figure 2.11*G, H).

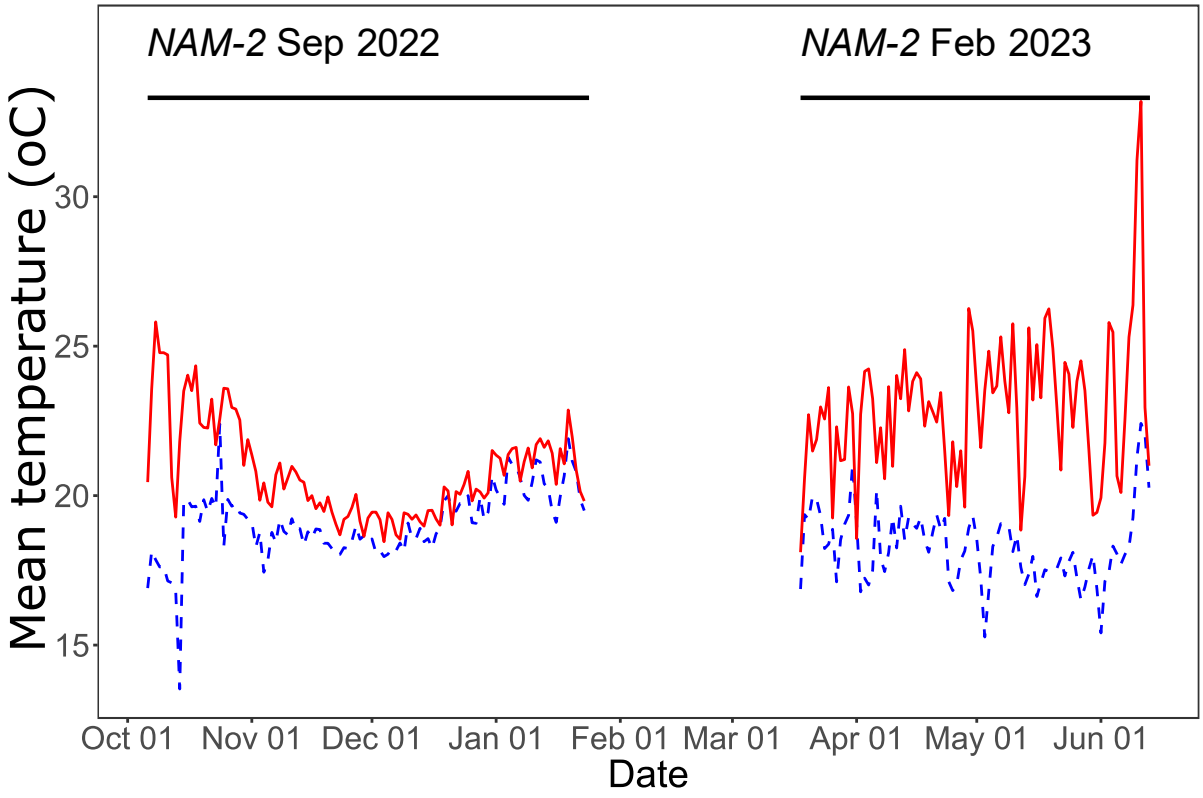


Figure 2.10 Air temperature for NAM-2 glasshouse experiments. NAM-2 lines were grown in the glasshouse in two experiments starting September 2022 and February 2023. Air temperature at wheat canopy height was measured with an EasyLog at 15 minute intervals. Mean glasshouse air temperature in day-time 8am – 8pm (red solid lines) and night-time 8pm – 8am (blue dotted lines).

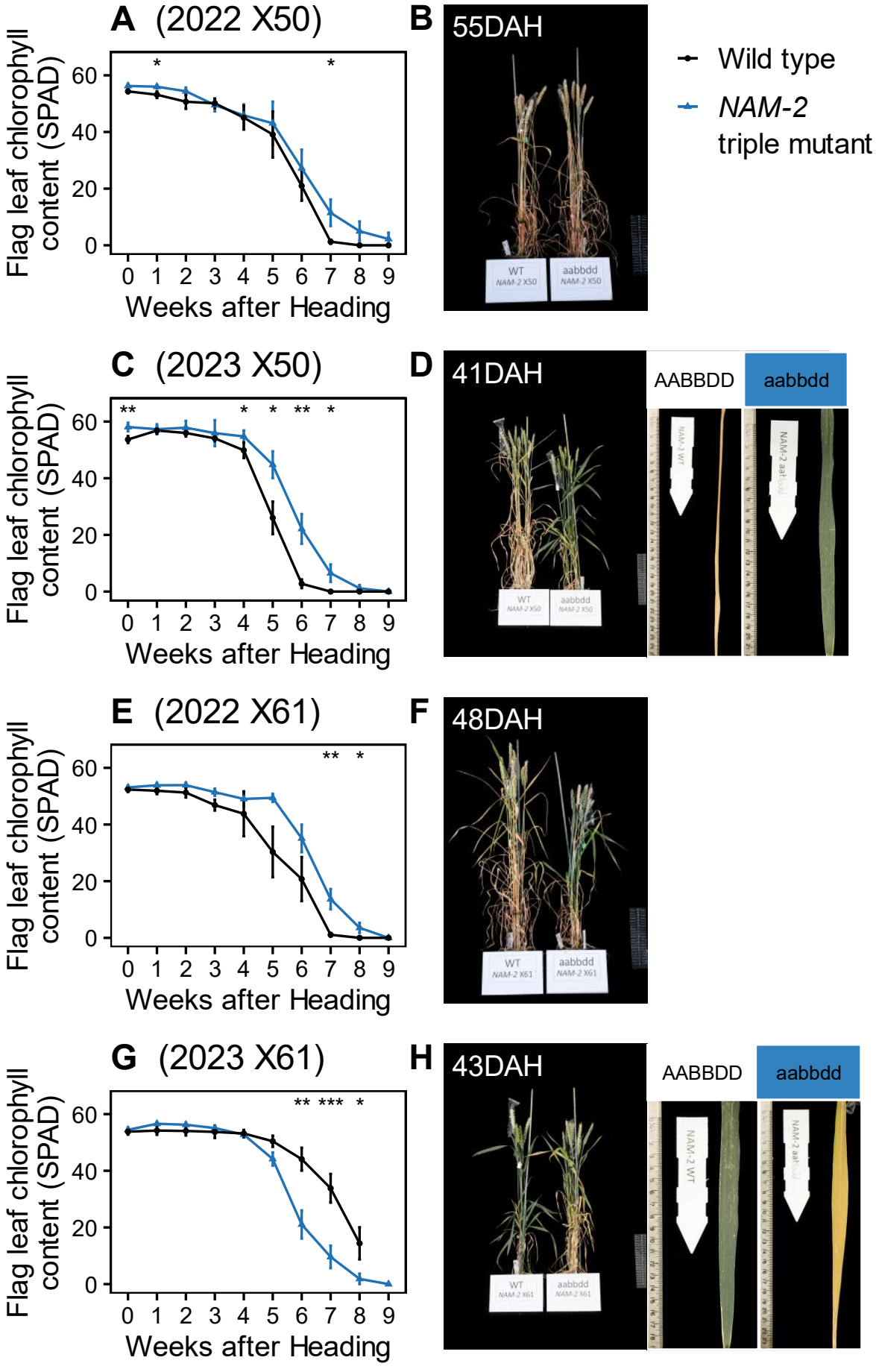

A (2022 X50)
B
55DAH
Wild type
NAM-2 triple mutant
Flag leaf chlorophyll content (SPAD)
Weeks after Heading
C (2023 X50)
D
41DAH
AABBDD
aabbdd
E (2022 X61)
F
48DAH
G (2023 X61)
H
43DAH

*Figure 2.11 Leaf senescence timing of NAM-2 triple mutant lines and controls varies between trials and crosses. TILLING lines from two independent crosses with mutations in NAM-2 and wild-type segregant controls were grown in the glasshouse in 2022 and 2023. (A, C, E, G) Flag leaf chlorophyll content (SPAD) in weeks after heading +/- 2 days. Average SPAD value at each timepoint was compared by Wilcoxon test, *=p<0.05 / **=p<0.01 / **=p<0.001. (B, F) Representative plants of NAM-2 triple mutant and control at 55DAH and 48DAH. (C, H) Representative plants of NAM-2 triple mutant and control at 41DAH and 43DAH, alongside flag leaves of the same plants. (A, B) Cross X50 grown in 2022. (C, D) Cross X50 grown in 2023. (E, F) Cross X61 grown in 2022. (G, H) Cross X61 grown in 2023.*

In 2022, X61 “aa” and “aadd” lines trended towards later heading than the control, although it was not significant, while heading dates were similar across X50 lines (*Figure 2.12*A). In 2023, X61 lines did not differ in heading date while X50 triple mutants trended toward earlier heading (*Figure 2.12*B). In both years, X54 “aabb” headed significantly later than at least two X50 lines (*Figure 2.12*A, B). The onset of leaf senescence was significantly later than control in X61 “aa”, “aadd” and “bbdd” in 2022, but earlier in X61 “bb” and “aadd” in 2023 (*Figure 2.12*C, D). Senescence onset did not differ between X50 lines in 2022, while double mutant “bbdd” showed later senescence onset in 2023 (*Figure 2.12*C, D).

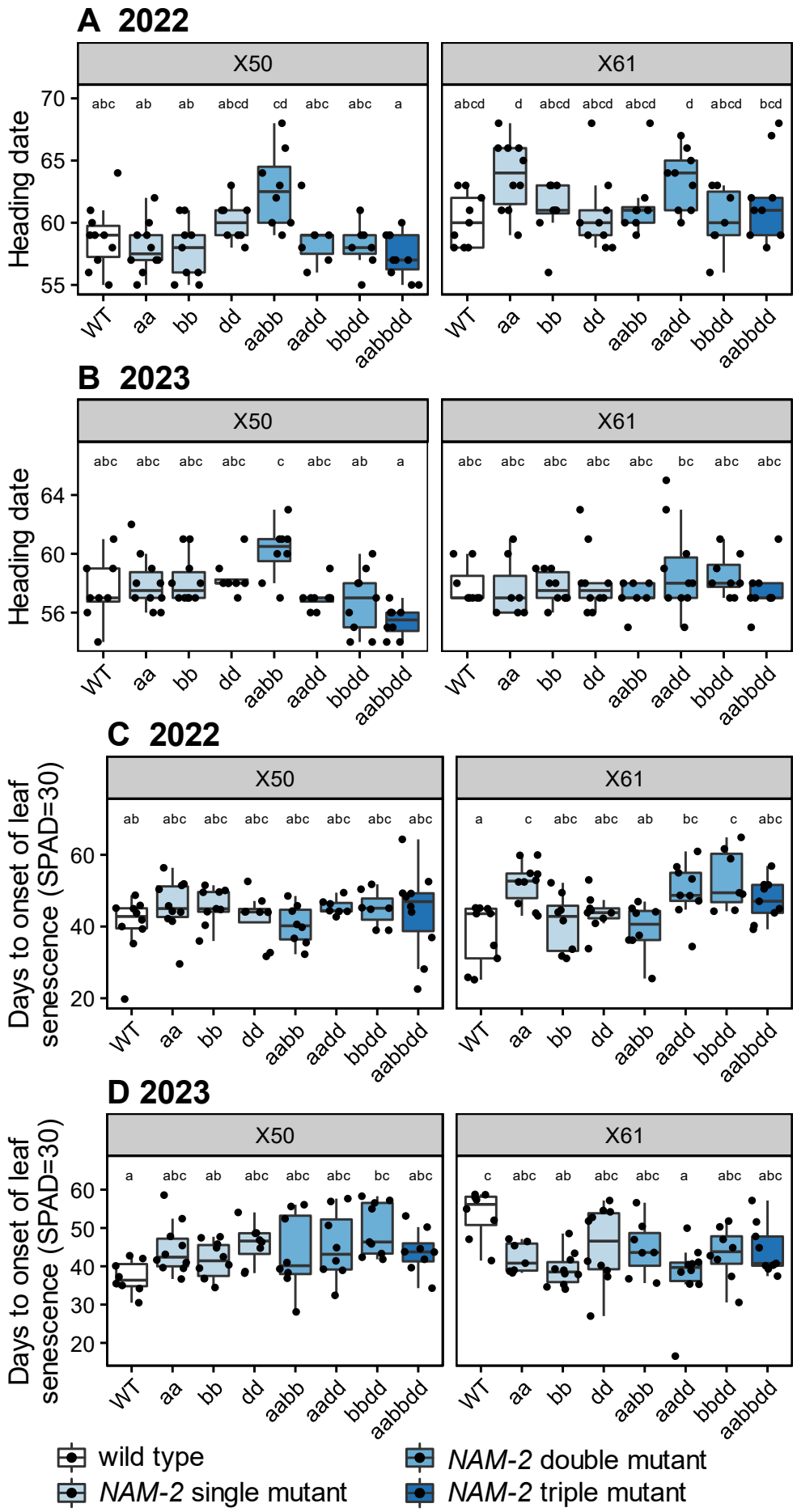

A 2022
X50
X61
Heading date
70
65
60
55
abc ab ab abcd cd abc abc a
abcd d abcd abcd abcd d abcd bcd
WT aa bb dd aabb aadd bbdd aabbdd
B 2023
X50
X61
Heading date
64
60
56
abc abc abc abc c abc ab a
abc abc abc abc abc bc abc abc
WT aa bb dd aabb aadd bbdd aabbdd
C 2022
X50
X61
Days to onset of leaf senescence (SPAD=30)
60
40
20
ab abc abc abc abc abc abc abc
a c abc abc ab bc c abc
WT aa bb dd aabb aadd bbdd aabbdd
D 2023
X50
X61
Days to onset of leaf senescence (SPAD=30)
60
50
40
30
20
a abc ab abc abc abc bc abc
c abc ab abc abc a abc abc
WT aa bb dd aabb aadd bbdd aabbdd
wild type
NAM-2 single mutant
NAM-2 double mutant
NAM-2 triple mutant

*Figure 2.12 Some NAM-2 mutants showed later onset of leaf senescence than controls among X61 in 2022 and X50 in 2023, but some NAM-2 mutants showed earlier senescence onset among X61 in 2023. (A, B) Heading date (DAS); (C, D) Days from heading to SPAD=30. (A, C) 2022 Experiment. (B, D) 2023 Experiment. (A-D) ANOVA with post-hoc Tukey test, formula ~ Row + Block + Cross*Genotype, letters show significance groups at p<0.05. In graphs for X50, the "aabb" genotype derived from X54.*

Area under curve (AUC) of leaf senescence was higher in X61 lines "aa", "aadd" and "bbdd" in 2022, and lower in X61 lines "bb" and "aadd" in 2023, matching the result for onset of senescence (*Figure 2.13*A, B). For X50, *NAM-2* mutants did not differ significantly from controls in either year, but with a slight trend toward higher AUC in 2023 (*Figure 2.13*A, B). There were no significant differences in duration of leaf senescence in either year (*Figure 2.13*C, D).

When scored visually, for X61, lines "bb" and "aadd" reached 25% leaf yellowing earlier than controls in 2023, consistent with SPAD-derived senescence metrics (*Figure 2.14*A). For X61, peduncle senescence was similar between lines (*Figure 2.14*B). *NAM-2* X50 mutant lines trended slightly toward later 25% leaf yellowing and 100% peduncle senescence than wild-type (*Figure 2.14*A, B).

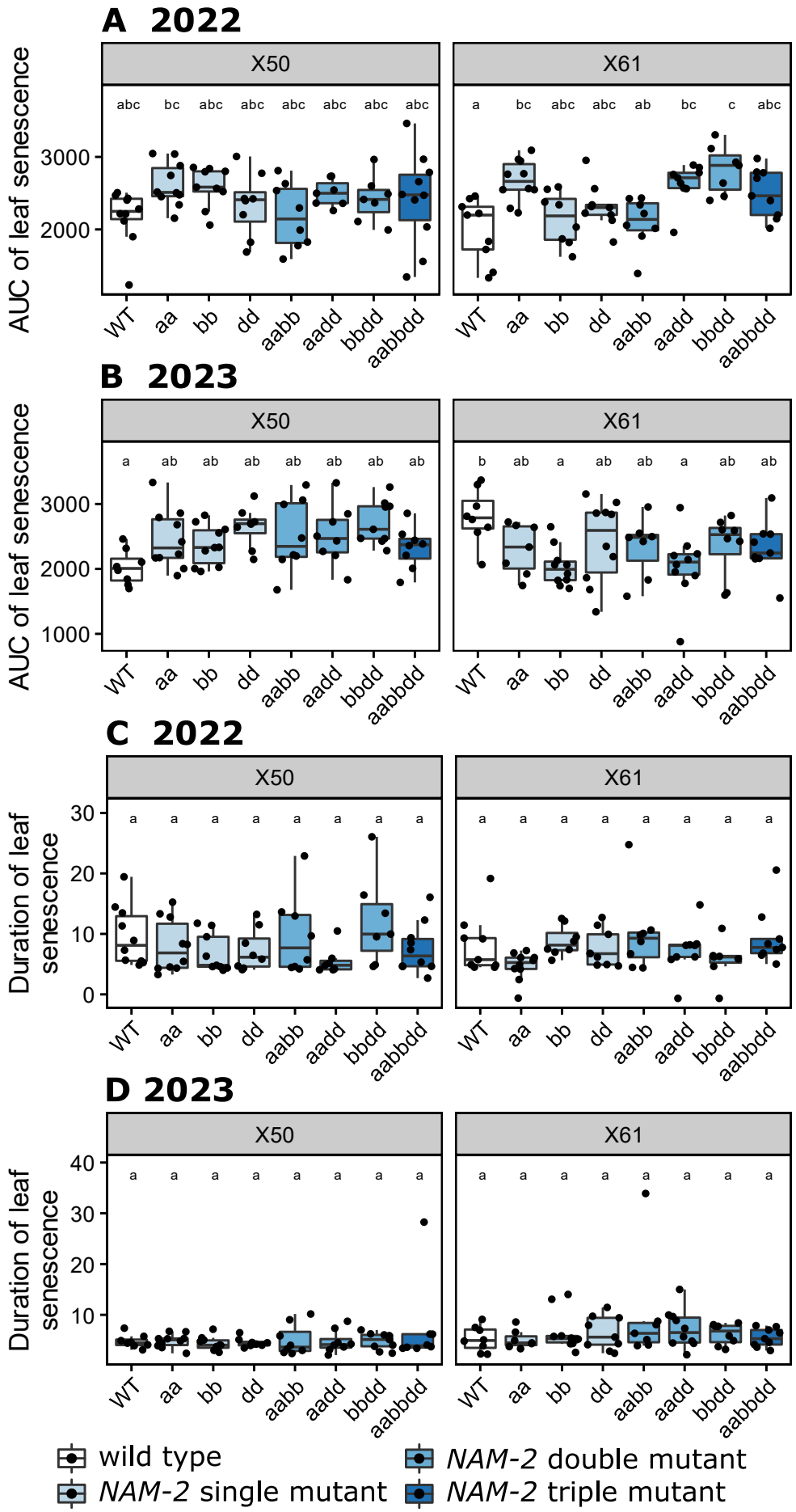

A 2022
X50
X61
AUC of leaf senescence
3000
2000
abc bc abc abc abc abc abc abc
a bc abc abc ab bc c abc
WT aa bb dd aabb aadd bbdd aabbdd
B 2023
1000
a ab ab ab ab ab ab ab
b ab a ab ab a ab ab
C 2022
Duration of leaf senescence
30
20
10
0
a a a a a a a a
D 2023
40
wild type
NAM-2 single mutant
NAM-2 double mutant
NAM-2 triple mutant

*Figure 2.13 NAM-2 genotype affects AUC of leaf senescence, dependent on cross and experiment, but has no impact on Duration of leaf senescence. (A, B) Area under curve (AUC) of leaf senescence; (C, D) Duration of leaf senescence. (A, C) 2022 Experiment. (B, D) 2023 Experiment. (A-D) ANOVA with post-hoc Tukey test, formula ~ Row + Block + Cross*Genotype, letters show significance groups at p<0.05. In graphs for X50, the "aabb" genotype derived from X54.*

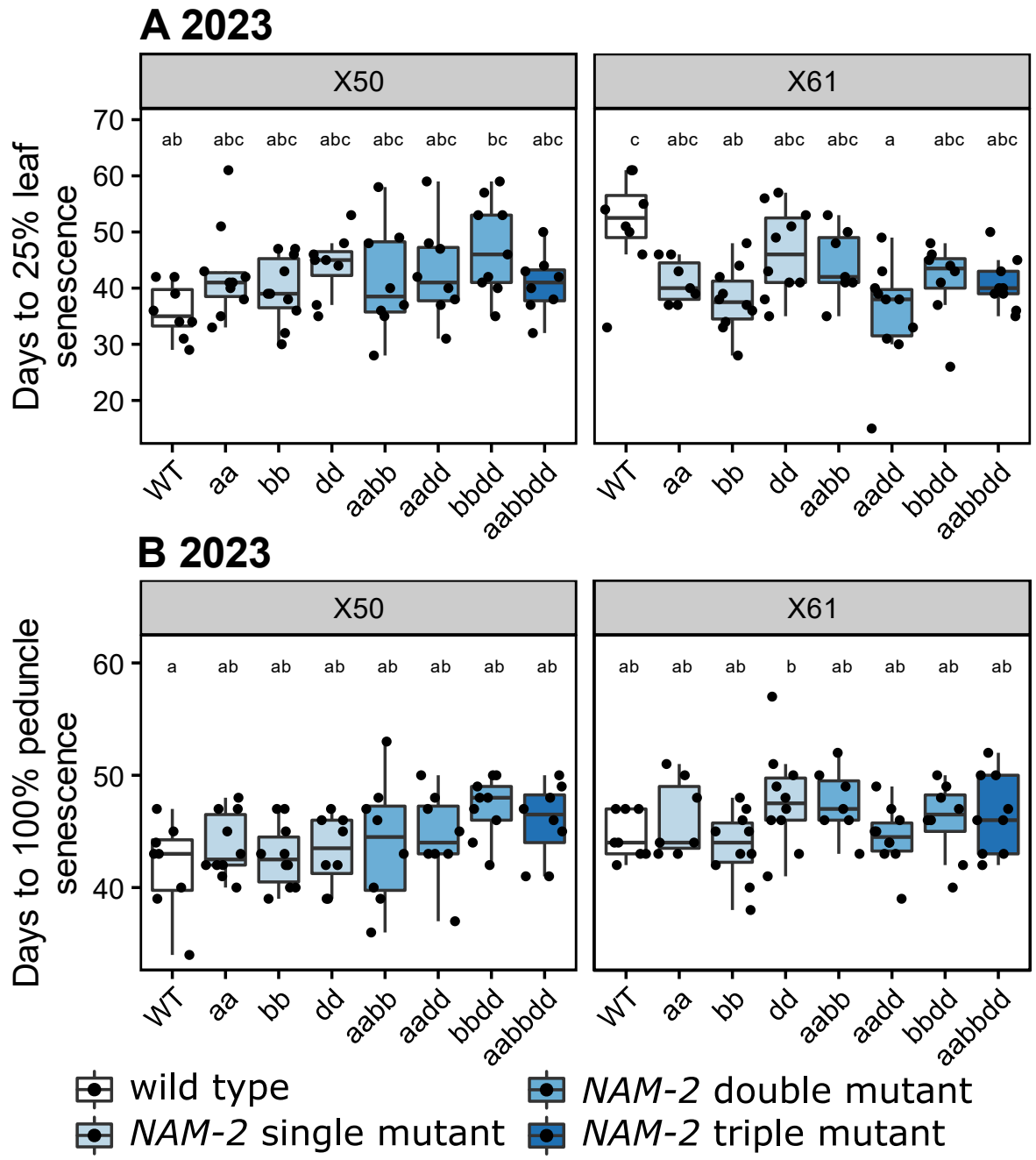


*Figure 2.14 In 2023, NAM-2 triple mutants in cross X50 trend towards later peduncle senescence and 25% leaf yellowing, while triple mutants in cross X61 trend towards earlier 25% leaf yellowing. (A) 25% flag leaf yellowing in 2023 Experiment; (B) 100% peduncle yellowing in 2023 Experiment. (A-B) ANOVA with post-hoc Tukey test, formula ~ Row + Block + Cross*Genotype, letters show significance groups at p<0.05. NB: 25% flag leaf yellowing and 100% peduncle yellowing were not shown for 2022 Experiment as a high number of missing values made these data unreliable. In graphs for X50, the "aabb" genotype derived from X54.*

2.3.4 Agronomic traits in *NAM-2* TILLING lines

Tiller number, height and flag leaf length were also measured in these experiments. Tiller number ranged widely in both experiments. In 2022, the highest average tiller number was found in X61 wild-type, while the lowest were found in X50 “aa”, X54 “aabb”, X61 “aa” and X61 “bbdd” (*Figure 2.14*A). In 2023, tiller number was not significantly different between lines (*Figure 2.14*B). On average, X54 “aabb” had a significantly taller primary tiller than X50 wild-type in 2022 (*Figure 2.14*C). X54 “aabb” also had a wider tiller angle, with 4 out of 10 plants scoring 4 or 5 on a qualitative scale from 1 to 5, compared to an average of 1 out of 10 across X50. Cross X61 showed overall reduced primary tiller height relative to cross X50 in 2023 (*Figure 2.14*D).

NAM-2 mutations showed no effect on flag leaf length in either year (*Figure 2.15*A, B). Interestingly, cross X61 showed overall narrower flag leaves than cross X50 (*Figure 2.15*C).

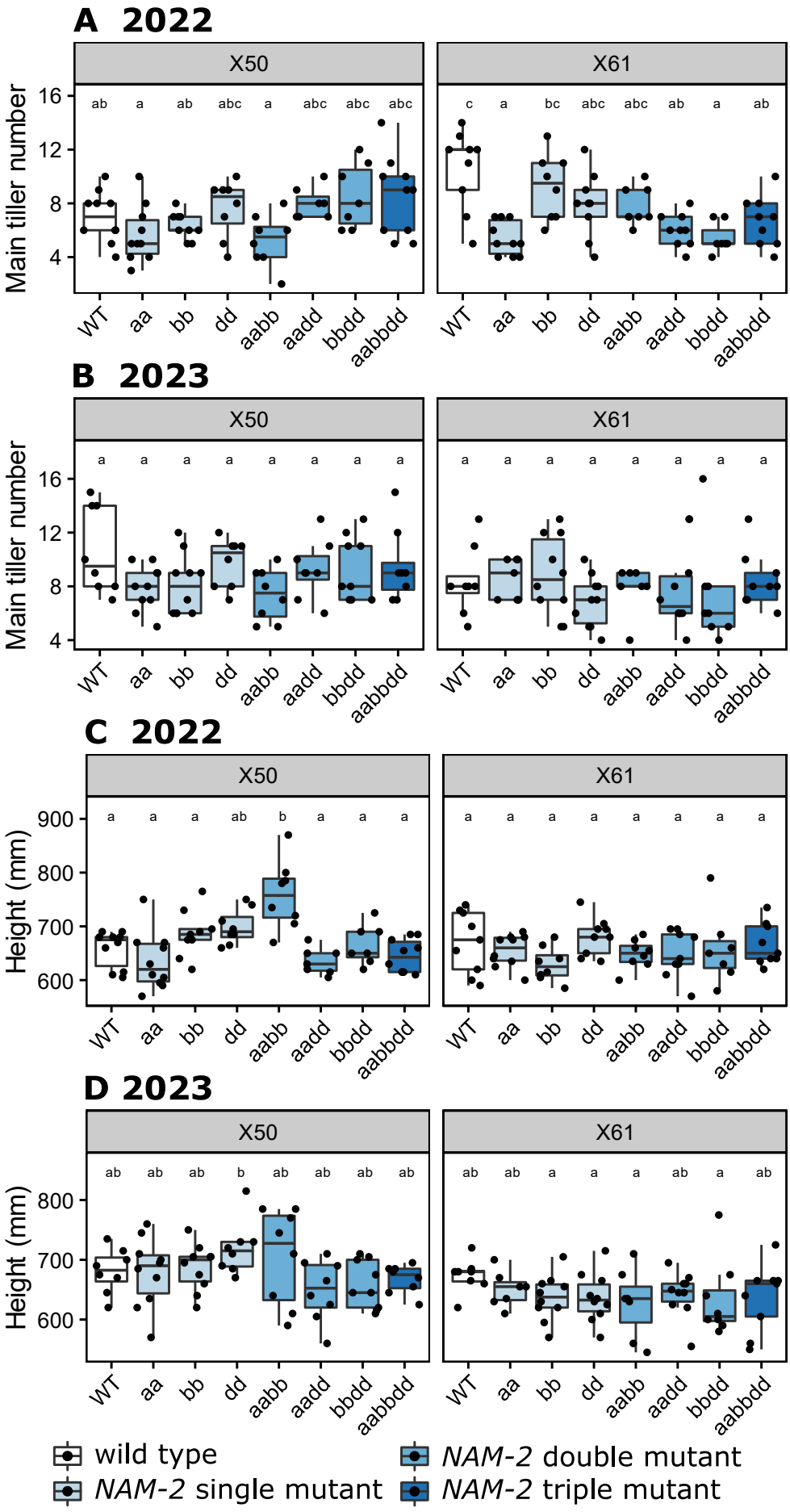

A 2022
X50
X61
Main tiller number
16
12
8
4
ab a ab abc a abc abc abc
c a bc abc abc ab a ab
WT aa bb dd aabb aadd bbdd aabbdd
B 2023
a a a a a a a a
C 2022
Height (mm)
900
800
700
600
a a a ab b a a a
D 2023
ab ab ab b ab ab ab ab
ab ab a a a ab a ab
wild type
NAM-2 single mutant
NAM-2 double mutant
NAM-2 triple mutant

*Figure 2.15 Tiller number varied between NAM-2 TILLING lines in 2022 but was consistent in 2023, while NAM-2 X50 "aabb" was significantly taller than other lines in 2022, likely due to its distinct pedigree from other X50 lines. (A, B) Main tiller number; (C, D) Height of primary tiller (mm). (A, C) 2022 Experiment. (B, D) 2023 Experiment. (A-D) ANOVA with post-hoc Tukey test, formula ~ Row + Block + Cross*Genotype, letters show significance groups at p<0.05. In graphs for X50, the "aabb" genotype derived from X54.*

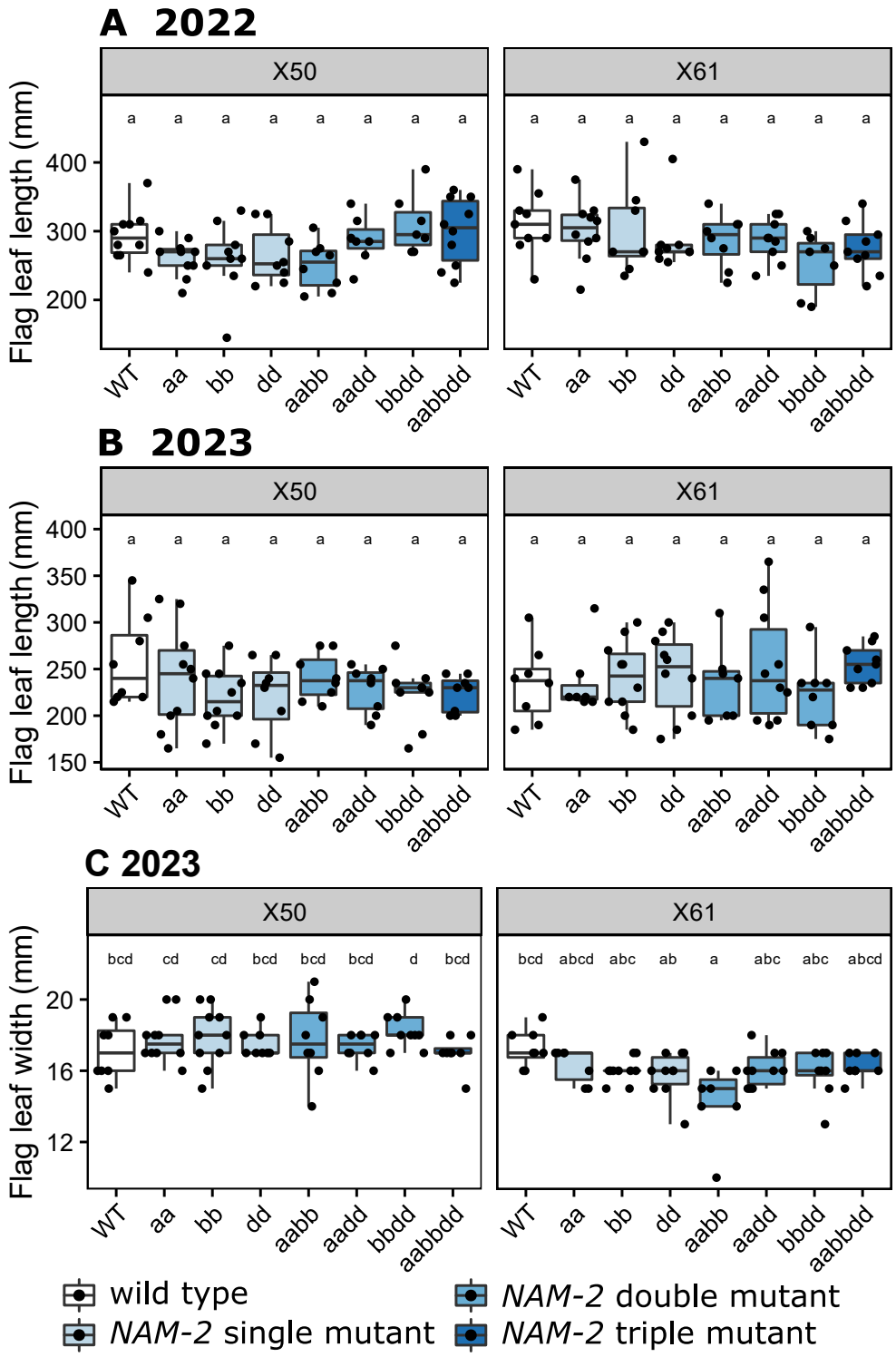


*Figure 2.16 Flag leaf length was lower in 2023 than 2022, but consistent between genotypes and crosses, while flag leaf width was higher across NAM-2 X50 compared to NAM-2 X61 in 2023. (A, B) Flag leaf length (mm); (C) Flag leaf width (mm). (A) 2022 Experiment. (B, C) 2023 Experiment. (A-C) ANOVA with post-hoc Tukey test, formula ~ Row + Block + Cross*Genotype, letters show significance groups at p<0.05. In graphs for X50, the "aabb" genotype derived from X54.*

2.3.5 Grain mass and protein content of *NAM-2* TILLING lines in the glasshouse

Grain traits and protein content of *NAM-2* mutant lines varied between experiments. For X61 in 2022, *NAM-2* mutant lines showed lower grain number and total grain mass than null segregant controls, while grain number and grain mass did not differ between lines in other experiments (Figure 2.17A, B, C, D). For X50, kernel weight was higher than controls in *nam-b2* single mutants in 2022 and 2023, and *nam-b2/nam-d2* double mutants in 2023 (Figure 2.18A, B). There were no significant differences in X61 (Figure 2.18A, B). X54 “aabb” showed higher grain length than X50 lines in both 2022 and 2023 (Figure 2.18C, D). For X61, *NAM-2* triple mutants along with some single and double mutants had higher grain length than controls in 2022 and 2023 (Figure 2.18C, D). Consistent with results for kernel weight, in X50 *nam-b2* single mutants showed increased grain width and area in 2022 and 2023, while *nam-b2/nam-d2* double mutants showed increased grain width and area in 2023 (Figure 2.19A, B, C, D). Within X61, the *nam-d2* single mutant had higher grain width and area compared to the *nam-a2/nam-b2* double mutant in 2022, but otherwise grain width and area did not differ between lines (Figure 2.19A, B, C, D).

In 2022, *NAM-2* triple mutants from X61 as well as “aa” and “bbdd” genotypes had significantly higher GPC than controls (Figure 2.20A). *NAM-2* mutants trended towards decreased GPC in X50 in 2023, but the difference was not significant (Figure 2.20B). Protein content was normalised by multiplying by thousand kernel weight to obtain protein mass per thousand grains. The trend of increased protein in *NAM-2* triple mutants of X61 in 2022 was also seen in these normalised data (Figure 2.21A). Across all genotypes, while GPC was higher in 2023 than 2022, protein

mass per thousand grains was similar across years, with most samples between 5g-7g protein per thousand grains (Figure 2.20A, B, Figure 2.21A, B).

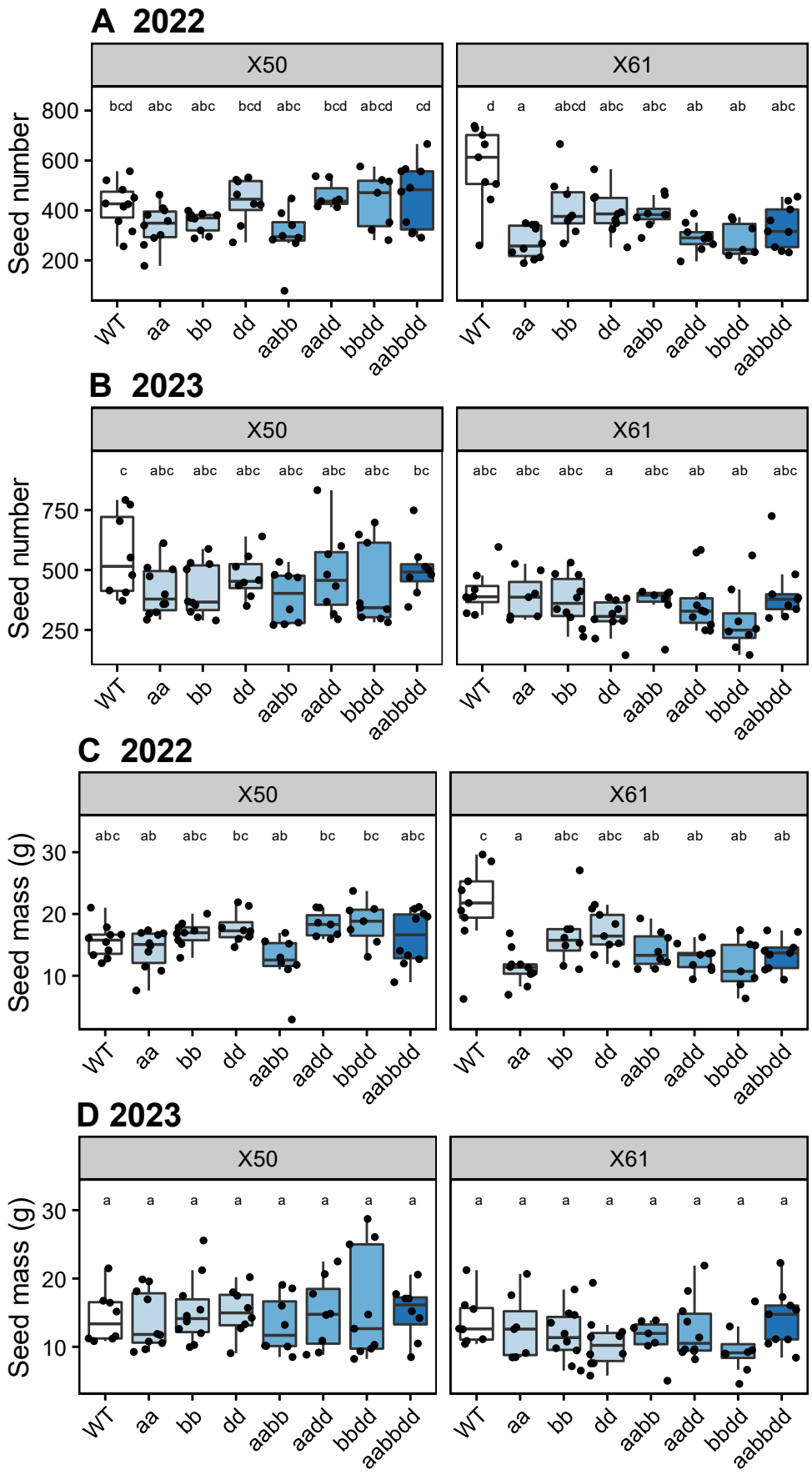

A 2022
X50
X61
Seed number
800
600
400
200
bcd abc abc bcd abc bcd abcd cd
d a abcd abc abc ab ab abc
WT aa bb dd aabb aadd bbdd aabbdd
B 2023
X50
X61
Seed number
750
500
250
c abc abc abc abc abc abc bc
abc abc abc a abc ab ab abc
WT aa bb dd aabb aadd bbdd aabbdd
C 2022
X50
X61
Seed mass (g)
30
20
10
abc ab abc bc ab bc bc abc
c a abc abc ab ab ab ab
WT aa bb dd aabb aadd bbdd aabbdd
D 2023
X50
X61
Seed mass (g)
30
20
10
a a a a a a a a
a a a a a a a a
WT aa bb dd aabb aadd bbdd aabbdd
wild type
NAM-2 single mutant
NAM-2 double mutant
NAM-2 triple mutant

*Figure 2.17 Grain number and grain mass did not differ across the majority of NAM-2 TILLING lines. (A, B) Grain number; (C, D) Grain mass (g). (A, C) 2022 Experiment. (B, D) 2023 Experiment. (A-D) ANOVA with post-hoc Tukey test, formula ~ Row + Block + Cross*Genotype, letters show significance groups at p<0.05. In graphs for X50, the "aabb" genotype derived from X54.*

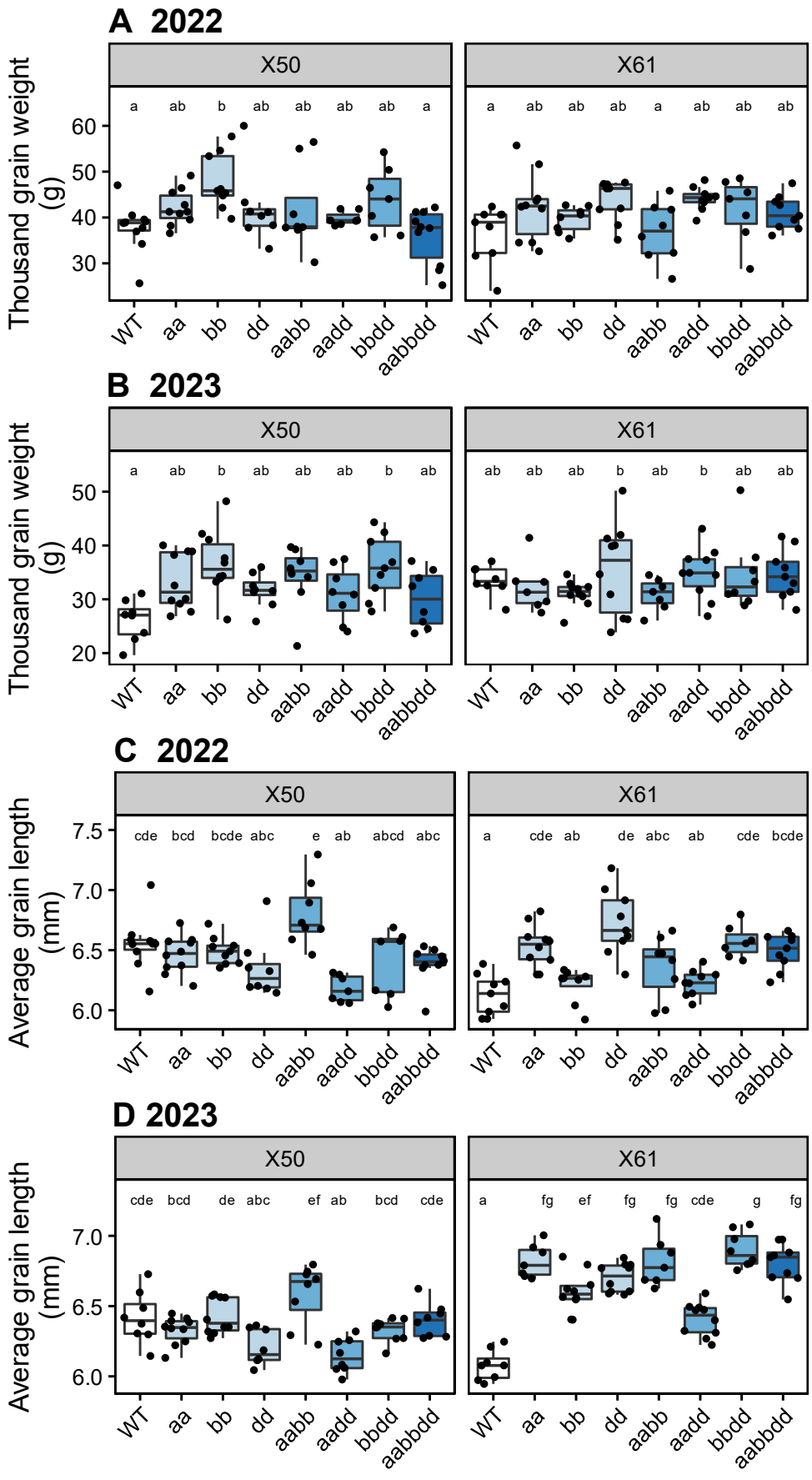

A 2022
X50
X61
Thousand grain weight (g)
a ab b ab ab ab ab a
a ab ab ab a ab ab ab
60
50
40
30
WT aa bb dd aabb aadd bbdd aabbdd
B 2023
X50
X61
Thousand grain weight (g)
a ab b ab ab ab b ab
ab ab ab b ab b ab ab
50
40
30
20
WT aa bb dd aabb aadd bbdd aabbdd
C 2022
X50
X61
Average grain length (mm)
cde bcd bcde abc e ab abcd abc
a cde ab de abc ab cde bcde
7.5
7.0
6.5
6.0
WT aa bb dd aabb aadd bbdd aabbdd
D 2023
X50
X61
Average grain length (mm)
cde bcd de abc ef ab bcd cde
a fg ef fg fg cde g fg
7.0
6.5
6.0
WT aa bb dd aabb aadd bbdd aabbdd
wild type
NAM-2 single mutant
NAM-2 double mutant
NAM-2 triple mutant

*Figure 2.18 Some NAM-2 mutants showed increased thousand kernel weight in X50, with no differences within X61. (A, B) Thousand kernel weight (g); (C, D) Average grain length (mm). (A, C) 2022 Experiment. (B, D) 2023 Experiment. (A-D) ANOVA with post-hoc Tukey test, formula ~ Row + Block + Cross*Genotype, letters show significance groups at p<0.05. In graphs for X50, the "aabb" genotype derived from X54.*

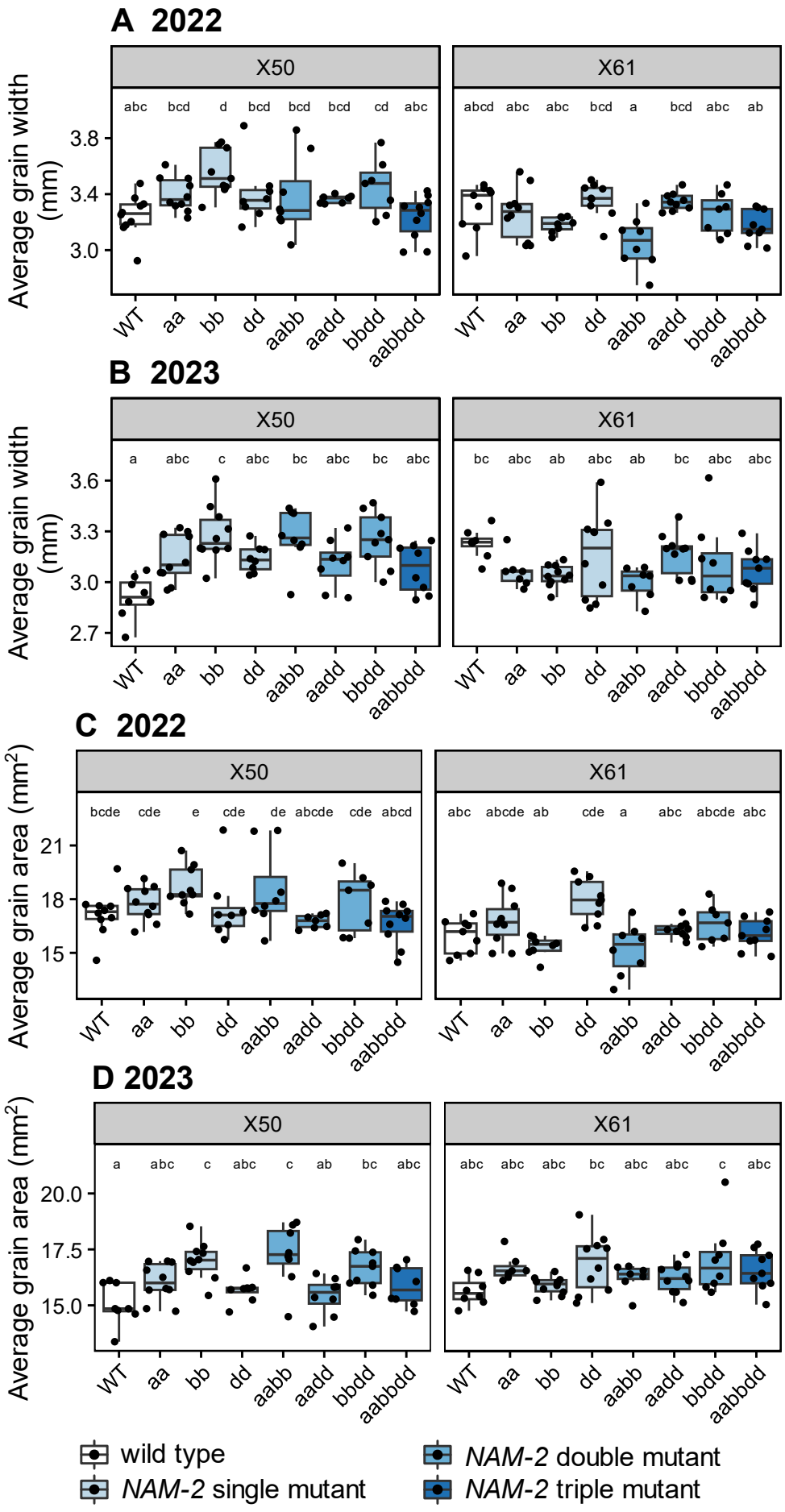

A 2022
X50
X61
Average grain width (mm)
3.8
3.4
3.0
abc bcd d bcd bcd bcd cd abc
abcd abc abc bcd a bcd abc ab
WT aa bb dd aabb aadd bbdd aabbdd
B 2023
3.6
3.3
3.0
2.7
a abc c abc bc abc bc abc
bc abc ab abc ab bc abc abc
C 2022
Average grain area (mm²)
21
18
15
bcde cde e cde de abcde cde abcd
abc abcde ab cde a abc abcde abc
D 2023
20.0
17.5
15.0
a abc c abc c ab bc abc
abc abc abc bc abc abc c abc
wild type
NAM-2 single mutant
NAM-2 double mutant
NAM-2 triple mutant

*Figure 2.19 NAM-2 lines show some variability in grain width and area. (A, B) Average grain width (mm); (C, D) Average grain area (mm^2). (A, C) 2022 Experiment. (B, D) 2023 Experiment. (A-D) ANOVA with post-hoc Tukey test, formula ~ Row + Block + Cross*Genotype, letters show significance groups at $p<0.05$. In graphs for X50, the "aabb" genotype derived from X54.*

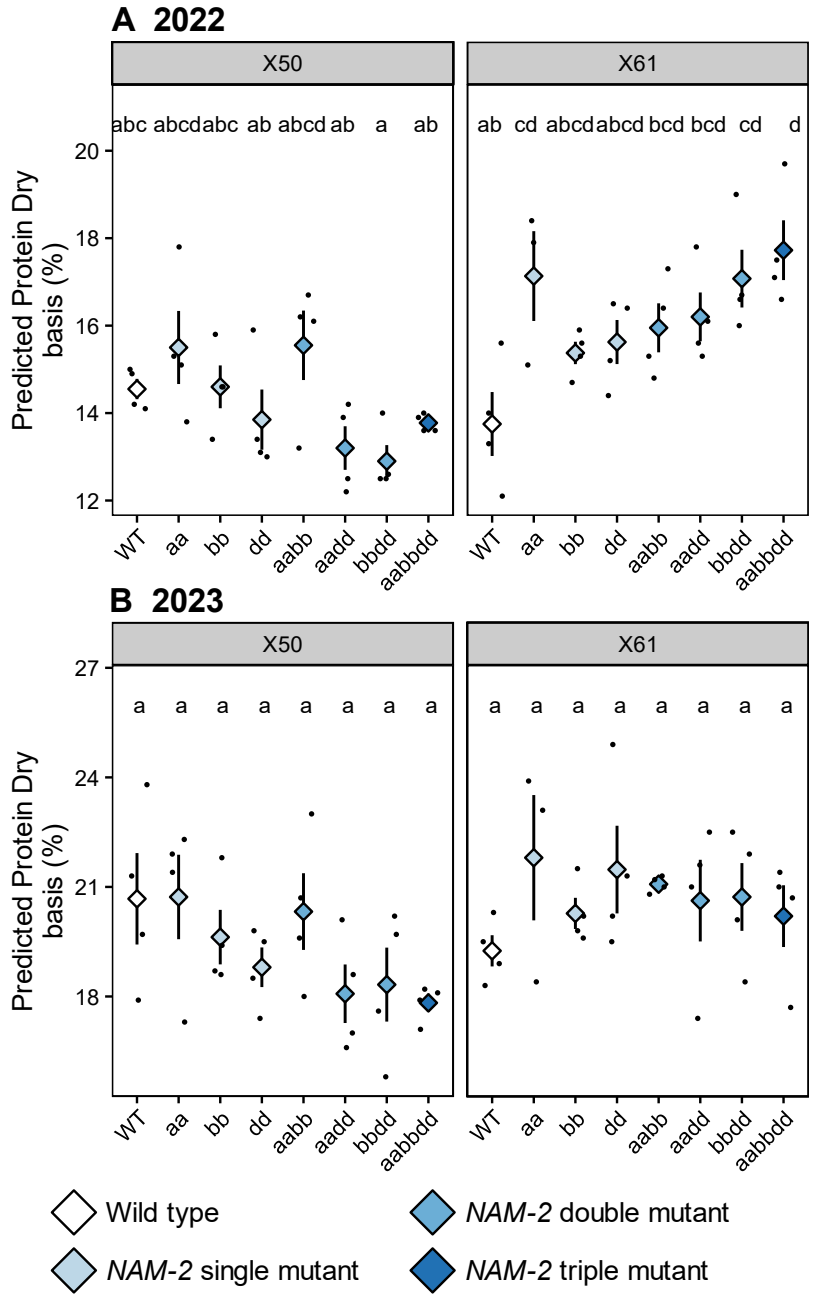


*Figure 2.20 NAM-2 triple mutants showed increased grain protein content compared to controls in X61 in 2022, but not in other experiments. (A) Predicted grain protein content (%) in 2022; (B) Predicted grain protein content (%) in 2023. (A-D) ANOVA with post-hoc Tukey test, formula ~ Row + Block + Cross*Genotype, letters show significance groups at p<0.05. In graphs for X50, the "aabb" genotype derived from X54. Diamonds and bars represent mean and standard error.*

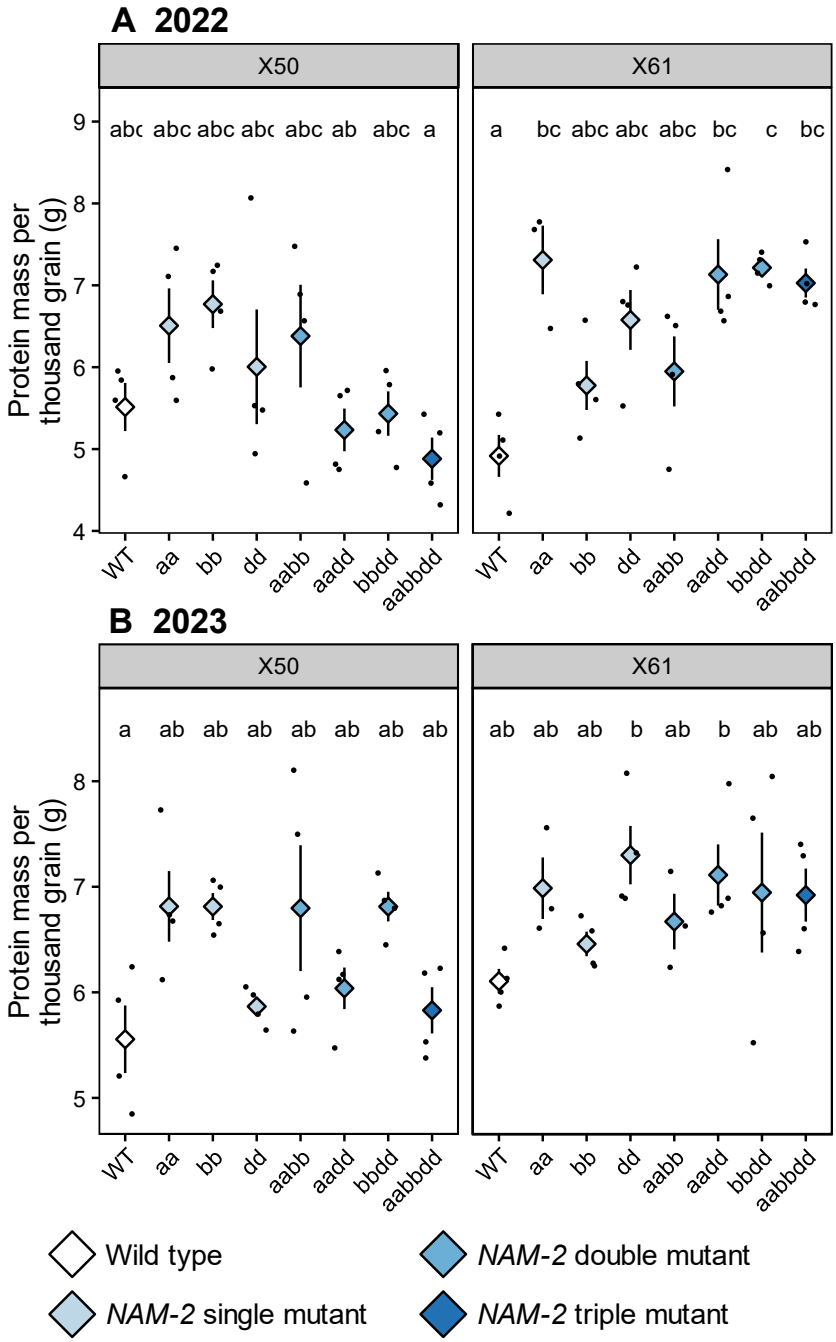


*Figure 2.21 Normalising for thousand grain weight accounts for differences in protein content between 2022 and 2023. (A) Predicted protein mass per thousand grains (g) in 2022; (B) Predicted protein mass per thousand grains (g) in 2023. (A-D) ANOVA with post-hoc Tukey test, formula ~ Row + Block + Cross*Genotype, letters show significance groups at p<0.05. In graphs for X50, the "aabb" genotype derived from X54. Diamonds and bars represent mean and standard error.*

2.3.6 Effect of Cross and blocking factors on *NAM-2* dataset

Phenotypic variables were analysed with Row and Block as blocking factors, to account for spatial variability in the environment which may affect senescence. Row represented the distance from plants to glasshouse lights in 2022, and to a lesser extent in 2023. Row accounted for significant variability in thousand kernel weight in 2022, with reduced kernel weight in the row furthest from the lights (*Table 2.21*). Otherwise, row did not account for significant variation in any phenotypes except peduncle senescence in 2022 and grain mass in 2023, with borderline p-values of 0.042 and 0.043 (*Table 2.21*). Similarly, block did not account for significant variation in any phenotype (*Table 2.21*). Overall, this demonstrates that phenotypes, and by implication environmental conditions, were spatially uniform in these experiments.

Cross (X50 versus X61) impacted multiple phenotypes, with significant variation explained through either main effect or interaction with genotype for all traits except flag leaf length and kernel weight in 2023 and Heading date, Height, flag leaf length, tiller number and all grain traits in 2022 (*Table 2.21*). In some cases, the main effect of Cross was stronger than the main effect of Genotype or the interaction. In 2022, cross X61 showed later heading than cross X50, and higher protein content (*Figure 2.12*, Figure 2.20). In 2023, X61 showed slightly longer duration of leaf senescence, slightly later peduncle senescence, reduced primary tiller height, slightly reduced tiller number, and reduced flag leaf width (*Figure 2.13*, *Figure 2.14*, *Figure 2.15*, *Figure 2.16*). X61 also showed reduced seed number, reduced seed mass, and slightly increased protein content compared to X50 in 2023 (Figure 2.17, Figure 2.20). Because of these differences, all data were shown separately for X50 and X61.

*Table 2.21 P-values from Analysis of Variance of NAM-2 glasshouse experiments. Variables were analysed with formula ~ Row + Block + Cross*Genotype. Degrees of freedom for each explanatory factor in brackets. Significant p-values (threshold 0.05) in bold. Grain protein content was analysed with formula ~ Cross*Genotype, as seed from two plants was pooled for each measurement.*

Year	Variable	Row (1df)	Block (1df)	Cross (1df)	Genotype (7df)	Cross: Genotype (7df)
2022	Heading_date	0.752	0.581	**4.46E-09**	**0.012**	**8.97E-04**
2022	Leaf_senescence_DAH	0.340	0.269	0.259	**7.32E-04**	0.388
2022	TT_SPAD30	0.965	0.682	0.153	**9.12E-05**	0.156
2022	Dur_Leaf_Sen	0.831	0.137	0.434	0.245	0.105
2022	AUC_Leaf_Sen	0.688	0.302	0.793	**1.32E-05**	0.110
2022	Peduncle_senescence_DAH	**0.042**	0.912	0.285	0.074	0.614
2022	Height	0.581	0.892	0.061	**3.93E-04**	**6.34E-05**
2022	Flag_leaf_length	0.366	0.785	0.154	0.507	**0.019**
2022	Tiller_1	0.540	0.627	0.344	**3.48E-04**	**1.89E-06**
2022	Seed_number	0.984	0.194	0.086	**2.06E-06**	**9.60E-07**
2022	Seed_mass	0.142	0.159	0.051	**3.62E-05**	**4.15E-05**
2022	TKW	**7.19E-03**	0.823	0.595	**2.27E-03**	**0.018**
2022	O_length	0.084	0.747	0.128	**1.61E-06**	**4.46E-10**
2022	Protein			**9.29E-08**	**0.016**	**7.34E-04**
2023	Heading_date	0.923	0.317	0.373	**0.047**	**1.84E-03**
2023	Leaf_senescence_DAH	0.616	0.617	0.796	**0.046**	**6.45E-04**
2023	TT_SPAD30	0.655	0.611	0.818	0.117	**1.90E-04**
2023	Dur_Leaf_Sen	0.771	0.419	**0.029**	0.724	0.373
2023	AUC_Leaf_Sen	0.643	0.680	0.079	0.209	**2.11E-03**
2023	Peduncle_senescence_DAH	0.877	0.071	**5.24E-03**	**0.024**	0.252
2023	Height	0.872	0.610	**6.68E-06**	0.396	0.154
2023	Flag_leaf_length	0.997	0.110	0.175	0.729	0.401
2023	Tiller_1	0.474	0.122	**0.021**	0.494	0.175
2023	Flag_leaf_width	0.298	0.086	**1.85E-11**	0.285	**0.016**
2023	Seed_number	0.086	0.747	**6.80E-06**	0.050	0.425
2023	Seed_mass	**0.043**	0.656	**5.96E-04**	0.853	0.600
2023	TKW	0.986	0.390	0.271	0.165	**3.51E-03**
2023	O_length	0.905	0.743	**<2E-16**	**<2E-16**	**<2E-16**
2023	Protein			**3.73E-03**	0.292	0.306

2.3.7 Field trials of *NAM-2* TILLING lines

To assess how loss-of-function of *NAM-2* affects senescence timing in field conditions, *NAM-2* TILLING mutant lines were grown in the field in 2023. Temperature data was collected for calculation of thermal time. The daily air temperature at Church Farm was on average 12.4°C between 1st May 2023 and 9th June 2023 (*Figure 2.22*). After this, temperatures increased, averaging 18.6°C between 10th June 2023 and 31st July 2023. For context, heading occurred between 31st May 2023 and 13th June 2023, all plots had reached 10% leaf yellowing by 6th July 2023 and all plots had reached 100% leaf yellowing by 24th July 2023 (*Figure 2.22*).

No obvious spatial pattern was observed for phenotyped traits along x-axis (Block) or y-axis, as shown for thermal time to 70% leaf senescence (*Figure 2.23*). Given the lack of spatial pattern and small sample size, Block was omitted as a factor to maintain degrees of freedom. Grain mass and GPC were not presented for this trial, due to the likelihood of low data reliability from a combination of variable plot cover and lodging between the end of senescence and harvest.

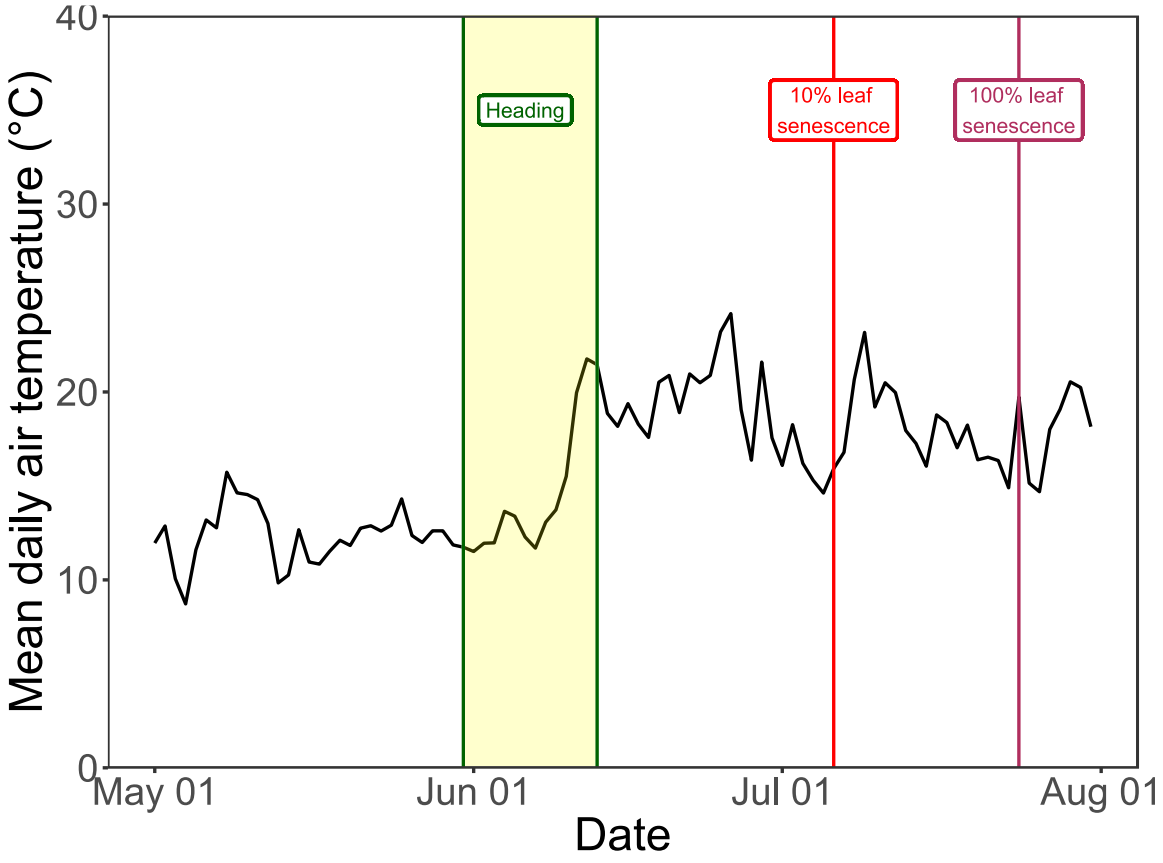


Figure 2.22 Mean daily air temperature at JIC Church Farm weather station from 01/05/2023 to 31/07/2023. NAM-2 TILLING lines were grown in the field at JIC Church Farm in the 2023 season. Air temperature was averaged across a 24-hour period. Annotations mark the time interval of heading, and dates when all plots had reached 10% and 100% leaf senescence.

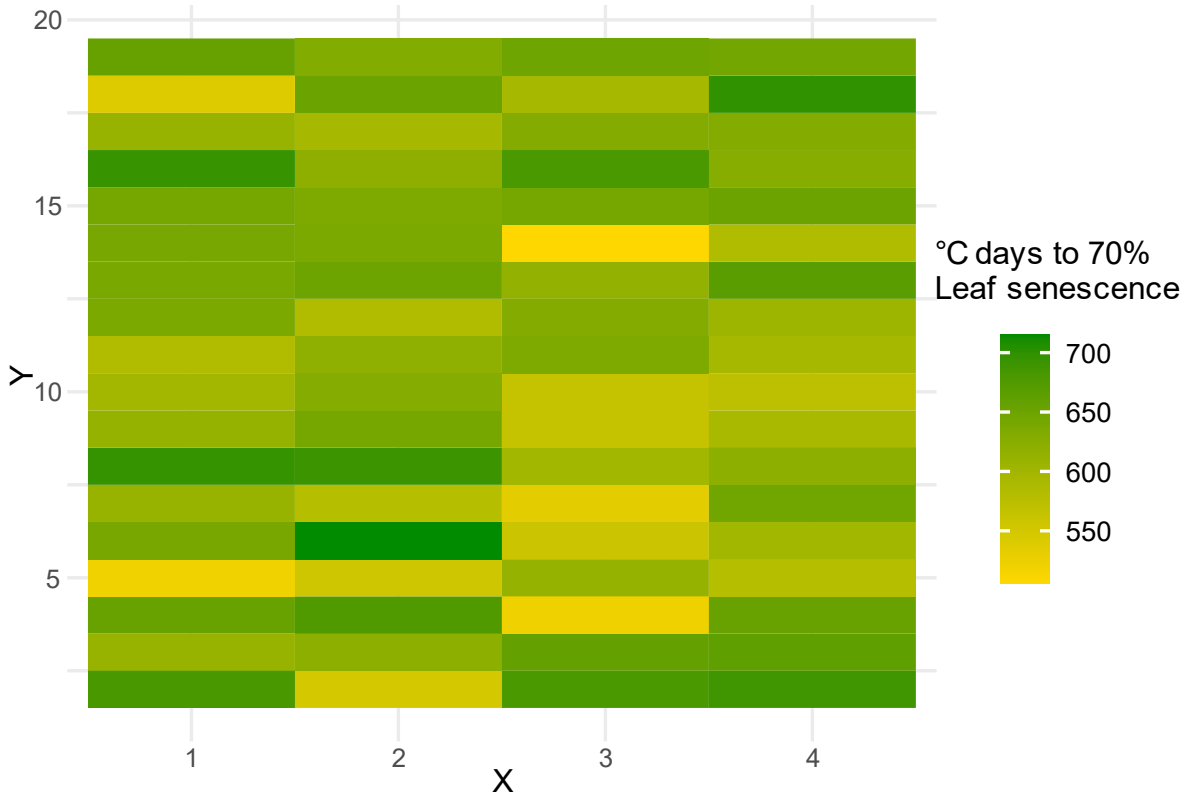


Figure 2.23 Thermal time to 70% leaf senescence does not show an obvious spatial pattern. Tile plot shows thermal time to 70% leaf senescence (°C days) of each 1m^2 plot as arranged in the field. Each x-axis column represents one block.

The percentage of the 1m plot covered with wheat plants in March differed significantly between TILLING lines, although non-mutagenized Cadenza showed 80-100% coverage (*Figure 2.24*A). Lines in cross X50 “WT”, “bb”, “dd” and “bbdd”, and lines in cross X61 “WT”, “bbdd” and “aabbdd” had significantly reduced coverage (*Figure 2.24*A). The same seven lines had a height of around 20cm on 5th May, compared to around 40cm in non-mutagenized Cadenza (*Figure 2.24*B). As wild-type TILLING lines were among those with reduced height and coverage, this phenotype has no relation to mutation in *NAM-2*.

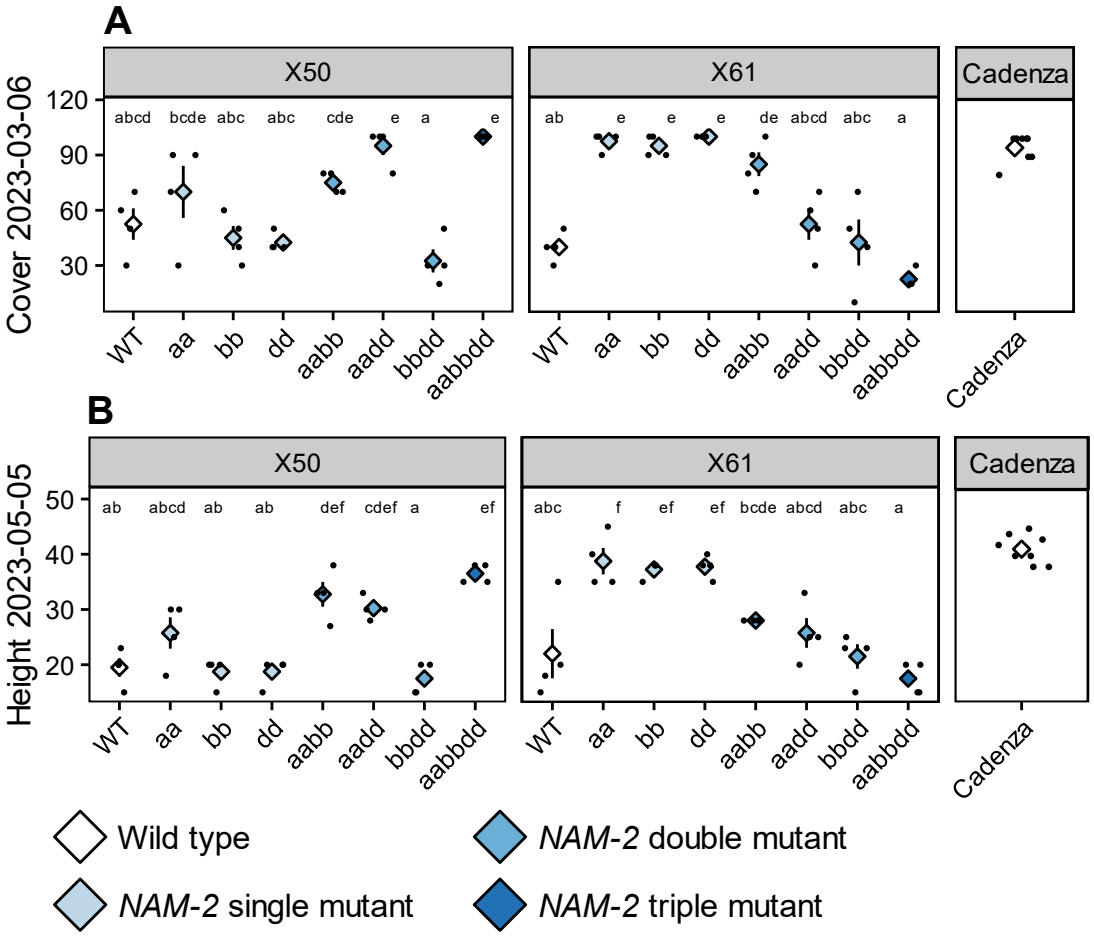


*Figure 2.24 Seedling establishment significantly differed between NAM-2 TILLING lines, however this did not relate to the number of functional copies of NAM-2. (A) Percentage of 1m^2 plot covered with plants in March; (B) Average height across plot (cm) in May. (A, B, C, D) Analysed by ANOVA with post-hoc Tukey test, formula ~ Cross*Genotype, p<0.05. In graphs for X50, the "aabb" genotype derived from X54. Diamonds and bars represent mean and standard error. Non-mutagenized Cadenza (right hand panel) not included in statistical analysis.*

Differences in plant establishment began early in the growing season. In November, seedling vigour (a combination of seedling size and number of seedlings per plot) was qualitatively categorized into Good, OK and Poor. Plots in the OK category had significantly reduced cover in March compared to the Good category, while seedlings in the Poor category had reduced cover compared to the OK category (*Figure 2.25*A). This shows that the reduced cover may be due to failed germination or death

of seedlings within two months of drilling. Both OK and Poor vigour plots had reduced height in May (*Figure 2.25*B). This indicates that the plants had a slower rate of development, as they remained in the tillering phase while Good vigour plants had entered the stem elongation phase. Thus, these categories simply express seedling establishment and rate of development.

Good vigour plots showed earlier heading (ear emergence), and higher AUC of leaf senescence indicating earlier senescence relative to heading (*Figure 2.25*C, D). There were no differences in duration of leaf senescence (*Figure 2.25*E). Both Good and Poor vigour plots reached 30% and 90% leaf senescence later than OK vigour plots (*Figure 2.25*F, G). On 17th July, more peduncles were senesced among Good vigour plots (*Figure 2.25*H). This shows that while, on average, Good vigour plots had slightly later senescence relative to heading, they senesced earlier in absolute time because heading was notably earlier.

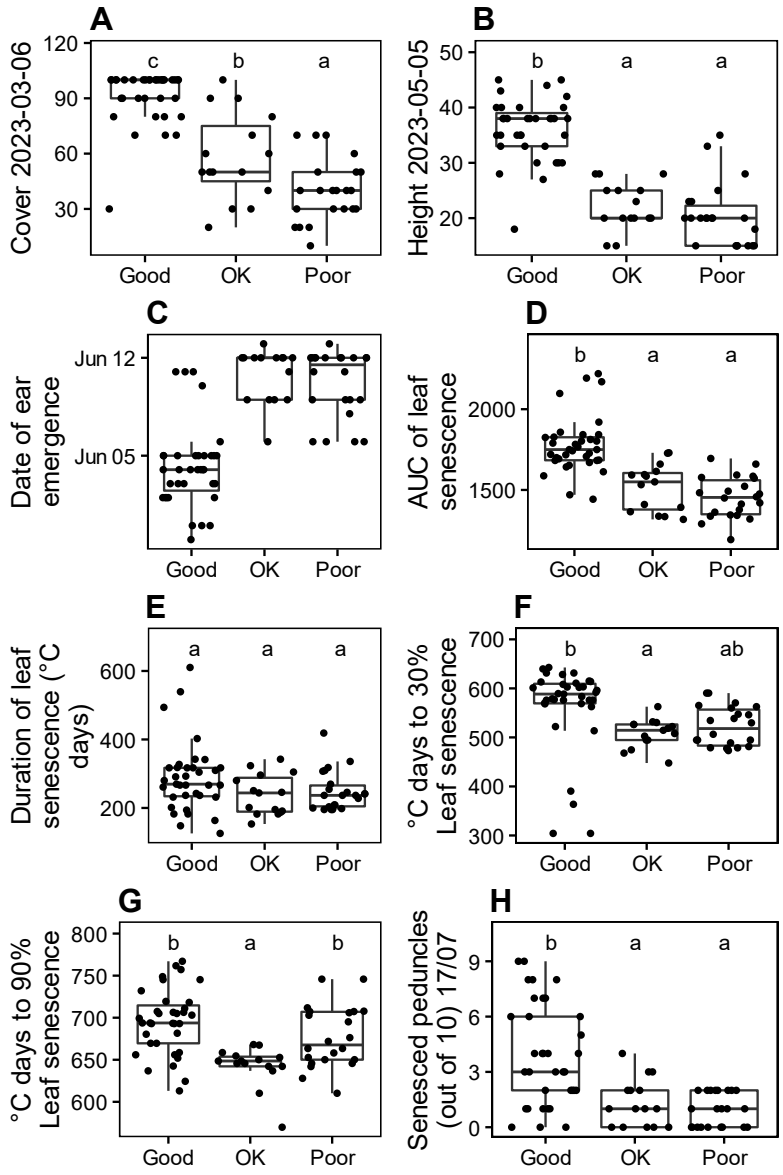


Figure 2.25 Poor seedling establishment correlated with late heading, earlier 30% leaf senescence relative to heading, and later peduncle senescence in absolute time. Seedling vigour in November was categorised: Good = many large seedlings, similar to guard plots (Soissons). OK = several medium seedlings. Poor = few small seedlings, empty gaps in plot. Seedling vigour plotted against (A) Percentage of 1m^2 plot covered with plants in March; (B) Average height across plot (cm) in May; (C) Date of ear emergence; (D) Area under curve (AUC) of leaf senescence; (E) Duration of leaf senescence; (F) Thermal time to 30% leaf senescence (°C days); (G) Thermal time to 90% leaf senescence (°C days); (H) Number of senesced peduncles out of 10 on 17/07/2023. (A-H) Analysed by ANOVA with post-hoc Tukey test, formula ~ Vigour.2023-11-10, p<0.05.

2.3.8 Senescence data for field trials

To explore how *NAM-2* affects senescence in the field, a time-course of leaf yellowing was scored visually in *NAM-2* triple mutant lines and controls from crosses X50 and X61 (*Figure 2.26*). As an “aabb” mutant was not available from X50, an “aabb” mutant with the same original TILLING mutations derived from cross X54 was used instead. X54 “aabb” appeared taller, with a wider tiller angle and more twisted leaves than other lines (*Figure 2.26*). All other single and double mutants from X50 and X61 were also included (not shown).

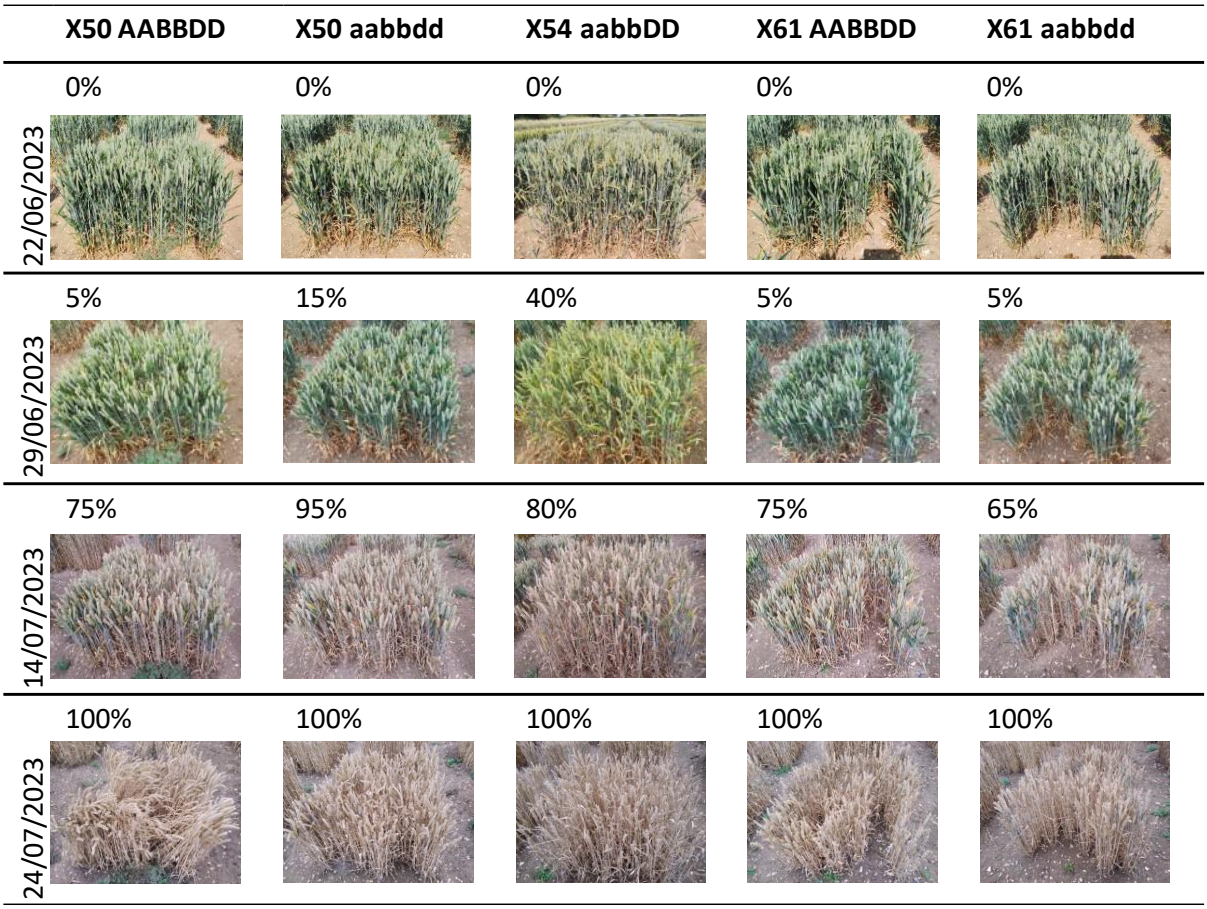


Figure 2.26 Representative field plots from NAM-2 field trial. Field plots from replicate 2 photographed from the same angle before, during and after leaf senescence. Dates on left hand side; cross and genotype above. Percentage leaf yellowing for each plot is shown above the photograph.

Notably, the same seven lines with reduced coverage also showed later heading (X50 “WT”, “bb”, “dd” and “bbdd”, and X61 “WT”, “bbdd” and “aabbdd”) (*Figure 2.27*). *NAM-2* triple mutants headed 9 days earlier than wild-type sibling lines (*Figure 2.27*).

NAM-2 triple mutants from X50 showed delayed leaf yellowing compared to the corresponding control line, but there was no difference in X61(*Figure 2.28*). To assess peduncle senescence, the number of completely yellowed peduncles was counted out of ten picked at random (Chapman et al. 2021a). *NAM-2* triple mutants from X50 reached 10/10 peduncles senesced earlier relative to heading (*Figure 2.29*). In X61, peduncle senescence did not differ between *NAM-2* triple mutants and controls (*Figure 2.29*).

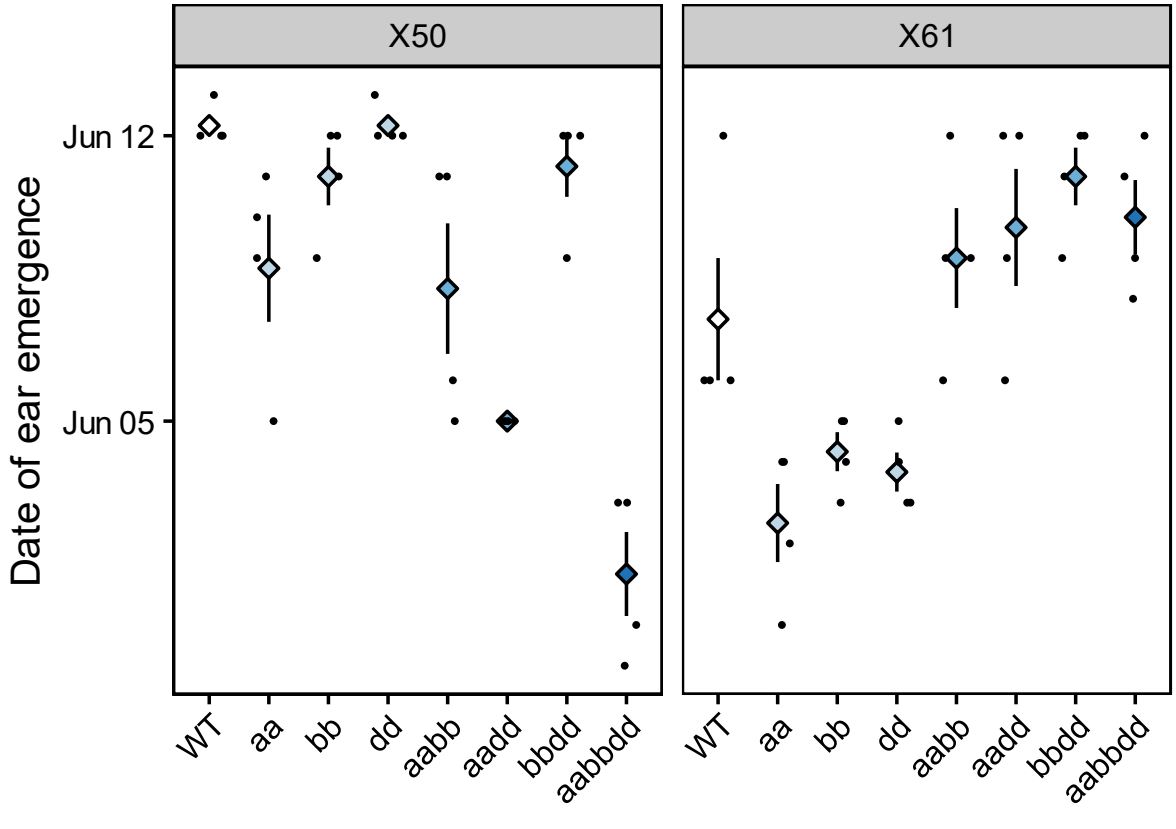


Figure 2.27 NAM-2 TILLING lines vary in heading (ear emergence) date in the field. In graphs for X50, the “aabb” genotype derived from X54. Diamonds and bars represent mean and standard error.

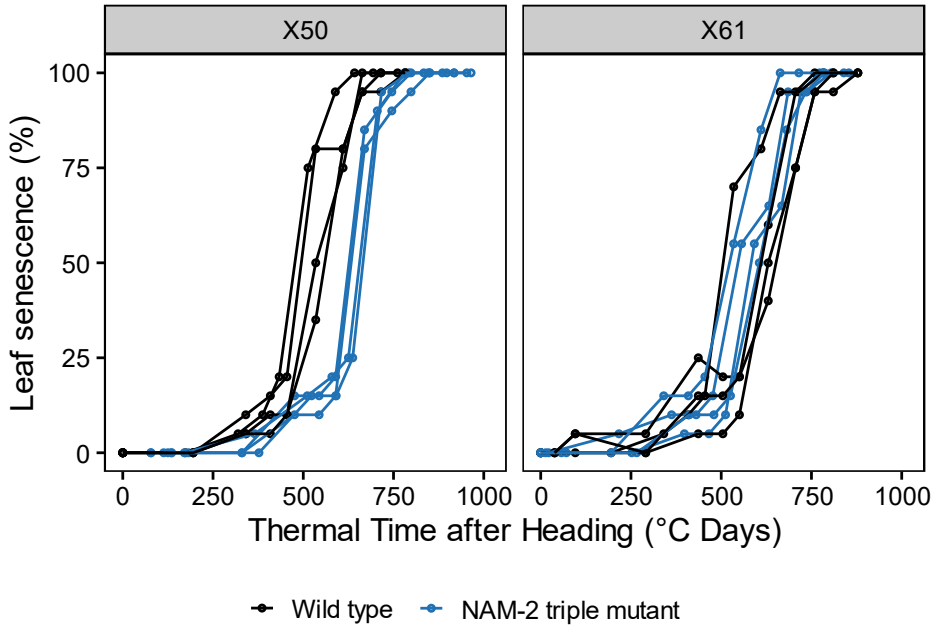


Figure 2.28 NAM-2 triple mutant lines showed later leaf senescence than controls in cross X50 but not cross X61 in the field. Percentage leaf yellowing scored visually, for each 1m^2 plot, against thermal time after heading (°C days).

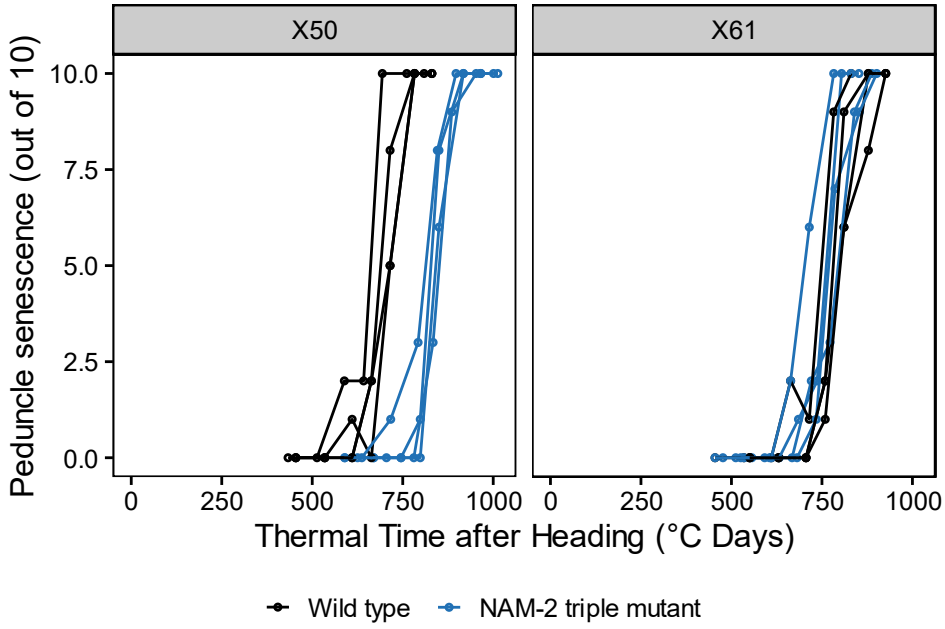


Figure 2.29 NAM-2 triple mutant lines showed later peduncle senescence than controls in cross X50 but not cross X61 in the field. Number of senesced peduncles out of 10, for each 1m^2 plot, against thermal time after heading (°C days).

Line X54 “aabb” had a significantly higher AUC of leaf senescence and duration of leaf senescence than all other lines (*Figure 2.30*A, B). The longer duration of senescence occurred because X54 “aabb” had an earlier onset of leaf senescence, reaching 10% and 30% leaf senescence earlier than all other lines (*Figure 2.30*C, D). Meanwhile, the termination of leaf senescence was not changed, as X54 “aabb” reached 90% leaf senescence at a similar time to other lines (*Figure 2.31*C). Together with the distinct appearance of the plants (*Figure 2.26*), this suggests that line X54 “aabb” cannot be compared alongside lines from cross X50.

For X50 *NAM-2* triple mutants and “aadd” double mutants showed higher AUC of leaf senescence than the control, while for X61 *NAM-B2* and *NAM-D2* single mutants had higher AUC of leaf senescence (*Figure 2.30*A). Excepting X54 “aabb”, the duration of leaf senescence and thermal time to 10% leaf senescence did not differ between lines (*Figure 2.30*B, C). X50 *NAM-2* triple mutants were delayed in reaching 30%, 50%, 70% and 90% leaf senescence, X50 “aadd” double mutants showed delayed 30% and 50% leaf senescence, and X61 “aa” single mutants showed delayed 30% leaf senescence compared to corresponding controls (*Figure 2.30*D, *Figure 2.31*A, B, C). For X61, double and triple mutants showed a trend toward earlier 50% leaf senescence than single mutants and controls, but it was not significant (*Figure 2.31*A). The number of senesced peduncles on 20th July was highest in the triple mutant and lowest in the “dd” single mutant for X50, and highest in the “aa” single mutant and lowest in the “aadd” and “bbdd” double mutants and the triple mutant for X61 (*Figure 2.31*D).

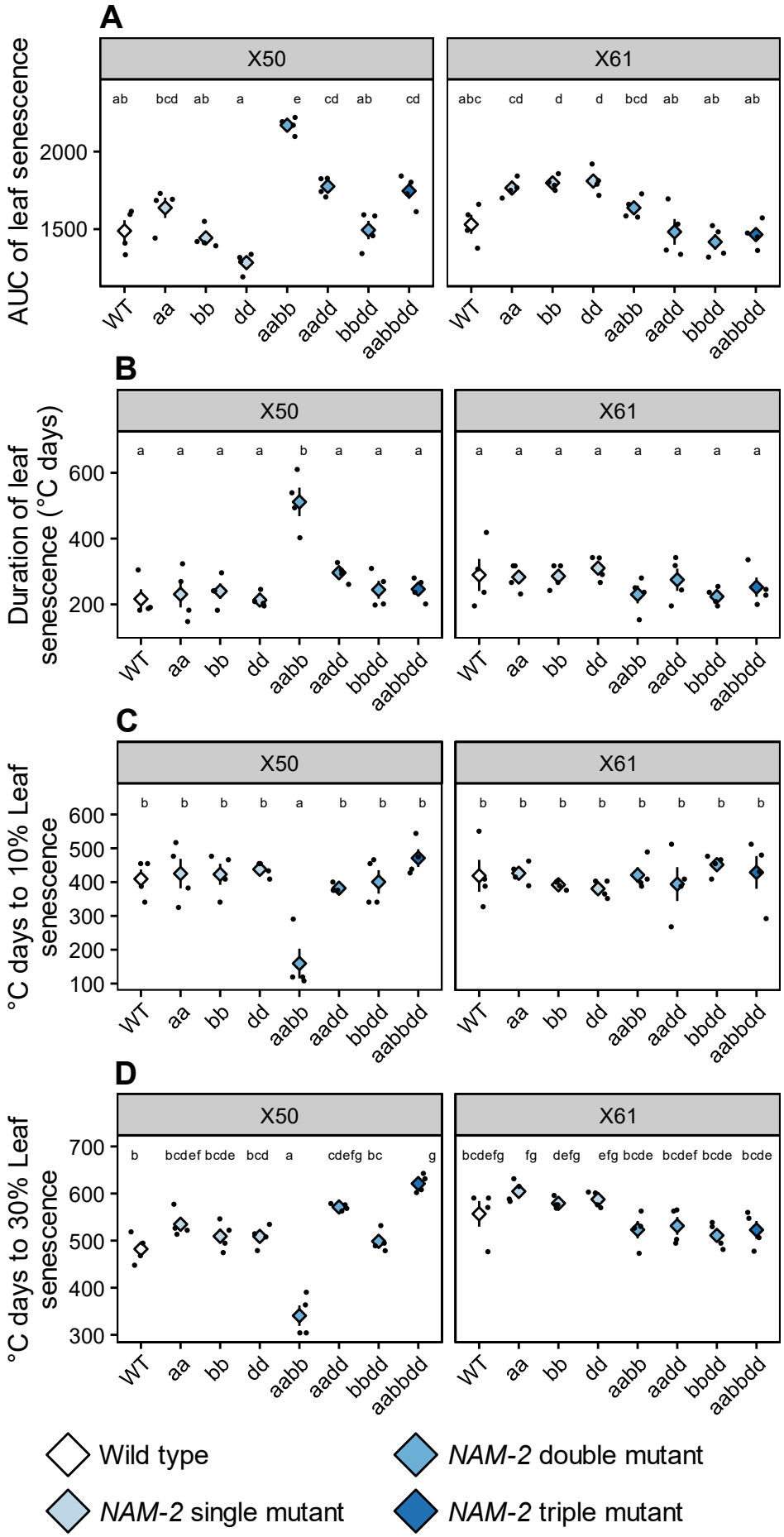

A
X50
X61
AUC of leaf senescence
2000
1500
ab bcd ab a e cd ab cd
abc cd d d bcd ab ab ab
B
Duration of leaf senescence (°C days)
600
400
200
a a a a b a a a
a a a a a a a a
C
°C days to 10% Leaf senescence
600
500
400
300
200
100
b b b b a b b b
b b b b b b b b
D
°C days to 30% Leaf senescence
700
600
500
400
300
b bcdef bcde bcd a cdefg bc g
bcdefg fg defg efg bcde bcdef bcde bcde
WT
aa
bb
dd
aabb
aadd
bbdd
aabbdd
Wild type
NAM-2 double mutant
NAM-2 single mutant
NAM-2 triple mutant

*Figure 2.30 NAM-2 X50 "aabb" showed earlier onset and longer duration of senescence, while AUC of leaf senescence varied between NAM-2 TILLING lines. (A) Area under curve (AUC) of leaf senescence; (B) Duration of leaf senescence; (C) Thermal time to 10% leaf senescence (°C days); (D) Thermal time to 30% leaf senescence (°C days). (A, B, C, D) Analysed by ANOVA with post-hoc Tukey test, formula ~ Cross*Genotype, p<0.05. In graphs for X50, the "aabb" genotype derived from X54. Diamonds and bars represent mean and standard error.*

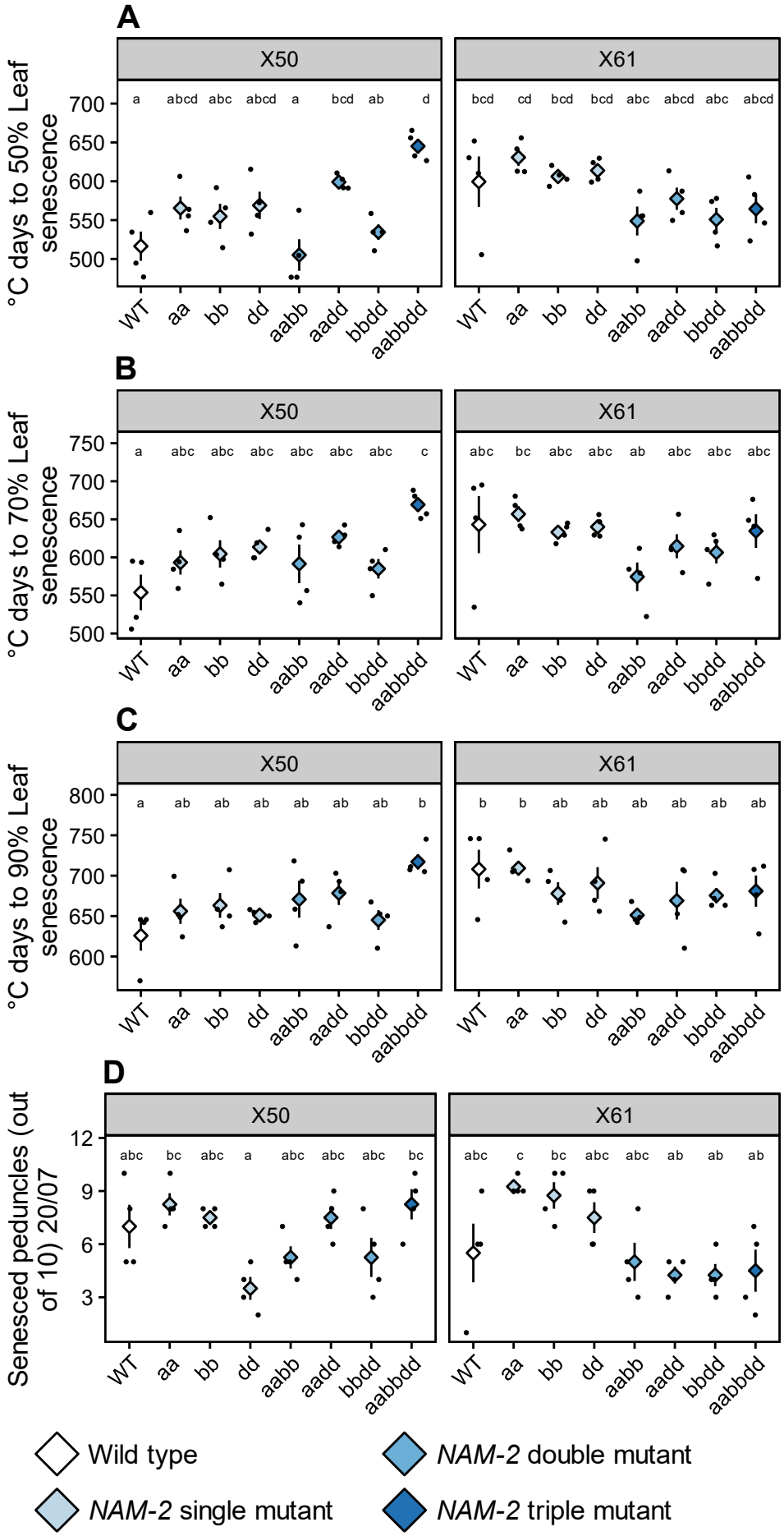

A
X50
X61
°C days to 50% Leaf senescence
700
650
600
550
500
a abcd abc abcd a bcd ab d
bcd cd bcd bcd abc abcd abc abcd
WT aa bb dd aabb aadd bbdd aabbdd
B
°C days to 70% Leaf senescence
750
700
650
600
550
500
a abc abc abc abc abc abc c
abc bc abc abc ab abc abc abc
C
°C days to 90% Leaf senescence
800
750
700
650
600
a ab ab ab ab ab ab b
b b ab ab ab ab ab ab
D
Senesced peduncles (out of 10) 20/07
12
9
6
3
abc bc abc a abc abc abc bc
abc c bc abc abc ab ab ab
Wild type
NAM-2 double mutant
NAM-2 single mutant
NAM-2 triple mutant

*Figure 2.31 NAM-2 X50 triple mutants reached 50% 70% and 90% leaf senescence later than controls. (A) Thermal time to 50% leaf senescence (°C days); (B) Thermal time to 70% leaf senescence (°C days); (C) Thermal time to 90% leaf senescence (°C days); (D) Number of senesced peduncles out of 10 on 20/07/2023. (A, B, C, D) Analysed by ANOVA with post-hoc Tukey test, formula ~ Cross*Genotype, p<0.05. In graphs for X50, the "aabb" genotype derived from X54. Diamonds and bars represent mean and standard error.*

2.4 Discussion

The objective of this chapter was to test the effect of loss-of-function of *NAM-2* in hexaploid wheat. Two independent lines with mutations in all homoeologs of *NAM-2* were successfully generated. It follows that if a phenotype is observed in both triple mutant lines, compared to wild-type sibling lines, that this phenotype results from mutation of *NAM-2* (Krasileva et al. 2017).

2.4.1 Unravelling inconsistent senescence phenotyping data

To test the effect of mutations in *NAM-2* on senescence, hexaploid *NAM-2* TILLING lines were grown in two glasshouse experiments and one field trial. Cross X50 contained stop codons in all homoeologs of *NAM-2*, predicted to lead to a truncated protein lacking subdomains iv and v of the NAC domain. *NAM-2* triple mutants of cross X50 showed delayed leaf senescence and trended toward delayed peduncle senescence in the glasshouse in 2023 and in the field in 2023, but did not differ in senescence from controls in the glasshouse in 2022. Cross X61 contained a missense mutation in a conserved residue of the NAC domain of *NAM-A2,* and stop codons in subdomain v of *NAM-B2* and subdomain ii of *NAM-D2*, predicted to lead to truncated peptides. *NAM-2* triple mutants of cross X61 showed later leaf senescence in the glasshouse in 2022, earlier leaf senescence in the glasshouse in 2023, and no

significant difference in the field. How can these inconsistent phenotypes be understood?

Multiple environmental factors can accelerate leaf senescence: drought, darkness, nitrogen limitation, pathogen infection and wounding (Yang and Zhang 2006; Schippers 2015; Lim, Kim,Nam 2007). Within both glasshouse and field experiments, phenotypes were not skewed by spatial variation in environmental factors. Spatial variation was accounted for in the randomized complete block design, and in the glasshouse experiments, blocking factors generally did not contribute to explaining phenotypic variation, showing that the environment was uniform. Nevertheless, environmental conditions differ between glasshouse and field, and the glasshouse reached higher temperatures in the 2023 experiment than the 2022 experiment. Apart from a few outliers, the duration of senescence was shorter in 2023 than 2022, implying more rapid senescence under higher temperatures.

In the field, seven out of sixteen TILLING lines had reduced plot cover, noticeable from an early seedling stage onwards, and delayed stem elongation (X50 “WT”, “bb”, “dd” and “bbdd”, and X61 “WT”, “bbdd” and “aabbdd”). The same seven lines showed delayed heading of 2-9 days, and decreased AUC of leaf senescence indicating overall earlier senescence relative to heading. Number of senesced peduncles on 20th July was either not significantly different or fewer. Overall, this indicates that compared to other TILLING lines and Cadenza, these seven lines senesced at the same time or later relative to sowing, but earlier relative to heading because heading was delayed. This phenotype of reduced germination or seedling survival and delayed growth was not observed in the glasshouse, and does not relate to *NAM-2,* as these lines included X50 wild-type, X61 wild-type and X61 triple mutants. It is possible that these lines contain background mutations which are

detrimental only under field conditions. Thus, it is probable that delayed senescence between X50 triple mutants and controls is an artifact of delayed heading of the X50 control.

Another case was the *nam-a2/nam-b2* mutant from X54. Although it derived from the same three original TILLING lines as X50, this line consistently showed distinct phenotypes to all the X50 lines. X54 “aabb” headed later and had increased grain length in both glasshouse experiments. This line grew taller in the glasshouse in 2022, had a wider tiller angle in the glasshouse in 2023, and appeared to also show these traits in the field. It showed earlier 10% leaf senescence and longer duration of leaf senescence in the field - although as the early stages of leaf senescence were hard to distinguish from *Septoria* infection, this might instead reflect susceptibility to *Septoria.* It is suggested that one or more background mutations led to these phenotypes, and that during the crossing program and subsequent rounds of selfing, these mutations were fixed in X54 but not in X50. In conclusion, this line from X54 cannot be compared with X50 lines in the context of *NAM-2.*

Together, these two occurrences illustrate that background mutations are a drawback of using TILLING populations. Cadenza TILLING lines contain, on average, 5,351 mutations in exons per line, so the single backcross lines in this experiment would contain around half as many (Krasileva et al. 2017). This issue could be overcome by generating a population with multiple backcrosses, halving the mutation load with each backcross – for example the effect of the *gw2-a1* mutation on grain weight was confirmed by testing in BC_2 and BC_4 backgrounds (Uauy, Wulff,Dubcovsky 2017; Simmonds et al. 2016). To test lines in the field, backcrosses could be made against a parent known to perform well in the target field conditions.

2.4.2 There is some evidence that *NAM-2* promotes earlier senescence

Based on cross X50, there is some evidence that loss-of-function of *NAM-2* is associated with delayed senescence. In the glasshouse in 2023, triple mutants retained higher chlorophyll content than controls, double “bbdd” mutants showed a later onset of senescence, measured as both days to a SPAD of 30 and days to 25% leaf senescence, and all *NAM-2* mutant lines showed a non-significant trend toward higher AUC and later peduncle senescence. Little difference in senescence timing was seen in the glasshouse in 2022. In the field, X50 triple mutants headed earlier and reached 30% leaf senescence later after heading than *nam-a2* single mutants which had similar plot cover. Overall, this suggests that stop codons in all copies of *NAM-2* can lead to delayed leaf and peduncle senescence.

For cross X61, *NAM-2* triple mutants reached onset of leaf senescence marginally later than controls in 2022 and earlier in 2023, and did not differ from controls in peduncle senescence in 2023. *NAM-2* single and double mutants showed a similar onset of leaf senescence as triple mutants in both years. In 2023, *NAM-2* mutant lines from X61 reached peduncle senescence shortly after, or at a similar time to, onset of leaf senescence. However, some control plants from X61 reached peduncle senescence before leaf senescence, resulting in an unusual phenotype of a green flag leaf with a yellowed ear and peduncle. If peduncle yellowing reduces or terminates nutrient export to the grain through the peduncle, this could potentially have the effect of further delaying leaf senescence. When half of the spikelets are removed from a wheat ear, the leaves senesce more slowly (Lv et al. 2020b). The mechanism for this could be a reduction in nitrogen demand and decrease in the C:N ratio of the flag leaf, given that wheat senesces faster under sugar excess and under

nitrogen deficiency (Distelfeld, Avni,Fischer 2014; Kong et al. 2016; Lv et al. 2020b). This suggests that something unusual may have occurred with the X61 control plants in 2023. By excluding this control, remaining evidence indicates that overall, mutations in *NAM-2* in X61 do not affect the timing of senescence.

In summary, mutation of *NAM-2* correlated with delayed leaf and peduncle senescence in one out of two mutant combinations, in two out of three experiments. This lends limited support to the hypothesis that *NAM-2* promotes earlier senescence – limited because the finding is based on a single TILLING mutant combination. This is somewhat in agreement with mutation of *NAM-2* in tetraploid wheat, which was associated with significantly delayed leaf and peduncle senescence (Borrill et al. 2019). It is also similar to mutation of *NAM-B2* along with *NAM-A1* using the same subdomain iii stop codon mutation, which led to a subtle delay in senescence in some experiments, and no effect in others (Distelfeld et al. 2012; Pearce et al. 2014). It is possible that in line X61, the missense mutation in *NAM-A2* or the later stop codon in *NAM-B2* did not lead to a complete loss-of-function, although unlikely as mutations in the same positions of *NAM-A2* and *NAM-A1* respectively were associated with a phenotypic effect (Borrill et al. 2019; Avni et al. 2014).

Specifically, *NAM-2* X50 TILLING lines had delayed onset of leaf senescence, but did not differ in duration from onset to completion of leaf senescence. This indicates that they may fall more into the “Type A” (late onset) than the “Type B” (slower rate) category of stay-green (Thomas and Howarth 2000). Future research could include measurements of functional photosynthetic capacity in *NAM-2* mutant lines, to verify whether retention of chlorophyll is accompanied by prolonged photosynthesis.

Nevertheless, it is likely that this is the case, as prolonged photosynthesis and chloroplast integrity occurs in *NAM* RNAi lines (Checovich et al. 2016).

Finally, given that these results and those of previous studies implicate both *NAM-2* and *NAM-1* in affecting senescence, it is likely that these closely related paralogs are redundant in function (Borrill, Harrington,Uauy 2019; Uauy et al. 2006). If *NAM-1* and *NAM-2* act redundantly, all six copies of *NAM-1* and *NAM-2* must be knocked out to quantify the full effect on senescence timing. One way to achieve this would be to cross together *NAM-2* TILLING mutants, generated in this chapter, with existing *NAM-1* TILLING mutants (Avni et al. 2014). Alternatively, *NAM-1* and *NAM-2* could be targeted using CRISPR gene editing (Borrill, Harrington,Uauy 2019). A caveat to both of these approaches would be that from a heterozygous plant with six segregating mutations, the probability of a full loss-of-function would decrease to 2^{-12}, or one plant in 4096. Thus, it would be impractical to generate sister lines of all genotypes from the same segregating population.

2.4.3 The impact of *NAM-2* on grain mass and protein content

How does *NAM-2* affect grain traits and protein content? In the glasshouse experiment where mutation of *NAM-2* delayed senescence (X50 in 2023), “bbdd” double mutants showed both delayed senescence onset and increased kernel weight, with a slight trend towards increased kernel weight in all mutant lines. Double and triple mutant lines showed a non-significant trend toward decreased protein content – however this trend was lost when protein content was normalised against kernel weight. This lends some support to the hypothesis that *NAM-2* promotes decreased kernel weight, but does not support the hypothesis that *NAM-2* promotes increased protein content, as reported for *NAM-1* (Uauy, Brevis,Dubcovsky 2006; Brevis and Dubcovsky 2010; Distelfeld et al. 2012).

Results for grain traits and protein content were mixed from the three other glasshouse experiments. The higher grain protein content in *NAM-2* mutant lines compared to controls in X61 in 2022 is opposite to the expected trend. This may be explained by the dilution effect: X61 control lines produced more tillers and grains in 2022, diluting the available nitrogen and reducing the protein content per grain. It should also be noted that across the 2023 experiment, thousand kernel weight was lower and protein content was higher than in 2022, with some protein contents recorded at over 20%. When protein content was normalised relative to thousand kernel weight, this fully accounted for the difference between 2023 and 2022. This implies that the observed high relative protein content derives from reduced starch accumulation, with no change in absolute protein accumulation. It is possible that in the 2023 experiment, frequent high temperatures during grain filling impaired starch accumulation, thereby reducing kernel weight and increasing relative protein content.

2.4.4 Conclusion

In conclusion, mutations with predicted loss-of-function of *NAM-A2, NAM-B2* and *NAM-D2* were successfully combined in hexaploid wheat. Loss-of-function of *NAM-2* delayed senescence in one out of two mutant lines, and two out of three experiments, indicating that *NAM-2* can be associated with earlier onset of leaf senescence and peduncle senescence. In one of the experiments where senescence was delayed, mutation of *NAM-2* increased kernel weight but did not have a consistent effect on protein content. This supports the hypothesis that *NAM-2* retains a conserved function with its paralog *NAM-1* to promote senescence in wheat but provides limited evidence for a role for *NAM-2* in the protein-yield trade-off. Conversely, the unchanged senescence timing in other experiments implies that *NAM-2* has a more subtle effect on senescence than *NAM-1*. Transcription factors

with subtle effects on senescence, including *NAM-2,* could still be useful to fine-tune senescence timing for the optimal balance of photosynthesis and nitrogen remobilization.

3 DO *NAC5-1* AND *NAP-1* AFFECT THE TIMING OF SENESCENCE?

3.1 Introduction: wheat orthologs of *OsNAC5* and *OsNAP* are candidate senescence regulators

This thesis sought to investigate the genetic regulation of senescence in wheat by focussing on NAC transcription factors. As 60% of senescence-related rice genes had similar expression patterns to their ortholog in wheat, there is a reasonable chance that wheat genes may retain a conserved function to their rice orthologs (Borrill et al. 2019). This chapter explores whether two NAC transcription factors known to be associated with leaf senescence in rice regulate leaf senescence in wheat.

3.1.1 *OsNAC5* plays a role in nutrient remobilization during senescence.

In rice, the NAC transcription factor *OsNAC5 / NAC071* (Os11g0184900) has been linked to both senescence and grain protein content (GPC). *OsNAC5* is upregulated during both age-induced leaf senescence and environmental stress-induced leaf senescence (Sperotto et al. 2009; Sharma et al. 2019). A cultivar of *Oryza sativa* ssp. *japonica* with high grain protein, iron, and zinc contents had higher expression of *OsNAC5* (Sperotto et al. 2009). Similarly, in *O. sativa* ssp. *indica,* a high-GPC rice cultivar expressed *OsNAC5* more highly in flag leaves during grain filling than a low-GPC cultivar (Sharma et al. 2019). Among recombinant inbred lines developed from these high-GPC and low-GPC cultivars, lines with higher protein content showed increased leaf and panicle *OsNAC5* expression, suggesting a direct genetic

correlation between *OsNAC5* expression and grain protein content (Sharma et al. 2019). *OsNAC5* overexpression lines had higher expression of a nicotianamine synthase *OsNAS2* and an iron-nicotianamine transporter *OsYSL2* (nicotianamine is a chelating agent required for systemic transport of metal ions such as iron) (Jeong et al. 2013). Together, these findings suggest that *OsNAC5* may be involved in promoting remobilization of nitrogen, iron and zinc to the grain during senescence (Ricachenevsky, Menguer,Sperotto 2013).

OsNAC5 is also known for its role in abiotic stress tolerance. Overexpression of *OsNAC5* increased survival of 3 days salt stress from 40% to 70%, increased survival of 4 days drought from 40% to 80%, and increased survival of cold stress (Takasaki et al. 2010; Song et al. 2011). How does *OsNAC5* work to regulate abiotic stress tolerance and nutrient remobilization? *OsNAC5* acts as a typical NAC transcription factor: it is a transcriptional activator, it can form homodimers and heterodimers, and it binds to the NAC binding motif CACG (Takasaki et al. 2010). *OsNAC5* is involved with ABA signalling, as ABA upregulates *OsNAC5* expression and overexpression lines are more sensitive to ABA (Song et al. 2011). *OsNAC5* is also a direct downstream target of the salt-stress related transcription factor *OsNAC106* (Sakuraba et al. 2015). Direct downstream targets of *OsNAC5* from two independent datasets include an amino acid transporter, a heavy metal transporter, and genes involved in carbohydrate metabolism and ABA response (Chung et al. 2018). *OsNAC5* improves drought tolerance by upregulating expression of a gene in the lignin biosynthesis pathway, leading to lignin accumulation in roots (Bang et al. 2022).

Given the link between *OsNAC5*, leaf senescence and grain nutrient content it was hypothesized that the ortholog of *OsNAC5* in wheat may also regulate nitrogen remobilization, impacting the timing of senescence and grain protein content.

3.1.2 *OsNAP* promotes leaf senescence and osmotic stress tolerance in rice.

A second rice NAC transcription factor, *OsNAP / NAC58* (Os03g0327800) is expressed during leaf senescence, with gradual increase in expression from 7 days after anthesis (DAA) (Liang et al. 2014). Both gain-of-function mutant and overexpression lines of *OsNAP* have earlier leaf senescence, while RNAi lines have delayed leaf senescence (Liang et al. ; Zhou et al.). *OsNAP* overexpression lines have increased transcript levels of multiple senescence-associated genes (Liang et al. 2014). Overexpression lines have increased proportions of protein, iron, zinc, sulphur and magnesium in the grain (Zhou et al. 2013). Interestingly, *OsNAP* is expressed in the phloem and adjacent to vascular tissues, opening the possibility of a role in regulating nutrient transport (Zhou et al. 2013). Overall, this demonstrates that *OsNAP* promotes earlier senescence and increased grain protein content.

OsNAP also promotes abiotic stress tolerance. Overexpression lines were more tolerant to drought at both vegetative and flowering stages, and showed a higher germination rate under salt stress (Chen et al. 2014).

It was hypothesized that as *OsNAP* promotes leaf senescence, the ortholog of *OsNAP* in wheat may also regulate leaf senescence timing and grain protein content.

3.1.3 Objectives

In this chapter, the following questions will be addressed.

1. What are the wheat orthologs of *OsNAC5* and *OsNAP*?
2. How are *NAC5-1* and *NAP-1* expressed in wheat?

3. How does overexpression and loss-of-function of *NAC5-1* affect senescence timing?
4. How does overexpression and loss-of-function of *NAP-1* affect senescence timing?

To address these questions, the wheat orthologs of *OsNAC5* and *OsNAP* were determined. The role of wheat *TaNAC5-1* and *TaNAP-1* in the context of senescence and grain protein content had not yet been reported. The expression level of *NAC5-1* and *NAP-1* during wheat leaf senescence was explored. Experiments were carried out to test how overexpressing *NAC5-A1* and *NAP-A1* affects senescence timing and grain mass. Experiments were carried out to test how loss-of-function of *NAC5-1* and *NAP-1* affects senescence timing, grain mass, and grain protein content.

3.2 Methods

3.2.1 Assessment of wheat orthologs of *OsNAC5* and *OsNAP*

To find the wheat ortholog of *OsNAC5 / NAC071* (Os11g0184900), a BLASTP search was carried out using the canonical peptide sequence of *OsNAC5* (Os11t0184900-02 peptide) against the *Triticum aestivum* (Chinese Spring RefSeq v1.1) peptide database and the *Oryza sativa* ssp. *japonica* peptide database, using Ensembl Plants with Search Sensitivity = Near Match (Yates et al. 2022). For each species, peptide sequences from the 15 hits with lowest E-value were recovered. Peptide sequences from wheat and rice were aligned with Clustal Omega 1.2.2 and a consensus tree was generated using the Neighbour-Joining method with 100 bootstrap replicates, in Geneious software (Biomatters 2022). One of the many-to-many orthologs of the *OsNAC5* and *OsNAP* in *Physcomitrium patens* (Pp3c13_10800V3_2) was included as an outgroup for the subclade (Nakashima et

al. 2012). This gene tree was not intended as a full depiction of the phylogeny, but as sufficient to establish the orthology of *OsNAC5*. Figures were created in Geneious software (Biomatters 2022).

To find the wheat ortholog of *OsNAP* / *NAC58* (Os03g0327800) the same process was repeated as for *OsNAC5*. Homoeologs of wheat genes were added to ensure wheat genes in the tree were presented as complete triads. In the initial tree for *OsNAP*, one cluster of wheat genes lacked an ortholog in rice. Further investigation led to *ONAC103*, which was not found in the BLASTP as the Ensembl annotation predicted a stop codon truncating the peptide sequence to 82 amino acids. However, the MSU annotation predicts a full-length NAC domain containing protein of 346 amino acids. To display this, the alignment and tree were supplemented with truncated and full-length alternatives for *ONAC103*, full length sequences of *ONAC103* from *Oryza rufipogon* and *Oryza sativa* ssp. *indica*, and *OsNAP* from *Oryza rufipogon.* Displayed multiple alignments were aligned with Clustal Omega 1.2.2 and formatted with MView. Percent identities were derived from pairwise percent identity matrix output by Clustal Omega.

3.2.2 Transformation of hexaploid wheat with constructs to overexpress *NAC5-A1* and *NAP-A1*

To overexpress *NAC5-A1* in wheat, the *NAC5-A1* coding sequence was PCR-amplified from cDNA using a proof-reading Taq polymerase, adding an N-terminal FLAG tag, and cloned into the PCR8 vector (ThermoFisher). The *NAC5-A1* sequence was cloned into the *pSc4Act-R1R2-SCV* vector (NIAB) by a Gateway LR reaction under control of the rice *ACTIN* promoter (pActin::3xFLAG-*NAC5-A1*) (*Figure 3.1*). The vector was transformed into hexaploid Fielder wheat, selected for its high transformation efficiency. Cloning was carried out by Philippa Borrill, and

transformation was carried out by Emma Wallington, Charline Soraru and Matt Hope (NIAB).

NAC5-A1 constructs were transformed in two batches, 5 and 8, labelled in the initial digit of the line name (e.g. line 5.4 comes from batch 5). Each batch had its own non-transformed control (5.con and 8.con). *NAP-A1* constructs were generated and transformed into wheat by the same method, in batches 7 and 10. The construct copy number of all plants in T_0 and segregating single-copy lines in T_1 was tested by a copy number assay (*Figure 3.1*).

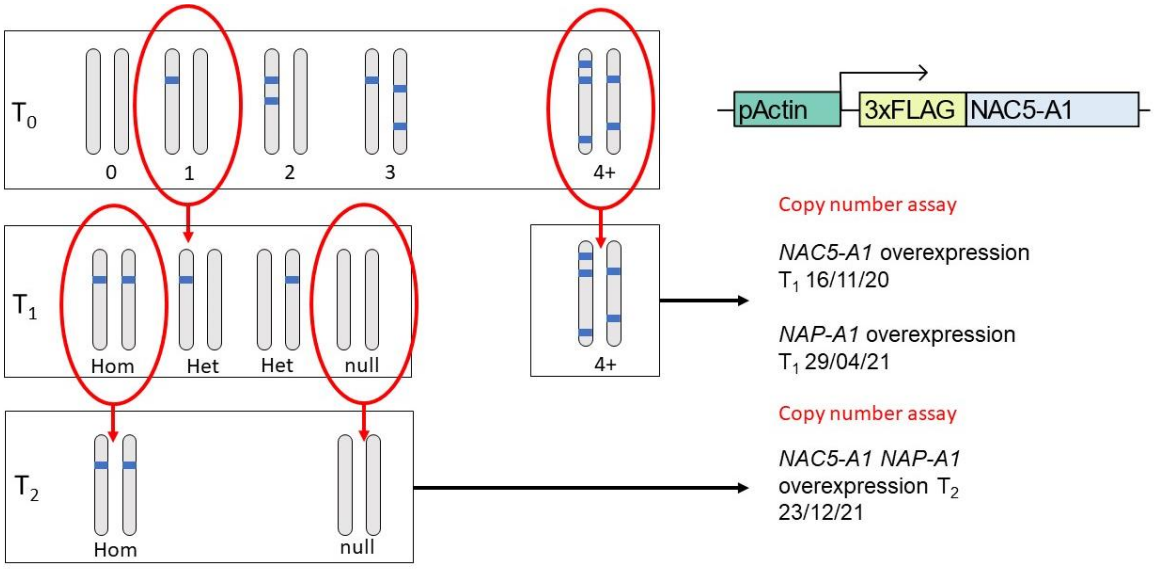


Figure 3.1 Overview of NAC5-A1 and NAP-A1 overexpression lines. Hexaploid Fielder wheat was transformed with a construct to express NAC5-A1 or NAP-A1 from a rice actin promoter (top right). Single-copy T_0 lines with 1 construct copy and multi-copy T_0 lines with 4+ construct copies were selected with a copy number assay (red ovals). T_1 progeny were grown in glasshouse experiments (bottom right). From the T_1 lines, homozygous and null segregants were selected with a copy number assay (red ovals). T_2 progeny were grown in glasshouse experiments (bottom right). Blue bars represent transgenic construct insertions. Sowing dates of glasshouse experiments are used as unique identifiers for each experiment.

3.2.2.1 Primer design

To assess whether *NAC5-A1* and *NAP-A1* transgenic lines overexpress these genes, three types of quantitative PCR (qPCR) primers were designed (*Table 3.1*).

1. To amplify transgenic construct only, primer pairs included one primer specific to the NAC gene and one within the N-terminal FLAG tag.
2. To amplify coding sequence of *NAC5-A1* (both endogenous and transgenic constructs, but not B or D homoeologs), primer pairs included one primer crossing the junction between two exons (specific to cDNA) and one with an A-homoeolog-specific SNP (single nucleotide polymorphism) at the 3' end.
3. To amplify all coding sequences of *NAC5-1*, including A, B and D homoeologs, primer pairs included one primer crossing the junction between two exons (specific to cDNA) and both primers had a sequence conserved across all three homoeologs.

Primers were designed manually in Snapgene Viewer with the criteria: product size less than 200bp, primer length 16-25bp, GC 40-70%, T_m 57-63˚C and T_m similar in the two primers. *ACT2* was used as the reference gene (Tenea et al. 2011).

Table 3.1 Primers used for qPCR of NAC5-1 and NAP-1 transgenic lines. Primer pairs were designed to amplify transgenic construct only, the A homoeolog or all three homoeologs. ACT2 is the reference gene (Tenea et al. 2011).

Primer name	Sequence	Amplifies	Specificity
CENAC5-1-F	GCTCAGGCTGGATGACT	*NAC5-A1*	cDNA
CENAC5-7-R	GGCTTGACGTCGGCCA	*NAC5-A1*	A homoeolog
CENAC5-3-F	TGGATCATGCACGAGTACCG	*NAC5-1*	*NAC5-1*
CENAC5-3-R	CACCCAGTCATCCAGCCTG	*NAC5-1*	cDNA
CENAC5-5-F	AAGGACGATGACGATAAGGAC	*3*FLAG-NAC5-A1*	FLAG

CENAC5-5-R	GCAAAGGTAGTACATCACCAGC	*3*FLAG-NAC5-A1*	*NAC5-1*
CENAP-7-F	CCCTGCCATCCAAGGCTA	*NAP-A1*	cDNA
CENAP-2-R	TGGCTTTCCAGTAGCCAGAG	*NAP-A1*	A homoeolog
CENAP-8-F	CTCCATGAGGCTGGATGACT	*NAP-1*	cDNA
CENAP-13-R	CTTGGCTGGTCTTCTTGTAG	*NAP-1*	*NAP-1*
CENAP-5-F	GACGATGACGATAAGATCATGTCCG	*3*FLAG-NAP-A1*	FLAG
CENAP-5-R	GTCGGCGATGATGGAGACG	*3*FLAG-NAP-A1*	*NAP-1*
PB441_Act2_F	CAAATCATGTTTGAGACCTTCAATG	*ACT2*	
PB441_Act2_R	ACCAGAATCCAACACGATACCTG	*ACT2*	

At least two primer pairs of each type were designed. To determine the most effective primers for qPCR, a primer efficiency analysis was performed. A cDNA dilution series was prepared from RNA extracted from a multi-copy transgenic plant and qPCR was run.

Primer efficiency = -1+10^(-1/Gradient)

Gradient is the slope of a straight line between Ct and log10(relative cDNA concentration). Primers were selected with a single peak melt curve, a straight-line relationship between Ct and log10(concentration), and primer efficiency closest to that of *ACT2* primers (*Table 3.2*). As expected, construct-specific primers do not amplify wild-type cDNA (*Table 3.2*).

Table 3.2 Primer efficiency results for NAC5-1 and NAP-1 qPCR primer pairs. Many primer pairs were tested, but only primer pairs selected for qPCR experiments are shown. These primer efficiency values were used in qPCR analysis.

Gene name	Primer pair	Specificity	Product T_m	Melt curve	WT CT at 1:4 dilution	Product size	Line shape (CT vs log10 concentration)	Efficiency 11/12/20	Efficiency 09/09/21
ACTIN	PB441_Act2_F PB441_Act2_R	Reference	80.7	single peak	23.1		Straight	0.91	0.97
NAC5-A1	CENAC5-1-F CENAC-7-R	A copy	85.6	single peak	30.6	99	Straight	0.99	
NAC5-A1	CENAC5-3-F CENAC5-3-R	All homoeologs	88.7	small shoulder	25.9	96	Straight	1.02	
NAC5-A1	CENAC5-5-F CENAC5-5-R	FLAG	86.6	single peak	No amplification	105	Straight	0.89	
NAP-A1	CENAP-7-F CENAP-2-R	A copy	87.1	single peak	31.12	120	Straight		1.07
NAP-A1	CENAP-8-F CENAP-13-R	All homoeologs	80.2	single peak	30.94	56	Straight		0.92
NAP-A1	CENAP-5-F CENAP-5-R	FLAG	89.7	single peak	No amplification	141	Straight		0.92

3.2.3 Development of tetraploid TILLING mutant lines for *NAC5-1* and *NAP-1*

To generate wheat lines with probable loss-of-function of *NAC5-1* or *NAP-1* in wheat, TILLING mutant lines were selected in tetraploid Kronos wheat and KASP primers designed as described previously (Methods 2.2.2). At every generation, SNP alleles were tracked with Kompetitive Allele-Specific PCR (KASP) using the following primers (Methods 2.2.3) (Table 3.3). The crossing scheme was similar to that for hexaploid wheat, except that mutations in A and B homoeologs only were combined (Methods 2.2.2).

TILLING lines were developed by Philippa Borrill as far as BC_2F_2 plants for *NAC5-1* and BC_2F_1 plants for *NAP-1*.

Table 3.3 KASP primers used to genotype TILLING mutations in NAC5-1 and NAP-1. A pair of allele-specific WT and MUT primers and a homoeolog-specific COM primer are used for each KASP reaction.

Primer name	Sequence	Line name	SNP description	Cross ID
PB462_COM	tccatcatcgccgacgtT	Kronos0255	*NAP-A1* stop	X585
PB462_MUT	GAAGGTGACCAAGTTCATGCTaggtactaacatggcagggcT	Kronos0255	*NAP-A1* stop	X585
PB462_WT	GAAGGTCGGAGTCAACGGATTaggtactaacatggcagggcC	Kronos0255	*NAP-A1* stop	X585
PB463_COM	tGtttctcttTGGGTCCCttG	Kronos3959	*NAP-B1* stop	X585
PB463_MUT	GAAGGTGACCAAGTTCATGCTccctcggcgtgaagaagtaT	Kronos3959	*NAP-B1* stop	X585
PB463_WT	GAAGGTCGGAGTCAACGGATTccctcggcgtgaagaagtaC	Kronos3959	*NAP-B1* stop	X585
PB479_COM	tacttcttctcgccgcgC	Kronos2546	*NAC5-A1* missense	X388+X392
PB479_MUT	GAAGGTGACCAAGTTCATGCTcGgtggccttccagtacT	Kronos2546	*NAC5-A1* missense	X388+X392
PB479_WT	GAAGGTCGGAGTCAACGGATTcGgtggccttccagtacC	Kronos2546	*NAC5-A1* missense	X388+X392
PB480_COM	gggtactggaaggccacG	Kronos2036	*NAC5-B1* best missense	X388
PB480_MUT	GAAGGTGACCAAGTTCATGCTacgagAgccttcttgatggT	Kronos2036	*NAC5-B1* best missense	X388
PB480_WT	GAAGGTCGGAGTCAACGGATTacgagAgccttcttgatggC	Kronos2036	*NAC5-B1* best missense	X388
PB481_COM	gcaaggtggttaccctgagA	Kronos3328	*NAC5-B1* backup missense	X392
PB481_MUT	GAAGGTGACCAAGTTCATGCTtctcgtcttctacgccgA	Kronos3328	*NAC5-B1* backup missense	X392
PB481_WT	GAAGGTCGGAGTCAACGGATTtctcgtcttctacgccgG	Kronos3328	*NAC5-B1* backup missense	X392

3.2.4 Working with transgenic lines

3.2.4.1 Copy number assay

A Taqman copy number assay was run against the marker gene *npt*II, found in the pSc4ActR1R2 vector used for transformation (Milner et al. 2018). *GAMYB* is used as reference as it exists as a single triad in the wheat genome (Haseneyer et al. 2008). Genomic DNA was extracted from leaves of 2-3-week-old wheat plants (Methods 2.2.3). A primer mix was prepared containing primers to amplify both *npt*II and reference gene *GAMYB*, and Taqman fluorescent probes (*Table 3.4*). Each well of a 96-well plate was loaded with:

12.5µl ABsolute qPCR mix with ROX
1µl genomic DNA (200-300ng/µl)
1µl primer mix
10.5µl ddH_2O

Quantitative PCR was run with the following program (*Table 3.5*). The copy number was calculated by first normalizing for DNA input concentration by comparing to *GAMYB*, then assigning copy number by normalizing to the median value in the single-copy cluster. Copy number assays were analysed and figures generated in Excel.

*Table 3.4 Primers for Taqman copy number assay, from Additional file 1 in (Milner et al. 2018). The transgenic construct contains npt*II *while GAMYB is the reference. Primers were provided by JIC Molecular Genetics platform.*

Primer name	**Sequence**	**Amplifies**	**Specificity**
GamyB1F	GATCCGAATAGCTGGCTCAAGTAT	*GAMYB*	Forward
GamyB2R	GGAGACTGCAGGTAGGGATCAAC	*GAMYB*	Reverse
GamyB1P	[Joe]CGTGGCTCCTGCGATGCAGC[TAMRA]	*GAMYB*	Taqman probe
Npt2B2F	CTCCTGCCGAGAAAGTATCCA	*npt*II	Forward
Npt2B4R	GCCGGATCAAGCGTATGC	*npt*II	Reverse
Npt2B2P	[FAM]TGGCTGATGCAATGCGGCG[TAMRA]	*npt*II	Taqman probe

Table 3.5 qPCR program for Taqman copy number assay.

Programme	**Temperature**	**Time**
		40 cycles
pre increase	95C	15min
amplification	95C	15sec
	60C	60sec read

3.2.4.2 RNA extraction and cDNA synthesis

For gene expression assays, 100mg leaf tissue samples from 2–3-week-old wheat seedlings were placed in 1.5ml tubes and snap-frozen in liquid N_2. For pooled samples, 0.5cm leaf tissue from 12 plants of one line was collected in the same 1.5ml tube. Frozen tissue was ground with a micro-pestle pre-chilled in liquid N_2.

To extract RNA, 1ml TRI-reagent (Invitrogen) was added to the tube. After 5 minutes, 200µl chloroform was added. The tube was mixed, left for 2 minutes then spun for 5 minutes. All spin steps were carried out at 13,000rpm at 4˚C. 600µl of the upper aqueous layer was transferred into 500µl isopropanol. Tube was left for 3 minutes then spun for 10 minutes, and the supernatant was discarded. The pellet was washed in 300µl 70% ethanol, spun for 10 minutes, and the supernatant was discarded. The pellet was dried for 3-5 minutes and resuspended in 50µl RNAse-free water. RNA concentrations were tested using a Nanodrop (ThermoFisher).

RNA was DNAse treated by incubating the following reaction for 30 minutes at 37˚C:

1,000ng RNA (equivalent to 8µl at 125ng/µl)
1µl DNase 10X reaction buffer
1µl DNase 1 (ThermoFisher)
ddH_2O to 10µl total reaction volume

The reaction was terminated by adding 1µl DNase stop solution and incubating at 65˚C for 10 minutes.

To synthesize cDNA required the following components:

11µl DNAse-treated RNA
1µl dNTPs 10µM
1µl oligo dT primers 1:2
1µl random primers 1:20
4µl First strand buffer
2µl 0.1M DTT
1µl RNAse inhibitor Ribolock (ThermoFisher)
1µl M-MLV reverse transcriptase (Invitrogen)

RNA, dNTPs and primers were incubated at 65˚C for 5 minutes then placed on ice. Remaining reagents were added. Tubes were incubated with the following program (*Table 3.6*).

Table 3.6 PCR program for cDNA synthesis.

Programme	**Temperature**	**Time**
incubate	25C	10min
	37C	50min
inactivate reaction	70C	15min

3.2.4.3 Gene expression testing

Transcript levels of transgenic constructs, *NAC5-A1, NAP-A1*, combined homoeologs of *NAC5-1* and *NAP-1* and reference gene *ACT2* were tested by qPCR using three technical replicates per sample, using the designed primers (*Table 3.1*). Into each well of a 384-well plate was added:

5µl SYBR Green master mix
2µl cDNA
1.25µl F Primer (2µM)
1.25µl R Primer (2µM)
0.5µl ddH_2O

qPCR was run with the following program (*Table 3.7*). Fold change in expression was analysed using *ACT2* as the reference gene. Pooled samples were analysed by the ΔΔCt method, normalised to either a non-transformed control sample, or a single-copy line for construct-specific primers where non-transformed controls did not amplify. Individual samples were analysed by the Pfaffl method which accounts for primer efficiency, using the calculated primer efficiencies in *Table 3.2* (Pfaffl 2001). If

the standard deviation of three technical replicates exceeded 1, the outlier technical replicate was removed. The average of all samples in the single-copy lines was used to normalise transcript levels (lines 5.4, 8.9 and 8.26 for *NAC5-1* or lines 10.5 and 10.9 for *NAP-1*). Scripts for qPCR analysis are available on Github (Evans 2023).

Table 3.7 qPCR program for testing for overexpression of NAC5-A1 and NAP-A1.

Programme	**Temperature**	**Time**
		45 cycles
pre increase	95C	5min
amplification	95C	10sec
	60C	15sec
	72C	20sec
	78C	1sec read
cooling to	60C	
melt curve to	95C	

3.2.5 Experimental design

3.2.5.1 Summary of growth conditions and senescence phenotyping methods

Growth conditions for glasshouse experiments;phenotyping methods for senescence, grain mass and number, grain protein content and other traits; and calculation of senescence metrics were as for *NAM-2* experiments (Methods 2.2.4; 2.2.5; 2.2.7). The dates, location of plants grown and number of replicates for each experiment in this chapter are detailed below (Table 3.8). SPAD readings were taken over a longer duration and more frequently in later experiments, while grain mass, grain number and protein content were measured in only some experiments due to

constraints on time and equipment availability (Table 3.8). Further detail follows on the design of each experiment.

Table 3.8 Summary of experimental design in this chapter. Sowing dates of glasshouse experiments are used as unique identifiers for each experiment. Growth conditions and measurements which differed between experiments are included. Location corresponds to Table 2.3. Most experiments were laid out in a randomized complete block design (RCBD).

Sowing date	**Harvest date**	**Plant material**	**Location**	**Experimental layout**	**Timing of SPAD reading**	**Grain mass / number measured**	**GPC measured**
16/11/2020	05/03/2021	*NAC5-A1* overexpression T_1	Glasshouse UoB	Not randomized. 12 reps per genotype	Weekly 18-20DAH to 39-41DAH	Some (by hand)	No
29/04/2021	18/08/2021	*NAP-A1* overexpression T_1	Glasshouse UoB	RCBD 12 reps per genotype	At Heading; Weekly 18-20DAH to 39-41DAH	Some (by hand)	No
23/12/2021	20/04/2022	*NAC5-1 NAP-1* overexpression T_2	CER JIC	RCBD 10 reps per genotype	At Heading; Weekly 6-8DAH to SPAD<10	Yes	No

01/12/2021	19/04/2022	*NAC5-1 NAP-1* Kronos TILLING	Glasshouse JIC	RCBD 12 reps per genotype	At Heading; Weekly 6-8DAH to SPAD<10	Yes	Yes

3.2.5.2 *NAC5-A1* overexpression T_1 (16/11/2020)

To explore whether overexpression of *NAC5-A1* affects the timing of senescence, gene expression assays and preliminary phenotyping were carried out on T_1 lines in the glasshouse (*Table 3.9*).

Table 3.9 Plant material for NAC5-A1 overexpression T_1 (16/11/2020). T_1 progeny of single-copy, multi-copy and non-transformed control plants from transformation batches 5 and 8 were grown in the glasshouse.

Gene name	Line name	Generation	Category	Copy number of T_0	Plants per line
NAC5-1	5.con1	T_1	non-transformed control	0	12
NAC5-1	8.con1	T_1	non-transformed control	0	12
NAC5-1	5.4	T_1	single	1	12
NAC5-1	8.9	T_1	single	1	12
NAC5-1	8.10	T_1	single	1	12
NAC5-1	8.23	T_1	single	1	12
NAC5-1	8.25	T_1	single	1	12
NAC5-1	8.26	T_1	single	1	12
NAC5-1	5.1	T_1	multi	4	12
NAC5-1	5.2	T_1	multi	4	12
NAC5-1	5.5	T_1	multi	4	12
NAC5-1	8.1	T_1	multi	4	12
NAC5-1	8.2	T_1	multi	4	12
NAC5-1	8.3	T_1	multi	4	12
				Total	168

3.2.5.3 *NAP-A1* overexpression T_1 (29/04/2021)

To explore whether overexpression of *NAP-A1* affects the timing of senescence, gene expression assays and preliminary phenotyping were carried out on T_1 lines in the glasshouse (*Table 3.10*). These plants were arranged in a randomized complete block design (RCBD) with 6 blocks of 24; i.e. 2 plants per genotype in each block. Senescence measurements in this experiment were carried out with assistance from Ramesh Arunkumar, Muhammad Ali, James Milson, Sophie Mogg, and Philippa Borrill.

Table 3.10 Plant material for NAP-A1 overexpression T_1 (29/04/2021). T_1 progeny of single-copy, multi-copy and non-transformed control plants from transformation batches 7 and 10 were grown in the glasshouse.

Gene name	Line name	Generation	Category	Copy number of T_0	Plants per line
NAP-1	7.con1	T_1	non-transformed control	0	12
NAP-1	10.con1	T_1	non-transformed control	0	12
NAP-1	7.5	T_1	single	1	12
NAP-1	7.19	T_1	single	1	12
NAP-1	10.3	T_1	single	1	12
NAP-1	10.5	T_1	single	1	12
NAP-1	10.9	T_1	single	1	12
NAP-1	7.7	T_1	multi	4+	12
NAP-1	7.8	T_1	multi	4+	12
NAP-1	7.9	T_1	multi	4+	12
NAP-1	10.1	T_1	multi	4+	12
NAP-1	10.8	T_1	multi	4+	12
				Total	144

3.2.5.4 *NAC5-1 NAP-1* overexpression T_2 (23/12/2021)

To test whether *NAC5-A1* or *NAP-1* overexpression affects senescence timing, a time-course of flag leaf senescence was measured in transgenic lines and null segregant controls, grown in a controlled environment chamber (*Table 3.11*). Plants were arranged in an RCBD with 10 blocks of 8 plants across two CER shelves for each gene (*Figure 3.2*). R Formula for analysis:

lm(Heading_date ~ Shelf * Line_name)

Table 3.11 Plant material for NAC5-1 NAP-1 overexpression T_2 (23/12/2021).T_2 progeny of homozygous and null / wild-type segregating single-copy T_1 lines were grown, as were T_2 multi-copy lines.

Gene name	Line name	Generation	Genotype	Copy number of T_1	qPCR: no amplification of construct at plant level	qPCR: significant overexpression of A homoeolog at plant level	Plants per line
NAC5-1	5.4	T_2	Hom	2		Y	10
NAC5-1	5.4	T_2	WT	0	Y		10
NAC5-1	8.9	T_2	Hom	2		N	10
NAC5-1	8.9	T_2	WT	0	?		10
NAC5-1	8.23	T_2	Hom	2		?	10
NAC5-1	8.23	T_2	WT	0	?		10
NAC5-1	8.2	T_2	multi	?		Y	10
NAC5-1	8.3	T_2	multi	?		Y	10
NAP-1	10.5	T_2	Hom	2		Y	10
NAP-1	10.5	T_2	WT	0	Y		10
NAP-1	10.9	T_2	Hom	2		Y	10
NAP-1	10.9	T_2	WT	0	Y		10
NAP-1	7.19	T_2	Hom	2		?	10
NAP-1	7.19	T_2	WT	0	?		10
NAP-1	10.1	T_2	multi	?		Y	10
NAP-1	7.9	T_2	multi	?		Y	10
						Total	160

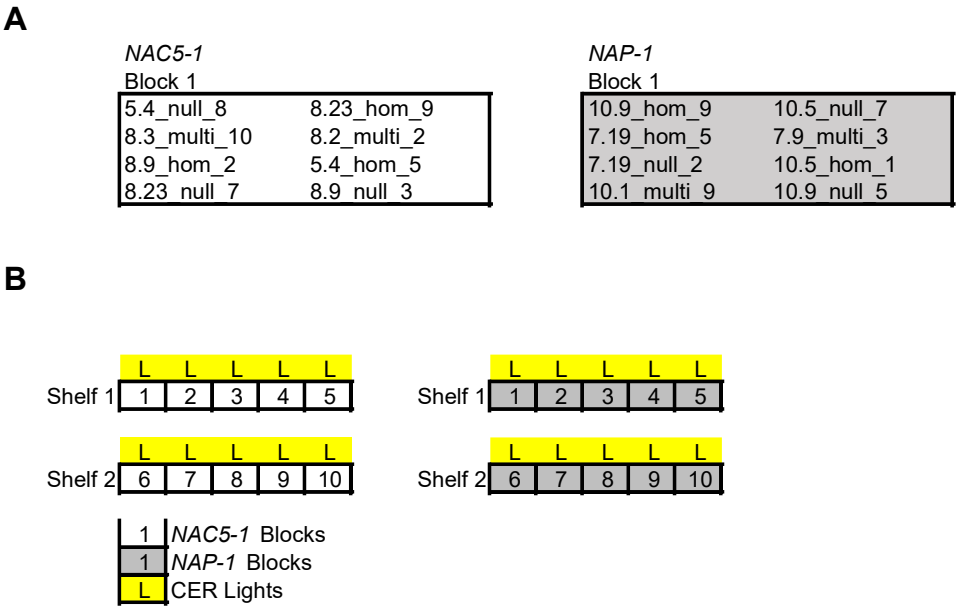


Figure 3.2 Randomized complete block design for NAC5-1 NAP-1 overexpression T_2 (23/12/2021). (A) Each block consisted of one plant per genotype, arranged at random in an 8-cell tray. (B) Blocks were split across upper and lower shelves of two identical CER cabinets lit by panels of LED lights.

3.2.5.5 *NAC5-1 NAP-1* Kronos TILLING (01/12/2021)

To test whether loss-of-function of *NAC5-1* or *NAP-1* affects senescence timing, a time-course of flag leaf chlorophyll content was measured in *NAC5-1* and *NAP-1* TILLING lines in the glasshouse. The lines used were BC_2F_3 lines of all three crosses, expected to have homozygous genotypes (Table *3.12*). Twelve plants per line were grown, and organised after potting up into a randomized complete block design (RCBD), with 12 blocks of 8 plants for *NAC5-1* and 6 blocks of 8 plants for *NAP-1 (Figure 3.3*A*)*. Blocks were shuffled every two weeks for more even light exposure (*Figure 3.3*B). R Formula for analysis:

lm(Heading_date ~ Light + Block + Genotype)

Table 3.12 Plant material for NAC5-1 NAP-1 Kronos TILLING (01/12/2021). Cross ID refers to Table 3.15. Generation: BC = number of backcrosses, F = generations since last cross. Genotype: capitals indicate wild-type allele, small letters indicate TILLING mutant allele. 27 plants were resown later due to seeds which failed to germinate or died.

Gene name	Cross ID	Cross description	Generation	Genotype	Plants per line total	Plants sown 01/12/23	Plants resown 23/12/23
NAC5-1	X388	K2546*K2036 "best"	BC2F3	AABB	12	6	6
NAC5-1	X388	K2546*K2036 "best"	BC2F3	AAbb	12	12	0
NAC5-1	X388	K2546*K2036 "best"	BC2F3	aaBB	12	12	0
NAC5-1	X388	K2546*K2036 "best"	BC2F3	aabb	12	11	1
NAC5-1	X392	K2546*K3328 "backup"	BC2F3	AABB	12	11	1
NAC5-1	X392	K2546*K3328 "backup"	BC2F3	AAbb	12	12	0
NAC5-1	X392	K2546*K3328 "backup"	BC2F3	aaBB	12	12	0
NAC5-1	X392	K2546*K3328 "backup"	BC2F3	aabb	12	12	0
NAP-1	X585	K0255*K3959	BC2F3	AABB	12	10	2
NAP-1	X585	K0255*K3959	BC2F3	AAbb	12	1	11
NAP-1	X585	K0255*K3959	BC2F3	aaBB	12	7	5
NAP-1	X585	K0255*K3959	BC2F3	aabb	12	11	1
				Total	**144**	**117**	**27**

A

NAC5-1
Block 1

K_X392_aa_62	K_X388_aa_23
K_X392_aabb_89	K_X392_WT_53
K_X388_aabb_43	K_X392_bb_76
K_X388_WT_7	K_X388_bb_27

NAP-1
Block 1

K_X585_aabb_133	K_X585_bb_128
K_X585_WT_107	K_X585_bb_129
K_X585_aabb_141	K_X585_aa_111
K_X585_aa_109	K_X585_WT_108

B

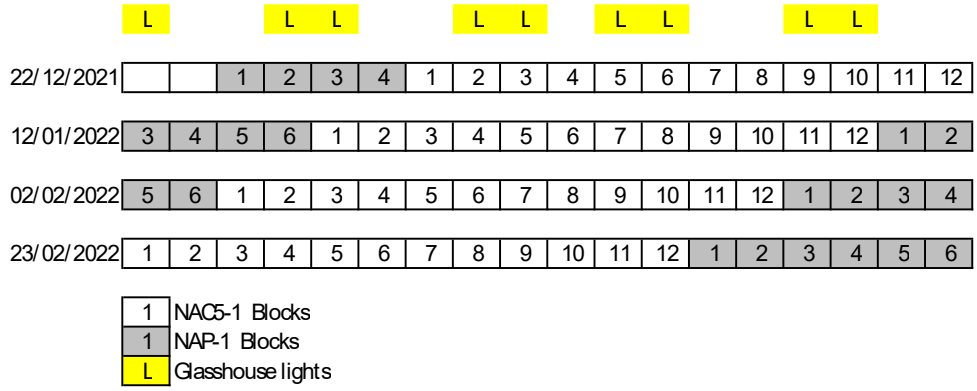


Figure 3.3 Randomized complete block design for NAC5-1 NAP-1 Kronos TILLING (01/12/2021). (A) Each block consisted of one plant per genotype for NAC5-1 or two plants per genotype for NAP-1, arranged at random in an 8-cell tray. (B) Blocks were shuffled laterally along the glasshouse bench every two weeks to balance exposure to glasshouse lights.

3.3 Results

3.3.1 Identification of the orthologs of *OsNAC5* and *OsNAP* in wheat

To identify the ortholog of *OsNAC5* (Os11g0184900) in wheat, the peptide sequence of *OsNAC5* was searched against *Triticum aestivum* and *Oryza sativa* ssp. *japonica* to find similar peptide sequences, which were aligned to construct a tree. The *OsNAC5* peptide clustered in a monophyletic group with the wheat triad TraesCS4A02G219700 / TraesCS4B02G098200 / TraesCS4D02G094400, therefore it was concluded that these wheat genes are the 1:1 orthologs of *OsNAC5* (*Figure 3.4*). It is proposed to name these genes *TaNAC5-A1, TaNAC5-B1* and

TaNAC5-D1 respectively, in accordance with guidelines on wheat gene nomenclature based on homology (Boden et al. 2023). *TaNAC5-A1* aligns to *OsNAC5* with few gaps, and has 81.9% pairwise identity to *OsNAC5* and 97.3% and 98.5% identity to *TaNAC5-B1* and *TaNAC5-D1* respectively (Figure 3.5). There is one substitution in the NAC domain between *TaNAC5-B1* and its homoeologs; this A64T residue in subdomain III is not conserved with *OsNAC5* (Figure 3.5).

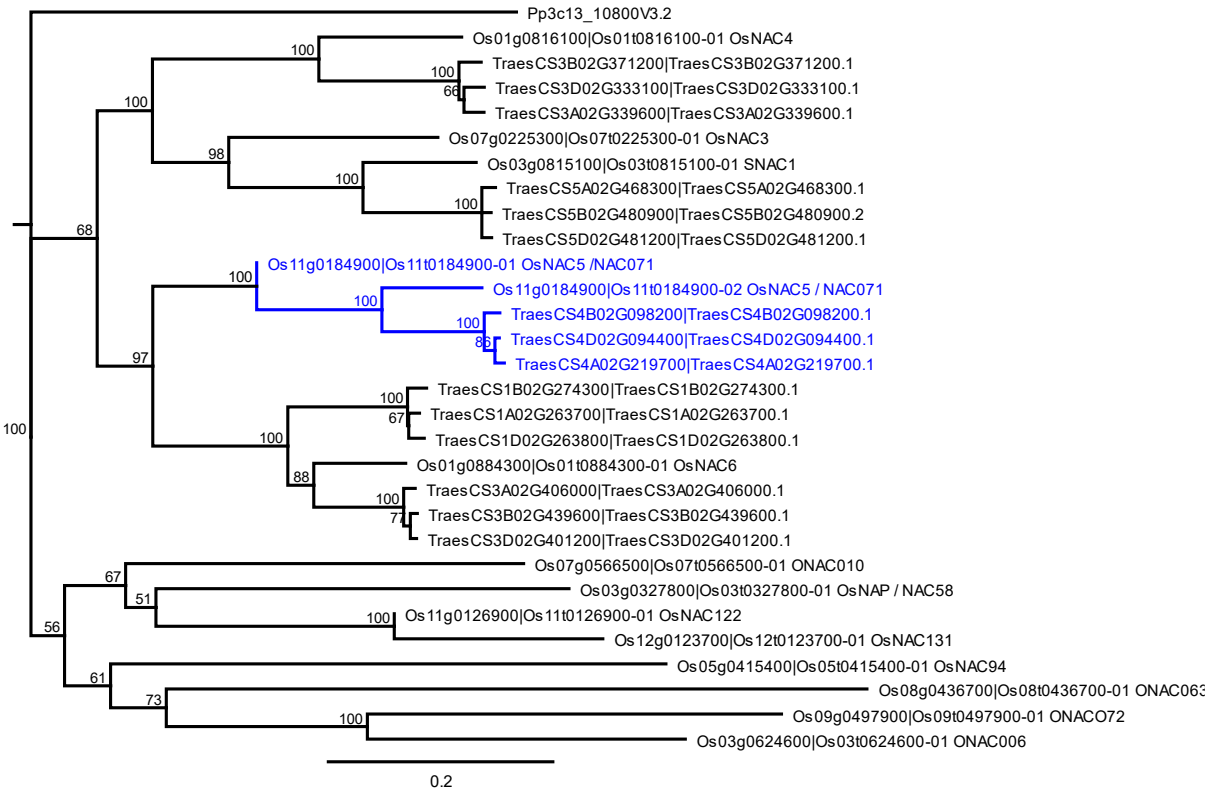


Figure 3.4 TraesCS4A02G219700 and its homoeologs are the orthologs of OsNAC5. Peptide sequences of the 15 top BLAST hits of OsNAC5 in Triticum aestivum and Oryza sativa ssp. japonica were aligned in Clustal Omega. A rooted tree was built with the Neighbour-Joining method. The node containing OsNAC5 is highlighted. Numbers show support values from 100 bootstrap replicates. Scale bar shows number of substitutions per site.

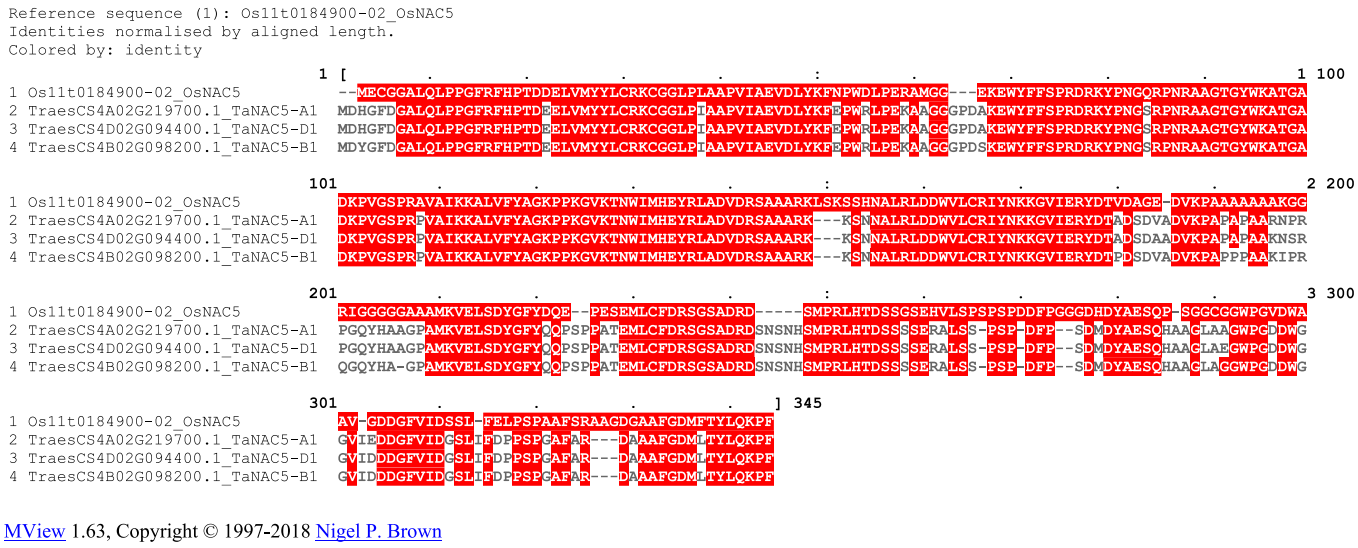


Figure 3.5 Peptide alignment of OsNAC5, TraesCS4A02G219700 and its homoeologs. Alignment in Clustal Omega, displayed with MView. Amino acid residues with identity to OsNAC5 are highlighted red.

The ortholog of *OsNAP* in wheat was identified through the same process as for *OsNAC5.* The *OsNAP* peptide clustered in a monophyletic group with the wheat triad TraesCS4A02G131000 / TraesCS4B02G173600 / TraesCS4D02G175700, therefore it was concluded that these wheat genes are the 1:1 orthologs of *OsNAP* (*Figure 3.6*). It is proposed to name these genes *TaNAP-A1, TaNAP-B1* and *TaNAP-D1* respectively.

TraesCS4A02G131000 *(TaNAP-A1)* has two closely related paralogs on the A subgenome of wheat, TraesCS2A02G101900 and TraesCS2A02G102000. This tandemly duplicated gene pair clusters with *ONAC103* on this gene tree (*Figure 3.6*). This is consistent with another phylogeny of NAC transcription factors in rice (Nakashima et al. 2012). The RAPDB annotation (Os07t0683200-01) shows a stop codon within *ONAC103*, translating as a truncated peptide lacking most of the NAC domain. The MSU annotation (LOC_Os07g48450.1.1) presents *ONAC103* as a full-length peptide, which matches the annotations in *Oryza sativa* ssp. *indica* and *Oryza rufipogon*. Therefore, it is unclear whether *ONAC103* produces a functional protein in *Oryza sativa* ssp. *japonica*.

TraesCS4A02G131000 *(TaNAP-A1)* has 72.3% identity with *OsNAP,* whereas TraesCS2A02G101900 and TraesCS2A02G102000 have 55.8% and 57.2% identity with *OsNAP* respectively (Figure 3.7). Therefore, *TaNAP-1,* rather than its paralogs, was selected to investigate its role in senescence. *TaNAP-A1* shows 94.2% identity to *TaNAP-B1* and 94.3% to *TaNAP-D1* (Figure 3.7). There are two substitutions in the NAC domain between *TaNAP-D1* and its homoeologs; both are outside the core subdomains.

Whilst alternative names have been used for TraesCS4A02G219700, TraesCS4A02G131000 and their homoeologs, no rationale was given for those gene names (Lv et al. 2020a; Mao et al. 2020). Therefore, these wheat gene triads orthologous to *OsNAC5* and *OsNAP* will be referred to as *NAC5-1* and *NAP-1* in this thesis (*Table 3.13*).

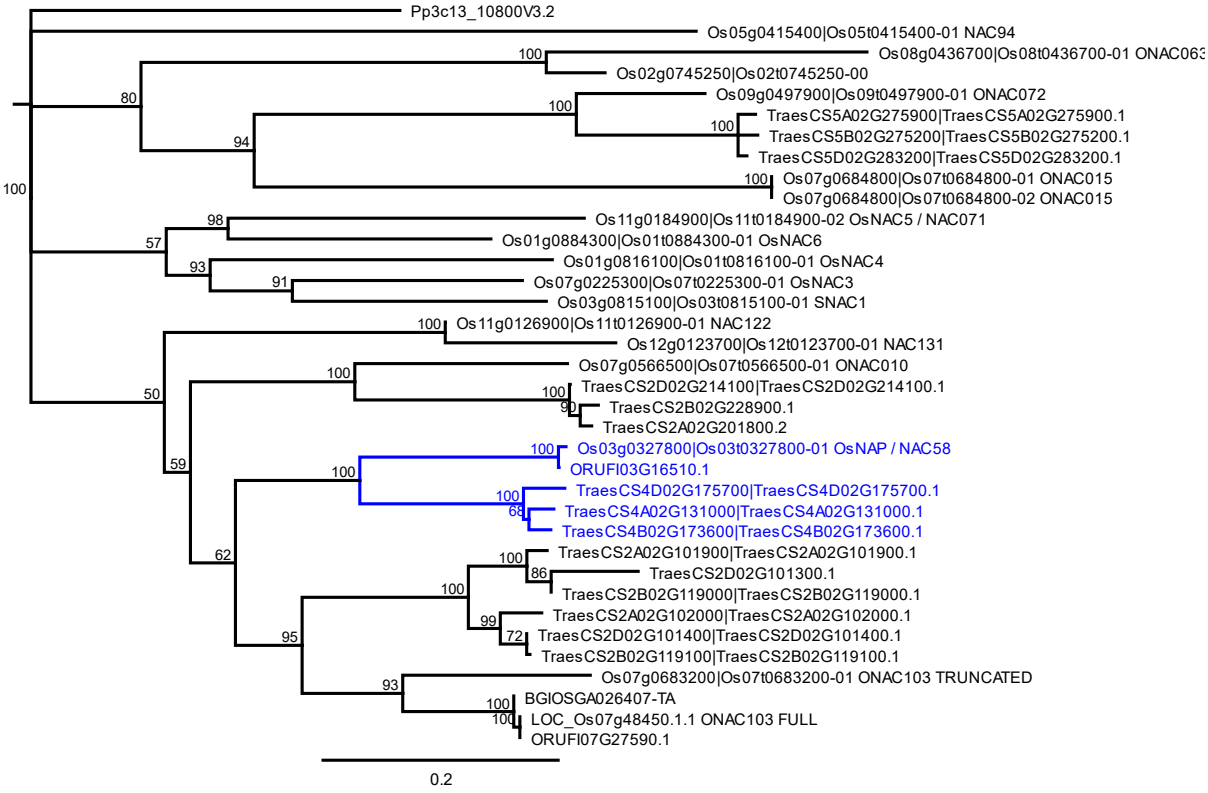
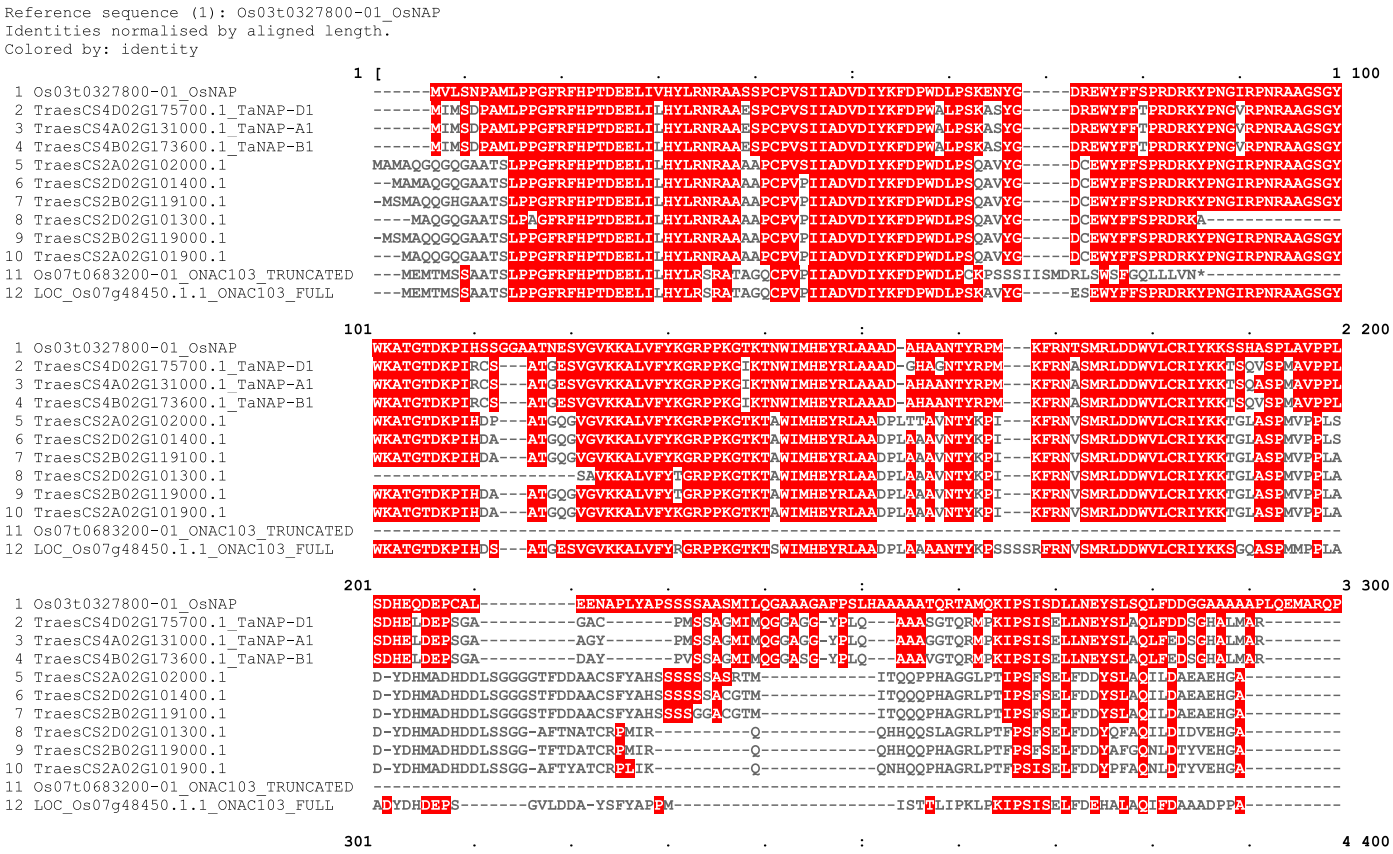


Figure 3.6 TraesCS4A02G131000 and its homoeologs are the orthologs of OsNAP. Peptide sequences of the 15 top BLAST hits of OsNAP in Triticum aestivum and Oryza sativa ssp. japonica were aligned in Clustal Omega. A rooted tree was built with the Neighbour-Joining method. The node containing OsNAP is highlighted. Numbers show support values from 100 bootstrap replicates. Scale bar shows number of substitutions per site.


Reference sequence (1): Os03t0327800-01_OsNAP
Identities normalised by aligned length.
Colored by: identity
1 Os03t0327800-01_OsNAP
2 TraesCS4D02G175700.1_TaNAP-D1
3 TraesCS4A02G131000.1_TaNAP-A1
4 TraesCS4B02G173600.1_TaNAP-B1
5 TraesCS2A02G102000.1
6 TraesCS2D02G101400.1
7 TraesCS2B02G119100.1
8 TraesCS2D02G101300.1
9 TraesCS2B02G119000.1
10 TraesCS2A02G101900.1
11 Os07t0683200-01_ONAC103_TRUNCATED
12 LOC_Os07g48450.1.1_ONAC103_FULL

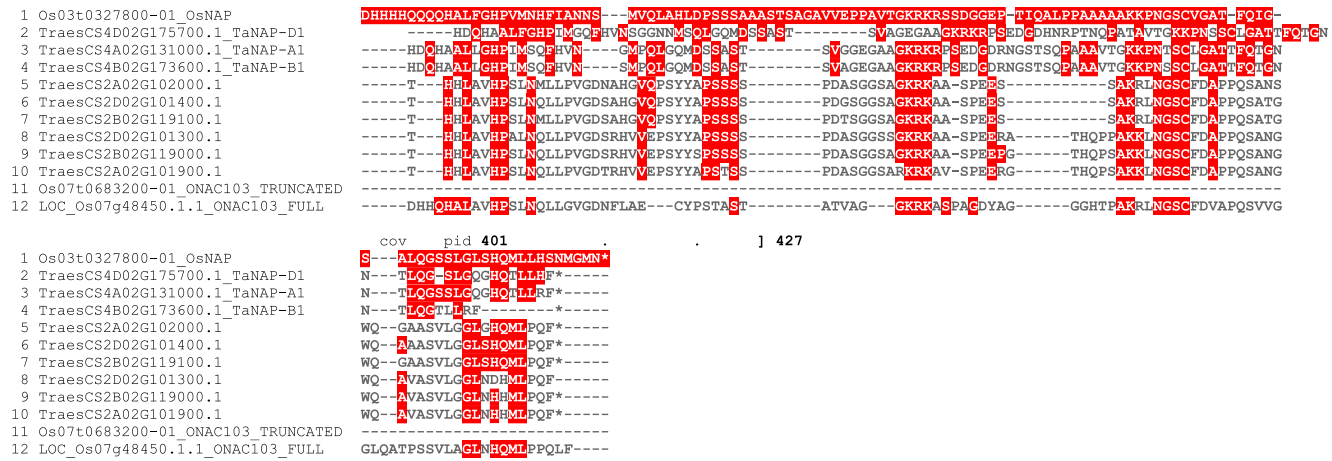


Figure 3.7 Peptide alignment of OsNAP and ONAC103 with TraesCS4A02G131000, TraesCS2A02G101900, TraesCS2A02G102000 and their homoeologs. Alignment in Clustal Omega, displayed with MView. Amino acid residues with identity to OsNAP are highlighted red.

Table 3.13 Naming of wheat genes used in this thesis. These wheat triads will be referred to as TaNAC5-1 and TaNAP-1 or NAC5-1 and NAP-1 after their orthologs in rice, OsNAC5 and OsNAP. Alternative names coined for these wheat genes are also shown.

***Oryza sativa ssp. japonica* genes**			***Triticum aestivum* orthologous genes**				
***O. sativa* Gene stable ID**	***O. sativa* gene names**	**% Identity of peptide**	**Gene stable ID (IWGSC Refseq v1.1)**	***T. aestivum* gene name used in this thesis**	***T. aestivum* triad name used in this thesis**	**Alternative gene names**	
						(Lv et al. 2020a)	(Mao et al. 2020)
Os11g0184900	*OsNAC5 / NAC071 / ONAC009*	75.6	TraesCS4A02G 219700	*TaNAC5-A1*	*TaNAC5-1*	*TaNAC071-A*	*TaSNAC3-4A*
		75.6	TraesCS4B02G 098200	*TaNAC5-B1*		*TaNAC071-B*	*TaSNAC3-4B*
		75.6	TraesCS4D02G 094400	*TaNAC5-D1*		*TaNAC071-D*	*TaSNAC3-4D*
Os03g0327800	*OsNAP / PS1 / ONAC058*	64.5	TraesCS4A02G 131000	*TaNAP-A1*	*TaNAP-1*	*TaNAC034-A*	*TaSNAC11-4A*
		62.5	TraesCS4B02G 173600	*TaNAP-B1*		*TaNAC034-B*	*TaSNAC11-4B*
		63.7	TraesCS4D02G 175700	*TaNAP-D1*		*TaNAC034-D*	*TaSNAC11-4D*

3.3.2 Expression patterns of *NAC5-1* and *NAP-1* during flag leaf senescence

To explore whether *NAC5-1* and *NAP-1* are suitable candidates for regulating the onset of flag leaf senescence in wheat, their expression level in flag leaves in early senescence was assessed. Expression data were extracted from an RNA-seq time-course of flag leaf tissue between 3 and 26 days after anthesis (DAA) (Borrill et al. 2019). All *NAC5-1* homoeologs were upregulated in flag leaves at 23–26 DAA, while *NAC5-D1* also showed a peak in expression at 15DAA (*Figure 3.8*A). *NAC5-A1* is also expressed in seedling leaves, seedling roots, anthers, glumes and lemma according to the Azhurnaya wheat development atlas (Ramírez-González et al. 2018).

All *NAP-1* homoeologs were highly upregulated at 23-26DAA while *NAP-A1* also showed a minor peak at 15DAA (*Figure 3.8*B). This is consistent with the Azhurnaya wheat development atlas, where the tissue with highest expression of *NAP-A1* throughout development is the senescing flag leaf (Ramírez-González et al. 2018). *NAP-A1* and *NAP-D1* were more highly expressed than *NAP-B1*.

Paralogs TraesCS2A02G101900, TraesCS2A02G102000, TraesCS2B02G119000, TraesCS2B02G119100, TraesCS2D02G101300 and TraesCS2D02G101400 were also expressed highly in the flag leaf at 23–26DAA (*Figure 3.8*C, D). *NAP-1* homoeologs increased in expression gradually from around 7DAA while TraesCS2A02G101900, TraesCS2A02G102000 and their homoeologs were upregulated rapidly at 23DAA (*Figure 3.8*B, C, D).

In conclusion, *NAC5-1* and *NAP-1* are expressed in flag leaves in the time window leading up to the first symptoms of senescence, therefore they are suitable candidate genes for regulating the onset of flag leaf senescence.

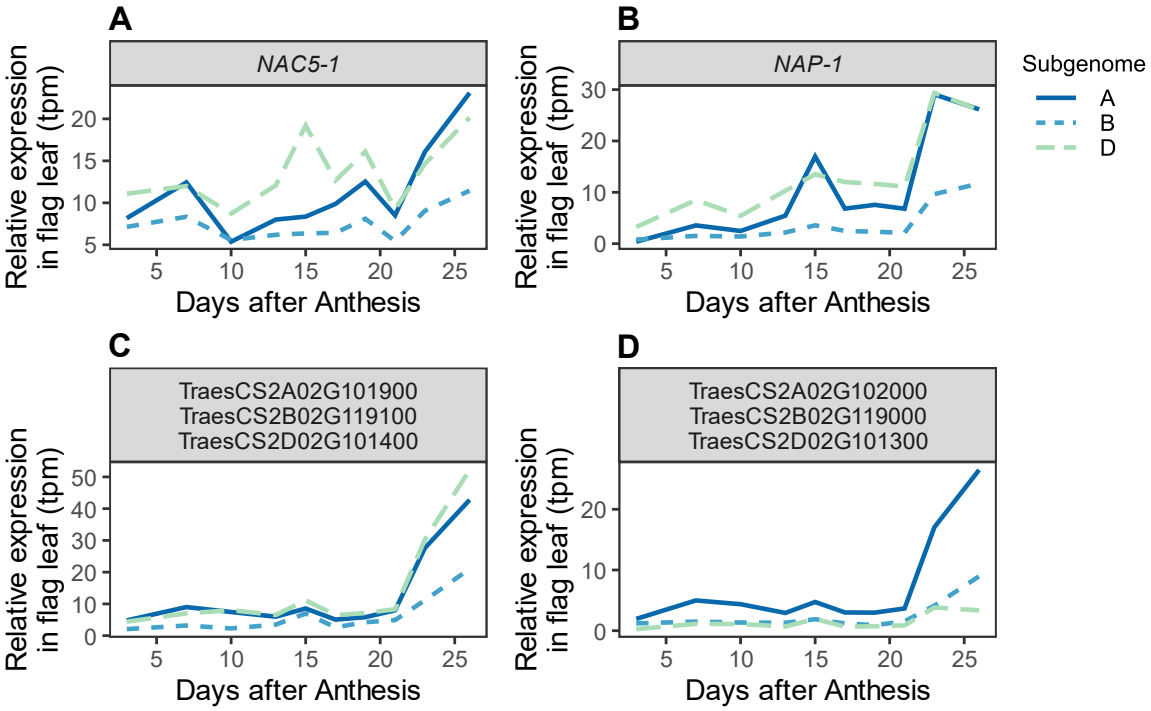


Figure 3.8 NAC5-1 and NAP-1 are upregulated in wheat flag leaves in a time-course of early senescence. Expression level in transcripts per million (tpm) in flag leaves from 3DAA to 26DAA. (A) NAC5-1; (B) NAP-1; (C, D) Paralogs of NAP-1. Re-analysed from (Borrill et al. 2019).

3.3.3 Overexpression of *NAC5-A1* in wheat

3.3.3.1 Identification of transgenic lines overexpressing *NAC5-A1*

If *NAC5-1* promotes the onset of flag leaf senescence, it follows that plants overexpressing *NAC5-1* would senesce earlier. To test this hypothesis, *NAC5-A1* was expressed constitutively in hexaploid wheat plants using a rice Actin promoter. Due to the similarity in the NAC domain between *NAC5-A1, NAC5-B1,* and *NAC5-D1* peptides, overexpression of any one of the homoeologs is likely to have a similar result (Figure 3.5). Twelve T_0 individuals from independent transformation events were selected using a copy number assay: six with a single copy of the construct in T_0 (hereafter “single-copy”), and six with four or more copies of the construct in T_0 (hereafter “multi-copy”). T_1 progeny were grown in the glasshouse.

For a preliminary screen of expression level of *NAC5-A1* in T_1 progeny, average transcript levels were tested by qPCR from pooled leaf samples of 12 T_1 plants per transformation event. Transcript levels were measured using primers designed to amplify either the construct, *NAC5-A1* or all homoeologs of *NAC5-1* (Methods 3.2.2.1). All transgenic lines expressed the construct (*Figure 3.9*A). Out of the single-copy lines, lines 5.4 and 8.26 showed the highest average transcript level of *NAC5-A1,* including both construct-derived and endogenous mRNA (*Figure 3.9*B). Line 8.9 had lower expression of *NAC5-A1* overall but high expression of the construct. Out of the multi-copy lines, lines 8.2 and 8.3 showed the highest average transcript level of *NAC5-A1*. Therefore, lines 5.4, 8.26, 8.9, 8.2 and 8.3 were selected as priority lines.

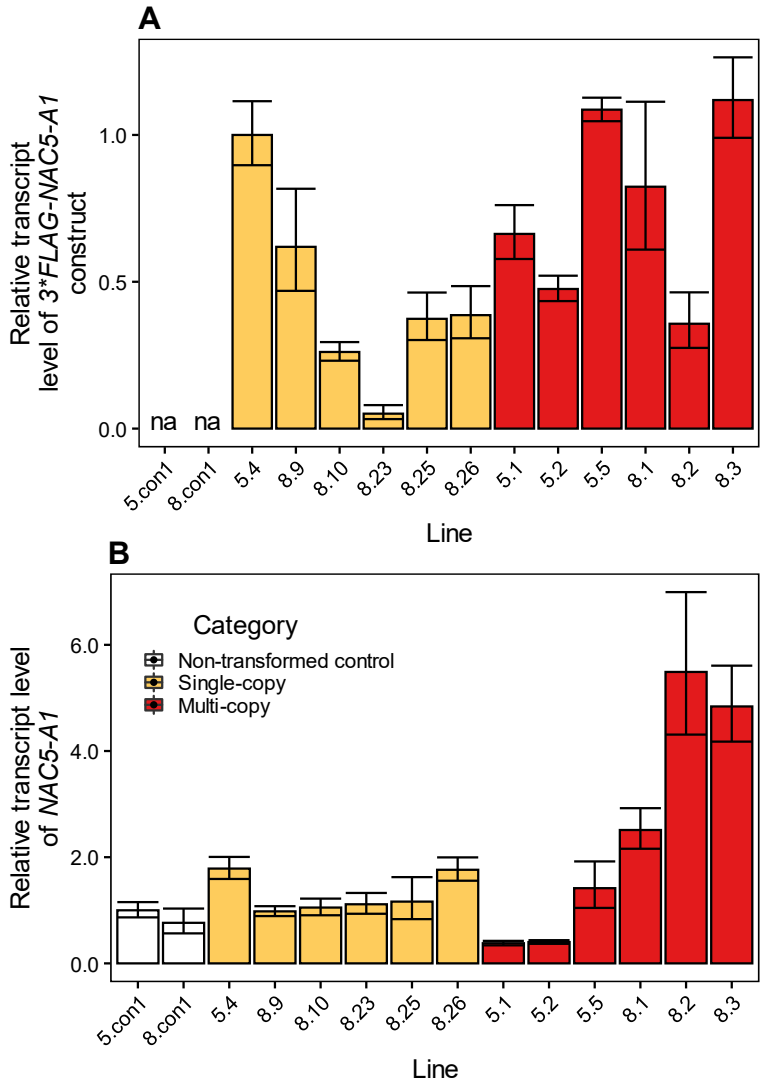


*Figure 3.9 Average expression of NAC5-A1 varies between independent T_1 transgenic lines. Average relative transcript level of (A) 3*FLAG::NAC5-A construct normalized to 5.4; (B) NAC5-A1 normalized to 5.con. RNA was extracted from pooled leaf samples of 12 T_1 plants per transgenic line, at 3 weeks. Relative transcript level was analysed by RT-qPCR using ΔΔCt method with Actin as reference gene, mean ±SD (n=3 technical replicates). "na" marks samples that were not amplified.*

To further screen *NAC5-A1* expression levels, transcript levels were tested by RT-qPCR in leaf samples from each individual in the five priority lines. Consistent with the pooled samples, individuals from all lines expressed the construct, although there was variability especially within lines 5.4 and 8.3 (*Figure 3.10*A). The median

NAC5-A1 expression of multi-copy line 8.2 was double that of non-transformed control 8.con, and multi-copy line 8.3 showed a trend toward higher expression (*Figure 3.10*B). The single-copy lines did not overexpress *NAC5-A1* compared to controls on average. This is unsurprising given that these T_1 populations are likely to contain null segregants lacking the construct. Some individuals within line 5.4 expressed *NAC5-A1* more highly than all 8.con individuals. Similar trends were seen when comparing the combined expression of *NAC5-A1, NAC5-B1* and *NAC5-D1* (*Figure 3.10*C).

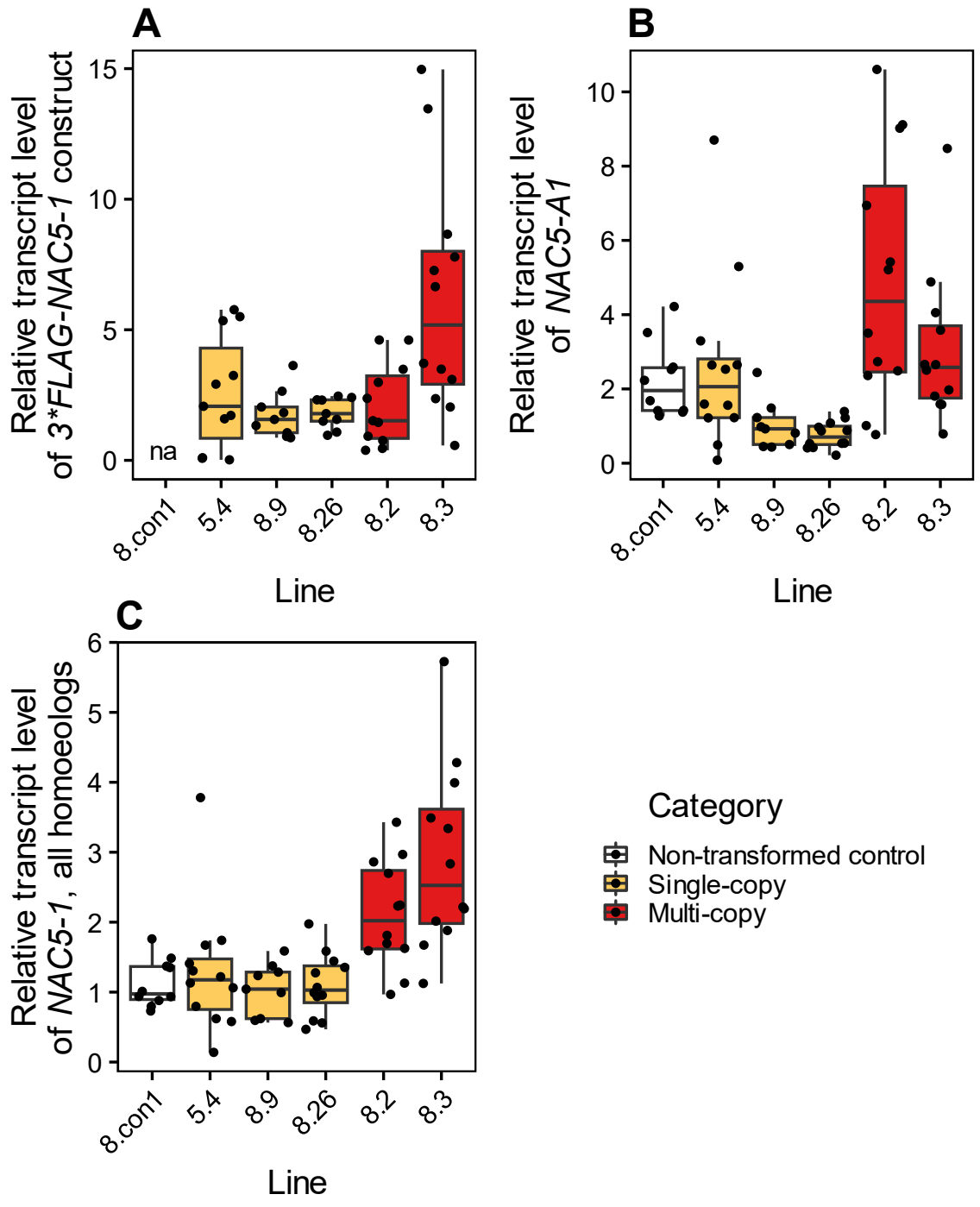


*Figure 3.10 Lines 5.4, 8.2 and 8.3 contain individuals with higher expression of NAC5-A1 than controls. Relative transcript level by RT-qPCR of (A) 3*FLAG::NAC5-A1 construct; (B) NAC5-A1; (C) NAC5-A1, NAC5-B1 and NAC5-D1 combined. RNA was extracted from leaves of individual T_1 plants at 3 weeks. Relative transcript level calculated the Pfaffl method with primer efficiencies and Actin as reference gene, normalised against the average of the single copy category, average of 3 technical replicates (n=12 plants). "na" marks samples that were not amplified.*

3.3.3.2 Phenotyping of T_1 transgenic lines in the glasshouse

To explore whether overexpression of *NAC5-A1* affects the timing of senescence, preliminary phenotyping was carried out on T_1 lines in the glasshouse (Methods 3.2.5.2). On this occasion, transgenic lines were not randomized and glasshouse lights were widely spaced. As a result, some transgenic lines were directly under glasshouse lights whilst others were not. Lines under glasshouse lights headed sooner, grew shorter and senesced earlier than those that were not (*Figure 3.11*). As both control lines were under lights, only lines under lights were retained for phenotypic analysis. These lines were non-transformed controls 5.con and 8.con, line 8.10 which showed similar average expression of *NAC5-A1* to controls, *NAC5-A1* overexpressing lines 8.2 and 8.3, and line 8.1 with intermediate expression.

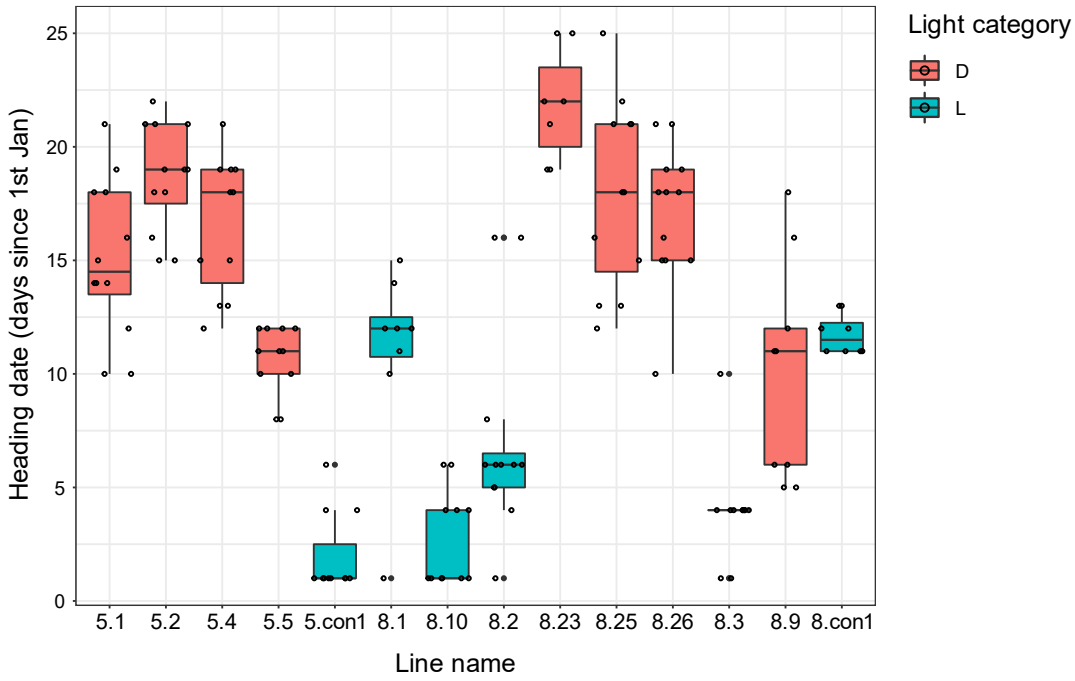


Figure 3.11 Multiple phenotypes varied with the light level in the glasshouse. Heading dates in NAC5-A1 T1 lines, directly under glasshouse lights (L) or further from lights (D). Heading date scored in days, where 1 = 1st January 2021.

The non-transformed controls differed in senescence timing: line 8.con headed later and senesced earlier (relative to heading) than line 5.con (*Figure 3.12*). *NAC5-A1* overexpressing lines 8.2 and 8.3 showed intermediate and early heading, respectively (*Figure 3.12*A). Flag leaves of lines 8.2 and 8.3 senesced earlier than 5.con, but did not differ from 8.con (*Figure 3.12*B, *Figure 3.12*D). Peduncles of lines 8.2 and 8.3 senesced earlier than 5.con, but did not differ from 8.con (*Figure 3.12*C). Line 8.10, which had low heterologous expression of *NAC5-A1,* showed similar timing of heading and senescence to control 5.con. Grain number and grain mass did not differ between lines 8.2, 8.3 and 8.con (*Figure 3.13*). Due to differences between controls and an experimental design that did not account for environmental variability, it is unclear from this experiment whether *NAC5-A1* overexpression leads to earlier senescence.

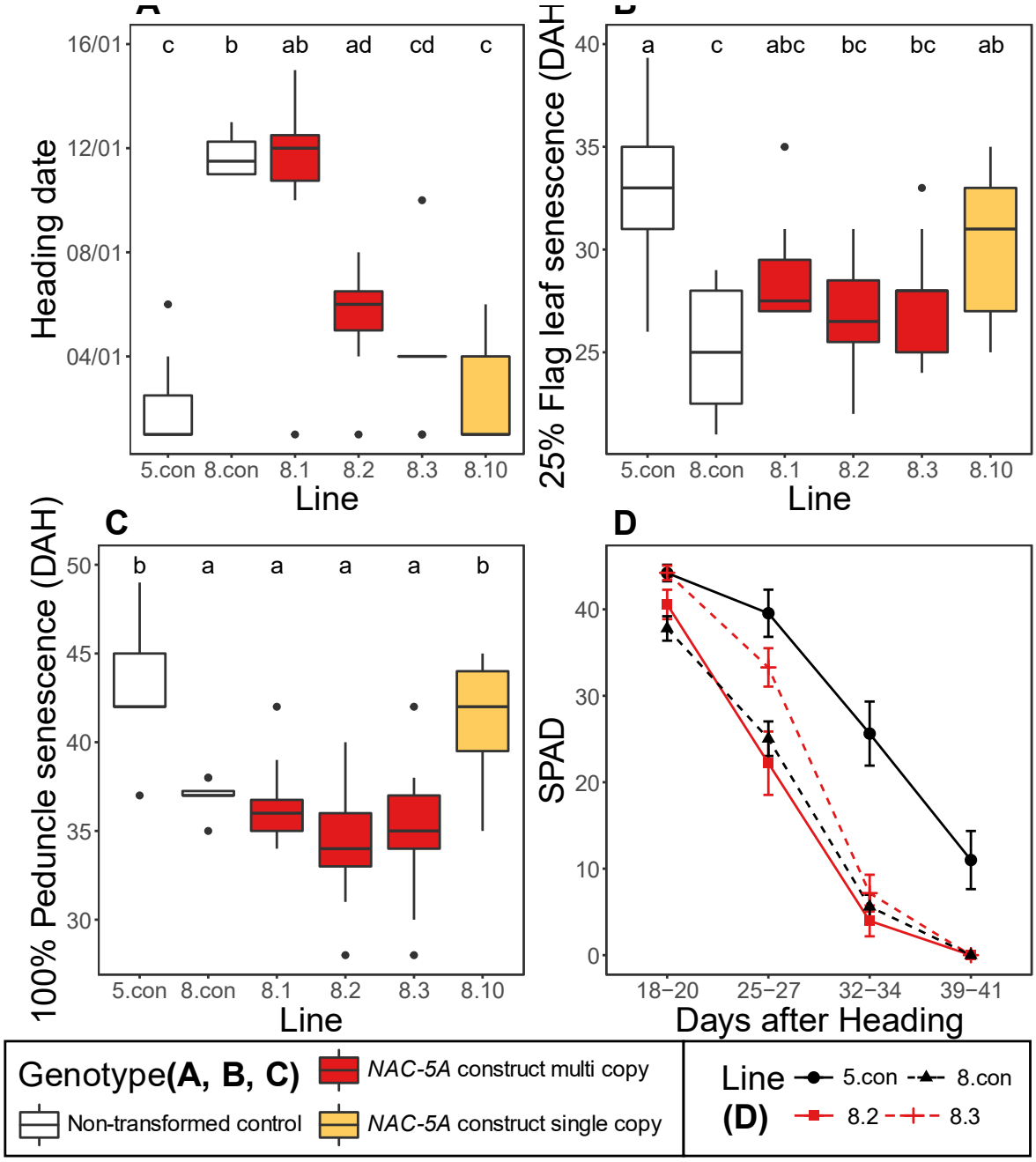


Figure 3.12 NAC5-A1 T_1 transgenic lines 8.2 and 8.3 senesced earlier than control 5.con but did not differ from control 8.con. Boxplots of (A) Heading date; (B) 25% flag leaf yellowing; (C) 100% peduncle yellowing (first tiller, n=12). DAH=Days after Heading. Letters show significance groups (post-hoc Tukey test, p<0.05). (D) Relative chlorophyll content of flag leaves measured by SPAD spectrophotometer, mean ±SE (n=12). Only lines directly under glasshouse lights are shown (see Methods 3.2.5.2).

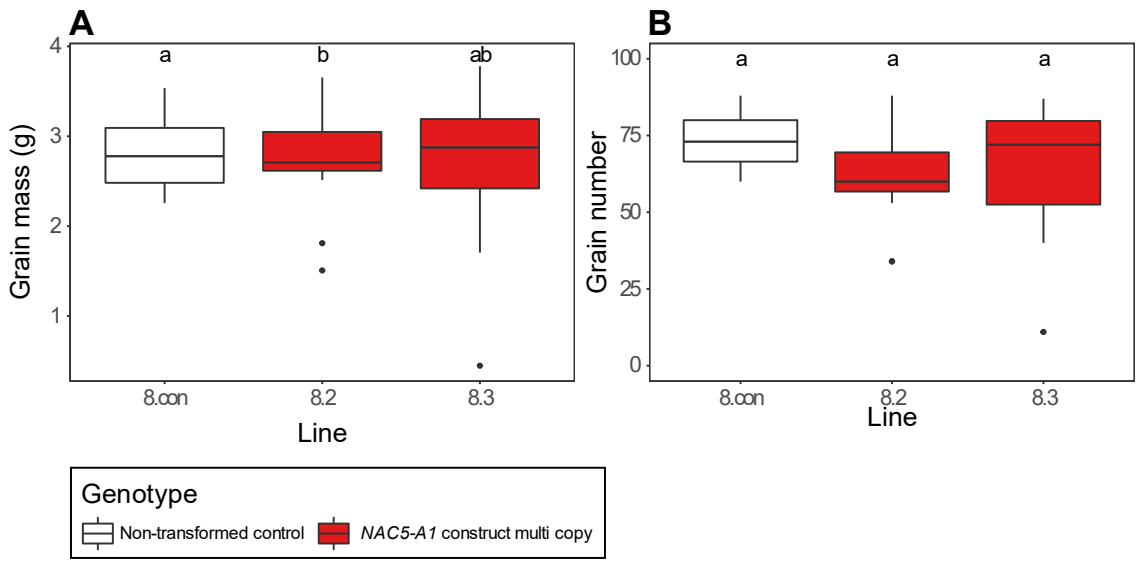


Figure 3.13 NAC5-A1 T_1 transgenic lines 8.2 and 8.3 do not differ in grain mass or number from control 8.con. Boxplots of (A) Grain number; (B) Grain mass (g). Letters show significance groups (post-hoc Tukey test, p<0.05).

3.3.3.3 Selection of homozygous transgenic lines by copy number analysis

To improve the genetic uniformity of the next experiment, single-copy T_1 plants with homozygous insertion of the *NAC5-A1* construct and corresponding null segregants lacking the *NAC5-A1* construct were selected. To achieve this, construct copy number of T_1 plants was assessed. If the T_0 parent contains a single construct insertion, the T_1 population will segregate in a 1:2:1 ratio of 0:1:2 construct copies. T_1 populations 5.4, 8.23, and 8.9 segregated consistently with this, confirming that T_0 parents contained a single insertion (*Figure 3.14*). However, some plants in lines 8.25, 8.26 and 8.10 putatively contained 3 construct copies, suggesting that the T_0 parents had two construct insertions. Therefore, lines 5.4, 8.23 and 8.9 were taken forward. For each line, the T_1 plant with 2 construct copies and highest *NAC5-A1* expression were selected, along with a T_1 plant with 0 construct copies and no expression of the construct (*Table 3.11*). In line 5.4, the selected homozygous transgenic plant showed two-fold higher expression of *NAC5-A1* than the selected

control plant. In line 8.9, the selected plants had similar expression, while in line 8.23 plant-level expression was not tested. T_2 progeny of these plants was used for the following experiment.

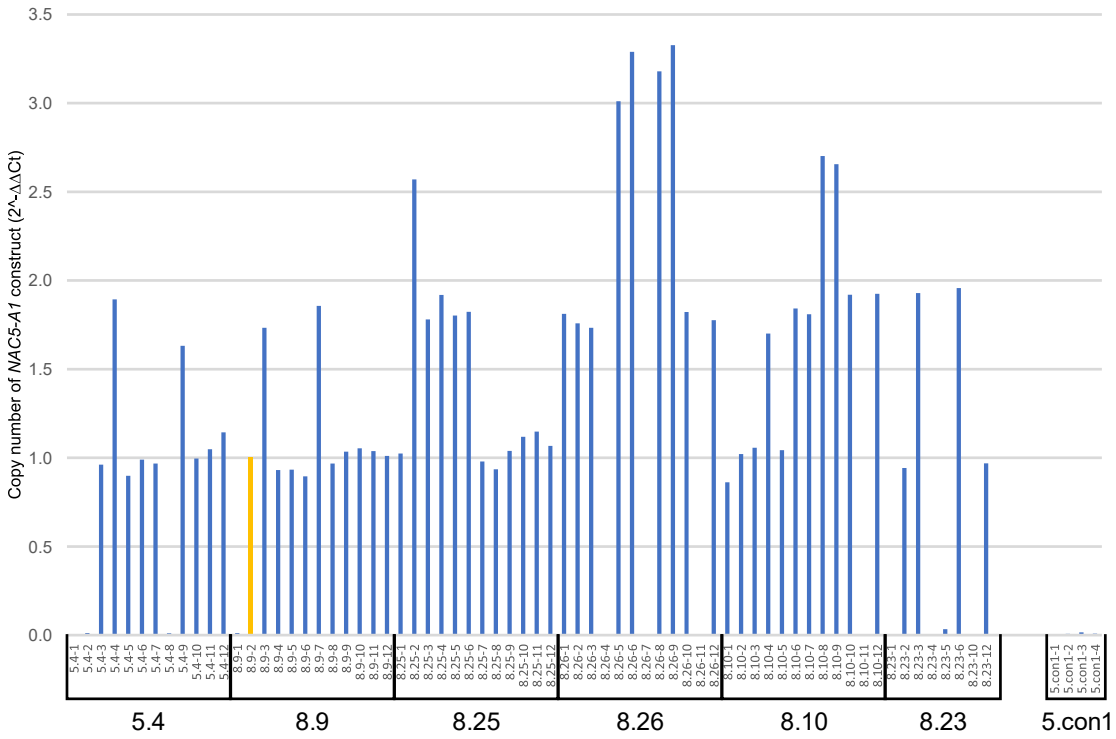


*Figure 3.14 Most, but not all, NAC5-A1 T_1 lines show expected segregation for the 3*FLAG::NAC5-A transgenic construct. Copy number of NAC5-1 construct in individual T_1 plants. Taqman qPCR was run against the nptII marker gene in the construct and analysed by ΔΔCt method, normalised against a known single-copy gene and the sample with median expression level in the "single copy" cluster (highlighted yellow).*

3.3.3.4 Overexpression of *NAC5-A1* in wheat promotes earlier leaf senescence but does not impact grain mass or protein content

To test whether *NAC5-A1* overexpression affects senescence timing, a time-course of flag leaf senescence was measured in *NAC5-A1* T_2 transgenic lines and null segregant controls, grown in a controlled environment chamber (Methods 3.2.5.4). *NAP-A1* transgenic lines were grown at the same time.

Unexpectedly, across both *NAC5-A1* and *NAP-A1* transgenic lines, plants on CER Shelf 2 headed earlier and senesced more rapidly after heading than plants on CER Shelf 1 (*Figure 3.15*A, D). Plants on Shelf 2 also grew fewer tillers, shorter flag leaves and more grains per plant than those on Shelf 1 (*Figure 3.15*B, C). Several plants on Shelf 1 were infected with powdery mildew, while few plants on Shelf 2 were infected. Although LED lights on both shelves were set to 300µmol, the light panels were different models (Hettich 1100µmol spec on Shelf 1 and 400µmol spec on Shelf 2), so it is possible that the colour spectrum, hence the photosynthetically active radiation, differed between shelves. As the plants were arranged in a randomized complete block design, all genotypes were divided equally between the two shelves. Therefore, results were shown separately for Shelf 1 and Shelf 2, and differences between Shelf 1 and Shelf 2 were accounted for in analysis by including Shelf as a blocking factor in the linear model.

Across *NAC5-A1* and *NAP-A1* overexpression experiments, 22 plants were excluded from analysis as the peduncle snapped before 100% peduncle senescence, potentially affecting grain filling. 14 plants infected by powdery mildew were retained in analysis, as senescence phenotypes did not differ significantly between infected and non-infected plants.

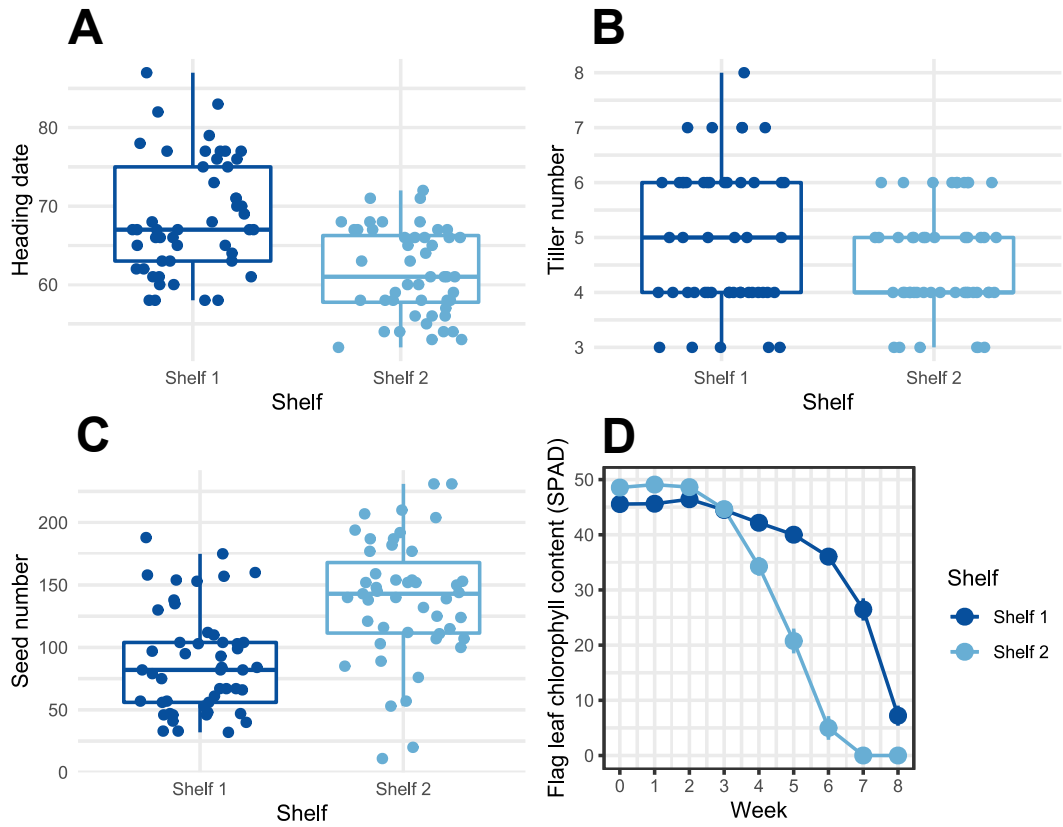


Figure 3.15 Multiple phenotypes of NAC5-1 and NAP-1 T2 lines vary between CER shelves. Plots of all genotypes in NAC5-1 and NAP-1 CER experiments categorised by CER shelf for (A) Heading date in days after sowing (DAS), (B) Main tiller number, (C) Seed number, (D) Flag leaf chlorophyll content (SPAD) in weeks after heading +/- 1 day.

In lines 8.23 and 8.9, which did not overexpress *NAC5-A1,* the time-course of flag leaf chlorophyll content was not significantly different between homozygous transgenics and corresponding null segregant controls grown on the same shelf (*Figure 3.16*). Average chlorophyll content deviates from a smooth curve at Weeks 5-6 in some graphs; this is an artifact of missing data in this time period. In *NAC5-A1* overexpressing line 5.4, transgenic plants showed significantly lower chlorophyll content 4 weeks after heading than controls on average on Shelf 2 (Wilcoxon test, $p < 0.05$) (*Figure 3.16*).

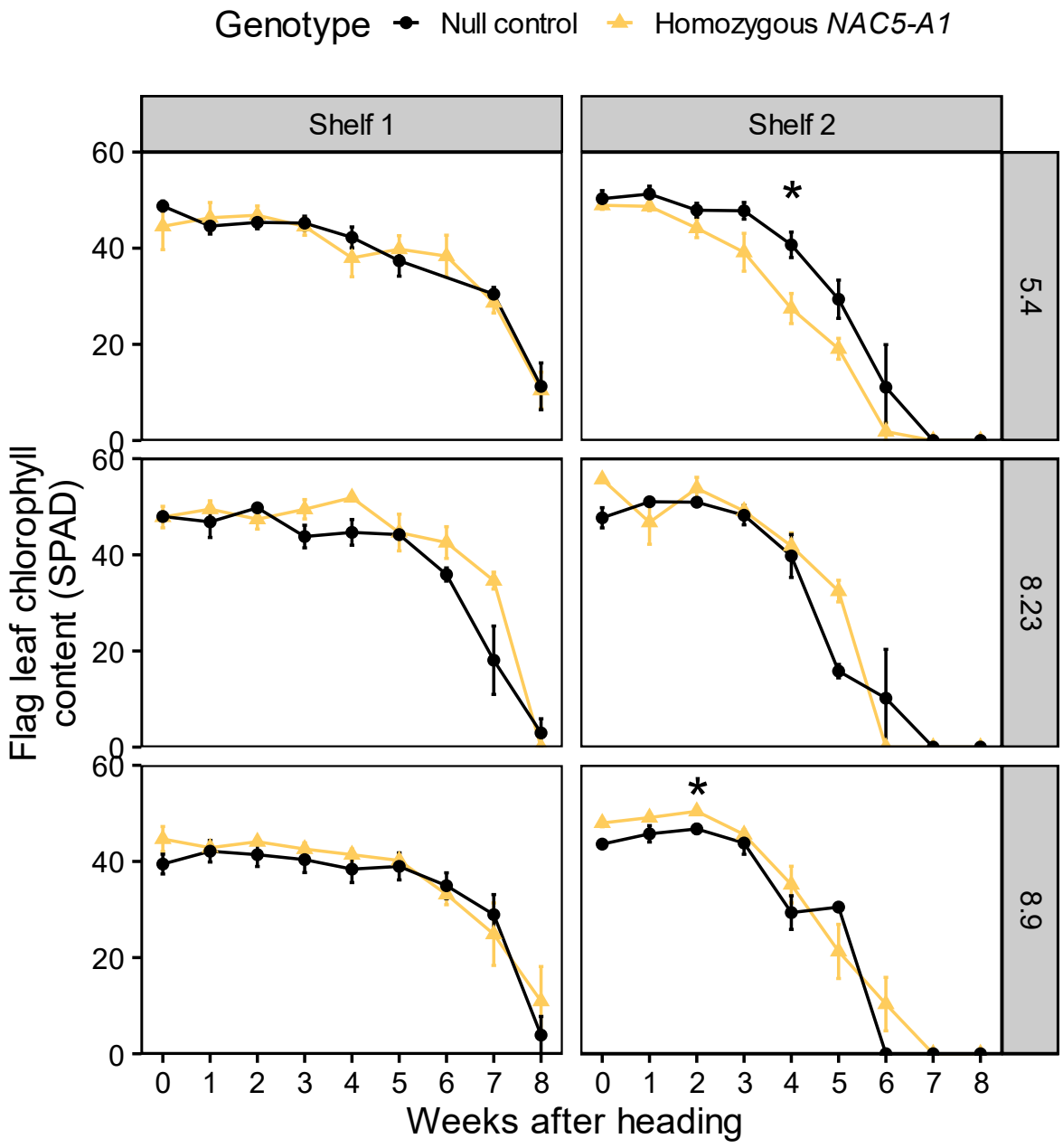


*Figure 3.16 Flag leaves senesce later in NAC5-A1 transgenic compared to control for line 5.4 on Shelf 2 only. Flag leaf chlorophyll content (SPAD) in weeks after heading +/- 1 day was compared between homozygous transgenic and null segregant controls in T2 transgenic lines 5.4, 8.23 and 8.9. Average SPAD value at each timepoint was compared by Wilcoxon test, *=p<0.05. NB: Averages were taken of 2-5 data points; timepoints with small sample sizes may result in apparent differences that are not statistically significant.*

Further traits are shown for *NAC5-A* overexpressing line 5.4 only. Heading date did not differ between line 5.4 homozygous transgenics and controls grown on the same shelf (*Figure 3.17*A). *NAC5-A* overexpressing plants trended towards earlier date of 25% leaf senescence by visual scoring and earlier peduncle senescence on both shelves, however this was not statistically significant (*Figure 3.17*B, C). On Shelf 2, the overexpression line reached a SPAD value of 30 significantly earlier than the control (*Figure 3.17*D), and showed a non-significant trend towards overall earlier senescence, measured as area under the curve (AUC), and longer duration of leaf senescence (*Figure 3.17*E, F). It should be noted that comparisons within one shelf have limited statistical power due to a sample size of five per genotype. In conclusion, these results indicate that overexpression of *NAC5-A1* leads to earlier flag leaf senescence in some environments, supporting the hypothesis that *NAC5-1* promotes the onset of senescence.

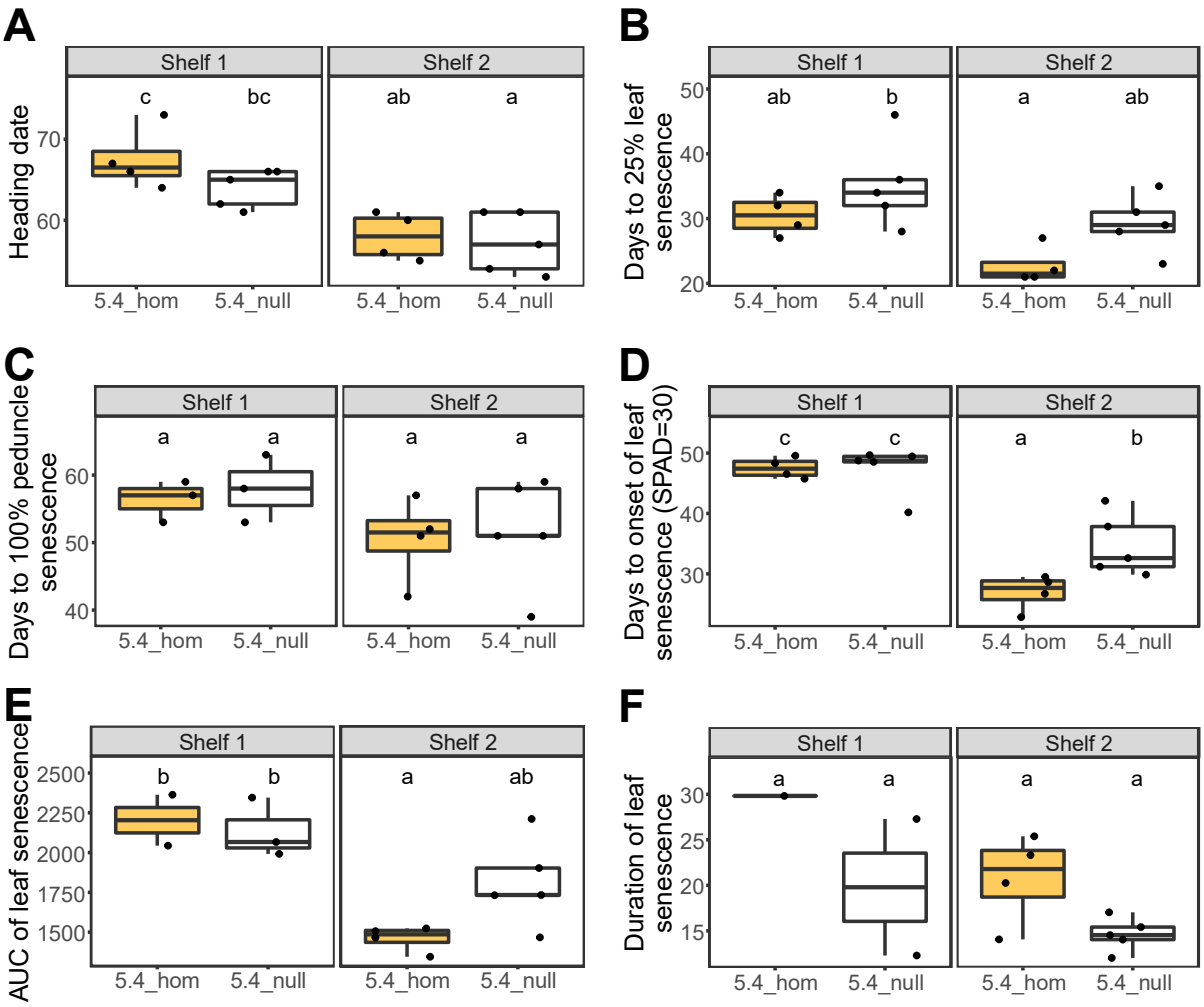


*Figure 3.17 Senescence phenotypes of NAC5-1 overexpression line 5.4. (A) Heading date (DAS); (B) 25% flag leaf yellowing; (C) 100% peduncle yellowing; (D) Days from heading to SPAD=30; (E) Area under curve (AUC) of leaf senescence; (F) Duration of leaf senescence (Days). (A-F) ANOVA with post-hoc Tukey test, formula ~ Shelf * Line_name, letters show significance groups at p<0.05. NB: Boxplots represent 2-5 individuals; small sample sizes may result in apparent differences that are not statistically significant.*

Tiller number, grain mass, grain number, thousand kernel weight, and grain length did not differ between transgenic and control plants of line 5.4 (*Figure 3.18*A-E). Grain width and area also did not differ between transgenics and controls (not shown). Because grain mass was less than 15g, it was not possible to measure grain protein content.

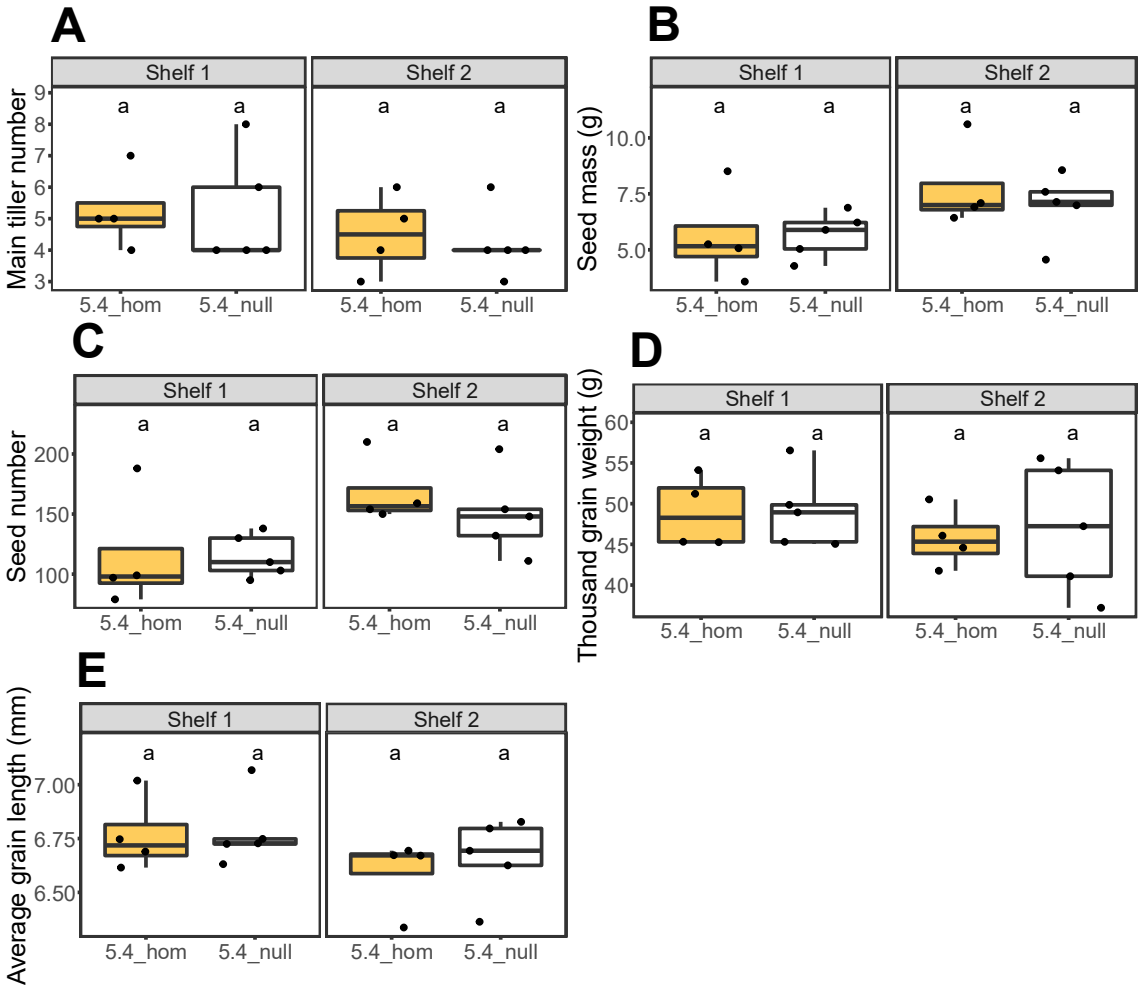


*Figure 3.18 Grain traits did not differ between homozygous NAC5-A1 transgenics and null segregants in line 5.4. (A) Main tiller number; (B) Seed mass (g); (C) Seed number; (D) Thousand grain weight; (E) Average grain length. ANOVA with post-hoc Tukey test, formula ~ Shelf * Line_name, letters show significance groups at p<0.05. NB: Boxplots represent 2-5 individuals; small sample sizes may result in apparent differences that are not statistically significant.*

The full range of traits measured and calculated include several correlated traits. Across this experiment, typically later heading correlates with later senescence (e.g. heading date and number of days to SPAD = 30, r^2 =0.48), and earlier senescence correlates with higher grain mass and number (e.g. number of days to SPAD = 30 and grain mass, r^2 = -0.39) (*Figure 3.19*). These correlation data are likely skewed by the differences between shelves.

The number of days to SPAD of 30 was calculated as a proxy for the onset of senescence. It showed a positive correlation with the independent visual scores of days to 25% leaf yellowing (r^2 =0.63) and days to complete peduncle yellowing (r^2 =0.57) (*Figure 3.19*). This indicates that the number of days to SPAD of 30 is a reliable metric for senescence. To simplify figures some highly correlated traits were omitted. In this experiment, the number of days to SPAD of 30 was positively correlated with the days to SPAD of 10 (r^2 =0.94) and days to SPAD of 40 (r^2 =0.77) which were not presented (*Figure 3.19*). Average grain area, average grain width, average grain length and thousand grain weight are highly correlated with each other (r^2 >=0.71). Of these, grain length and thousand grain weight were shown as representative grain traits. Other experiments in this thesis were simplified in the same way.

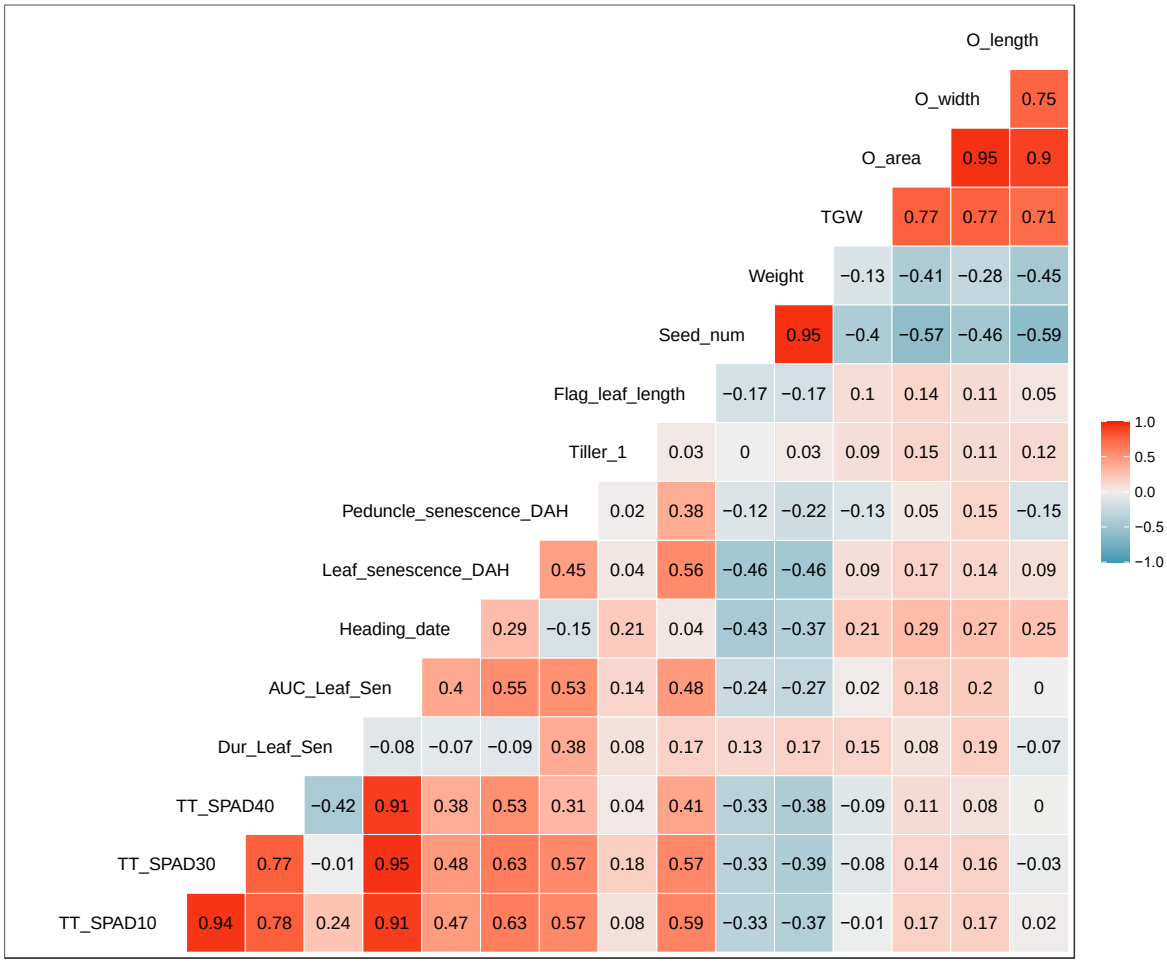


Figure 3.19 Correlations between senescence traits and other phenotypes for NAC5-A1 transgenics data. Pearson's correlation coefficient, r^2. TT_SPAD10 = Days from heading to SPAD = 10, TT_SPAD30 = Days from heading to SPAD = 30, TT_SPAD40 = Days from heading to SPAD = 40, Dur_Leaf_Sen = Days from SPAD = 40 to SPAD = 10, AUC_Leaf_Sen = Area under flag leaf senescence SPAD curve, Heading_date = Heading date (Days after sowing), Leaf_senescence_DAH = Days from heading to 25% leaf senescence, Peduncle_senescence_DAH = Days from heading to 100% peduncle senescence, Tiller_1 = number of main tillers, Seed_num = grain number per plant, Weight = grain mass per plant, TGW = thousand grain weight, O_area = mean area of grain, O_width = mean width of grain, O_length = mean length of grain.

3.3.4 Mutations in *NAC5-1* in tetraploid wheat

3.3.4.1 Development and phenotyping of *NAC5-1* and *NAP-1* TILLING mutant lines

If *NAC5-1* promotes the onset of senescence, loss-of-function of *NAC5-1* would delay senescence. To test this hypothesis, mutations in *NAC5-A1* and *NAC5-B1* likely to lead to loss-of-function were identified in the tetraploid Kronos TILLING population. Tetraploid Kronos was used as combining mutations in two rather than three homoeologs reduced the number of generations required in the crossing scheme.

For *NAC5-A1* and *NAC5-B1*, missense mutations in subdomains iii and iv of the NAC domain were selected (Table 3.14). The strongly negative PSSM scores of -4 and -8 demonstrate that the amino acids in the mutant alleles are rarely found at these positions in the NAC domains of NAC transcription factors across species, hence they are likely to be deleterious. For *NAP-A1* and *NAP-B1*, stop codon mutations in subdomains ii and iii of the NAC domain were selected (Table 3.14). These stop codon mutations are predicted to lead to a loss of function due to a truncated protein with an incomplete NAC domain.

For *NAC5-1,* plants with mutations in *NAC5-A1* and *NAC5-B1* were crossed to generate a heterozygous double mutant, then backcrossed twice to Kronos to reduce background mutation load by 75%. From the segregating BC_2F_2 population, wild-type, single and double mutants were selected. Two alternative mutations in *NAC5-B1* were used to create two independent sets of TILLING lines (Table 3.15). One set of TILLING lines was generated for *NAP-1* in the same way.

*Table 3.14 TILLING mutations selected in NAC5-A1, NAC5-B1, NAP-A1 and NAP-B1. Gene ID from IWGSC RefSeq v1.1. Variant ID is the wheat line containing the mutation and the SNP position. Consequence shows effect on the amino acid sequence. Subdomain shows where in five conserved NAC subdomains the mutation sits. PSSM score indicates the likelihood of a missense SNP in this position of the NAC domain across all NAC TFs. *Variant IDs could not be found for NAC5-A1 or NAP-B1 in RefSeq v1.1 as mutations were initially identified in previous gene annotation (TGAC).*

Gene name	**Gene ID**	**Variant ID**	**Alleles**	**Consequence**	**Amino acids**	**Amino acid position**	**Subdomain of NAC domain**	**PSSM score**
NAC5-A1	TraesCS4A02G219700	Kronos2546*	G/A	missense	G/E	93	iii	-8
NAC5-B1	TraesCS4B02G098200	Kronos2036.chr4B.103056075	G/A	missense	A/T	111	iv	-8
NAC5-B1	TraesCS4B02G098200	Kronos3328.chr4B.103056044	G/A	missense	G/D	121	iv	-4
NAP-A1	TraesCS4A02G131000	Kronos255.chr4A.174157340	G/A	stop gained	W/*	52	ii	
NAP-B1	TraesCS4B02G173600	Kronos3959*	G/A	stop gained	W/*	65	iii	

Table 3.15 Sets of TILLING lines for NAC5-1 and NAP-1. Two sets of TILLING lines were created for NAC5-1, and one for NAP-1. Cross ID is used to designate each set of lines in this thesis.

Cross ID	Gene name	A mutant	Consequence	B mutant	Consequence
X388	*NAC5-1*	Kronos2546	missense	Kronos2036	best missense
X392	*NAC5-1*	Kronos2546	missense	Kronos3328	missense
X585	*NAP-1*	Kronos0255	stop gained	Kronos3959	stop gained

Homozygous double mutant plants, single mutants and controls for *NAC5-1* and *NAP-1* were grown in the glasshouse (Methods 3.2.5.5). A few seeds in the *NAC5-1* TILLING lines and several seeds in the *NAP-1* TILLING lines, especially *NAP-A1* and *NAP-B1* single mutants, failed to germinate or died at the seedling stage. These individuals were replaced by seeds sown 3 weeks later and added into the original block design (Table *3.12*). Late-sown plants developed approximately half the number of tillers, and half the seed number and mass compared to early-sown plants (*Figure 3.20*C, D). This is likely due to tiller abortion as these plants had many back tillers that did not fully develop. Nevertheless, late sowing had no effect or only a small effect on the heading date or senescence phenotype of the primary tiller, therefore these plants were retained in the analysis (*Figure 3.20*A, B).

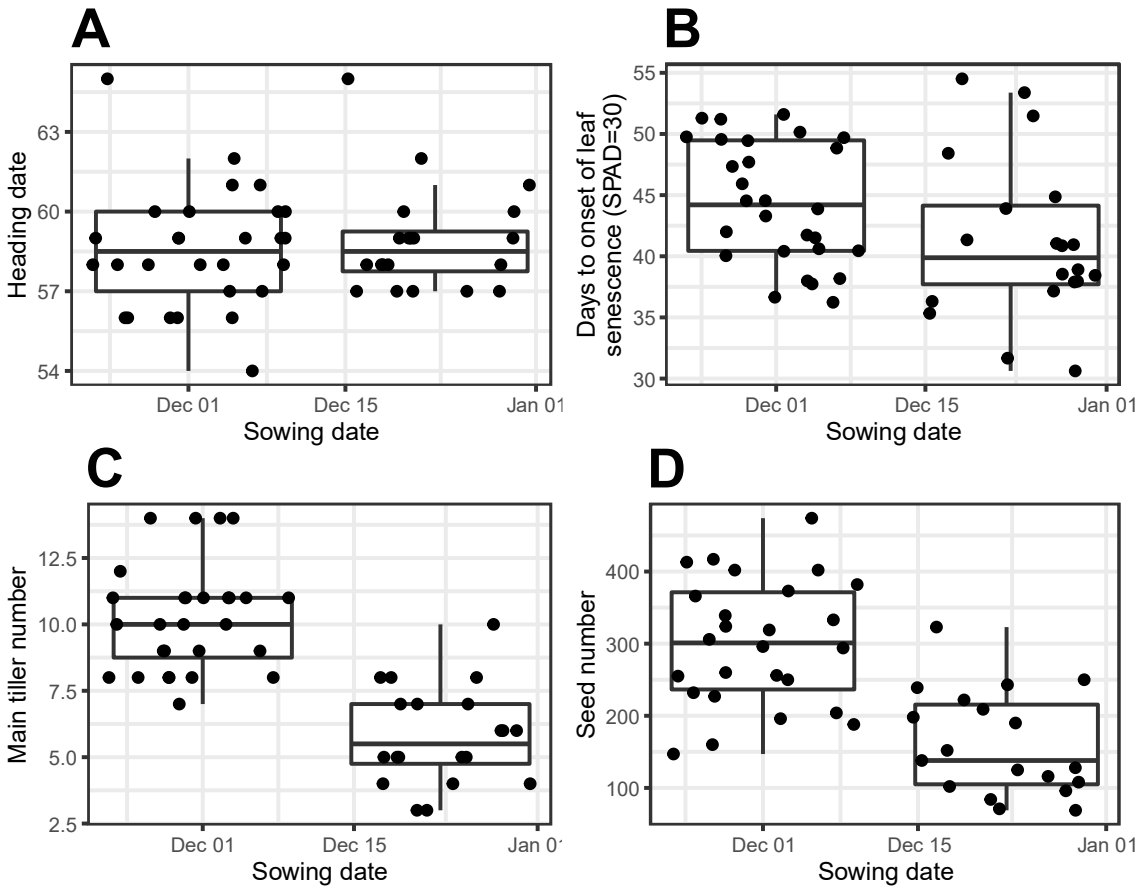


Figure 3.20 Plants with later sowing date had fewer tillers and seeds. Several plants in the NAP-1 TILLING experiment were re-sown three weeks later due to failed germination in the first batch. Plots show all plants in NAP-1 TILLING experiment categorised by sowing date, for (A) Heading date (DAS); (B) Days from heading to SPAD=30; (C) Number of main tillers and (D) Seed number.

The genotypes of plants in the glasshouse experiment were tested by KASP genotyping. Most plants for most *NAC5-1* and *NAP-1* TILLING lines showed the expected genotypes (*Table 3.16*, *Table 3.17*). NA values represent genotyping errors, while heterozygous genotypes may be either genotyping errors or rare cross-pollination events. However, the line labelled “X392_bb” segregated, showing *NAC5-B1* mutants (AAbb), double mutants (aabb) and heterozygotes (Aabb) (*Table 3.17*). This indicates that the parent plant was “Aabb” rather than the expected “AAbb”.

Similarly, the “X392_aabb” parent plant was probably “aaBb” rather than the expected “aabb”. Plants were recategorized, and all confirmed homozygous genotypes were included in the analysis (both expected and unexpected). In analysis, the sample size was less than 10 for genotypes X388_WT, X388_aa, X392_bb and X392_aabb.

*Table 3.16 Summary of KASP genotyping results for NAC5-1 Kronos TILLING lines (01/12/2021). Here, "Y" represents wild-type alleles and "X" represents mutant alleles. Expected genotypes are highlighted in green. *These lines appear to have a different genotype than expected.*

Row Labels	Y:Y.Y:Y	X:X.Y:Y	Y:Y.X:X	X:X.X:X	X:X.X:Y	X:Y.X:X	NA	Grand Total
X388_WT	5						7	12
X388_aa		7		3			2	12
X388_bb			11				1	12
X388_aabb				9		1	2	12
X392_WT	11						1	12
X392_aa		12						12
X392_bb*			4	2		6		12
X392_aabb*		5			7			12
Grand Total	16	24	15	14	7	7	13	96

Table 3.17 Summary of KASP genotyping results for NAP-1 Kronos TILLING lines (01/12/2021). Here, "Y" represents wild-type alleles and "X" represents mutant alleles. Expected genotypes are highlighted in green.

Row Labels	Y:Y.Y:Y	X:X.Y:Y	Y:Y.X:X	X:X.X:X	X:X.X:Y	Y:Y.X:Y	NA	Grand Total
X585_WT	12							12
X585_aa		12						12
X585_bb			8			3	1	12
X585_aabb				10	2			12
Grand Total	12	12	8	10	2	3	1	48

This glasshouse experiment ran December – April, therefore plants received supplementary light and heat from lights evenly spaced along the centre of the glasshouse bench. Plants were situated between the centre and edge of the bench. Plants at the centre of the bench headed sooner, and the flag leaves senesced more rapidly after heading (*Figure 3.21*). Therefore, position from centre of bench was added as a covariate to the linear model. Block in the randomised complete block design was added as a fixed-effect factor.

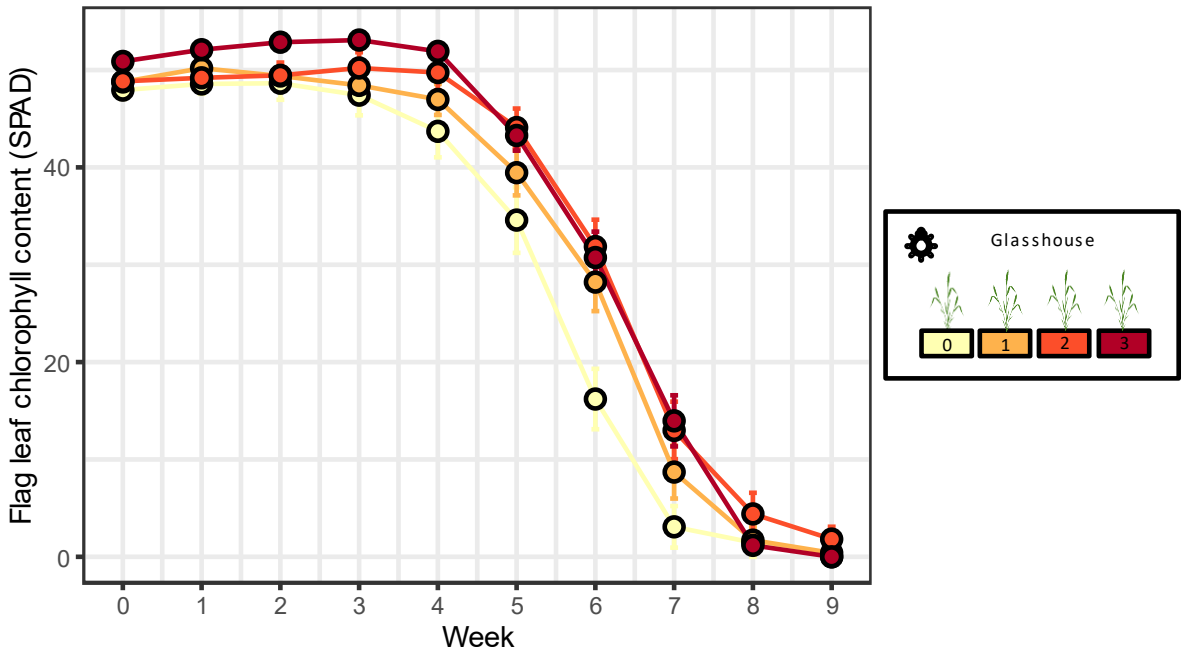


Figure 3.21 Plants directly under glasshouse lights senesced faster. Flag leaf chlorophyll content (Weeks after Heading ± 2 days) for all plants in NAC5-1 TILLING experiment categorised by distance from the centre of the bench, where glasshouse lights were situated.

3.3.4.2 *NAC5-1* double mutants showed delayed leaf senescence

To explore the effect of mutations in *NAC5-1* on senescence timing, data from crosses X388 and X392, sharing the same mutation in *NAC5-A1* but different mutations in *NAC5-B1*, were combined. *NAC5-1* double mutants retained higher flag leaf chlorophyll than controls between 14 and 35 days after heading (DAH) on average (*Figure 3.22*A). *NAC5-A1* and *NAC5-B1* single mutants also retained higher flag leaf chlorophyll than controls at and after heading (*Figure 3.22*B, C). *NAC5-1* mutants senesced more rapidly from 35-49DAH, completing flag leaf senescence at the same time as controls around 56DAH. As such, randomly selected plants and flag leaves photographed at later timepoints of 41DAH and 51DAH look similar across genotypes (*Figure 3.22*D-F). It is likely that the reason the *NAC5-A1* mutant at 51DAH looks more senesced is that this individual was directly under glasshouse lights, unlike any others shown. It should also be noted that flag leaves with SPAD values between 40 and 60 are difficult to distinguish visually.

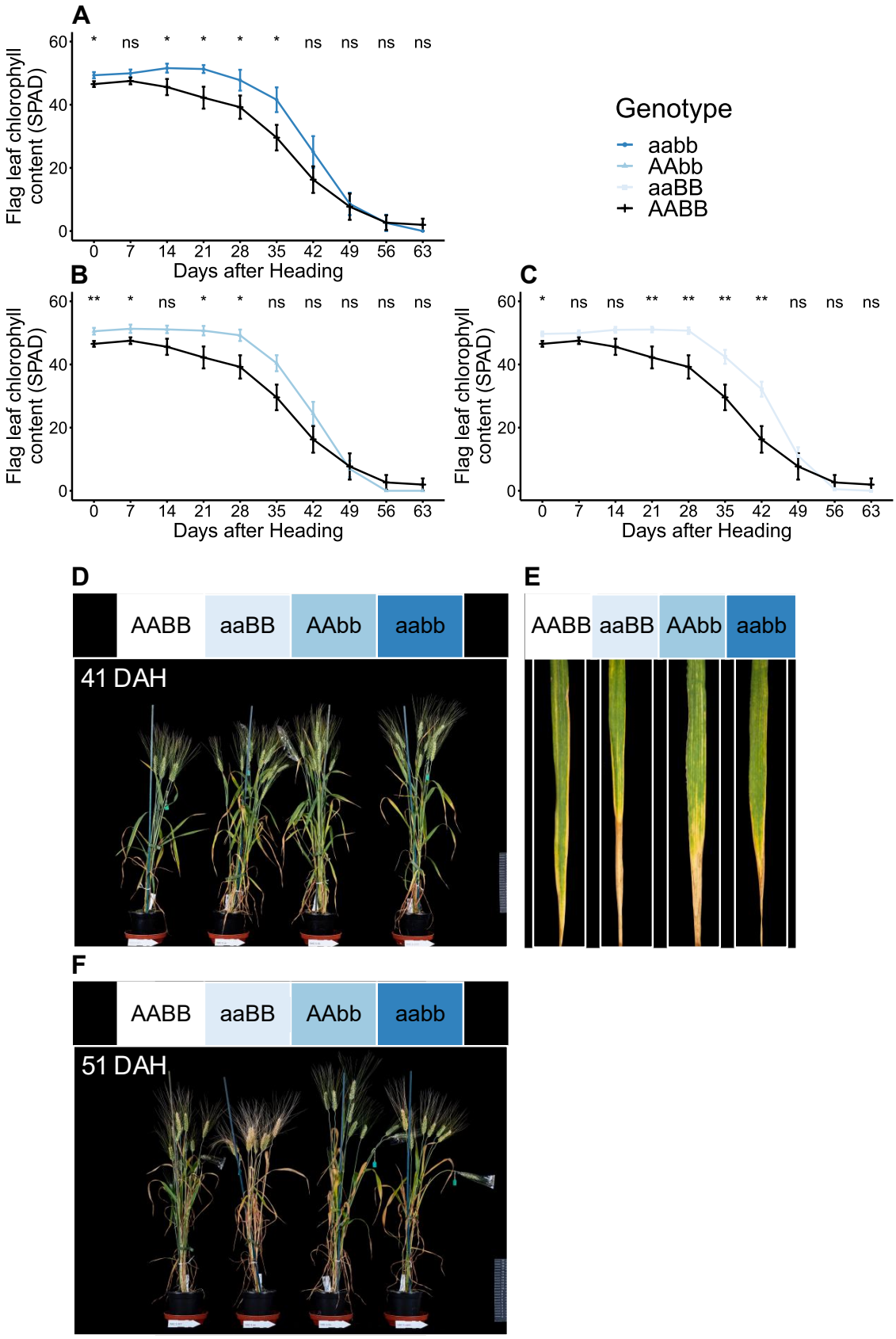


Figure 3.22 NAC5-1 double mutants retain flag leaf chlorophyll for longer than controls. (A-C) Flag leaf chlorophyll content (SPAD) in weeks after heading +/- 1 day

*was compared between NAC5-1 TILLING mutants and wild type segregant controls (AABB, n = 16). Average SPAD value at each timepoint was compared by Wilcoxon test, *=p<0.05. Data from crosses X388 and X392 were combined. (A) Double mutants (aabb, n = 14), (B) NAC5-B1 single mutants (AAbb, n = 14), NAC5-A1 single mutants (aaBB, n = 24). (B) Representative plants for wild type (AABB) single (aaBB / AAbb) and double (aabb) NAC5-1 mutants at 41DAH. (C) Flag leaves at 41DAH of plants in B. (D) Representative plants at 51DAH; different individuals to B.*

Interestingly, *NAC5-A1* single mutants headed earlier and reached 25% leaf senescence – by visual score – later after heading than controls, with intermediate phenotypes in *NAC5-B1* single mutants and double mutants (*Figure 3.23*A, B). *NAC5-1* single and double mutants showed a non-significant trend toward later onset and AUC of leaf senescence (*Figure 3.23*D, E). Onset measured as days to SPAD of 30 or days to 25% leaf senescence occurs around 30- 50DAA, so neither metric effectively captures the difference in chlorophyll content from 14-35DAA. The duration of leaf senescence and days to peduncle senescence did not differ between *NAC5-1* TILLING lines (*Figure 3.23*C, F). These results indicate that loss-of-function of *NAC5-1* delays the onset of leaf senescence, but does not delay peduncle senescence. This lends some evidence towards the hypothesis that *NAC5-1* promotes the onset of senescence.

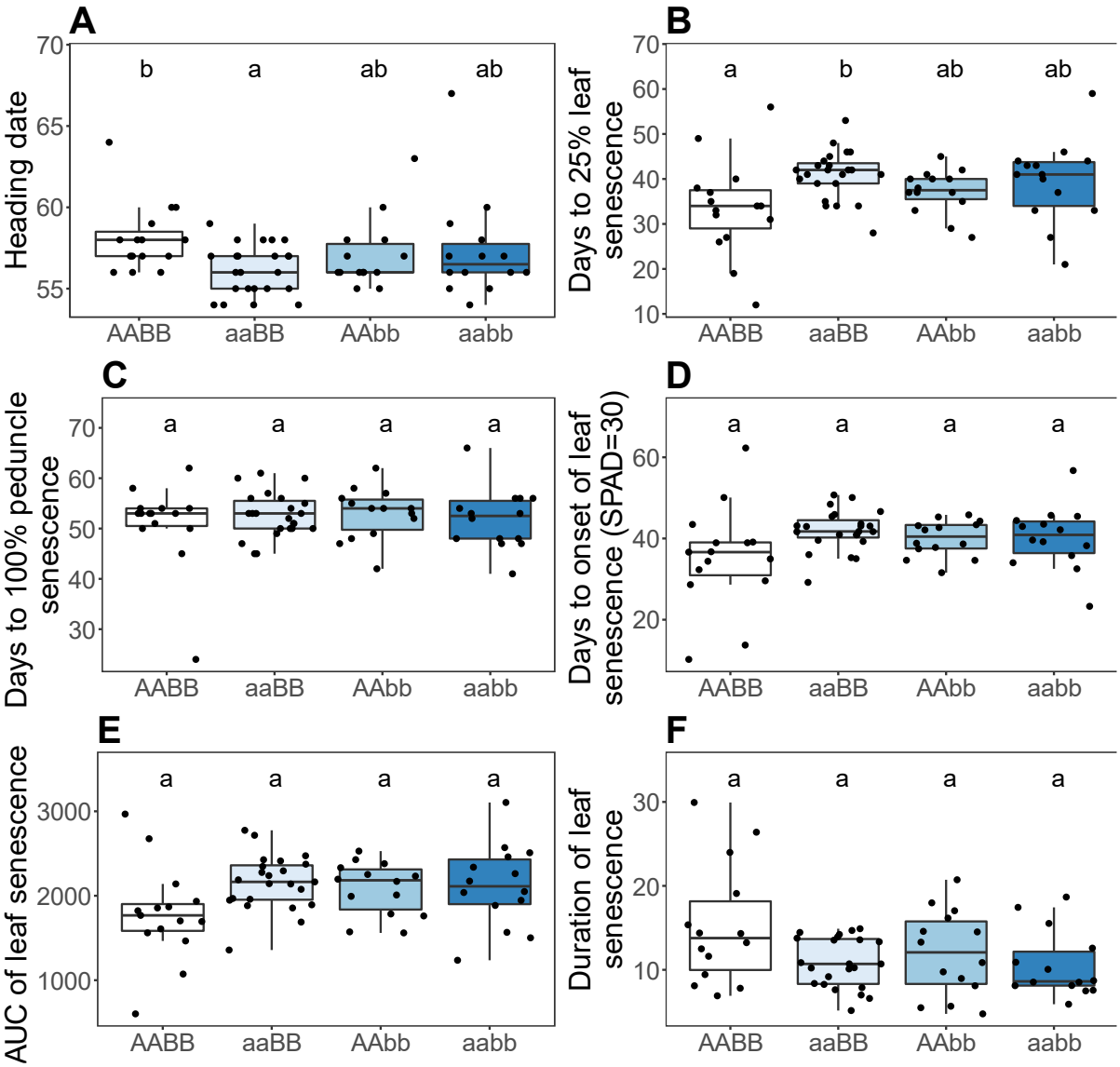


Figure 3.23 NAC5-1 double mutants show a trend toward later onset and AUC of leaf senescence however it is not statistically significant. (A) Heading date (DAS); (B) 25% flag leaf yellowing; (C) 100% peduncle yellowing; (D) Days from heading to SPAD=30; (E) Area under curve (AUC) of leaf senescence; (F) Duration of leaf senescence (Days). (A-F) ANOVA with post-hoc Tukey test, formula ~ Light + Block + Genotype, letters show significance groups at p<0.05. Data from crosses X388 and X392 were combined (n=14-24).

3.3.4.4 Mutations in *NAC5-1* do not affect grain number or protein content

All *NAC5-1* mutants and controls showed a similar growth phenotype, with no significant differences in tiller number or height (*Figure 3.24*A, B). *NAC5-A1* mutants had significantly higher grain mass than controls, although neither grain number nor thousand kernel weight were significantly affected (*Figure 3.24*C, D, E). Grain length increased in *NAC5-1* double mutants, while grain width and area did not differ between lines (*Figure 3.24*F, G, H). Grain protein content did not vary between *NAC5-1* genotypes (*Figure 3.24*I). When normalised for thousand grain weight, *NAC5-A1* single mutants displayed slightly higher protein mass per thousand grain than controls (*Figure 3.24*J). Neither loss-of-function nor overexpression of *NAC5-1* altered grain mass or protein content in these experiments. This indicates that *NAC5-1* does not affect grain mass and protein content, at least under well-watered, fertilised conditions.

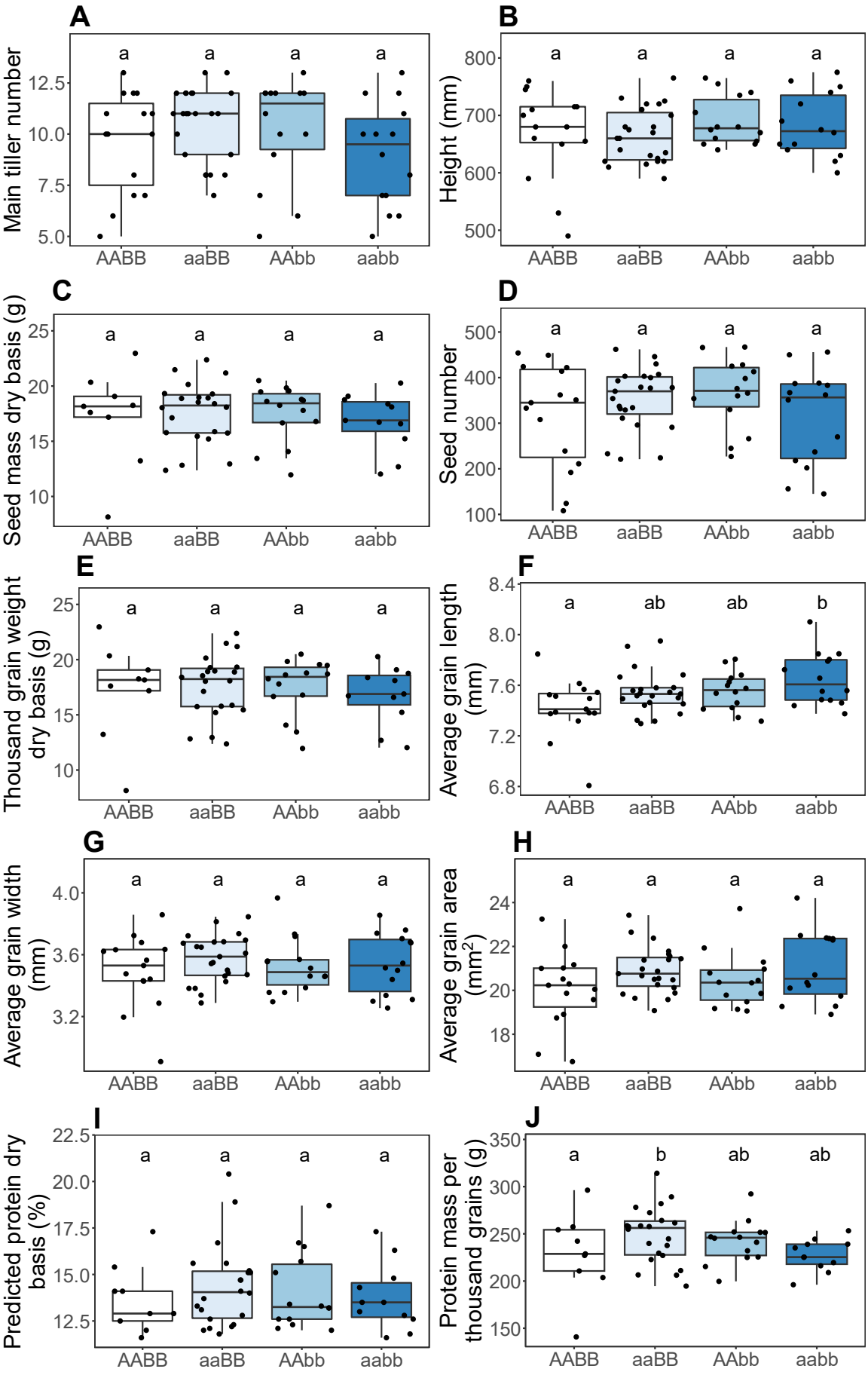

A
Main tiller number
12.5
10.0
7.5
5.0
a a a a
AABB aaBB AAbb aabb
B
Height (mm)
800
700
600
500
a a a a
AABB aaBB AAbb aabb
C
Seed mass dry basis (g)
25
20
15
10
a a a a
AABB aaBB AAbb aabb
D
Seed number
500
400
300
200
100
a a a a
AABB aaBB AAbb aabb
E
Thousand grain weight dry basis (g)
25
20
15
10
a a a a
AABB aaBB AAbb aabb
F
Average grain length (mm)
8.4
8.0
7.6
7.2
6.8
a ab ab b
AABB aaBB AAbb aabb
G
Average grain width (mm)
4.0
3.6
3.2
a a a a
AABB aaBB AAbb aabb
H
Average grain area (mm²)
24
22
20
18
a a a a
AABB aaBB AAbb aabb
I
Predicted protein dry basis (%)
22.5
20.0
17.5
15.0
12.5
a a a a
AABB aaBB AAbb aabb
J
Protein mass per thousand grains (g)
350
300
250
200
150
a b ab ab
AABB aaBB AAbb aabb

Figure 3.24 Grain number, grain protein content, tiller number, and height did not differ between NAC5-1 TILLING lines, although grain length was higher in NAC5-1 double mutants. (A) Main tiller number; (B) Height of primary tiller (mm), (C) Seed mass (g); (D) Seed number; (E) Thousand grain weight; (F) Average grain length; (F) Grain protein content (%, subset of plants with seed mass > 15g). Data from crosses X388 and X392 were combined (n=14-24).

3.3.5 Overexpression of *NAP-A1* in wheat

3.3.5.1 Identification of transgenic lines overexpressing *NAP-A1*

To test whether *NAP-1* overexpression promotes earlier senescence in wheat, *NAP-A1* was constitutively expressed in wheat. Nine T_0 individuals from independent transformation events were selected using a copy number assay: four single-copy lines and five multi-copy lines.

For a preliminary analysis of *NAP-1* expression, leaf tissue from the twelve plants of each T_1 transgenic line was pooled. Transcript levels were measured using primers designed to amplify either the construct, *NAP-A1* or all homoeologs of *NAP-1* (Methods 3.2.2.1). Transgenic lines expressed the construct, apart from lines 10.3 and 7.7 which had negligible construct expression (*Figure 3.25*A). Out of the single-copy lines, lines 10.5 and 10.9 expressed *NAP-A1* the highest on average (*Figure 3.25*B). Out of the multi-copy lines, lines 7.9 and 10.1 showed the highest *NAP-A1* expression (*Figure 3.25*B). NB: Line 7.con1 is missing from this figure due to accidental tube explosion. Based on these data, single-copy lines 10.5 and 10.9 and multi-copy lines 7.9 and 10.1 were selected as priority lines.

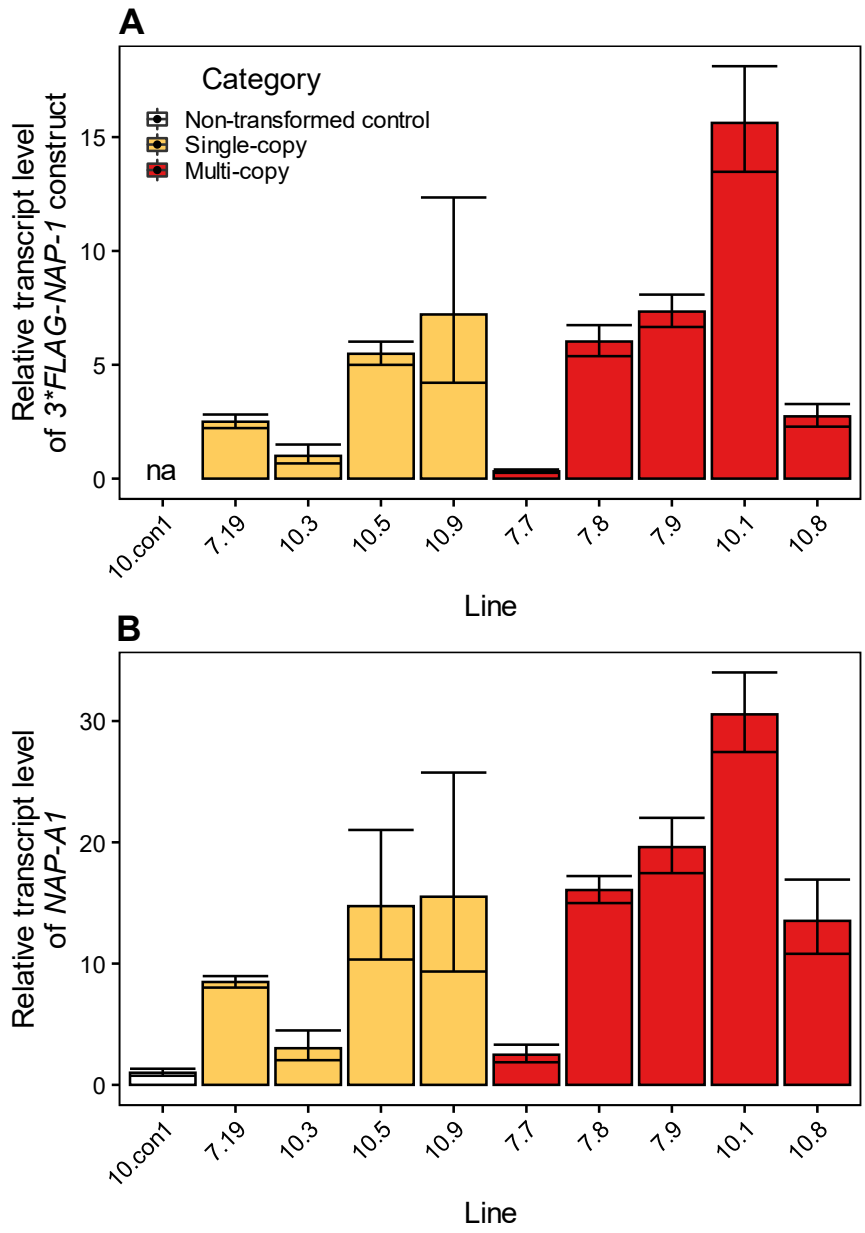


*Figure 3.25 Average expression of NAP-A1 varies between independent T_1 transgenic lines. Average relative transcript level of (A) 3*FLAG::NAP-A1 construct; (B) NAP-A1. RNA was extracted from pooled leaf samples of 12 T_1 plants per transgenic line, at 3 weeks. Relative transcript level was analysed by RT-qPCR using ΔΔCt method with Actin as reference gene, mean ±SD (n=3 technical replicates). "na" marks samples that were not amplified.*

To select individuals with high expression of *NAP-1*, transcript levels were tested in each individual from the priority transgenic lines. Most individuals in the priority transgenic lines expressed the construct (*Figure 3.26*A). In multi-copy lines 7.9 and

10.1, most individuals overexpressed *NAP-A1* and showed an increase in the total expression of all homoeologs of *NAP-1* compared to non-transformed controls (*Figure 3.26*B, C). In single-copy lines 10.5 and 10.9, some individuals showed higher expression of *NAP-A1* than non-transformed controls (*Figure 3.26*B). Total transcript level of all homoeologs of *NAP-1* was similar between single-copy lines and controls (*Figure 3.26*C).

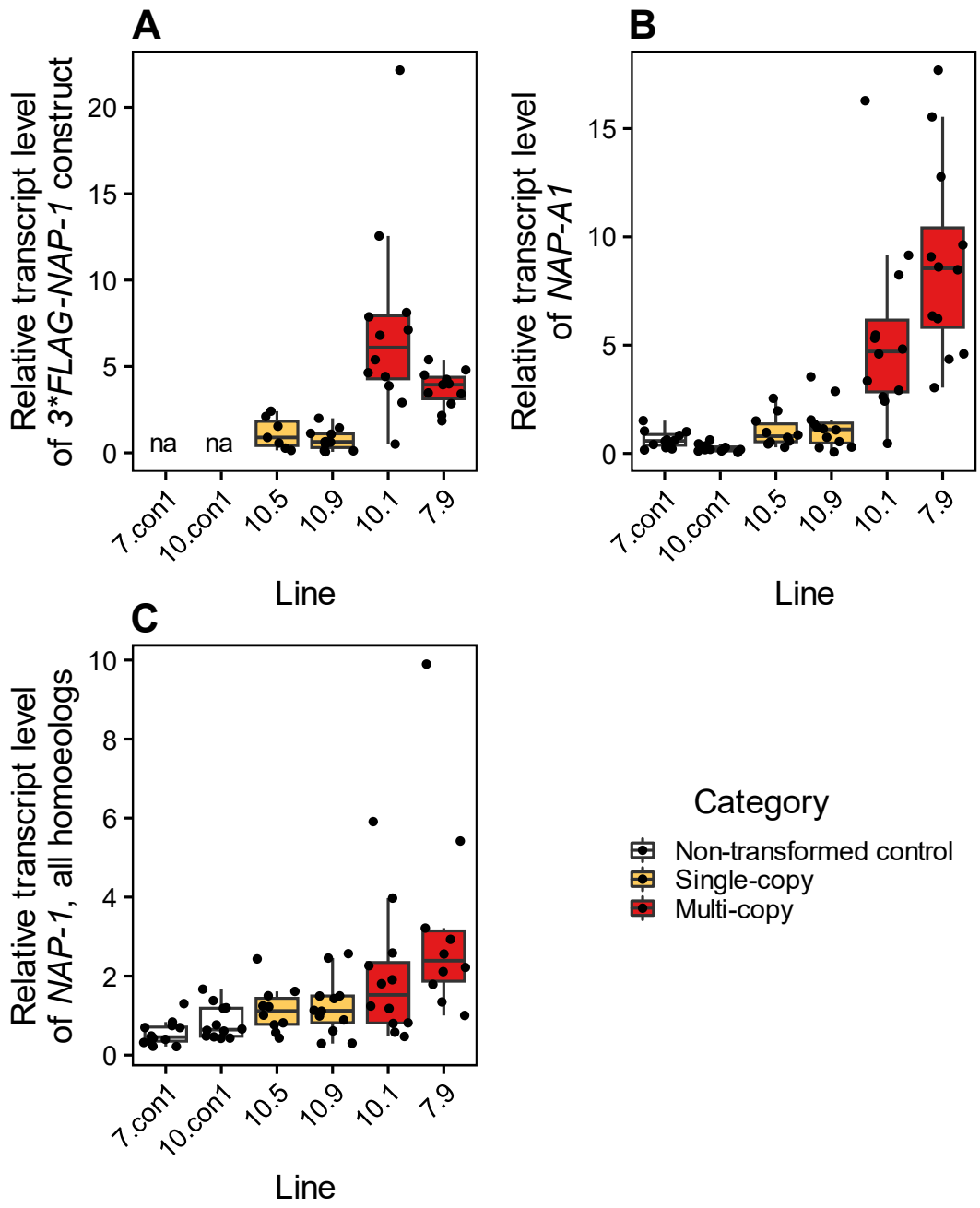


*Figure 3.26 Lines 7.9, 10.1, 10.5 and 10.9 contain individuals with higher expression of NAP-A1 than controls. Relative transcript level by RT-qPCR of (A) 3*FLAG::NAP-A1 construct; (B) NAP-A1; (C) NAP-A1, NAP-B1 and NAP-D1 combined. RNA was extracted from leaves of individual T_1 plants at 3 weeks. Relative transcript level calculated by the Pfaffl method with primer efficiencies and Actin as reference gene, normalised against the average of the single-copy category, average of 3 technical replicates (n=12 plants). "na" marks samples that were not amplified.*

3.3.5.2 Preliminary phenotyping of senescence in *NAP-A1* transgenics

To test the effect of overexpressing *NAP-A1* on senescence, leaf senescence was measured in T_1 transgenics in the glasshouse (Methods 3.2.5.3). Heading dates varied widely across the trial, with the earliest heading in single-copy T_1 line 10.9 and non-transformed control 10.con1, and latest heading in lines 10.5 and 7.9 (*Figure 3.27*A). In lines with the earliest heading, leaves and peduncles senesced later counted in days after heading, however lines did not differ in senescence timing when counted in days after sowing (*Figure 3.27*B, C). Latest-heading lines 10.5 and 7.9 had the highest grain mass (*Figure 3.27*D). Overall, *NAP-A1* transgenic lines showed phenotypes within the same range as non-transformed controls.

As a different approach, heading date was plotted directly against transcript level of *NAP-A1* (*Figure 3.28*). Heading date was positively correlated with transcript level *NAP-A1* in seedlings ($r^2 = 0.468$), implying that plants which highly expressed *NAP-A1* were more likely to head later (*Figure 3.28*). Because of the variability in non-transformed controls, pairs of homozygous and null T_2 lines segregating from the same genetic background were used for the next experiment.

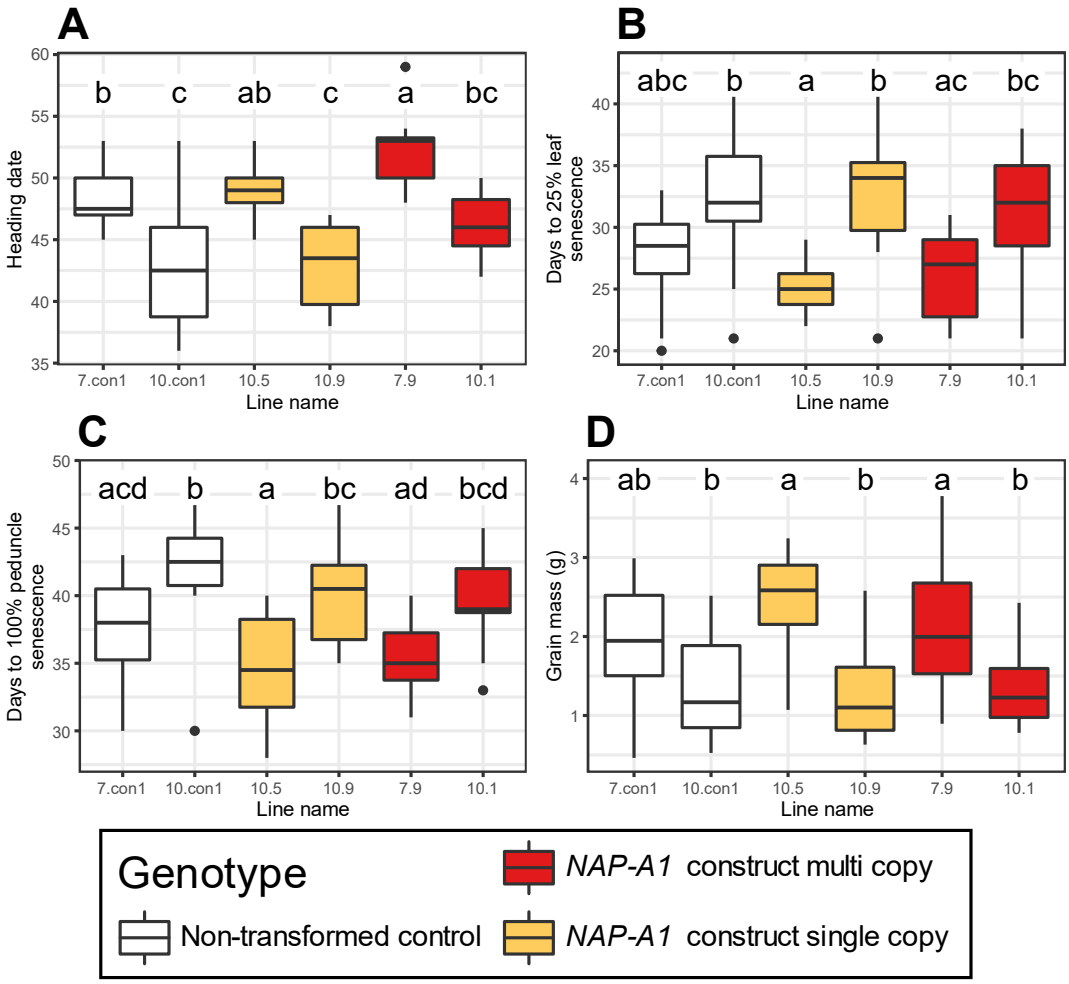


Figure 3.27 Heading date varies dramatically among both NAP-A1 T_1 transgenic lines and non-transformed controls. (A) Heading date; (B) 25% flag leaf yellowing in days after heading (DAH); (C) 100% peduncle yellowing (DAH); (D) Grain mass. ANOVA with post-hoc Tukey test, significance groups at p<0.05.

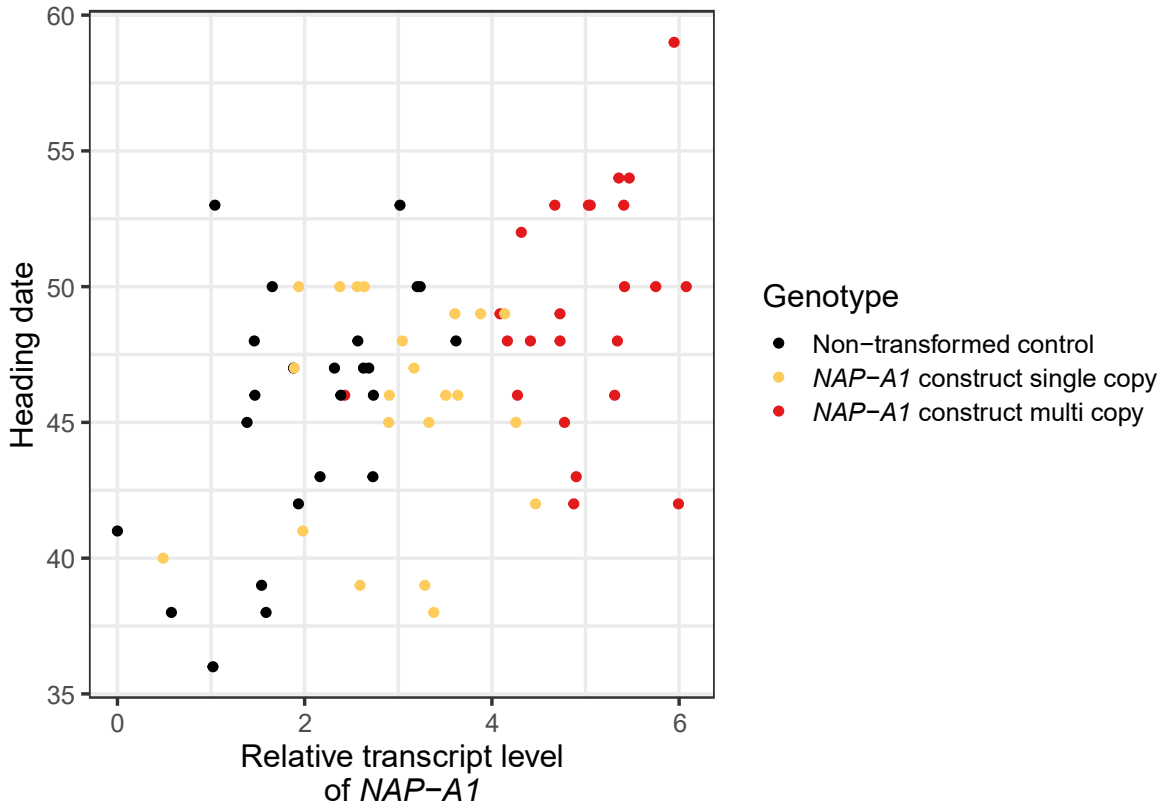


Figure 3.28 Higher expression of NAP-A1 correlates with later heading. Heading date plotted against transcript level of NAP-A1 in seedlings for individual plants. Correlation coefficient $r^2 = 0.468$, p = 4.36e-05.

3.3.5.3 Selection of homozygous transgenic lines by copy number analysis

To improve the genetic uniformity of the next experiment, construct copy number of T_1 plants was assessed. If the T_0 parent contains a single construct insertion, the T_1 population will segregate in a 1:2:1 ratio of 0:1:2 construct copies. *NAP-1* T_1 populations segregated consistently with this, confirming that T_0 parents contained a single insertion (*Figure 3.29*). Lines 10.5, 10.9, and 7.19 were taken forward based on higher transcript levels. For each line, the T_1 plant with 2 construct copies (homozygous) and highest *NAP-A1* expression were selected, along with a T_1 plant with 0 construct copies (wild type) and no expression of the construct (*Table 3.11*). T_2 progeny of these plants was used for the following experiment.

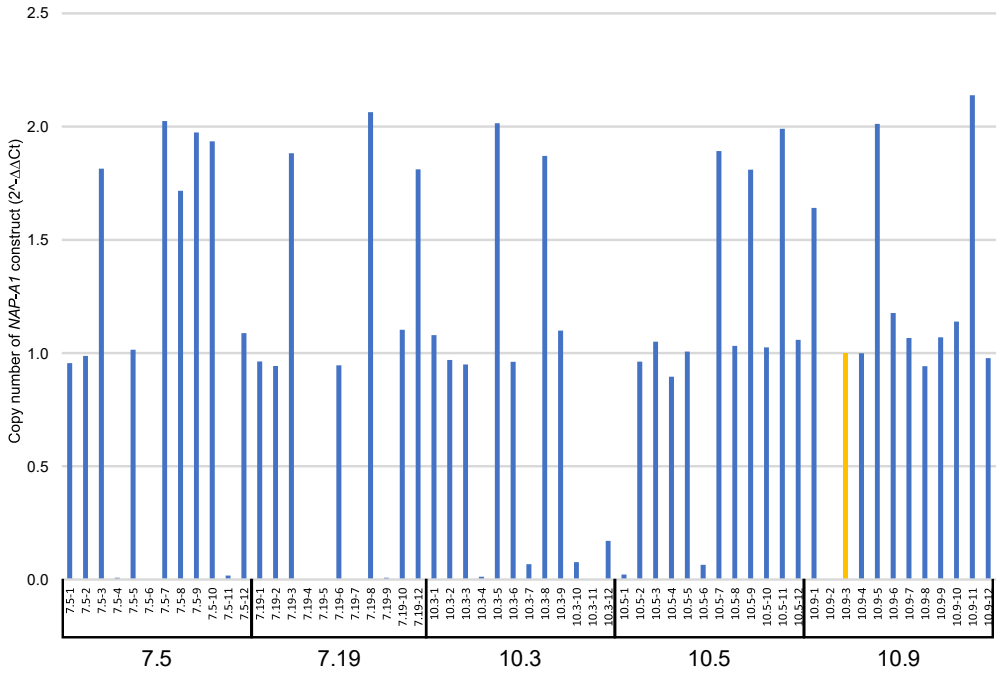


*Figure 3.29 NAP-A1 T_1 lines show expected segregation for the 3*FLAG::NAP-A1 transgenic construct. Copy number of NAP-1 construct in individual T_1 plants. Taqman qPCR was run against the nptII marker gene in the construct and analysed by ΔΔCt method, normalised against a known single-copy gene and the sample with median expression level in the "single copy" cluster (highlighted yellow).*

3.3.5.4 *NAP-A1* overexpression does not alter senescence timing or grain mass

To further test whether *NAP-A1* overexpression impacts senescence timing, senescence was measured in *NAP-A1* T_2 overexpression lines grown in a CER (Methods 3.2.5.4). As for *NAC5-A1*, Shelf 1 and Shelf 2 are shown separately due to the distinct plant phenotypes (Results 3.3.3). Overall, from heading to harvest, flag leaf chlorophyll content decreased at the same pace in *NAP-A1* homozygous transgenics and corresponding null segregants (*Figure 3.30*). For one exception, chlorophyll content was higher in *NAP-A1* overexpressing plants in line 7.19 on Shelf 2 at 4 weeks after heading (*Figure 3.30*). Wider error bars around Weeks 5-6 are the result of missing data.

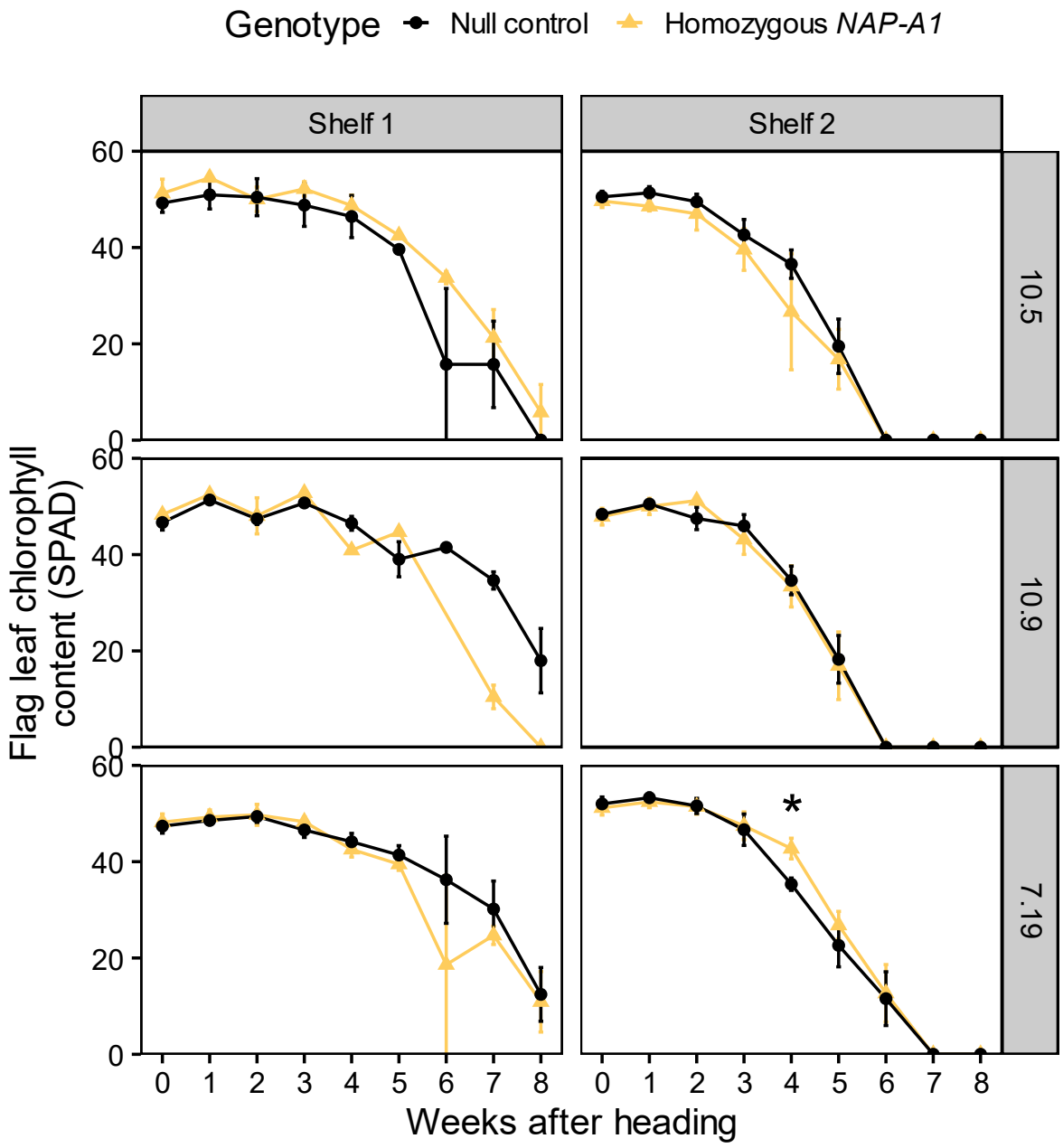


*Figure 3.30 Flag leaf chlorophyll through senescence does not differ between NAP-A1 transgenics and control. Flag leaf chlorophyll content (SPAD) in weeks after heading +/- 1 day was compared between homozygous transgenic and null segregant controls in T2 transgenic lines 10.5 and 10.9. Average SPAD value at each timepoint was compared by Wilcoxon test, *=p<0.05. NB: Averages were taken of 2-5 data points; timepoints with small sample sizes may result in apparent differences that are not statistically significant.*

Further traits are shown for lines 10.5 and 10.9, which had higher expression of *NAP-A1* than line 7.19. Heading date was later on Shelf 1 than Shelf 2 but did not differ between *NAP-A1* transgenics and controls (*Figure 3.31*A). *NAP-A1* overexpressing lines trended towards later 25% leaf senescence on Shelf 1, however this is based on small sample sizes (*Figure 3.31*B). There were no statistically significant differences in peduncle senescence timing, days to reach a SPAD value of 30, AUC of leaf senescence, or duration of leaf senescence between single-copy transgenic lines and the corresponding control grown on the same shelf (*Figure 3.31*C-F).

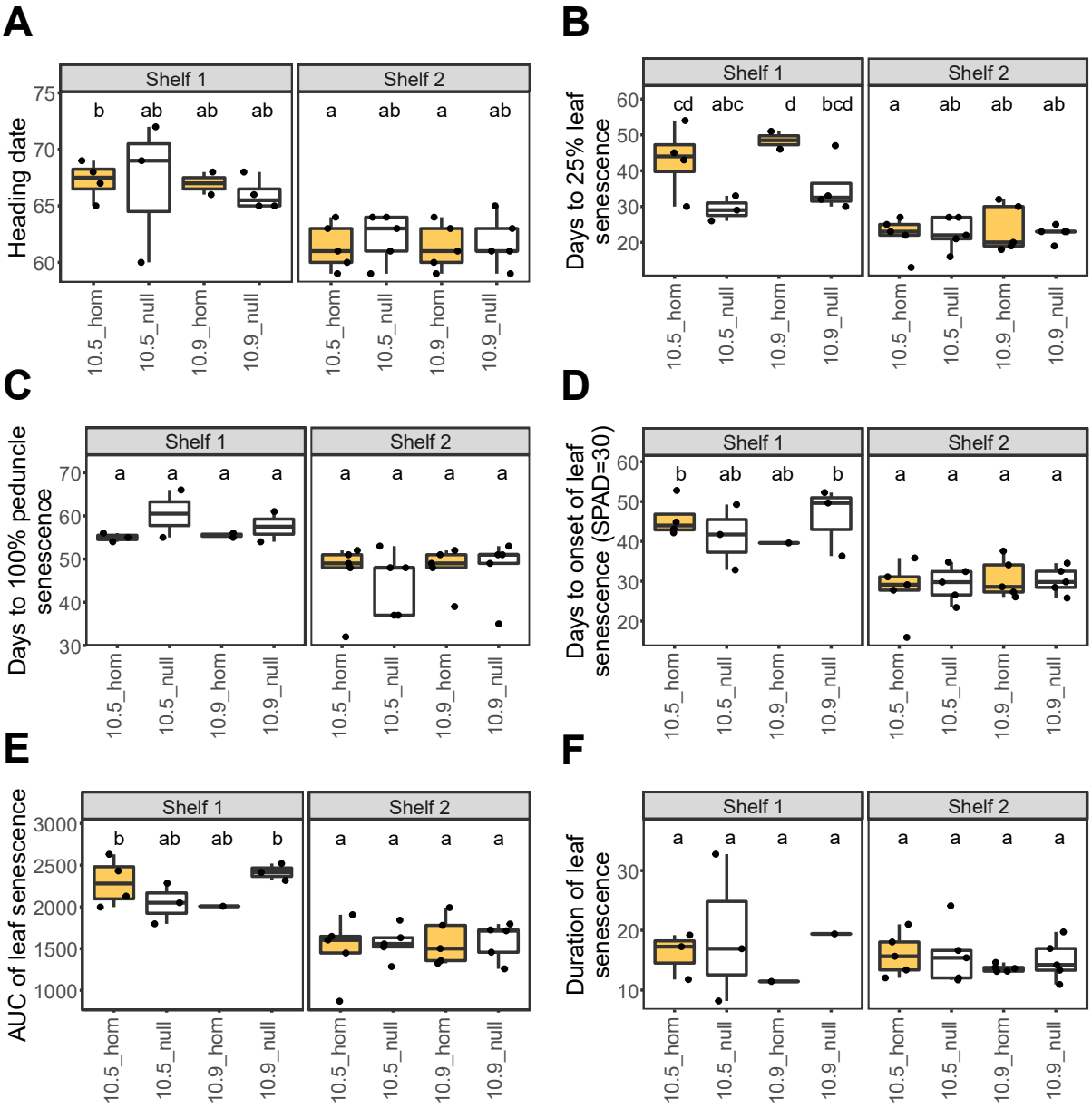


*Figure 3.31 Senescence phenotypes do not differ between NAP-A1 overexpression lines 10.5 and 10.9 and corresponding controls. (A) Heading date (DAS); (B) 25% flag leaf yellowing; (C) 100% peduncle yellowing; (D) Days from heading to SPAD=30; (E) Area under curve (AUC) of leaf senescence; (F) Duration of leaf senescence (Days). (A-F) ANOVA with post-hoc Tukey test, formula ~ Shelf * Line_name, letters show significance groups at p<0.05. NB: Boxplots represent 2-5 individuals; small sample sizes may result in apparent differences that are not statistically significant.*

Plants produced a consistent tiller number across genotypes and shelves (*Figure 3.32*A). On Shelf 2, *NAP-A1* overexpression lines trended slightly towards higher grain mass and number, together with reduced grain length and thousand kernel weight, compared to the corresponding control (*Figure 3.32*B-E). Grain width and area were not significantly different (not shown). Overall, grain traits did not differ significantly between *NAP-A1* overexpression lines and controls.

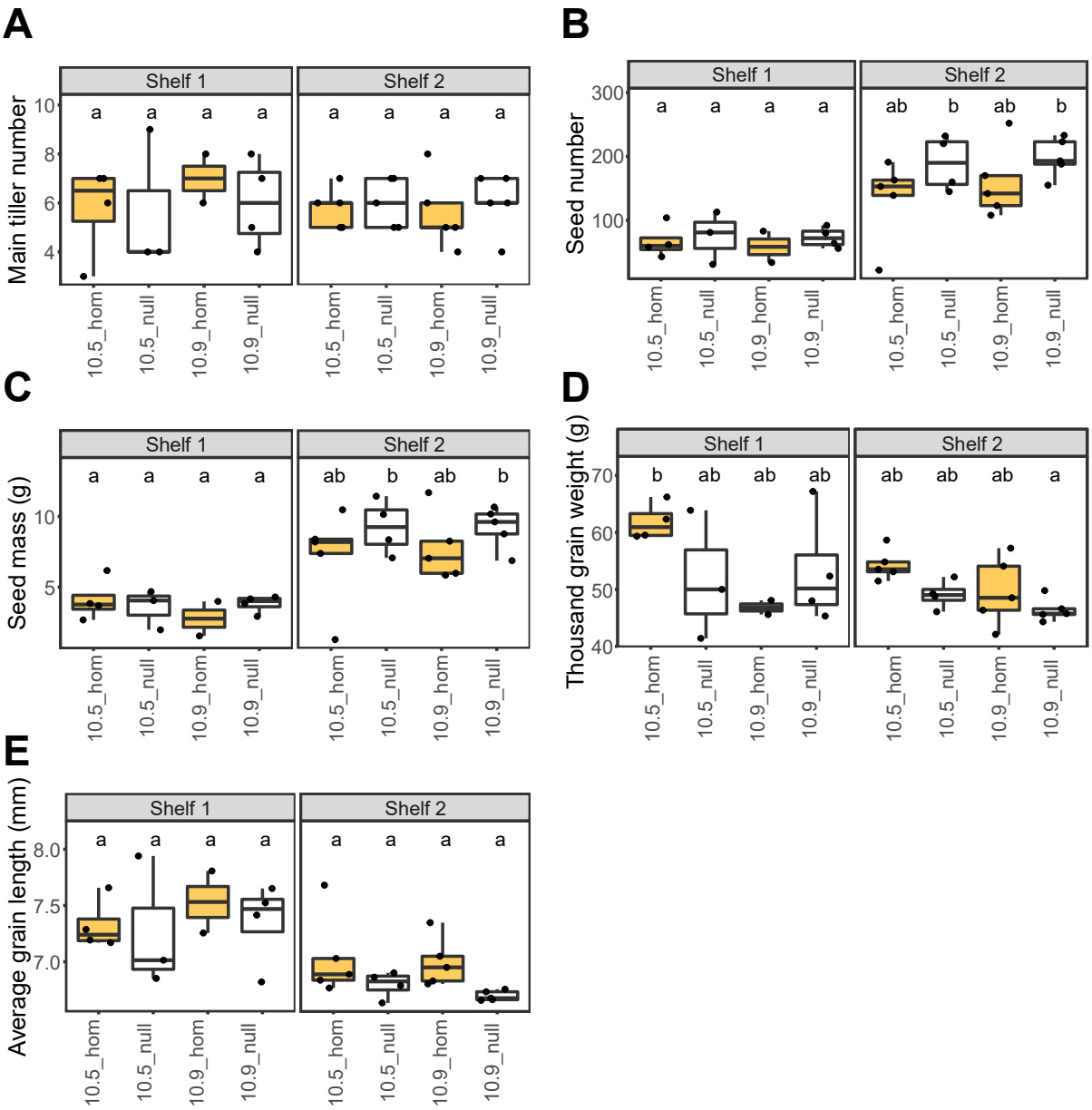
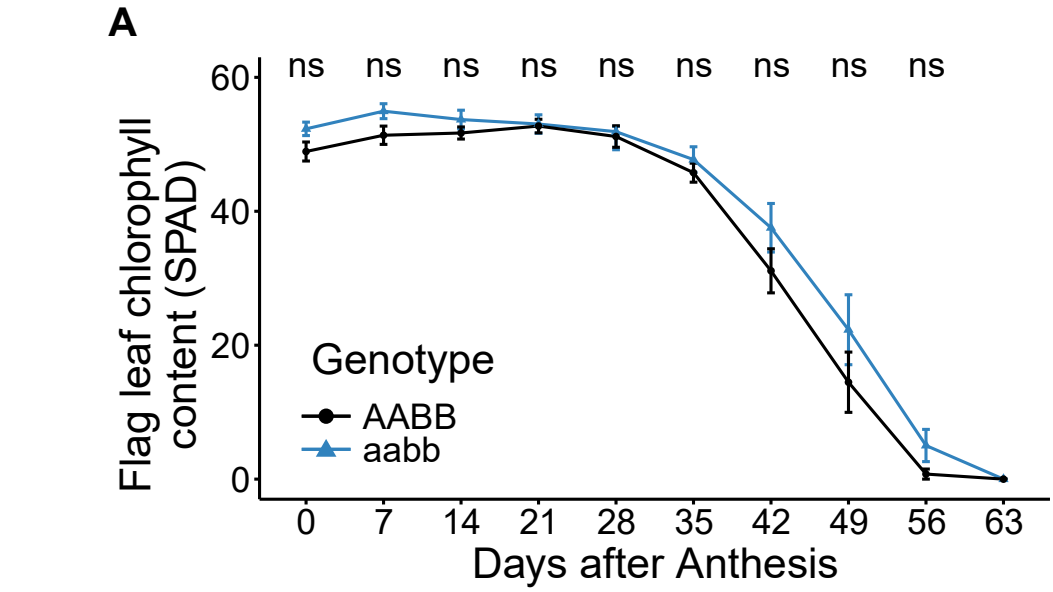


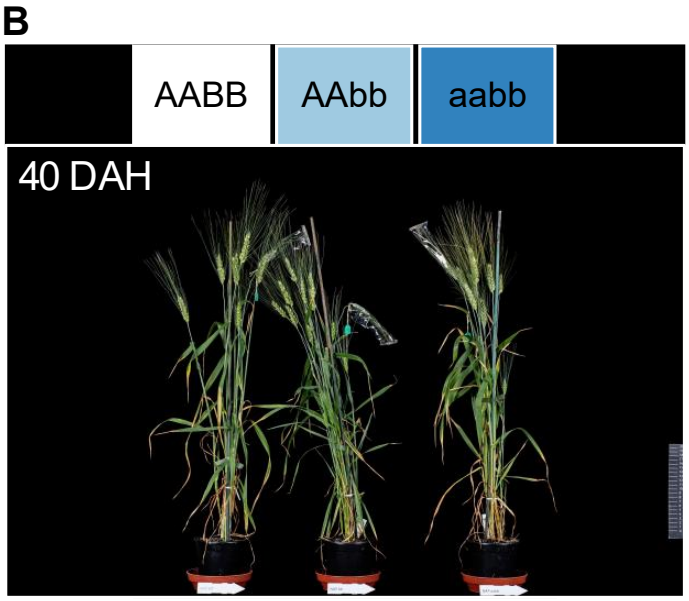
*Figure 3.32 Grain traits did not differ between homozygous NAP-A1 transgenics and null segregants in lines 10.5 and 10.9. (A) Main tiller number; (B) Seed mass (g); (C) Seed number; (D) Thousand grain weight; (E) Average grain length. (A-E) ANOVA with post-hoc Tukey test, formula ~ Shelf * Line_name, letters show significance groups at p<0.05. NB: Boxplots represent 2-5 individuals; small sample sizes may result in apparent differences that are not statistically significant.*

3.3.6 Mutations in *NAP-A1* in tetraploid wheat

3.3.6.1 *NAP-1* mutants do not differ in leaf senescence timing but may have later peduncle senescence

To assess the impact of mutations in *NAP-1* on the timing of senescence, stop codon mutations likely to lead to loss-of-function of *NAP-A1* and *NAP-B1* were identified in the tetraploid Kronos TILLING population. Homozygous *NAP-1* double mutants were generated by crossing and phenotyped for senescence in the glasshouse (Methods 3.2.5.5). The same issues apply as for *NAC5-1* TILLING lines (Results 3.3.4). On average, *NAP-1* double mutants and controls did not differ in flag leaf chlorophyll content at any time-point (Figure 3.33A). The plants were visually similar (Figure 3.33B-C). There were no differences in heading date or leaf senescence timing between *NAP-1* mutants and controls (Figure 3.34). In *NAP-A1* single mutants, peduncles senesced significantly later, and *NAP-1* double mutants were on the borderline for later peduncle senescence (Figure 3.34C).


A
ns ns ns ns ns ns ns ns ns
60
40
20
0
Flag leaf chlorophyll content (SPAD)
Genotype
AABB
aabb
0 7 14 21 28 35 42 49 56 63
Days after Anthesis


B
AABB
AAbb
aabb
40 DAH

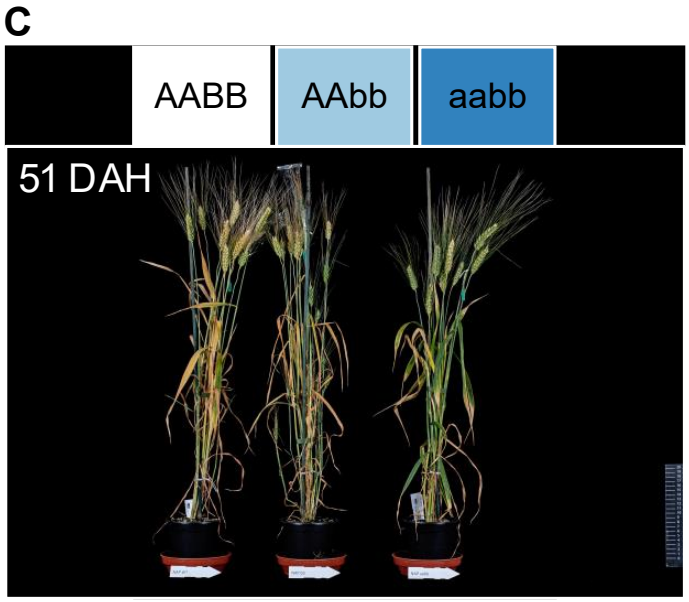

C
AABB
AAbb
aabb
51 DAH

*Figure 3.33 NAP-1 double mutants and controls show no difference in the timing of flag leaf senescence. (A) Flag leaf chlorophyll content (SPAD) in weeks after heading +/- 1 day was compared between NAP-1 TILLING mutants (aabb, n = 10) and wild type segregant controls (AABB, n = 12). Average SPAD value at each timepoint was compared by Wilcoxon test, *=p<0.05. (B) Representative plants for wild type (AABB) single (AAbb) and double (aabb) NAP-1 mutants at 40DAH. Single (aaBB) mutant plants were omitted as none shared the same heading date. (C) Representative plants at 51DAH; different individuals to B.*

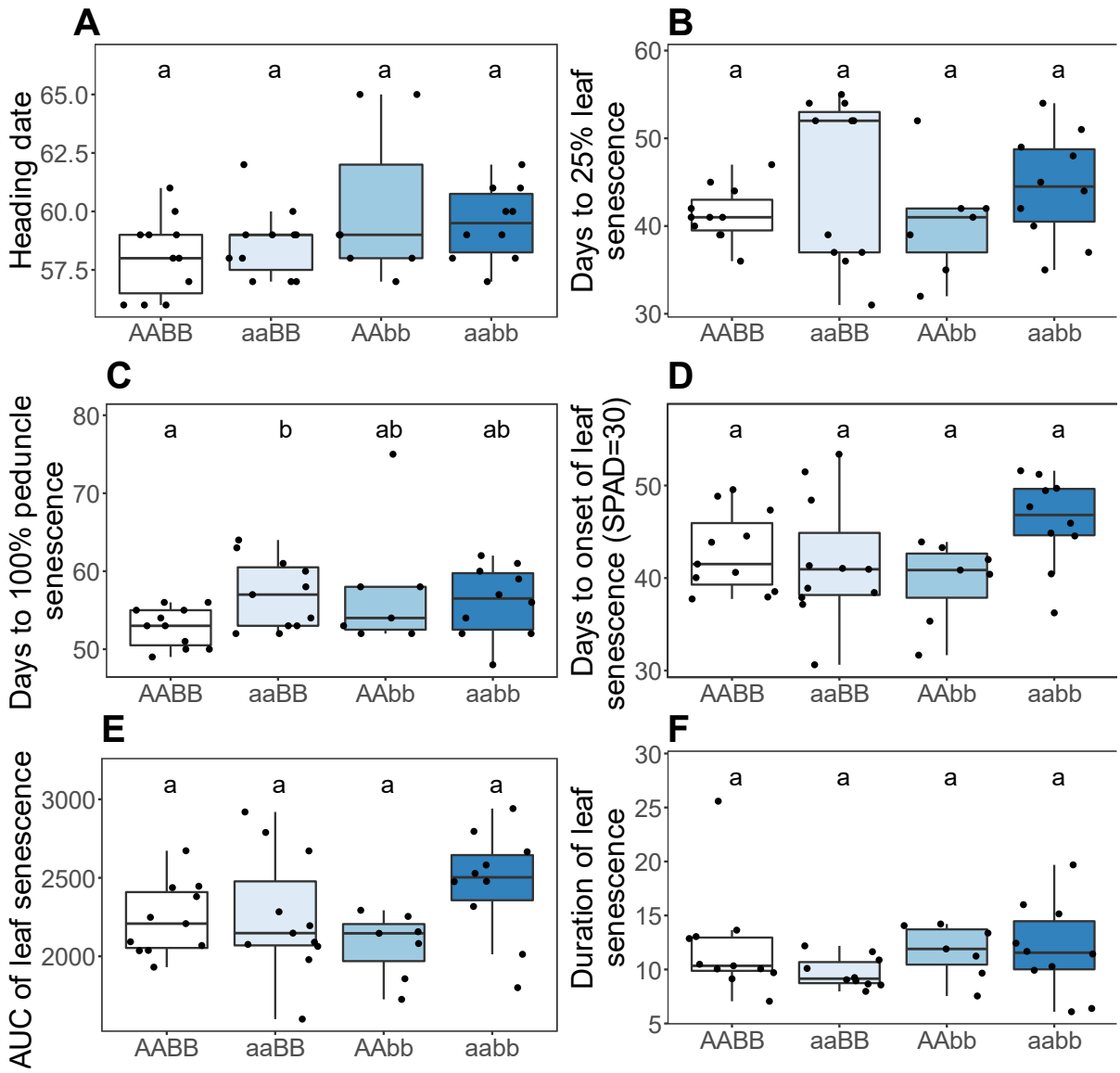


Figure 3.34 Peduncles senesce later in NAP-A1 single mutants (aaBB), while other senescence phenotypes do not differ significantly between NAP-1 mutants and controls. (A) Heading date (DAS); (B) 25% flag leaf yellowing; (C) 100% peduncle yellowing; (D) Days from heading to SPAD=30; (E) Area under curve (AUC) of leaf senescence; (F) Duration of leaf senescence (Days). (A-F) ANOVA with post-hoc Tukey test, formula ~ Light + Block + Genotype, letters show significance groups at p<0.05. Data from cross X585 (n = 8-12).

3.3.6.3 *NAP-1* double mutants do not differ in grain mass or protein content

NAP-1 double mutants grew to a similar number of tillers and height of the primary tiller (Figure 3.35A, B). Grain mass and grain number were no different between *NAP-1* double mutants and controls (Figure 3.35C, D). In contrast, *NAP-A1* and *NAP-B1* single mutants produced fewer grains and reduced grain mass than double mutants or controls, while *NAP-B1* single mutants also had fewer tillers (Figure 3.35A, C, D). These traits can be attributed to differences in sowing date, as a higher proportion of single mutants were resown later (Methods 3.2.5.5). Therefore, conclusions about the single mutant genotypes cannot be made from these data.

Mutations in *NAP-1* did not affect thousand grain weight or grain length (Figure 3.35E, F). Grain width and area were not significantly different (not shown). Grain protein content did not differ between *NAP-1* double mutants and controls (Figure 3.35G). Only individuals with a grain mass exceeding 15g were tested for protein, therefore there were negligible protein samples for single mutants.

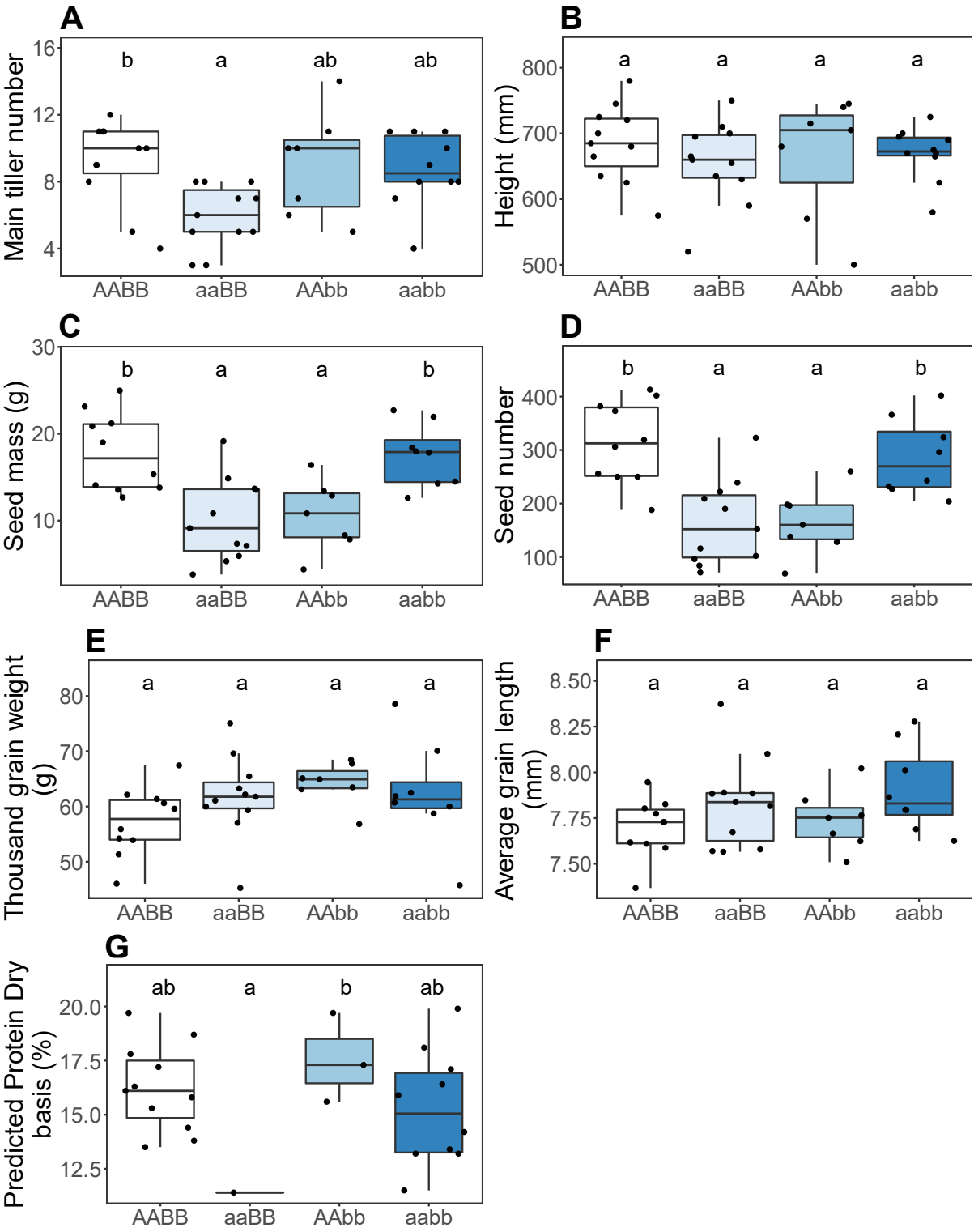

A
Main tiller number
16
12
8
4
b
a
ab
ab
AABB
aaBB
AAbb
aabb
B
Height (mm)
800
700
600
500
a
a
a
a
AABB
aaBB
AAbb
aabb
C
Seed mass (g)
30
20
10
b
a
a
b
AABB
aaBB
AAbb
aabb
D
Seed number
400
300
200
100
b
a
a
b
AABB
aaBB
AAbb
aabb
E
Thousand grain weight (g)
80
70
60
50
a
a
a
a
AABB
aaBB
AAbb
aabb
F
Average grain length (mm)
8.50
8.25
8.00
7.75
7.50
a
a
a
a
AABB
aaBB
AAbb
aabb
G
Predicted Protein Dry basis (%)
20.0
17.5
15.0
12.5
ab
a
b
ab
AABB
aaBB
AAbb
aabb

Figure 3.35 Grain number, grain protein content, tiller number, and height did not differ between NAP-1 double mutants and controls. (A) Main tiller number; (B) Height of primary tiller (mm), (C) Seed mass (g); (D) Seed number; I Thousand grain weight; (F) Average grain length; (G) Grain protein content (%, subset of plants with seed mass > 15g). (A-G) ANOVA with post-hoc Tukey test, formula ~ Light + Block + Genotype, letters show significance groups at p<0.05. Data from cross X585 (n = 8-12). NB: Grain traits of NAP-1 single mutants were affected by later sowing of some plants after failed germination (Methods 3.2.5.5).

3.4 Discussion

3.4.1 *NAC5-1* may promote earlier senescence in wheat

This chapter sought to investigate whether *NAC5-1* promotes earlier senescence and increased protein content in wheat. Overexpression of *NAC5-A1* was associated with earlier onset of flag leaf senescence and possibly earlier peduncle senescence. In contrast, loss-of-function of *NAC5-1* through TILLING mutations was associated with delayed onset of flag leaf senescence. *NAC5-1* loss-of-function did not impact the duration of leaf senescence or peduncle senescence. These findings support the hypothesis that *NAC5-1* acts to promote the onset of leaf senescence, consistent with the upregulation of *OsNAC5* during leaf senescence (Sperotto et al. 2009).

Specifically, this indicates that *NAC5-A1* and *NAC5-B1* promote earlier leaf senescence under well-watered, well-fertilized conditions. *NAC5-D1* was not explicitly tested, as the TILLING mutant lines were generated in tetraploid wheat. Nevertheless, it is likely that *NAC5-D1* has the same function as its homoeologs, given similar expression pattern in senescence and over 97% pairwise sequence similarity between *NAC5-1* peptide sequences. Similar results may or may not be obtained under different environmental conditions, such as drought, nitrogen

limitation, or field conditions, as senescence timing is also regulated by environmental factors.

Loss-of-function of *NAC5-1* did not affect GPC in glasshouse conditions. This supplies some evidence against the hypothesis that *NAC5-1* regulates grain protein content. This contrasts with the correlation between *OsNAC5* expression and grain protein content in rice recombinant inbred lines – although this correlation could be caused by a third, unknown factor (Sharma et al. 2019).

Interestingly, *NAC5-A1* mutants had increased grain number and *NAC5-1* double mutants had increased grain length. Conversely, overexpression of *NAC5-A1* did not affect grain mass or grain number. The phenotype of *NAC5-A1* mutants is consistent with findings in rice, where enhanced expression of *OsNAC5* resulted in decreased grain number, grain length and thousand grain weight (Wairich et al. 2023).

A recent study Identified *NAC5-A1* (TraesCS4A02G219700) through a GWAS for extreme seedling drought tolerance (Mao et al. 2022). A promoter insertion allele “In-693” was correlated with high expression of *NAC5-A1.* Near isogenic lines with the In-693 allele were more drought-tolerant than controls (Mao et al. 2022). It would be interesting to test whether the In-693 promoter insertion allele also promotes earlier senescence. This paper indicates that *NAC5-A1* promotes drought tolerance, like the rice ortholog *OsNAC5* (Mao et al. 2022; Takasaki et al. 2010). The results in this chapter show that *NAC5-1* may promote earlier leaf senescence. Together this suggests that *NAC5-1* retains at least two conserved functions with its ortholog in rice.

3.4.2 The role of *NAP-1* in wheat senescence

This chapter also sought to investigate whether *NAP-1* promotes earlier senescence and increased protein content in wheat. *NAP-1* homoeologs were expressed during early leaf senescence based on RNA-seq data, consistent with a recent study which found that *NAP-B1* (TraesCS4B02G173600) is upregulated in senescing flag leaves (Zhang, Liu,Guo 2020). Leaf and peduncle senescence timing did not differ in lines overexpressing *NAP-A1* or TILLING mutants of *NAP-1*. *NAP-A1* overexpression lines trended slightly toward later 25% leaf senescence on one shelf. Double mutants of *NAP-1* showed no difference in GPC. These data contradict the hypothesis, indicating that *NAP-1* may not regulate senescence timing or grain protein content. This contrasts with *OsNAP*, which promotes earlier leaf senescence and increased GPC (Zhou et al. 2013; Liang et al. 2014). In addition, heterologous expression of wheat *NAP-B1* in *Arabidopsis thaliana* resulted in earlier senescence and was sufficient to complement the *Arabidopsis nap* mutant (Zhang, Liu,Guo 2020). Here are several hypotheses to explain these observations, which are not mutually exclusive.

Hypothesis 1: *NAP-1* does not regulate senescence or protein content; *NAP-1* has evolved to diverge in function from *OsNAP*. This is possible as *NAP-A1*, *NAP-B1* and *NAP-D1* have only 64.5%, 62.5%, and 63.7% similarity to *OsNAP* in peptide sequence, compared to 75.6% between *NAC5-1* and *OsNAC5*. This hypothesis would contradict the recent paper that implied *NAP-1* has some conserved function with *AtNAP* (Zhang, Liu,Guo 2020). However, overexpression and loss-of function of *NAP-1* in wheat provides more insight into *NAP-1* function in the regulatory landscape of wheat compared to expressing this gene in *Arabidopsis*. Therefore,

while more experiments are needed, the results in this chapter indicate that *NAP-1* does not impact senescence timing in wheat.

Hypothesis 2: *NAP-1* does regulate senescence and/or protein content but it was not observed in these experiments. This could occur if the effect of *NAP-1* on senescence is only apparent in certain environments. It is also possible that the expression of *NAP-A1* from the transgenic constructs in lines 10.5 and 10.9 did not lead to physiologically relevant levels of overexpression, given the marginal increase in transcript levels of *NAP-1*, considering all homoeologs. In addition, overexpression was assessed at seedling stage where wild-type expression of *NAP-1* is very low, whereas wild-type expression of *NAP-1* is higher during senescence. This hypothesis could be tested by measuring whether transgenic lines overexpress *NAP-1* relative to controls in flag leaves around 23DAA, where endogenous *NAP-1* expression is highest. Levels of NAP-A1 protein could also be tested to check whether NAP-A1 protein is degraded in transgenic lines.

Hypothesis 3: *NAP-1* acts redundantly with other NAC transcription factors to regulate senescence and/or protein content. If this is the case, we would expect to see no phenotypic differences in *NAP-1* TILLING mutant lines. Specifically, *NAP-1* might act redundantly with its paralogs TraesCS2A02G101900 and TraesCS2A02G102000 and their homoeologs, which were also expressed during leaf senescence. Genetic redundancy is frequent in senescence-associated NAC transcription factors in *Arabidopsis*, especially between recently diverged paralogs (Li, Woo,Guo 2018). In an *in silico* senescence regulatory network, while all homoeologs of *NAP-1* and its paralogs were included in the network, 4/6 of the paralogs were in the top 30% of connected transcription factors (TraesCS2A02G101900, TraesCS2B02G119000, TraesCS2A02G102000,

TraesCS2B02G119100) compared to none of the homoeologs of *NAP-1* (Borrill et al. 2019). If the equivalent rice gene *ONAC103* is truncated in *Oryza sativa ssp. Japonica*, *OsNAP* would not have a redundant paralog. This could explain why *OsNAP* loss-of-function has a phenotypic effect, whilst *NAP-1* loss-of-function does not. This hypothesis could be tested by knocking out *NAP-1*, TraesCS2A02G101900 and TraesCS2A02G102000 together, perhaps using gene editing techniques if a common guide RNA could be designed.

3.4.3 Strengths and caveats of these glasshouse experiments

The statistical power of several experiments was weakened by confounding factors. For example, some *NAC5-1* Kronos TILLING lines had incorrect genotypes, reducing the sample size, and splitting the overexpression experiment into two differing environments effectively halved the sample size within each environment. Repeating experiments with larger sample sizes and a consistent environment would increase the statistical power to detect subtle differences between genotypes.

Significant overexpression was obtained in one single-copy transgenic line for *NAC5-A1*, and two for *NAP-A1*. Ideally, results would be validated by repeating transformation to obtain three independent single-copy transgenic lines per gene, to compare homozygous and null segregant T_2 lines for each. For Kronos TILLING lines, GPC measurements have missing data, as only individual plants with >15g seed could be measured accurately. For a more accurate assessment, GPC should be tested in “pooled” sets of more than one individual, or from a field trial.

Variability in light conditions occurred in three out of four experiments carried out in this chapter: *NAC5-1* T_1 overexpression lines, *NAC5-1* and *NAP-1* T_2 overexpression lines, and *NAC5-1* and *NAP-1* Kronos TILLING lines. For *NAC5-1* T_1 overexpression

lines and TILLING lines, spacing of lights in the glasshouse led to variable light intensity. In both experiments, plants closer to the lights, receiving higher light intensity, headed sooner and senesced more rapidly after heading. For *NAC5-1* and *NAP-1* T_2 overexpression lines grown in controlled environment conditions, light intensity was measured as equal across both shelves. Nevertheless, plants on Shelf 2 showed an early heading and senescence phenotype resembling the effect of higher light intensity. It is probable that due to the two different models of LED light box, the light spectrum differed between Shelf 1 and Shelf 2 such that plants on Shelf 2 received higher photosynthetically active radiation. In all three of these experiments, plants primarily relied on artificial light sources, as the glasshouse studies were run between November and April. In contrast, in the *NAP-1* T_1 overexpression lines, grown between April and August, light-related phenotypic differences were not observed. Whilst an attempt was made to account for differing light conditions by adding blocking factors to analyses, future research on senescence should not only plan experiments with uniform light intensity where possible, but measure light intensity and the light spectrum during the experiment to capture differences that are likely to impact senescence timing.

3.4.4 Conclusion

In conclusion, to identify regulators of senescence in wheat, this chapter investigated the orthologs of *OsNAC5* and *OsNAP,* both associated with senescence in rice. Both *NAC5-1* and *NAP-1* are expressed in early flag leaf senescence, making them suitable candidate genes. Results from overexpression and TILLING mutant lines indicate that the transcription factor *NAC5-1* promotes earlier flag leaf senescence in wheat, although it may not affect grain protein content. These results found no

evidence for an effect of *NAP-1* on either senescence or grain protein content. Further research is needed to decipher the function of *NAP-1* in wheat.

4 APPLYING UNDERSTANDING OF SENESCENCE TO WHEAT BREEDING

4.1 Introduction

4.1.1 The challenge of improving wheat grain protein content

Wheat grain protein content is a key determinant of bread quality. Glutenins, which comprise 30-45% of wheat grain protein, and gliadins, which comprise 40% of grain protein, give bread dough its elasticity and extensibility (Cauvain 2012). Total grain protein content correlates positively with bread-making quality traits such as water absorption and loaf volume (Bushuk, Briggs,Shebeski 1969; Fradgley et al. 2022). Therefore, wheat grain protein content is used as a proxy for breadmaking quality: in the UK, a threshold of 13% grain protein content must be exceeded to classify a variety as a “Group 1” breadmaking variety, and to obtain a premium price for a crop (AHDB 2023b). In 2023, 23% of UK land area planted with wheat comprised Group 1 varieties, with a range of 15-29% annually since 2005 (AHDB 2023a). Thus, developing wheat varieties with high grain protein content, while maintaining high yield, is an important target for breeders.

The trade-off between protein content and yield impedes improvement of wheat grain protein content (Simmonds 1995). The timing of leaf senescence may partially explain this trade-off, as the onset of flag leaf senescence determines the transition from leaf photosynthesis to nutrient remobilization (Thomas and Ougham 2014). Grain protein content is increased through an early onset of senescence, and increased nitrogen remobilization to the grain (Kong et al. 2016). Delayed

senescence, also described as functional stay-green, enables prolonged photosynthesis and starch accumulation, potentially increasing yield (Thomas and Ougham 2014).

4.1.2 Senescence timing and grain protein content have changed through wheat breeding

Over a century of targeted wheat breeding has altered yield, grain protein content and the timing of senescence. High-yielding Green Revolution varieties, along with intensification and more fertiliser input, led to an increase of almost 3t/ha in average UK wheat yield between the 1970's and the 1990's (FAO 2020). Compared to varieties from the 1920's, modern wheat varieties have altered development including a longer time from anthesis to maturity, higher yield, and reduced protein content (Maeoka et al. 2020). Similarly, UK winter wheat varieties released between 2002 and 2017 shift gradually towards increased yield, decreased protein content, and later maturity (Shorinola et al. 2022). The trend toward decreasing protein content was observed in Group 2 (breadmaking potential) and Group 4 (feed wheat) varieties – but not Group 1 varieties where high protein content is required (Shorinola et al. 2022). It is likely that artificial selection for yield, without selection for protein content, leads to reduced protein content because of the protein-yield trade-off. The trend towards delayed maturity suggests that wheat lines with delayed senescence or "stay-green" have been selected for, directly or indirectly, in modern breeding (Maeoka et al. 2020; Shorinola et al. 2022).

4.1.3 Introgression of functional *NAM-B1* increases protein content in diverse germplasm and field conditions

Gpc-B1 is a quantitative trait locus associated with grain protein content (GPC), with the high GPC allele carrying a functional copy of NAC transcription factor *NAM-B1*

(Uauy et al. 2006). Multiple field studies have assessed the impact of *Gpc-B1* on grain yield and quality traits. For example, six hexaploid and three tetraploid hard spring wheat near isogenic lines (NILs) containing the *Gpc-B1* locus were grown in a three year field experiment in three sites in California (Brevis and Dubcovsky 2010). *Gpc-B1* NILs had increased GPC (+5.8% in hexaploid and +10.4% in tetraploid) and protein yield (Brevis and Dubcovsky 2010). Change in GPC varied from 4.5-15.5 g kg^{-1} across genotypes. Kernel weight decreased (-2.8%), but yield was unchanged. Time of 50% flag leaf senescence and 50% spike senescence was 0-2 days earlier in *Gpc-B1* NILs (Brevis and Dubcovsky 2010). A larger effect on tetraploids could be a dosage effect, with a functional copy of the *NAM-B1* gene comprising ¼ of total *NAM* expression in tetraploid and 1/6 of total *NAM* expression in hexaploid.

Twenty-five studies testing introgression of *Gpc-B1* in field conditions were reviewed in a meta-analysis, including 11 durum wheat (*T. turgidum* ssp. *Durum,* AABB) and 14 bread wheat (*T. aestivum* ssp. *Aestivum,* AABBDD) studies spanning four continents (Argentina, Australia, Canada, India, Israel, Japan, US) (Tabbita, Pearce,Barneix 2017). The *Gpc-B1* locus increased GPC in 90% of comparisons, with an average increase of +21g/kg (Tabbita, Pearce,Barneix 2017). Overall, the *Gpc-B1* locus had negligible effect on yield relative to the variation from genotype and environment, although yield was impacted in 23% of comparisons, with an effect ranging from -300kg/ha to +600kg/ha (Tabbita, Pearce,Barneix 2017). Protein yield increased in 30% of comparisons and was non-significant in 70% of comparisons. The functional *Gpc-B1* allele led to earlier senescence in all durum wheat lines measured and a quarter of comparisons for bread wheat, however this could not be quantified as senescence was measured in a variety of ways (Tabbita, Pearce,Barneix 2017).

The *Gpc-B1* locus improves breadmaking parameters in both bread wheat and durum wheat, increasing flour water absorption and loaf volume, as well as improving parameters of semolina and pasta quality (Brevis et al. 2010; Kiszonas et al. 2021). Milling score (indicative of milling quality) was reduced, likely due to reduced kernel weight and increased flour ash content (Brevis et al. 2010; Kiszonas et al. 2021). The improved bread and pasta quality parameters imply that *Gpc-B1* improves grain protein content without a detrimental impact on protein composition (Brevis et al. 2010).

The functional allele of *Gpc-B1* has been incorporated into wheat breeding programs, with released varieties in the US and Canada such as Lillian and Glencross (Depauw et al. 2005; Randhawa et al. 2013). More recently, the *Gpc-B1* locus was combined with protein quality and rust resistance alleles in Indian wheat germplasm (Gupta et al. 2022). When targeting production to meet a threshold 14% grain protein content, it was estimated that a spring wheat cultivar with *Gpc-B1* required less fertilizer input, and therefore led to increased revenue, compared to a cultivar without *Gpc-B1* (Pan et al. 2020).

In summary, the *Gpc-B1* locus carrying a functional allele of *NAM-B1* can increase grain protein content in diverse germplasm and environments. However, the impact of *Gpc-B1* on GPC, yield and senescence timing has not been reported in UK elite germplasm and field conditions. The impact of *Gpc-B1,* especially upon yield, is affected by gene-by-genotype and gene-by-environment interactions (Brevis and Dubcovsky 2010; Tabbita, Pearce,Barneix 2017). Therefore, a targeted approach is needed for each context. The introgression of the *Gpc-B1* locus into wheat cultivars from multiple countries demonstrates that genetic variation in a senescence-regulating NAC transcription factor can be applied to alter senescence timing and

grain protein content in wheat breeding. Can the understanding of leaf senescence be further applied to wheat breeding?

4.1.4 Methods for phenotyping senescence vary across the literature.

To track the timing of senescence in wheat breeding, a practical method is needed to phenotype senescence timing through field trials. During senescence, the chlorophyll content of leaves, ears and peduncles gradually decreases, visible as a colour change from green to yellow, brown, or white. In the glasshouse, chlorophyll content can be quantified using a hand-held spectrometer, however this would be time-consuming for field studies (Uauy, Brevis,Dubcovsky 2006). In the field, leaf yellowing is commonly scored visually over multiple time-points to generate a time-course (Kumar et al. 2010; Bogard et al. 2011; Xie, Mayes,Sparkes 2016; Chapman et al. 2021a).

A delay in senescence may occur through either a later onset of senescence or a slower rate of senescence (Thomas and Howarth 2000). To distinguish these types of alteration in senescence timing, it is necessary to estimate the onset and rate of senescence. The plethora of methods used to calculate senescence onset, rate and other metrics from a leaf senescence time-course have been thoroughly reviewed (Chapman et al. 2021a). In this thesis, the following senescence metrics were selected, and were used to analyse leaf yellowing time-course data in the field. Thermal time to 30% leaf senescence was used as a proxy for leaf senescence onset, calculated by a linear interpolation approach following (Chapman et al. 2021a; Alhabbar et al. 2018). Thermal time to 70% leaf senescence was also presented, as it was found to be a robust measure of senescence timing (Chapman et al. 2021a). These metrics were expressed in thermal time after heading to account for variability in heading date and temperature (Chapman et al. 2021a). Duration of leaf

senescence can be interpreted as the inverse of senescence rate; it was calculated as the thermal time from 10% to 90% leaf senescence (Chapman et al. 2021a). In addition, the area under the curve (AUC) of leaf senescence was calculated (Kumar et al. 2010). Area under the curve gives a measure of the level of leaf yellowing throughout the time-course, and is a metric commonly used for disease progression curves in pathology (Joshi et al. 2007). These metrics were selected as being straightforward to calculate while providing information that aids in interpreting differences in senescence between lines.

4.1.5 Untapped genetic variation for senescence and grain protein content

Despite intensive selective breeding over the past century, there may still be untapped genetic variation that can alter senescence profiles or improve grain protein content. Advantageous alleles for traits such as protein content and grain quality present in wheat wild relatives or landraces may be absent from the gene pool of elite varieties (Winfield et al. 2018; Sansaloni et al. 2020). It is possible that alleles for higher protein content were not transmitted through the genetic bottlenecks of polyploidization and domestication (Haas, Schreiber,Mascher 2019; Doebley, Gaut,Smith 2006). Alleles for higher protein content may have been selected against due to negative pleiotropic effects, such as functional *NAM-B1* which decreased grain size (Lundstrom, Leino,Hagenblad 2017).

It Is likely that In this young polyploid, many homoeologous triads act redundantly to carry out the same function. In hexaploid bread wheat, over half of genes are present as three homoeologous copies, and typical homoeologs are >95% similar in their coding sequence (Adamski et al. 2020). The A subgenome progenitor evolved separately from the B and D genome progenitors for only around 7 million years since their last common ancestor (Haas, Schreiber,Mascher 2019). The 0.5 million

years since the formation of tetraploid wheat have also left little time for pseudogenization or divergent evolution of these gene copies (Haas, Schreiber,Mascher 2019; Wendel 2000). In addition, 94% of gene triads retain synteny, and 72% of syntenic triads show balanced expression across homoeologs within 15 tissue types (Ramírez-González et al. 2018; Appels et al. 2018). Redundancy means that a genetic variant leading to loss-of-function or reduced expression of the A homoeolog of a gene may be compensated by functional B and D homoeologs (Borrill, Adamski,Uauy 2015). Wheat lines carrying this genetic variant will show no phenotypic effect, so phenotype-based techniques such as GWAS and genomic selection will not detect this variant (Borrill, Adamski,Uauy 2015).

We showed that transcription factor genes are more likely to have retained three homoeologs in hexaploid wheat since polyploidization than other types of genes (Evans, Arunkumar,Borrill 2022). These homoeologs are also less likely to have acquired potentially deleterious mutations, such as stop codon and missense mutations, over recent evolution (Evans, Arunkumar,Borrill 2022). Transcription factor homoeologs show redundancy as they share a median of 40% of predicted downstream targets compared to 0% for a random pair of transcription factors (Harrington et al. 2020). Therefore, variants in transcription factors are more likely to be masked by redundancy with homoeologs, and untapped for breeding.

4.1.6 Techniques in this chapter: exome capture and Near Isogenic Lines

Allelic variation in wheat genes of interest can be identified effectively using exome capture datasets. By targeting coding DNA, which makes up only 6.7% of the wheat genome, a larger number of accessions can be tested (Appels et al. 2018). Exome capture has been carried out in both tetraploid and hexaploid wheat cultivars (Pont et

al. 2019; He et al. 2019). Untapped genetic diversity has been recorded using exome capture in the Watkins landrace collection, as well as wheat wild relatives such as wild emmer *(T. turgidum* ssp. *Dicoccoides,* AABB) and *Aegilops tauschii* (DD) (Gardiner et al. 2018; Avni et al. 2017; Singh et al. 2019).

To generate an exome capture array in wheat, contigs of wheat exon sequences were assembled by combining cDNA sequencing with expressed sequence tag collections and removing duplicates, and probes were designed to tile evenly across these contigs (Winfield et al. 2012). The probes were immobilised on a NimbleGen array (Roche), and genomic DNA libraries were hybridized to this array before sequencing and SNP calling (Winfield et al. 2012). Subsequently, exome capture probe sets have been designed based on a partial genome assembly of Chinese Spring, and based on the Chinese Spring reference sequence combined with wild emmer and *Aegilops tauschii* (Jordan et al. 2015; Gardiner et al. 2019). Exome capture techniques can capture sequences with limited mismatches relative to the probe sequence, enabling capture of a range of wheat accessions, but not of wide introgressions (Gardiner et al. 2019; Burridge et al. 2022).

Near-Isogenic Lines (NILs) consist of wheat lines which differ at markers surrounding a specific QTL (Quantitative Trait Locus) or SNP (Single Nucleotide Polymorphism) but are uniform in the rest of the genome. NILs are typically generated by repeated backcrossing of a donor variety, carrying the locus of interest, with a recipient variety, accompanied by marker-assisted selection (Tuinstra, Ejeta,Goldsbrough 1997). By controlling the genetic background, NILs enable more precise measurement of the phenotype associated with the QTL compared to a segregating population (Tuinstra, Ejeta,Goldsbrough 1997). Therefore, in this chapter NILs were

used to test the phenotype of the *Gpc-B1* locus and a SNP in *NAM-A1* under UK field conditions.

4.1.7 Allelic variation in *NAM-A1*

NAM-A1 provides an example of investigating allelic variation in a gene of interest across wheat populations. Two allelic variants were identified in *NAM-A1*: a missense mutation causing an alanine to valine substitution in exon 2 and a 1bp deletion causing a premature stop codon at the end of exon 3 (Cormier et al. 2015). These variants lead to four possible combinations or haplotypes (*Table 4.1*). The haplotype *NAM-A1b* was only found in a single accession, implying that the 1bp deletion mutation occurred in a line carrying the “A” allele in exon 2, forming the *NAM-A1d* haplotype, and the *NAM-A1b* accession is a rare recombinant (Cormier et al. 2015).

The haplotype *NAM-A1a* correlated with lower yield and higher GPC compared to *NAM-A1d* in European cultivars, with *NAM-A1c* intermediate (Cormier et al. 2015). Among 19 Australian cultivars, *NAM-A1a* had the opposite association: lines with *NAM-A1a* showed higher yield (2.2 vs 2.0 t/ha) and slightly lower GPC than lines with *NAM-A1c* or *NAM-A1d,* a result that the authors attribute to terminal heat stress (Alhabbar et al. 2018). *NAM-A1a* lines also had earlier senescence, as loss of leaf chlorophyll, and reduced kernel weight (Alhabbar et al. 2018). *NAM-A1* was within the most significant QTL for GPC in a panel of 93 Russian cultivars, of which GPC was lower for *NAM-A1d* than *NAM-A1c* cultivars, but yield and kernel weight did not differ (Leonova et al. 2022). Overall, this indicates that *NAM-A1a* is the functional haplotype of *NAM-A1*, as the alanine in exon 2 matches homoeologous proteins. *NAM-A1c* and *NAM-A1d* may be haplotypes with reduced protein function as they were more often associated with delayed senescence and reduced GPC, similar to

NAM-A1 TILLING mutant lines and *NAM* RNAi lines (Avni et al. 2014; Pearce et al. 2014).

Table 4.1 Haplotypes of SNPs 6A_77099397_G/A and 6A_77098609_TG/G in NAM-A1, adapted from (Cormier et al. 2015). Base pairs on forward strand of chromosome 6A (reverse complement of NAM-A1 transcript). Upper label is variant ID in this thesis; lower label is variant ID in (Cormier et al. 2015).

	6A_77099397_G/A	**6A_77098609_TG/G**
	SNP1	**SNP2**
NAM-A1a	G	TG
NAM-A1b	G	G
NAM-A1c	A	TG
NAM-A1d	A	G

4.1.8 *NAM-2, NAC5-1* and *NAP-1* are candidate senescence regulators

In earlier chapters, it was shown that the NAC transcription factors *NAM-2, NAC5-1* and *NAP-1* are expressed in early flag leaf senescence. Overexpression of *NAC5-A1* was correlated with earlier senescence, while loss-of-function of *NAC5-1* was correlated with delayed senescence, indicating that *NAC5-1* may promote earlier onset of senescence in wheat. Allelic variation in these candidate senescence regulators across wheat cultivars has not yet been explored.

4.1.9 Objectives

In this chapter, the following objectives will be addressed.

1. How do *NAM-A1* and *NAM-B1* affect senescence, yield and grain protein content in a UK context?
2. What allelic variation exists in the NAC transcription factors *NAM-1, NAM-2, NAC5-1* and *NAP-1* in wheat?

3. Development of markers to track allelic variation in NAC transcription factors

To achieve the first objective, senescence timing, yield and grain protein content were measured in near-isogenic lines carrying both the *Gpc-B1* locus and a loss-of-function allele of *NAM-A1* in UK germplasm and UK field conditions. To explore allelic variation in NAC transcription factors, variants were explored in an exome capture dataset of wheat breeding material. KASP markers were developed to track these variants, and were used to compare yield and protein content between NAC transcription factor alleles.

4.2 Methods

4.2.1 Experimental design

4.2.1.1 *NAM-1* Field trials

Near isogenic lines (NILs) segregating for both *NAM-A1* and *NAM-B1* alleles were generated by RAGT. The *Gpc-B1* locus, containing the full-length peptide of *NAM-B1,* was derived from a NIL in hexaploid spring wheat Yecora rojo (Brevis and Dubcovsky 2008; Qualset, Vogt,Borlaug 1985) (*Table 4.2*). An allele of *NAM-A1* with a stop codon in subdomain v of the NAC domain was derived from an EMS-induced mutation, with at least three backcrosses into a hexaploid spring wheat (*Table 4.2*). Both the *Gpc-B1* locus and *NAM-A1* stop codon allele were introgressed into UK hexaploid winter wheat cultivar “RGT Bowen” (which carries a loss-of-function allele of *NAM-B1,* either a >100kb deletion or +1bp frameshift). Between 7 and 13 independent NILs were generated for each genotype combination (*Table 4.3*).

Table 4.2 NAM-A1 and NAM-B1 alleles used to generate near-isogenic lines in UK hexaploid wheat. NAM-B1 is absent from RefSeq v1.1 so Genbank ID is given (Uauy et al. 2006).

Gene	Gene ID	Genetic background	Conse-quence	Allele	Amino acids	Amino acid position	Sub-domain
NAM-B1	DQ869673	Yecora rojo (GPC-B1)	complete peptide	*Gpc-B1* locus			
NAM-A1	TraesCS6A02G108300	Hexaploid spring wheat (unknown)	stop codon		W/*	199	v

Table 4.3 Near isogenic lines (NILs) for NAM-A1 and NAM-B1 grown in field trials. WT marks the genotype of the recurrent parent (UK hexaploid winter wheat cultivar "RGT Bowen"). Capital letters indicate functional gene copies; small letters indicate loss-of-function.

Genotype	*NAM-A1*	*NAM-B1*	*NAM-D1*	Number of NILs
aabbDD	stop codon	loss-of-function	complete peptide	13
AabbDD (WT)	complete peptide	loss-of-function	complete peptide	9
aaBBDD	stop codon	complete peptide	complete peptide	7
AABBDD	complete peptide	complete peptide	complete peptide	7

The 36 *NAM-1* NILs were grown in treated field trials at RAGT Seeds Ltd., Ickleton, Essex, in 6m*1.3m plots in a randomized design with two replicates in 2021 and one replicate in 2022. Field trials were managed according to standard agronomic practice. Leaf senescence and ear senescence were scored and senescence metrics calculated as described previously (Methods 2.2.6 and 2.2.7). In 2021, senescence scoring was assisted by the RAGT Pathology team.

Grain mass and grain moisture content were measured at harvest, and yield was calculated as tonnes/hectare at 15% grain moisture content. Grain protein content was analyzed by Near Infrared Spectrometer (NIR, Perten DA7250) by the RAGT Quality team, calibrated with manufacturer-supplied wheat grain data.

No obvious spatial variation in traits was observed in this trial. In 2021, ear emergence was only measured for replicate 1, and replicate 2 was inferred to have the same ear emergence for calculation of senescence metrics. This is unlikely to impact results as ear emergence fell within a 1.5 day range. Traits were analysed using a linear model and type III ANOVA with formula:

```
lm(Trait ~ NAMA1 * NAMB1)
```

4.2.2 Genetic variation analysis

4.2.2.1 Extraction of genetic variants in NAC TFs from Exome Capture data

An exome capture dataset from a panel of 286 wheat lines, including elite cultivars, breeding lines and “exotic” germplasm (anything with genetic diversity beyond the gene pool of elite cultivars) was provided by RAGT in variant call format (VCF). To select variants in NAC transcription factors, the transcript coordinates of all transcripts of all homoeologs of *NAM-1*, *NAM-2*, *NAC5-1* and *NAP-1* (except *NAM-*

B1) were downloaded from the bread wheat reference sequence, *Triticum aestivum* cv. Chinese Spring IWGSC RefSeq v1.1, on Ensembl Plants (*Table 4.4*) (Appels et al. 2018; Yates et al. 2022).

Variants were filtered for average read depth between 5 and 60, per-sample read depth between 2 and 120, less than 20% missing calls, and biallelic sites using vcftools (Danecek et al. 2011). Only biallelic sites (with two possible alleles) can be used to create KASP markers in Polymarker (Ramirez-Gonzalez, Uauy,Caccamo 2015). Variants were filtered using bcftools with the parameters “QD <2 || FS >60.0 || MQRankSum<-12.5 || ReadPosRankSum<-8.0 || SOR >3.0 || MQ <40” following (Scott et al. 2021) . This set of filters removes variants with low mapping quality, strand mapping biases and Alt vs Ref mapping biases. Variants called in more than one variety were retained. Scripts for this pipeline are available on Github (Evans 2023).

Table 4.4 Chromosome locations of NAC transcription factor genes used to select variants from exome capture data. Gene IDs and chromosome locations from RefSeq v1.1 via Ensembl Plants (Appels et al. 2018; Yates et al. 2022).

Gene name	Gene ID	Chromosome	Gene start (bp)	Gene end (bp)
NAM-A1	TraesCS6A02G108300	6A	77097709	77100361
NAM-D1	TraesCS6D02G096300	6D	60486167	60488033
NAM-A2	TraesCS2A02G201800	2A	175467301	175470007
NAM-B2	TraesCS2B02G228900	2B	223153810	223156266
NAM-D2	TraesCS2D02G214100	2D	175330859	175333525
NAC5-A1	TraesCS4A02G219700	4A	521917748	521920022

NAC5-B1	TraesCS4B02G098200	4B	103054108	103056465
NAC5-D1	TraesCS4D02G094400	4D	69677974	69680281
NAP-A1	TraesCS4A02G131000	4A	174155319	174157653
NAP-B1	TraesCS4B02G173600	4B	380653174	380655594
NAP-D1	TraesCS4D02G175700	4D	304689911	304692359

4.2.2.2 Variant effect prediction

To predict the effect of variants on NAC gene function, consequences of the 99 filtered variants were assessed using the Ensembl Variant Effect Predictor with default options, and SIFT scores (Sorting Intolerant From Tolerant) (McLaren et al. 2016; Kumar, Henikoff,Ng 2009). For *NAM-A1, NAM-A2* and *NAM-B2*, two alternative transcripts were available from RefSeq v1.1. All transcripts of homoeologous triads were multiple aligned using Clustal Omega 1.2.2 (Madeira et al. 2022). Transcripts with higher sequence similarity with homoeologous genes were selected (*Table 4.5*). The transcripts of *NAM-A1, NAM-A2* and *NAM-B2* that were not selected were alternatively spliced at the intron 2/exon 3 boundary, resulting in an in-frame insertion of 7 or 8 amino acids between subdomains iv and v of the NAC domain (*Table 4.5*).

Table 4.5 Transcripts selected for Variant Effect Predictor (VEP). Alternative transcripts not selected are annotated with the amino acid insertion compared to selected transcripts.

Gene	Transcript selected for VEP	Transcript not selected
NAM-A2	TraesCS2A02G201800.1	TraesCS2A02G201800.2 (R185 -> RCTSSSHQ)
NAM-B2	TraesCS2B02G228900.2	TraesCS2B02G228900.1 (R185 -> RCTSSSHQ)
NAM-A1	TraesCS6A02G108300.1	TraesCS6A02G108300.2 (R185 -> RVRTRVDRT)

4.2.2.3 Gene-level haplotypes

Gene-level haplotypes were built for the 99 filtered SNPs and RAGT exome capture data using a custom R script (Evans 2023). As this exome capture panel consisted of wheat cultivars and breeding lines expected to be predominantly homozygous, and sequencing data was unphased, heterozygous calls were treated as missing data. Briefly, the VCF file was rearranged to a matrix of variant calls with a row per variety and a column per variant. All rows with missing data were removed. Each row with a unique set of variant calls was defined as a haplotype. Haplotypes were numbered such that *h1* is the haplotype of the reference genome (RefSeq v1.1), then in order of the most common in this dataset. Finally, each variety was assigned to a haplotype, and possible haplotype(s) were imputed for varieties with missing data. Any variety that could not be narrowed down to one or two possible haplotypes was set as undefined.

4.2.2.4 KASP marker design for NAC transcription factor SNPs

To design KASP markers for variants in NACs, upstream and downstream flanking sequences for each SNP were determined using bedtools. KASP markers were designed using the Polymarker web interface (Ramirez-Gonzalez, Uauy,Caccamo 2015). Markers which passed a proprietary script for marker quality control were run on a panel of 1245 crossing parents, and markers with a non-zero allele frequency in French crossing parents were run on a larger panel of French breeding lines. Alleles of SNPs in NACs in the French panel were compared to yield and grain protein content data from field trials provided by RAGT (Table 4.7). Two published KASP markers that distinguish SNPs in *NAM-A1* were run on crossing parents, but not on the french panel (*Table 4.1*, *Table 4.6*) (Cormier et al. 2015). KASP genotyping was

carried out by the RAGT Genotyping team, and yield and protein comparison was assisted by Ruth Bryant.

Table 4.6 KASP markers used to genotype variants in NAC transcription factors. Marker ID includes chromosome, position, reference (REF) and alternative (ALT) alleles. KASP markers which functioned successfully are shown. Fluorescent "VIC" and "FAM" tags have been omitted from REF and ALT primers respectively for brevity. Specific = COM primer specific to one homoeolog; Semispecific = COM primer targets 2 homoeologs; Nonspecific = COM primer targets 3 homoeologs. [1] This thesis; [2] (Cormier et al. 2015).

Marker		KASP Primer	Primer type	Gene name	Gene ID	Consequence	Source	Axiom 35K array marker
2B_223154437_C/T	REF	aaCccatccatcatgcttatacC	Semispecific	*NAM-B2*	TraesCS2B02G228900	intron_variant	[1]	
	ALT	aaCccatccatcatgcttatacT						
	COM	caagcacgacaggatcacaT						
2B_223155153_G/A	REF	gctgtccTggtgatggagC	Specific	*NAM-B2*	TraesCS2B02G228900	synonymous_ variant	[1]	
	ALT	gctgtccTggtgatggagT						
	COM	gtcaccgcatacccgcTT						
2D_175333184_T/A	REF	ggaatagacccggccaaaaatA	Semispecific	*NAM-D2*	TraesCS2D02G214100	3_prime_UTR_ variant	[1]	
	ALT	ggaatagacccggccaaaaatT						
	COM	aacgagtcacaacaTagtTGgA						
4A_521919892_C/G	REF	tgaatggaccacggcttcG	Nonspecific	*NAC5-A1*	TraesCS4A02G219700	missense_variant	[1]	AX-94582821
	ALT	tgaatggaccacggcttcC						
	COM	tacatcaccagctcctcgtc						
4B_103054374_A/G	REF	aacctaaaagcgtcagccaA	Semispecific	*NAC5-B1*	TraesCS4B02G098200	3_prime_UTR_ variant	[1]	AX-95010248
	ALT	aacctaaaagcgtcagccaG						
	COM	gtgttgtgtagctagtgtagagT						
4B_103054985_A/G	REF	atcgacggctcGctGatT	Specific	*NAC5-B1*	TraesCS4B02G098200	synonymous_	[1]	

						variant		
	ALT	atcgacggctcGctGatC						
	COM	AgtctgacggatgcTgcC						
4B_103055511_T/C	REF	cgtacacgtacactagcttTAgttA	Semispecific	*NAC5-B1*	TraesCS4B02G098200	intron_variant	[1]	
	ALT	cgtacacgtacactagcttTAgttG						
	COM	gtctcagcgacggcgatA						
4D_304690264_G/A	REF	gacggggcagggcgattC	Nonspecific	*NAP-D*	TraesCS4D02G175700	missense_variant	[1]	
	ALT	gacggggcagggcgattT						
	COM	cgatgatcatgtccgacccg						
4D_304690554_G/C	REF	ccgtaagtaccccaacggtG	Nonspecific	*NAP-D*	TraesCS4D02G175700	missense_variant	[1]	
	ALT	ccgtaagtaccccaacggtC						
	COM	cttccagtagccggaaccc						
4D_304691224_T/G	REF	gcgtgttaatgactgattcaTcttT	Semispecific	*NAP-D*	TraesCS4D02G175700	intron_variant	[1]	
	ALT	gcgtgttaatgactgattcaTcttG						
	COM	agacggatcAcacgtagtattaaA						
4D_304691234_G/A	REF	tgattcaTctttcgcctgGttG	Semispecific	*NAP-D*	TraesCS4D02G175700	intron_variant	[1]	
	ALT	tgattcaTctttcgcctgGttA						
	COM	agacggatcAcacgtagtattaaA						
4D_304691983_A/T	REF	cagttcgccGgtcgtatataatT	Specific	*NAP-D*	TraesCS4D02G175700	3_prime_UTR_variant	[1]	
	ALT	cagttcgccGgtcgtatataatA						
	COM	ccatcagacgCtgctccA						
4D_69678642_C/T	REF	ccgaattacacgagacctgaC	Semispecific	*NAC5-D1*	TraesCS4D02G094400	3_prime_UTR_variant	[1]	AX-95069084
	ALT	ccgaattacacgagacctgaT						
	COM	cgtcagacCcctcTtcctT						
6A_77098019_T/C	REF	gcataagggccactcacataaT	Nonspecific	*NAM-A1*	TraesCS6A02G108300	3_prime_UTR_variant	[1]	

	ALT	gcataagggccactcacataaC					
	COM	gcatggtaattgcatacacggg					
6A_77098609_TG/G	REF	GGCGCCACCTCTGGTTTCCA	Specific	*NAM-A1*	TraesCS6A02G108300	frameshift	[2]
	ALT	GCGCCACCTCTGGTTTCCG					
	COM	GATTCCAGTTCACGCCGGATACTT					
6A_77099397_G/A	REF	ACCGCCTCACCGACGC	Specific	*NAM-A1*	TraesCS6A02G108300	missense	[2]
	ALT	TACCGCCTCACCGACGT					
	COM	TGTACGTACCCTCAGAGAGGC T					

Table 4.7 Number of data points for yield (YLD) and protein content (GPC) for KASP markers run on French breeding lines. LLC/POI are trial location codes, R1 is replicate 1. Phenotypic data are presented for these trials and some of the markers.

KASP marker	Allele	Data shown	Number of data points			
			YLD POI TT R1 2022	YLD LLC TT R1 2022	GPC POI TT R1 2022	GPC LLC TT R1 2022
2B_223155153_G/A	G		412	608	412	608
2B_223155153_G/A	A		0	0	0	0
4A_521919892_C/G	C	Y	348	483	348	483
4A_521919892_C/G	G	Y	63	124	63	124
4B_103054985_A/G	A		353	515	353	515
4B_103054985_A/G	G		58	93	58	93
4B_103055511_T/C	T	Y	352	517	352	517
4B_103055511_T/C	C	Y	59	95	59	95
4D_69678642_C/T	C	Y	232	317	232	317
4D_69678642_C/T	T	Y	182	293	182	293
2D_175333184_T/A	T	Y	407	605	407	605
2D_175333184_T/A	A	Y	115	165	115	165
4B_103054374_A/G	A		355	518	355	518
4B_103054374_A/G	G		60	96	60	96

4.2.2.5 Comparison of haplotypes of *NAM-A1*

To compare the frequency of four published haplotypes of two variants in *NAM-A1* between RAGT data and other datasets, counts and frequencies of haplotypes of *NAM-A1* in RAGT exome capture data were calculated using the data from the gene-level haplotype analysis (*Table 4.1*) (Cormier et al. 2015). Counts and frequencies of haplotypes in crossing parents were inferred from frequencies of 6A_77099397_G/A and 6A_7709609_TG/G by assuming that the frequency of haplotype *NAM-A1b* is zero, as was found in all other elite cultivar datasets. In addition, counts and frequencies of *NAM-A1* haplotypes were collected from the following sources.

1. Elite wheat cultivars from Europe (334 accessions). *NAM-A1* haplotype counts from (Cormier et al. 2015).
2. Elite wheat cultivars from Russia (93 accessions). *NAM-A1* haplotype counts from (Leonova et al. 2022).
3. INRA core collection (367 accessions). This collection was selected to capture the genetic diversity of 3,942 accessions from the INRA collection, and consists of 101 accessions from France, 102 from the rest of Europe, and 164 from the rest of the world (Balfourier et al. 2007). *NAM-A1* haplotype counts from (Cormier et al. 2015).
4. Watkins core collection (102 accessions). This collection was selected to capture the genetic diversity of the 826 accessions of the Watkins landrace collection, and consists of global landraces collected in the 1930's (Wingen et al. 2014). *NAM-A1* haplotype counts calculated from SNP calls generated by exome capture and accessed through Ensembl Biomart (Gardiner et al. 2018; Kinsella et al. 2011).

Other exome capture datasets were searched, but no variants mapping to *NAM-A1* transcripts were found (He et al. 2019; Pont et al. 2019). *NAM-A1* sequences in the wheat pangenome were identified using a BLASTN search on Ensembl Plants, and haplotypes were assigned based on multiple alignment with Clustal Omega 1.2.2 in Geneious software (Biomatters 2022; Madeira et al. 2022). *NAM-A1* haplotypes in the Watkins core collection were compared with phenotypic data from field trials at Church Farm, Bawburgh in 2010 and 2011, accessed with permission (Designing Future Wheat 2018).

4.3 Results

4.3.1 Impact of *NAM-A1* and *NAM-B1* on senescence, yield and protein content in the field in the UK

To test the impact of *NAM-A1* and *NAM-B1* on senescence, yield and protein content in a UK breeding context, near-isogenic lines (NILs) were developed in a UK hexaploid wheat cultivar segregating for functional *NAM-B1* from the *Gpc-B1* introgression, and a mutation in *NAM-A1* likely to lead to loss-of-function (Methods 4.2.1). NILs were grown in field trials with two replicates in 2021 and one replicate in 2022. Senescence timing is reported for both years, while yield and protein content is reported for 2021, but not for 2022.

4.3.1.1 Temperature data for field trials

For *NAM-1* field trials at RAGT Seeds Ltd., Ickleton, Essex, temperature data from a weather station 18.3 miles distant at Andrewsfield, Essex was used to calculate thermal time for senescence metrics (Methods 2.2.7) (Met Office 2023). Overall, 2022 was warmer than 2021, with mean daily air temperature exceeding 20°C more frequently (*Figure 4.1*,*Figure 4.2*). Maximum hourly temperatures in July were 29°C in 2021 and 36°C in 2022.

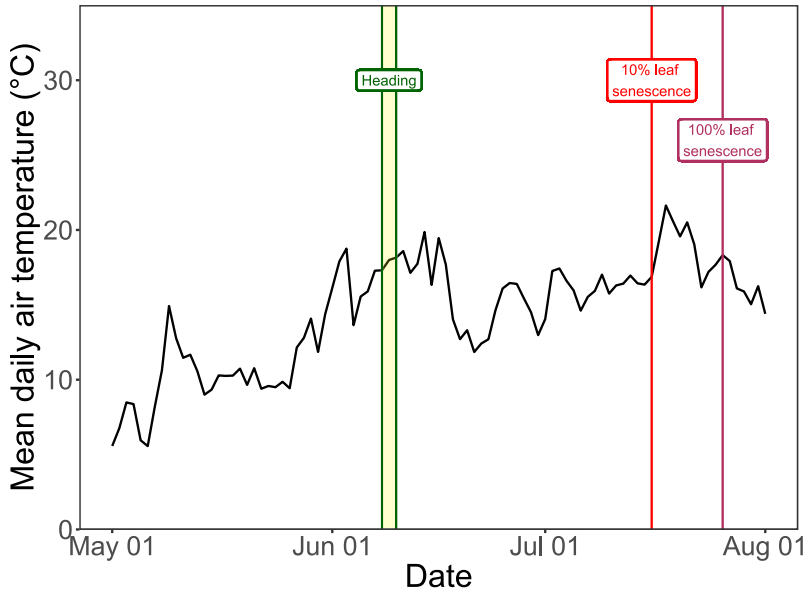


Figure 4.1 Mean daily air temperature from May to July 2021 used in calculating senescence metrics. Annotations mark the time interval of heading, and dates when all plots had reached 10% and 100% leaf senescence. Data from weather station at Andrewsfield, Essex (Met Office 2023).

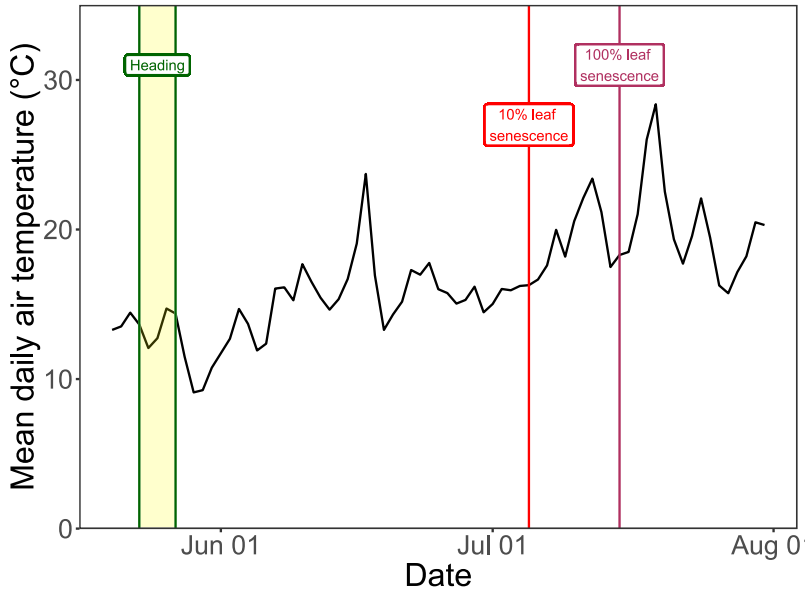


Figure 4.2 Mean daily air temperature from May to July 2022 used in calculating senescence metrics. Annotations mark the time interval of heading, and dates when all plots had reached 10% and 100% leaf senescence. Data from weather station at Andrewsfield, Essex (Met Office 2023).

4.3.1.2 Functional alleles of *NAM-B1* and *NAM-A1* promote earlier leaf and ear senescence and increased protein content in hexaploid wheat.

In 2021, the time-course of senescence scores captured the majority of leaf yellowing and was complete for ear yellowing, although the point of 10% leaf yellowing was missed for some plots (*Figure 4.3*). In absolute time, double loss-of-function lines displayed the latest leaf senescence, whilst lines with functional *NAM-A1* and *NAM-B1* displayed the earliest leaf senescence (*Figure 4.3*A). The progress of leaf senescence was very similar in single loss-of-function lines of *nam-b1* (wild-type) and *nam-a1* (*Figure 4.3*A). Overall, ear yellowing began later and occurred more rapidly than leaf yellowing, but the same patterns were seen between genotypes (*Figure 4.3*B).

Heading date was uniform, occurring within a 1.5-day window across all lines (*Figure 4.4*A). Functional *NAM-A1* resulted in earlier onset of leaf senescence, measured as thermal time to 30% leaf senescence, by an estimated 44 °C days, and *NAM-B1* earlier by 39 °C days (*Figure 4.4*B). Functional alleles of *NAM-A1* and *NAM-B1* led to significantly earlier 70% leaf senescence and increased AUC of leaf senescence (*Figure 4.4*C, D). The duration of leaf senescence was shortened by 39 °C days with the *NAM-B1* allele and 17 °C days, with the *NAM-A1* allele (*Figure 4.4*E). In 2021, the interaction term between *NAM-A1* and *NAM-B1* alleles was not significant for any leaf senescence metrics, indicating that *NAM-A1* and *NAM-B1* act additively to promote earlier leaf senescence.

Ear yellowing was also measured: functional *NAM-A1* and *NAM-B1* decreased thermal time to 30% ear senescence by an estimated 26 °C days and 27 °C days respectively (*Figure 4.5*A). As for leaf senescence, 70% ear senescence was earlier and AUC of ear senescence increased (*Figure 4.5*B, C). The duration of ear

senescence did not differ between genotypes (*Figure 4.5*D). This could be explained as in wild-type plants, the duration of ear senescence is only 130°C days, shorter than the duration of leaf senescence at 197°C days. The interaction term was just significant for AUC of ear senescence (p=0.03) – mutation of *NAM-A1* delayed ear senescence slightly less in a *NAM-B1* mutant background (*Figure 4.5*C).

In 2021, functional *NAM-B1* significantly decreased yield by 0.62 t/ha, however *NAM-A1* allele did not have a significant effect on yield (*Figure 4.6*A). Functional alleles of *NAM-1* increased grain protein content, with 0.71% increase for *NAM-B1* and a borderline significant 0.51% increase for *NAM-A1* (*Figure 4.6*B). For grain protein content, the interaction term was not significant, indicating that *NAM-A1* and *NAM-B1* act additively. Overall, this meant that *nam-b1* single mutant lines (wild-type) had the highest protein yield, although the difference was non-significant (*Figure 4.6*C).

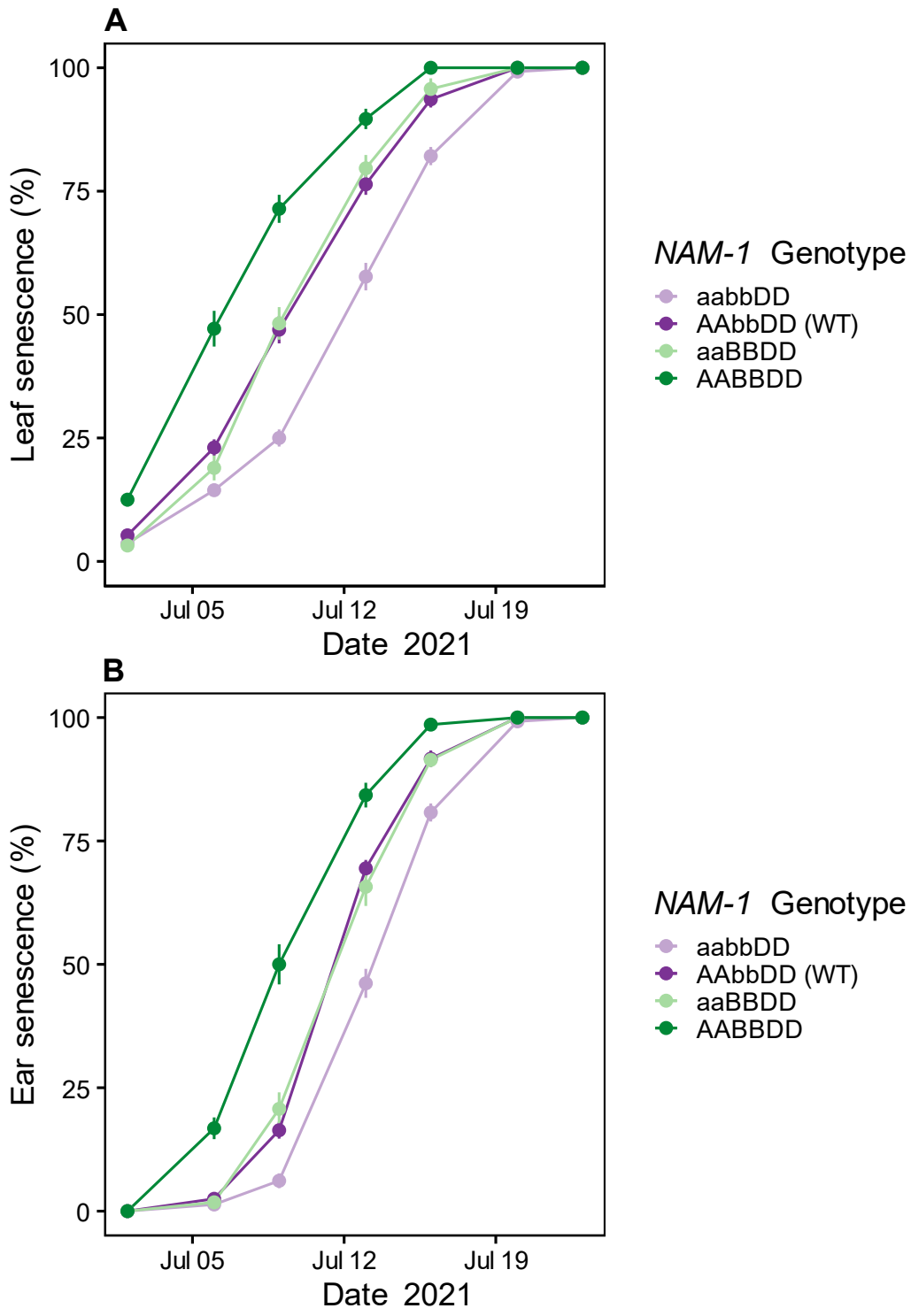


Figure 4.3 In 2021, loss-of-function of NAM-A1 and NAM-B1 delayed leaf and ear senescence. Percentage leaf and ear yellowing were scored in 6m plots twice weekly from 2nd to 23rd July. Mean + SE shown for each genotype (n = 14 – 26). Capitals functional NAM-1 alleles; lower case non-functional NAM-1 alleles. WT marks NILs with genotype matching the hexaploid cultivar background that has a non-functional allele of NAM-B1. (A) Percentage leaf senescence; (B) Percentage ear senescence.

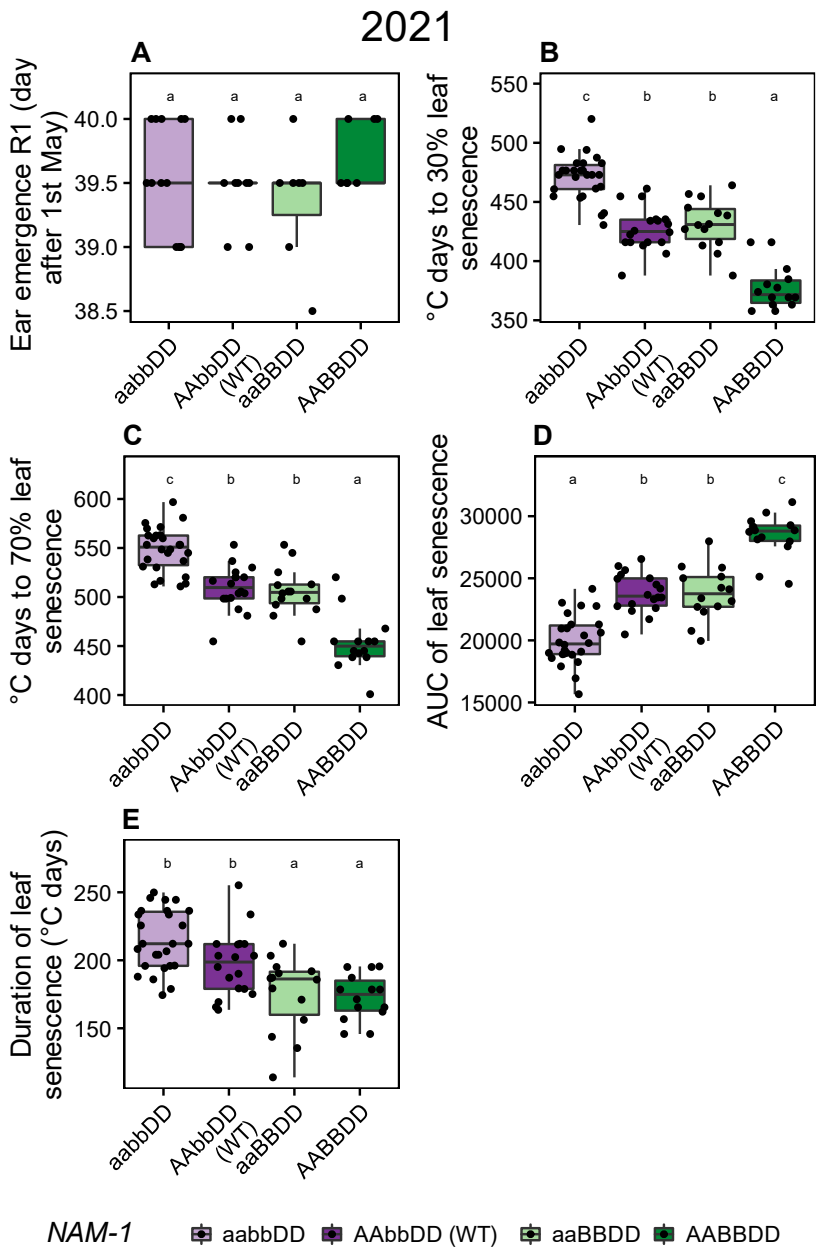


*Figure 4.4 Lines with functional NAM-A1 or NAM-B1 alleles reached 30% and 70% leaf senescence earlier and showed a shorter duration of leaf senescence in 2021. (A) Ear emergence in days after 1st May (0.5 values indicate borderline between two days); (B) Thermal time to 30% leaf senescence (°C days); (C) Thermal time to 70% leaf senescence (°C days); (D) Area under curve (AUC) of leaf senescence; (E) Duration of leaf senescence (°C days). (A) Replicate 1 (n = 7-13); (B-E) Replicates 1 and 2 (n = 14-26). Capitals functional NAM-1 alleles; lower case non-functional NAM-1 alleles. ANOVA with post-hoc Tukey test, formula ~ NAM-A1 * NAM-B1, letters show significance groups at p<0.05.*

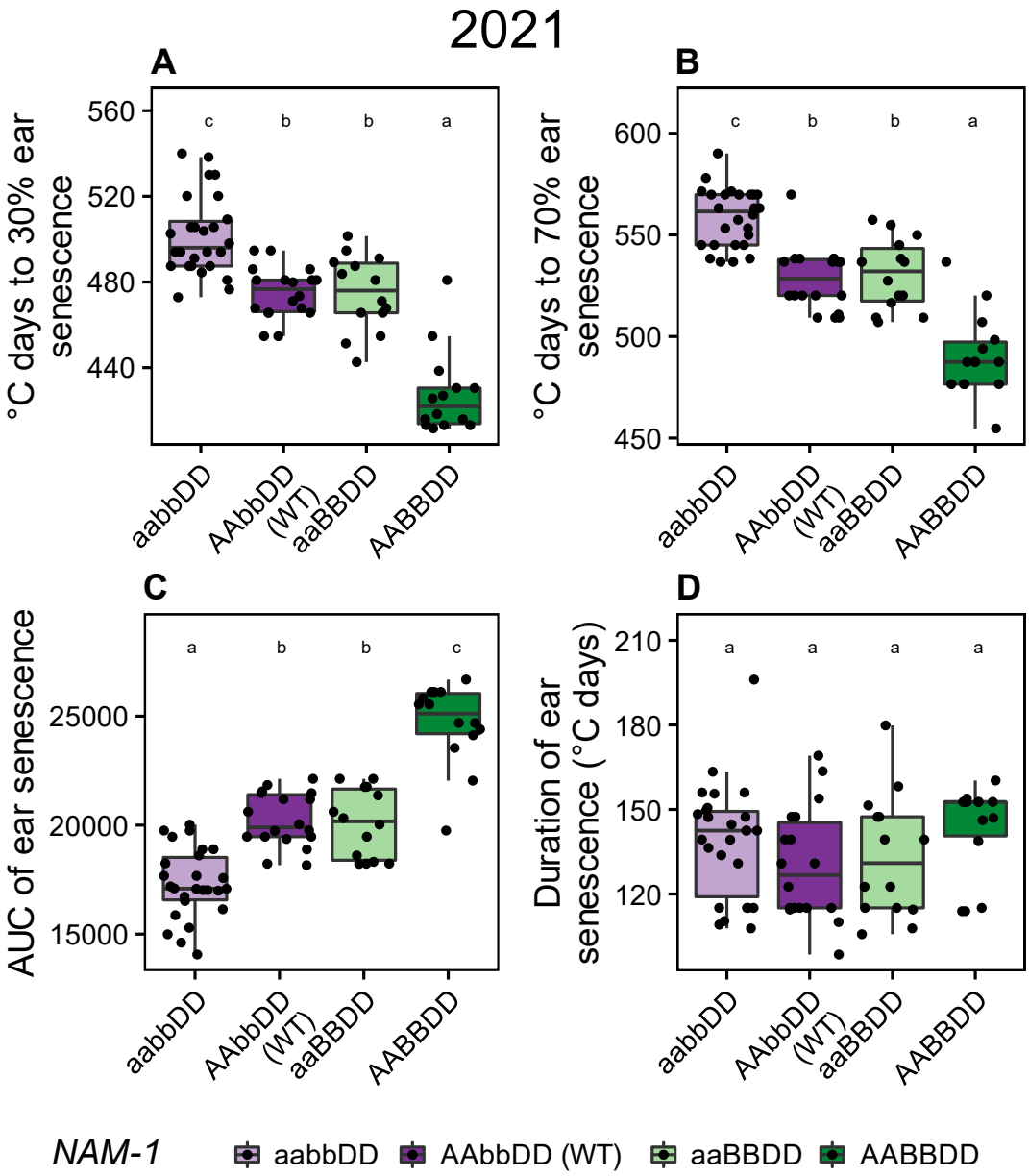


*Figure 4.5 Lines with functional NAM-A1 or NAM-B1 alleles reached 30% and 70% ear senescence earlier in 2021. (A) Thermal time to 30% ear senescence (°C days); (B) Thermal time to 70% ear senescence (°C days); (C) Area under curve (AUC) of ear senescence; (D) Duration of ear senescence (°C days). (A-D) Replicates 1 and 2 (n = 14-26). Capitals functional NAM-1 alleles; lower case non-functional NAM-1 alleles. ANOVA with post-hoc Tukey test, formula ~ NAM-A1 * NAM-B1, letters show significance groups at p<0.05.*

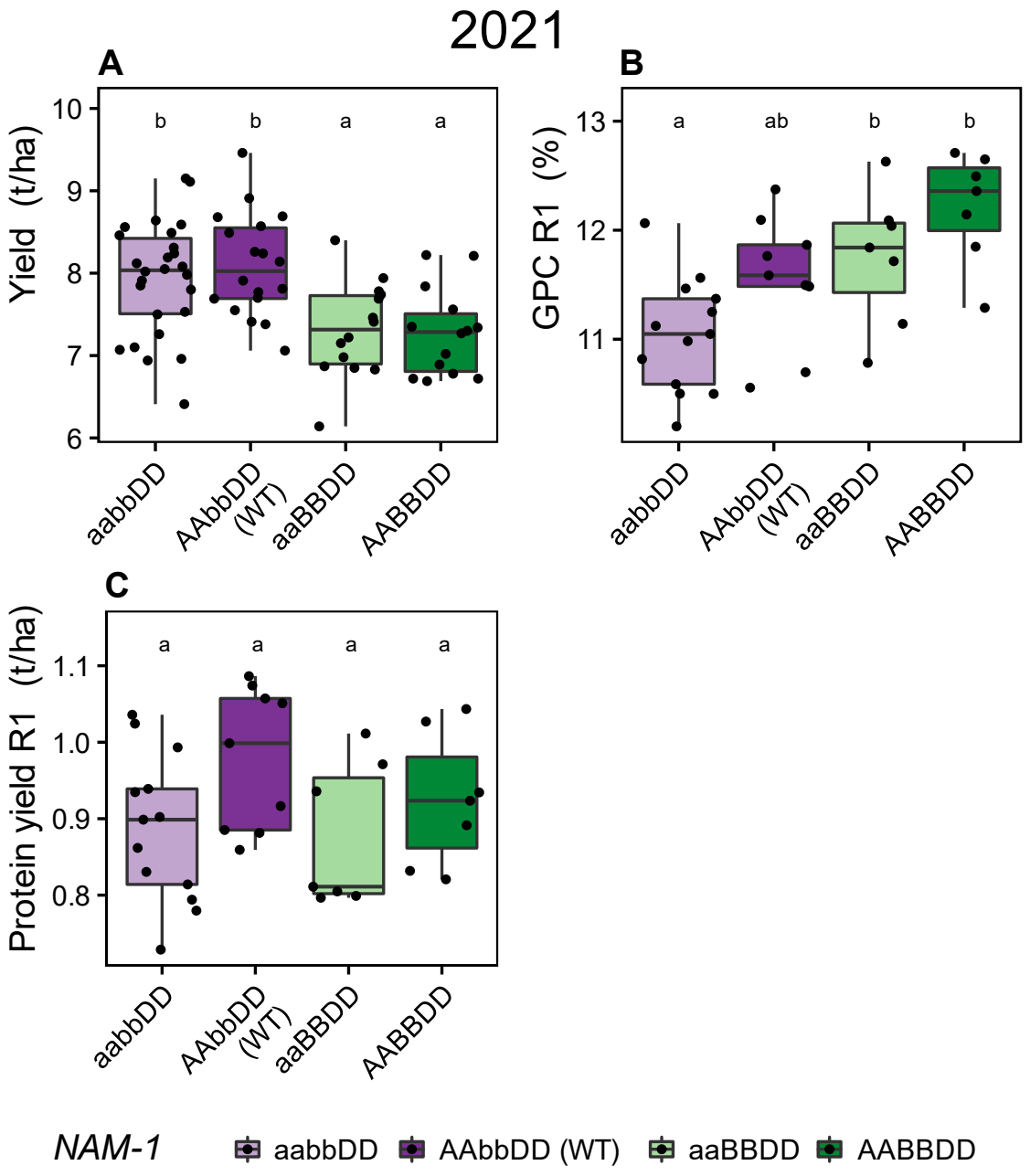


*Figure 4.6 Yield decreased and protein content increased with functional NAM-B1, while protein content decreased and yield did not differ with mutation of NAM-A1 in 2021. (A) Yield (t/ha) – Replicates 1 and 2 (n = 14-26); (B) Grain protein content (GPC) – Replicate 1 (n = 7-13); (C) Protein yield – Replicate 1 (n = 7-13). Capitals functional NAM-1 alleles; lower case non-functional NAM-1 alleles. ANOVA with post-hoc Tukey test, formula ~ NAM-A1 * NAM-B1, letters show significance groups at p<0.05.*

Overall, results from the same lines in 2022 were consistent with 2021. The overall patterns of leaf senescence and ear senescence were similar to 2021, and the full time-course from 0% to 100% leaf and ear yellowing was captured for all plots (*Figure 4.7*A, B). Date of ear emergence was uniform, within a window of four days (*Figure 4.8*A). Onset of senescence, as thermal time to 30% leaf senescence, was estimated at 47°C days earlier for functional *NAM-A1*, and 53°C days earlier for functional *NAM-B1* (*Figure 4.8*B). In 2022, as in 2021, functional *NAM-A1* and *NAM-B1* led to earlier 70% leaf senescence and higher AUC of leaf senescence (*Figure 4.8*C, D). In contrast to 2021, lines with *NAM-A1* showed a longer duration of leaf senescence by 77°C days, and *NAM-B1* allele did not impact duration of leaf senescence (*Figure 4.8*E). The longer duration in lines with *NAM-A1* occurred due to reaching 10% leaf senescence earlier.

Functional alleles of *NAM-A1* and *NAM-B1* resulted in 53°C days and 65°C days earlier 30% ear senescence, as well as earlier 70% ear senescence and increased AUC of ear senescence (*Figure 4.9*A, B, C). The duration of ear senescence did not differ between lines (*Figure 4.9*D). Double mutants lacking *NAM-A1* or *NAM-B1* had fewer senesced peduncles on 12th July (*Figure 4.9*E). It cannot be confirmed whether peduncle senescence differed between *NAM-1* single mutants and functional *NAM-1* lines from this single timepoint measurement.

Loss-of-function of *NAM-A1* increased plant height by an estimated 6.4cm, while *NAM-B1* did not affect plant height (*Figure 4.10*).

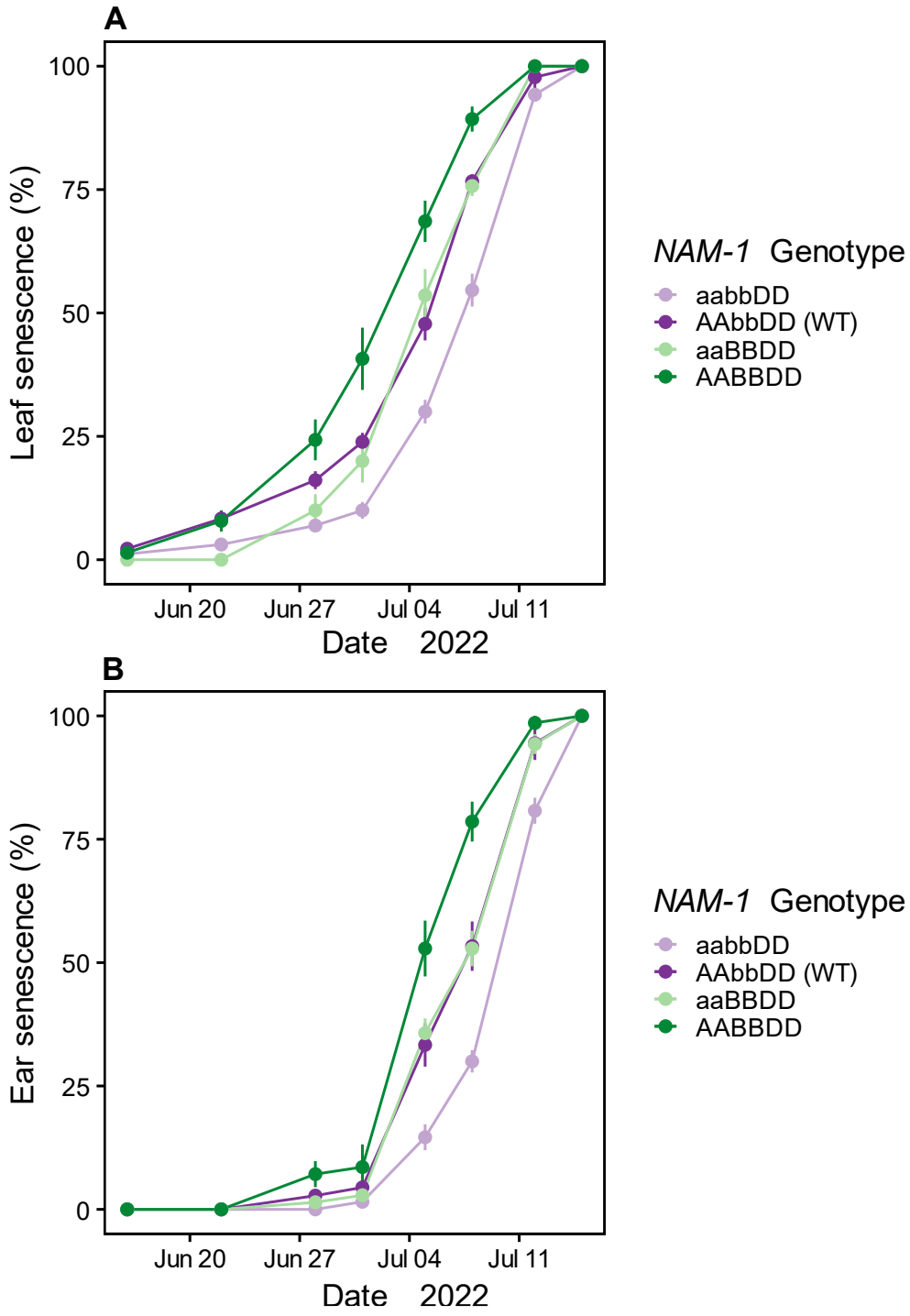
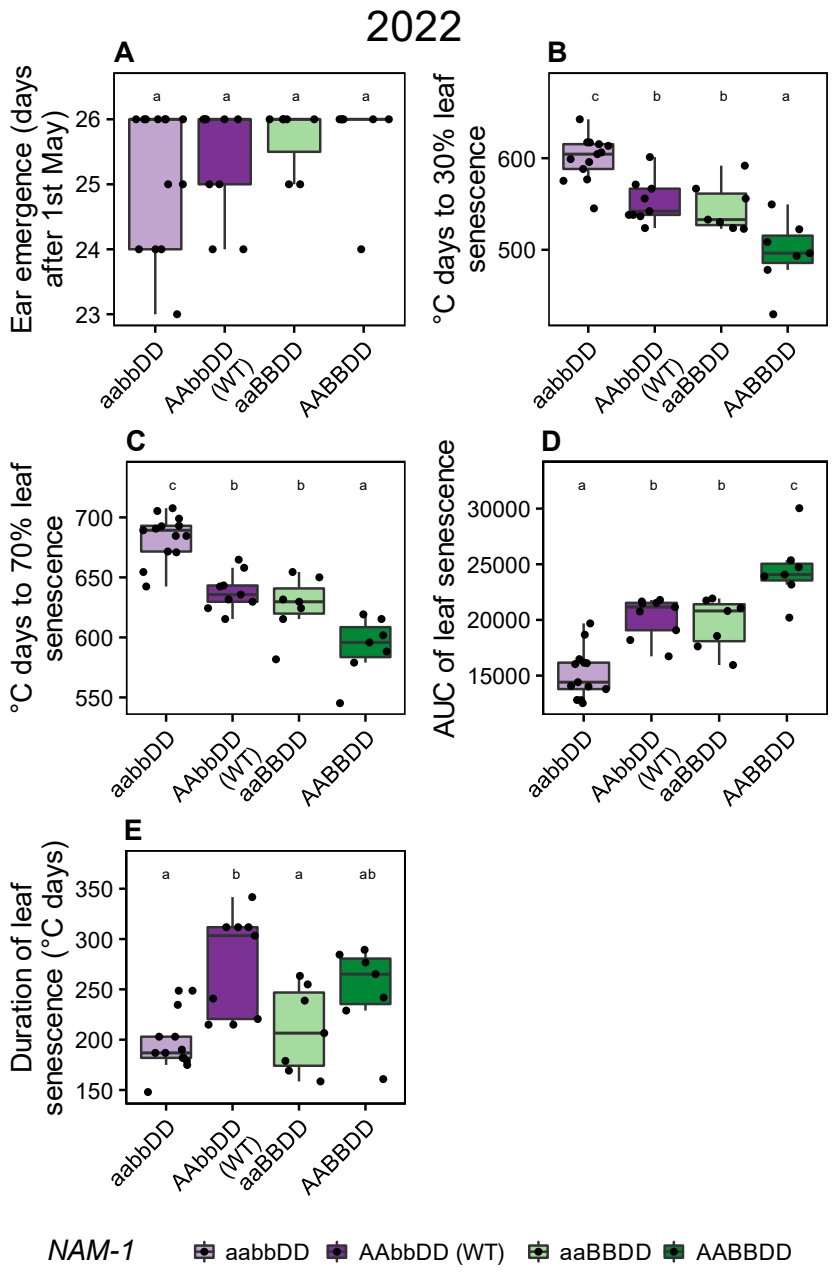


Figure 4.7 In 2022, loss-of-function of NAM-A1 and NAM-B1 delayed leaf and ear senescence. Percentage leaf and ear yellowing were scored in 6m plots weekly from 16th June and twice weekly from 28th June to 17th July. Mean + SE shown for each genotype (n = 14 – 26). Capitals functional NAM-1 alleles; lower case non-functional NAM-1 alleles. WT marks NILs with genotype matching the hexaploid cultivar background that has a non-functional allele of NAM-B1. (A) Percentage leaf senescence; (B) Percentage ear senescence.



.

*Figure 4.8 Lines with functional NAM-A1 or NAM-B1 alleles reached 30% and 70% leaf senescence earlier and NAM-A1 lines showed longer duration of leaf senescence in 2022. (A) Ear emergence in days after 1st May; (B) Thermal time to 30% leaf senescence (°C days); (C) Thermal time to 70% leaf senescence (°C days); (D) Area under curve (AUC) of leaf senescence; (E) Duration of leaf senescence (°C days). (A-E) Replicate 1 (n = 7-13). Capitals functional NAM-1 alleles; lower case non-functional NAM-1 alleles. ANOVA with post-hoc Tukey test, formula ~ NAM-A1 * NAM-B1, letters show significance groups at p<0.05.*

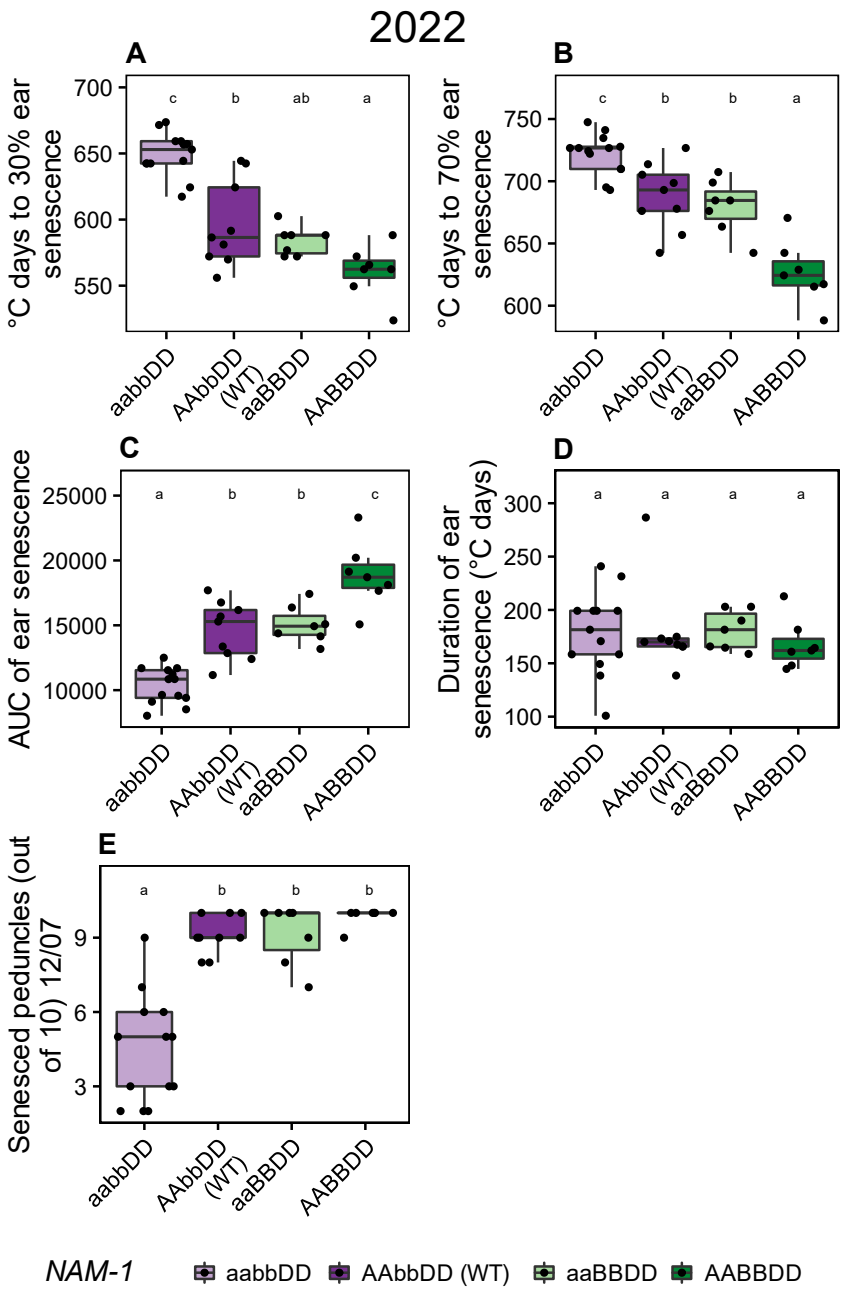


*Figure 4.9 Lines with functional NAM-A1 or NAM-B1 alleles reached 30% and 70% ear senescence earlier and double mutants showed reduced peduncle senescence in 2022. (A) Thermal time to 30% ear senescence (°C days); (B) Thermal time to 70% ear senescence (°C days); (C) Area under curve (AUC) of ear senescence; (D) Duration of ear senescence (°C days); (E) Number of yellowed peduncles out of 10 on 12th July. (A-E) Replicate 1 (n = 7-13). Capitals functional NAM-1 alleles; lower case non-functional NAM-1 alleles. ANOVA with post-hoc Tukey test, formula ~ NAM-A1 * NAM-B1, letters show significance groups at p<0.05.*

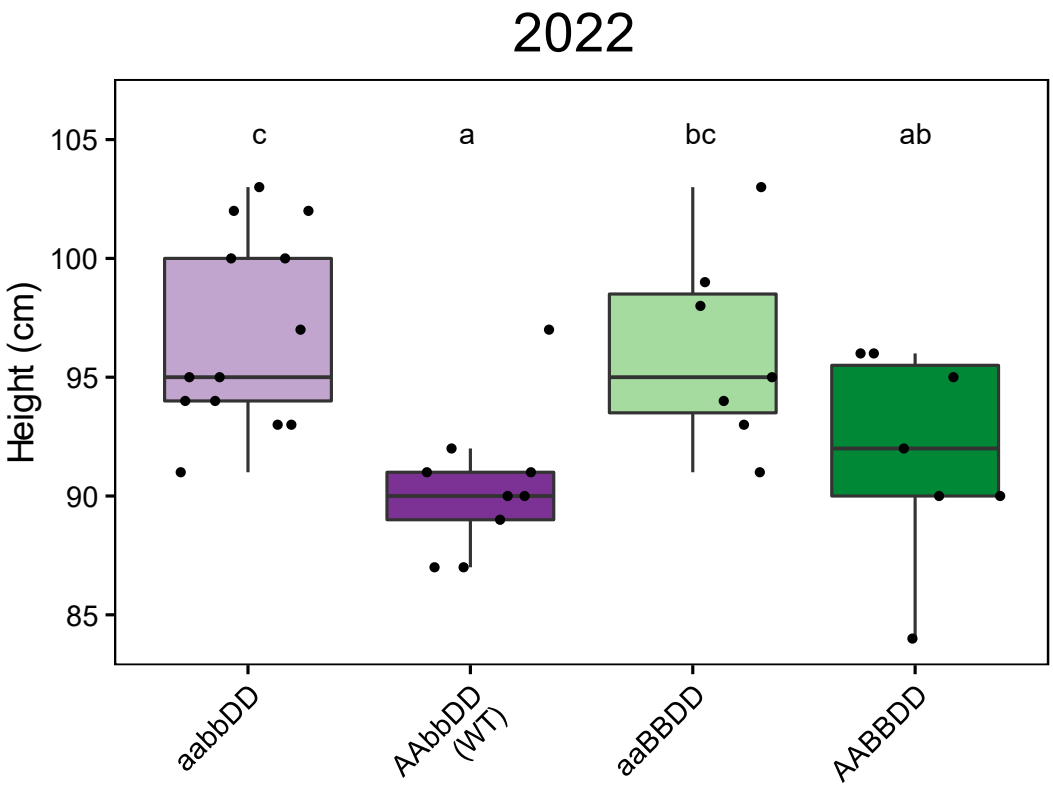


*Figure 4.10 Mutation of NAM-A1 leads to increased plant height. Plot height (cm) by genotype in 2022. Capitals functional NAM-1 alleles; lower case non-functional NAM-1 alleles. ANOVA with post-hoc Tukey test, formula ~ NAM-A1 * NAM-B1, letters show significance groups at p<0.05.*

In summary, functional alleles of *NAM-A1* and *NAM-B1* resulted in earlier leaf and ear senescence than non-functional alleles in an elite UK bread wheat background across two years (*Figure 4.4*, *Figure 4.5*, *Figure 4.8*, *Figure 4.9*). The effects of these alleles were additive, and the difference was subtly larger for *NAM-B1* than *NAM-A1*. Functional *NAM-B1* promoted increased protein content with decreased yield, while loss-of-function of *NAM-A1* decreased protein content with no effect on yield (*Figure 4.6*).

4.3.2 Genetic diversity: From genes regulating senescence to selectable markers

4.3.2.1 Natural genetic variation was identified in NAC transcription factors using Exome Capture data.

The previous section showed that a loss-of-function allele of *NAM-A1* delayed senescence and decreased GPC in an elite hexaploid wheat background. The genes *NAM-2, NAC5-1,* and *NAP-1* have also been explored as putative senescence regulators in this thesis. How could these genes be targeted in a wheat breeding context to alter senescence timing or protein content? The strategy taken here was to identify alleles of these genes already present in wheat breeding germplasm and develop markers to track these alleles. Single nucleotide polymorphisms (SNPs) and insertion-deletion sites (Indels) in homoeologs of *NAM-1*, *NAM-2*, *NAC5-A1,* and *NAP-1* were extracted from an exome capture dataset of 286 hexaploid wheat lines relevant to a breeding program (Methods 4.2.2.1). 705 variants from the exome capture panel overlapped NAC transcription factor transcripts, including single-nucleotide polymorphisms (SNPs) and short insertion/deletion alleles (Indels) (*Figure 4.11*). 499 out of 705 variants were biallelic and passed filters for read depth, missing calls, mapping quality and strand biases (*Figure 4.11*). Finally, the 99 variants called in more than one variety were selected for further analysis, as KASP markers from these variants would have a higher probability of a non-zero allele frequency (*Figure 4.11*). Of the 99 filtered variants, 23 had only homozygous calls, while 66 had at least one heterozygous call in the exome capture dataset.

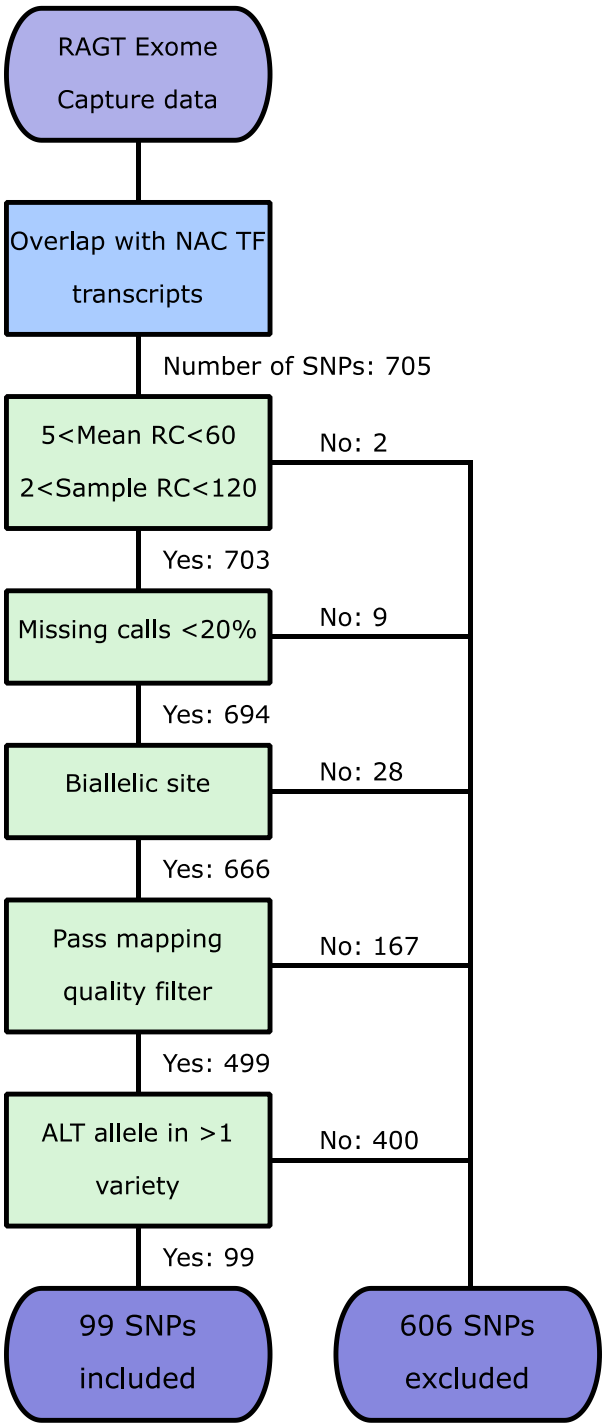


Figure 4.11 Pipeline to extract and filter single nucleotide polymorphisms (SNPs) in NAC transcription factors from RAGT Exome capture data. Of 705 SNPs, 99 SNPs passed quality filters, were biallelic, and the alternative allele was reported in more than one variety. RC = Read count, ALT = alternative allele. Purple oval: Input/Output. Blue rectangle: Process. Pale green rectangle: Decision. Scripts for this pipeline are available on Github (Evans 2023).

4.3.2.2 SNP variation in NAC transcription factors

The two previously reported polymorphisms in *NAM-A1* were found in the exome capture dataset (6A_77099397_G/A and 6A_7709609_TG/G), in addition to eight polymorphisms in the 3' UTR (Figure 4.12) (Cormier et al. 2015). The 1bp deletion allele effectively replaces 13 amino acids at the C-terminal of *NAM-A1* with a different 8 amino acids. 17 out of 18 varieties with the *NAM-A1a* haplotype (TG.G) also show a distinct allele for seven of the 3' UTR polymorphisms (Figure 4.12). The final 3' UTR SNP, 6A_77098068_A/C, is partially linked to the 1bp deletion allele, with 192 out of 197 varieties with the *NAM-A1d* haplotype (G.A) showing the C allele of this SNP (Figure 4.12). No varieties showed the haplotype *NAM-A1b* that was previously reported by Cormier et al., 2015 (G.G).

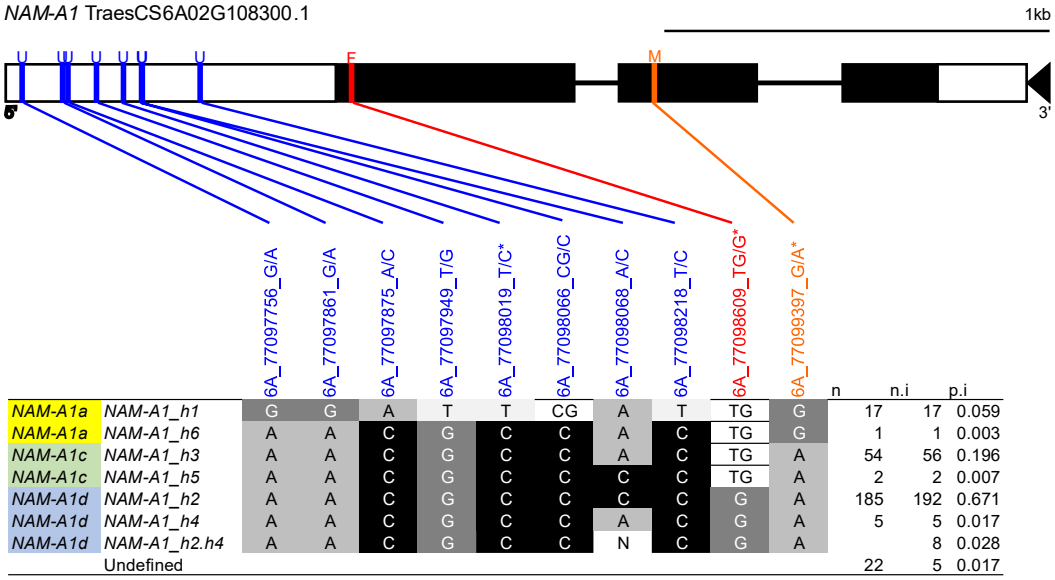


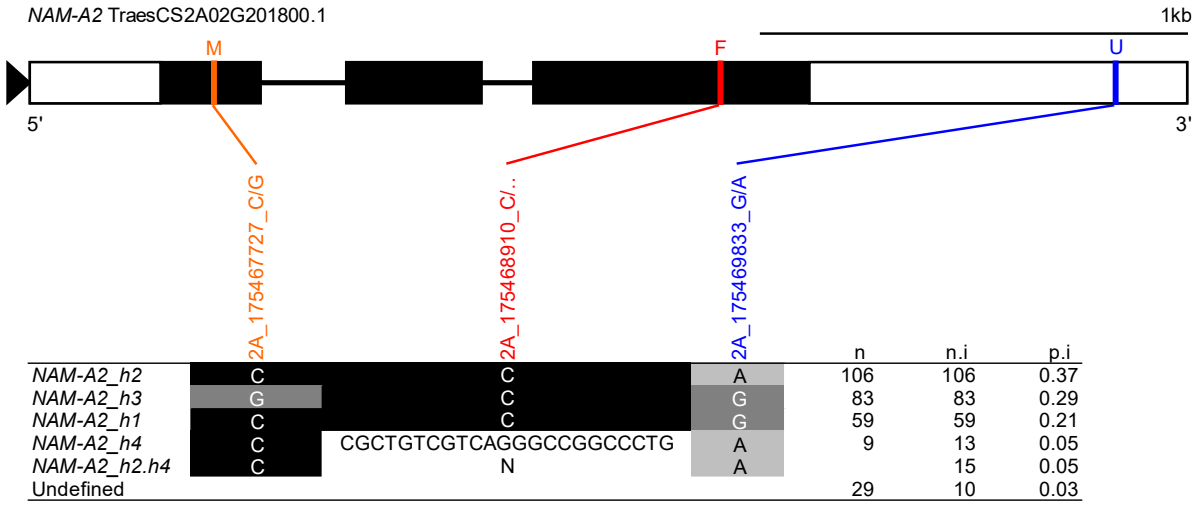
Figure 4.12 Haplotypes in NAM-A1 in exome capture dataset. Gene model for transcript TraesCS6A02G108300.1 shown with exons as black rectangles, 5' and 3' UTRs as white rectangles, introns as lines, transcription start site marked with a triangle, aligned left to right with respect to chromosome 6A. Positions of variants marked with U (UTR), I (Intron), S (Synonymous), M (Missense) or F (Frameshift).

*Haplotype table lists haplotypes in NAM-A1, with base pairs on forward strand of chromosome 6A. First column shows published haplotypes based on 6A_7709609_TG/G and 6A_77099397_G/A (Cormier et al. 2015); second column shows haplotypes based on all SNPs shown where h1 matches the reference sequence (Chinese Spring RefSeq v1.1), Table shows number of lines confirmed (n) number of lines imputed plus confirmed (n.i) and proportion of total lines with haplotypes assigned (p.i). * indicates variants with functioning KASP markers. Amino acid changes: 6A_7709609_TG/G, Q396RIPSKYPAX; 6A_77099397_G/A, A171V.*

For *NAM-A2* and *NAC5-A1*, mutations with a potential for altering protein function were discovered. In *NAM-A2*, three polymorphisms were identified: a missense mutation, a frameshift mutation, and a 3' UTR mutation (Figure 4.13). The missense mutation – proline at position 40 altered to arginine in 29% of varieties (P40R) – is interesting because senescence was delayed when the same proline was mutated to serine in tetraploid wheat (Figure 4.13) (Borrill et al. 2019). For *NAC5-A1,* 31% of varieties carried a missense variant D6H predicted to be deleterious by SIFT, outside the conserved NAC domain. For *NAC5-B1,* four SNPs with complete linkage were found in 54% of varieties. These SNPs are less likely to affect protein function, being two 3' UTR variants, one synonymous variant and one intron variant. Two other SNPs were also found.

For most of the NAC genes, polymorphism was rare. In *NAM-B2*, a total of 14 polymorphisms were identified, forming three haplotypes, with *NAM-B2_h2* found in four varieties and *NAM-B2_h3* in one variety. *NAM-B2_h2* included three missense mutations, T64A (subdomain ii of the NAC domain), A207G and G349R (C-terminal domain). In *NAM-D2*, one variety contained three UTR SNPs, one variety contained one UTR SNP, and the rest matched the reference sequence. In *NAC5-D1,* three varieties differed from the reference. Two of these contained a missense mutation S196P, however given that it is in the C-terminal domain, has a SIFT score of 0.44,

and proline is the amino acid at this position in A and B homoeologs, it is unlikely to be deleterious to protein function. In *NAP-D1,* five varieties differed from the reference sequence involving a total of 11 SNPs, and heterozygous calls across multiple SNPs were reported for three varieties. No allelic variation passed filtering for *NAM-D1, NAP-A1* or *NAP-B1.* Allelic variation was rare or non-existent in all of the D homoeologs investigated, consistent with the lower genetic diversity of the D subgenome (Pont et al. 2019).



				n	n.i	p.i
NAM-A2_h2	C	C	A	106	106	0.37
NAM-A2_h3	G	C	G	83	83	0.29
NAM-A2_h1	C	C	G	59	59	0.21
NAM-A2_h4	C	CGCTGTCGTCAGGGCCGGCCCTG	A	9	13	0.05
NAM-A2_h2.h4	C	N	A		15	0.05
Undefined				29	10	0.03

Figure 4.13 Haplotypes in NAM-A2 in exome capture dataset. Gene model for transcript TraesCS2A02G201800.1 shown with exons as black rectangles, 5' and 3' UTRs as white rectangles, introns as lines, transcription start site marked with a triangle, aligned left to right with respect to chromosome 2A. Positions of variants marked with U (UTR), I (Intron), S (Synonymous), M (Missense) or F (Frameshift). Haplotype table lists haplotypes in NAM-A2, with base pairs on forward strand of chromosome 6A. Table shows haplotypes where h1 matches the reference sequence (Chinese Spring RefSeq v1.1), number of lines confirmed (n) number of lines imputed plus confirmed (n.i) and proportion of total lines with haplotypes assigned (p.i). No NAM-A2 variants had functioning KASP markers. Amino acid changes: 2A_175467727_C/G, P40R; 2A_175468910_C/… , S330SLSSGPALX.

4.3.2.3 KASP markers were generated to genotype a subset of SNPs in NAC transcription factors

To track allelic variants in NAC transcription factors in larger panels of wheat lines, KASP markers were developed. From 99 filtered variants, 58 sets of KASP markers passing the primer criteria of Polymarker were generated (Figure 4.14). It was found that KASP markers could be generated for SNPs but not Indels using this pipeline. 26 markers were predicted to be effective using a proprietary script for marker quality control (Figure 4.14). A panel of crossing parents was genotyped using these markers.14 KASP markers from this pipeline and two published KASP markers in *NAM-A1* worked successfully (Figure 4.15) (Cormier et al. 2015).

The alternative allele of the missense SNP in *NAC5-A1* (4A_521919892_C/G) was more common in UK lines and less common in non-cultivar lines. The three markers in *NAC5-B1* each reported alternative allele frequencies of 0.68 across all crossing parents, consistent with the complete linkage of these SNPs in the exome capture data (Figure 4.15). The alternative alleles of *NAC5-B1* (4B_103055511_T/C, 4B_103054985, 4B_103054374) were more common in French lines, and less common in UK lines (Figure 4.15). Surprisingly, the SNP in *NAC5-D1* (4D_69678642_C/T) displayed a frequency of 0.55 in French lines, despite being present in only one variety from the exome capture dataset (Figure 4.15). Less surprisingly, SNPs in *NAM-B2, NAM-D2* and *NAP-D1* which were rare in exome capture data were rare or absent in the crossing parents. For SNPs where the alternative allele was not reported, it is also possible that the KASP primers did not amplify sufficiently to distinguish genotype clusters. The 3’ UTR SNP and missense SNPs in *NAM-A1* showed matching allele frequencies, consistent with their linkage in the exome capture data. *NAM-A1* will be discussed in more detail below. It should

be noted that three of the KASP markers target the same SNPs as markers in the Axiom 35K Breeders' Array, so are potentially implicitly targeted in breeding programs.

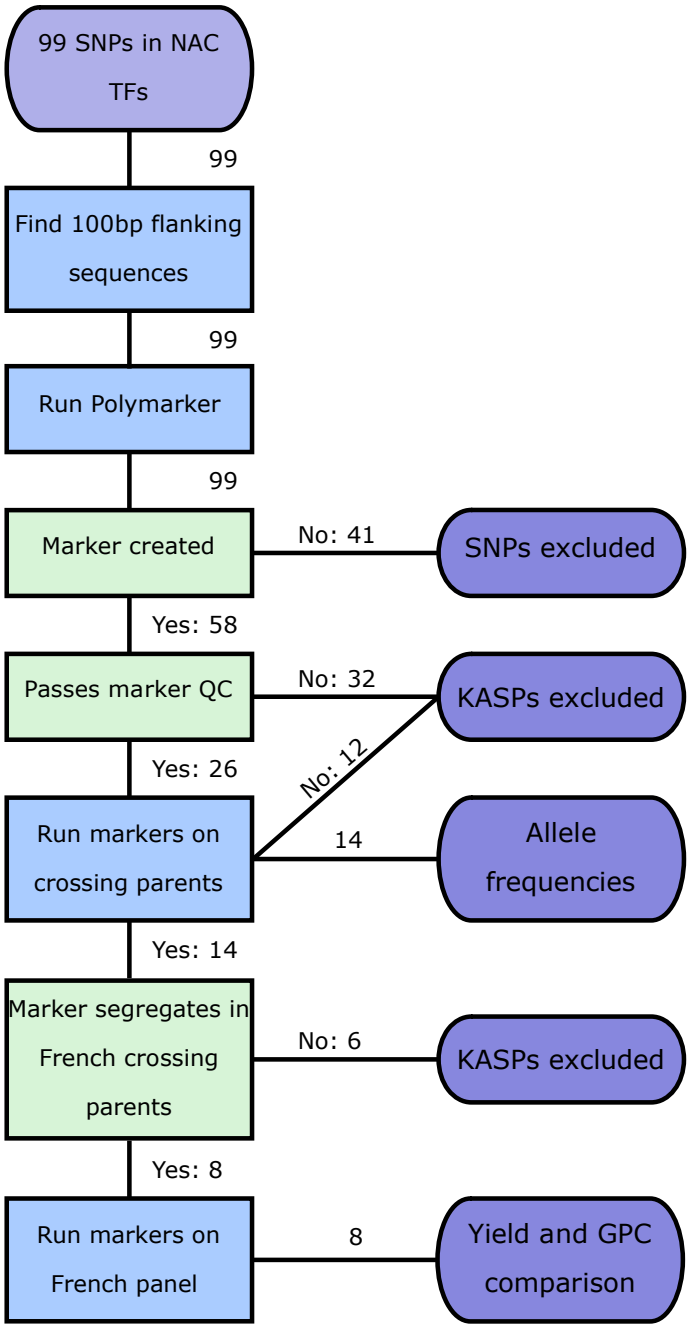


Figure 4.14 Pipeline to create and run KASP markers for SNPs in NAC TFs. KASP markers were generated using Polymarker (Ramirez-Gonzalez, Uauy,Caccamo 2015). Markers were run first on crossing parents, to determine the likely allele frequencies in each country (see Figure 4.15). Markers which had a non-zero allele frequency in French crossing parents were run on a French panel with associated phenotypic data (see Figure 4.16). Purple oval: Input/Output. Blue rectangle: Process. Pale green rectangle: Decision. QC: Quality Control. Scripts for this pipeline are available on Github (Evans 2023).

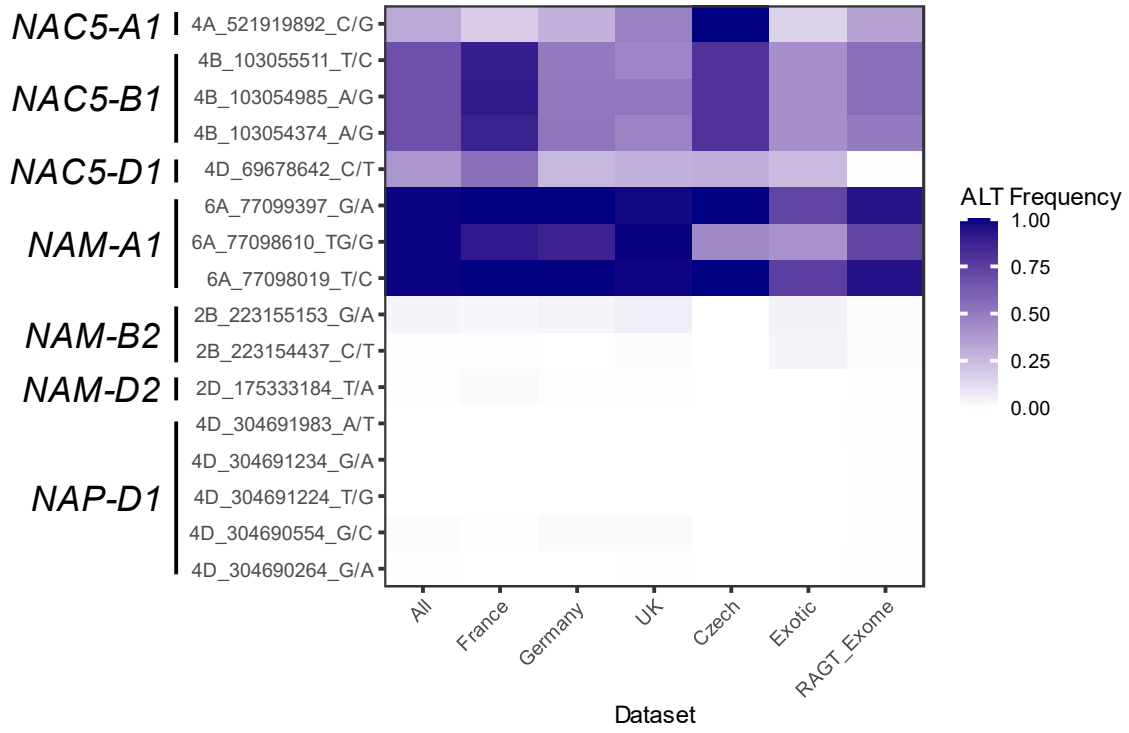


Figure 4.15 Frequencies of SNP alleles in NAC transcription factors in crossing parents. KASP markers were run on wheat crossing parents. ALT Frequency indicates the proportion of the alternative allele not found in the reference sequence (Chinese Spring RefSeq v1.1). Exotic includes germplasm not derived from cultivars. KASP marker names include chromosome, position, reference and alternative alleles.

4.3.2.4 SNP alleles of NAC transcription factors do not correlate with protein content or yield in a panel of breeding material.

To assess whether allelic variation in NAC transcription factors, known to be expressed during senescence, correlates with grain yield or protein content, eight KASP markers which had a non-zero allele frequency in French crossing parents were run on a larger panel of French wheat breeding lines (Figure 4.14). This panel was selected as yield and protein content data were available. For the markers tested, which were in *NAC5-A1, NAC5-B1, NAC5-D1* and *NAM-D2,* there were no obvious differences in yield and protein content between alleles (Figure 4.16). Two

trials from 2022 in different locations are shown; similar results were seen using data from 2021 and 2020. One marker is shown for *NAC5-B1* (4B_103055511_T/C); the two markers for linked alleles showed equivalent results (4B_103054985_A/G and 4B_103054374_A/G). Marker 2B_223155153_G/A was run for *NAM-B2,* but results are not shown as only three lines with the alternative allele were found.

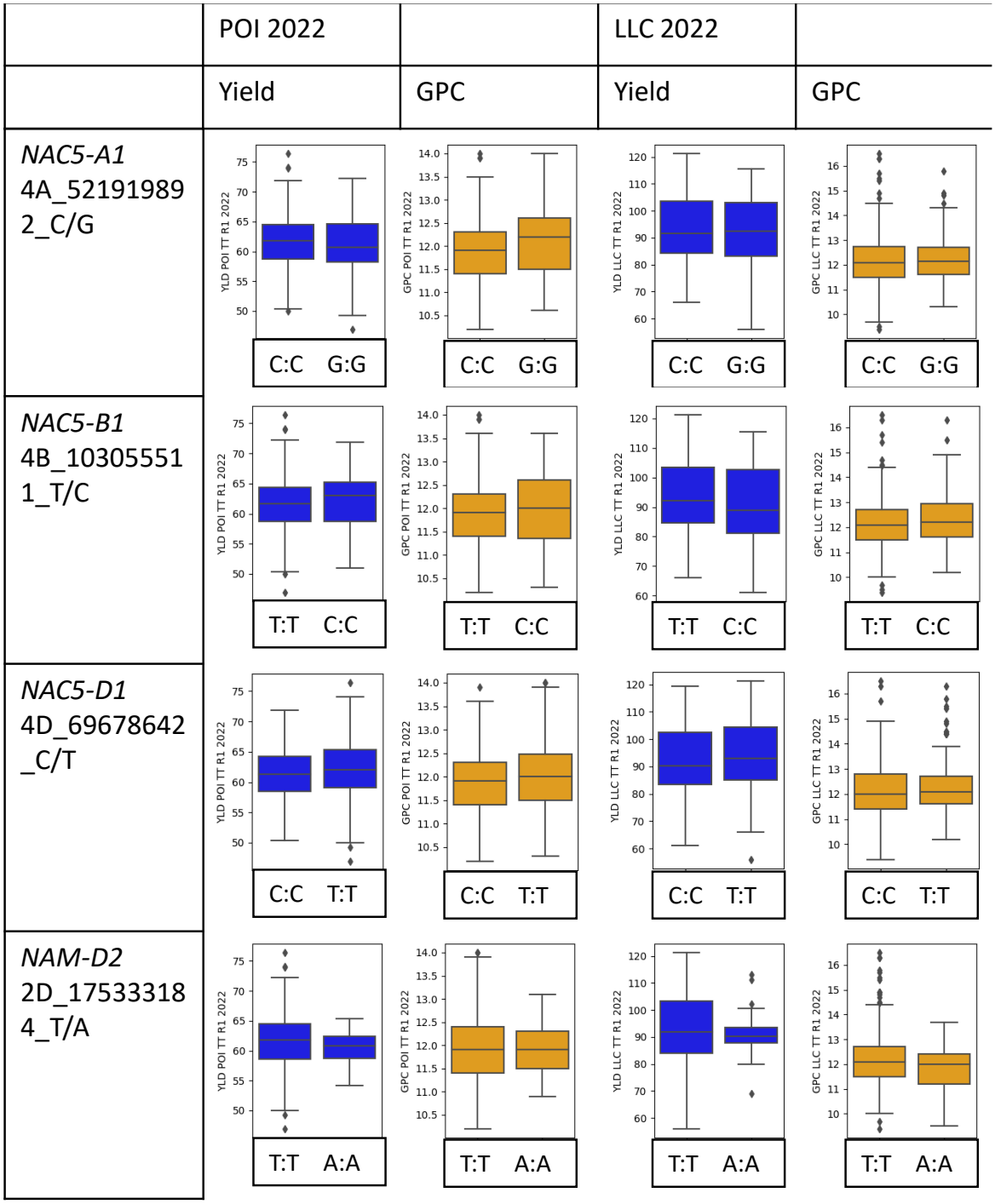


*Figure 4.16 Yield and grain protein content did not differ between alleles for tested markers in NAC5-1 and NAM-D2. "POI 2022" and "LLC 2022" represent field trials at different sites. Yield and GPC (grain protein content) are shown for each allele. Gene name and marker ID are shown on left hand side. In this figure, dots mark outliers more than 1.5 * interquartile range away from the 25% or 75% quartile.*

4.3.2.5 Further exploration of *NAM-A1* haplotypes

To further explore variation in *NAM-A1*, frequencies of published two-SNP haplotypes of *NAM-A1* were compared between datasets analysed in this chapter and published datasets. In the RAGT exome capture dataset, the most frequent haplotype was *NAM-A1d* (72%) followed by *NAM-A1c* (20%) and *NAM-A1a* (6%) with minimal missing data (2%). This distribution of haplotype frequencies is highly similar to that of a panel of European cultivars (Figure 4.17A). *NAM-A1d* was the most frequent haplotype among crossing parents from France, Germany and the UK (Figure 4.17A). The INRA and Watkins landrace core collections, which contain wider genetic diversity at the genome-wide level, show a more balanced distribution of *NAM-A1* haplotypes (Figure 4.17A). In the Watkins core collection, the most frequent haplotype was *NAM-A1c* (40%) followed by *NAM-A1d* (32%) and *NAM-A1a* (24%) (missing 4%). Consistent with this, all three haplotypes were represented in the non-cultivar crossing parents, despite the small number of accessions (Figure 4.17B). The combination *NAM-A1b* was not observed in the RAGT exome capture or Watkins datasets, supporting the hypothesis that *NAM-A1d* is the original haplotype containing the 1bp deletion allele.

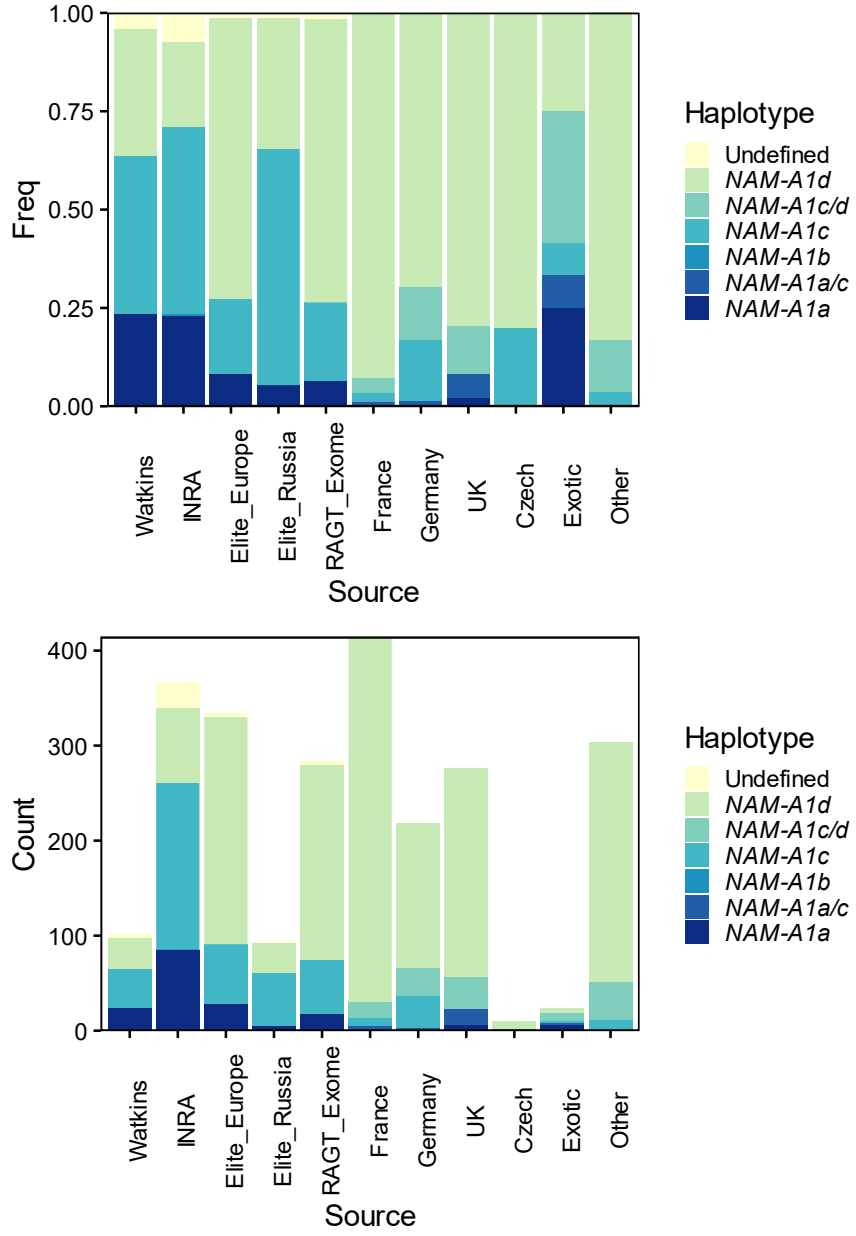


Figure 4.17 NAM-A1d is the most common haplotype in European elite wheat germplasm. (A) Frequencies and (B) counts of NAM-A1 haplotypes. "NAM-A1a/c" shows individuals that may have either a NAM-A1a or NAM-A1c haplotype. "Undefined" shows individuals with heterozygous or missing SNP calls. Hexaploid wheat (number of accessions in brackets) from Watkins core collection (102) (Gardiner et al. 2018), INRA core collection (367) and elite cultivars from Europe (334) (Cormier et al. 2015), elite cultivars from Russia (93) (Leonova et al. 2022), Exome capture data (286) (RAGT) and crossing parents (France, Germany, UK, Czech, Exotic, Other) (RAGT). Exotic includes germplasm not derived from cultivars. NB: Haplotype NAM-A1b was reported in one accession of the INRA core collection.

All three two-SNP haplotypes of *NAM-A1* are represented in the wheat pangenome (Table 4.8) (Walkowiak et al. 2020). Using this whole genome sequence data, gene-level haplotypes could also be assigned (Figure 4.12). The “C” allele of SNP 6A_77098068_A/C was not observed in pangenome varieties, which calls into question the validity of this SNP (Table 4.8, Figure 4.12). *NAM-A1_h6,* observed in one variety of RAGT exome capture, was also not found. In tetraploid wheat (AABB), *NAM-A1a (NAM-A1_h1)* was found in durum wheat and *NAM-A1c (NAM-A1_h3)* in wild emmer. This indicates that these haplotypes were inherited from tetraploid into hexaploid wheat, but it is unknown whether the 1bp deletion mutation that defines haplotype *NAM-A1d* occurred before or after the origin of hexaploid wheat. In the A genome progenitor *Triticum urartu* (AA), the two-SNP haplotype was *NAM-A1a,* however the gene-level haplotype was distinct (Table 4.8). *T. urartu* shared 3/7 3’ UTR SNP alleles with *NAM-A1_h1,* shared 4/7 3’ UTR SNP alleles with *NAM-A1_h3*, and contained four unique SNP mutations.

A QTL for days to ripening, found in UK winter wheat varieties, contained the *NAM-A1* gene, and authors speculated whether *NAM-A1* could be responsible (Shorinola et al. 2022). In this QTL region, the “T” allele of Axiom array marker AX-94490150, which is 6.5Mbp from *NAM-A1*, was associated with earlier ripening (Shorinola et al. 2022). Among sequenced genomes, the “T” allele of AX-94490150 was associated with *NAM-A1a* whilst the “C” allele was associated with *NAM-A1c* or *NAM-A1d*, with the exceptions of cv. Svevo and cv. Mattis (Table 4.8).

Table 4.8 NAM-A1 haplotypes in sequenced genomes of Triticum species containing an "A" genome. NAM-A1 genes were identified by BLASTN search of the NAM-A1 genomic sequence from RefSeq v1.1 against each genome, and BLAST hits were multiple aligned. Triticum urartu had a distinct gene-level haplotype to all accessions from RAGT exome capture. Genotypes at Axiom 35K marker AX-94490150 also identified through BLASTN. Genome sequences from [1] (Appels et al. 2018); [2] (Walkowiak et al. 2020); [3] (Maccaferri et al. 2019; Avni et al. 2017); [4] (Ling et al. 2018); [5] (10+ Consortium 2019); [6] (Avni et al. 2017).

Variety	**Species**	***NAM-A1* *haplotype* (SNP1 and SNP2)**	***NAM-A1* haplotype (full gene model)**	**AX-94490150 (reverse strand)**	**Source**
Chinese Spring	*T. aestivum ssp. aestivum*	*NAM-A1a*	*NAM-A1_h1*	T:T	[1]
Paragon	*T. aestivum ssp. aestivum*	*NAM-A1a*	*NAM-A1_h1*	T:T	[2]
Svevo.v1	*T. turgidum ssp. durum*	*NAM-A1a*	*NAM-A1_h1*	C:C	[3]
Cadenza	*T. aestivum ssp. aestivum*	*NAM-A1a*	*NAM-A1_h1*	T:T	[2]
Lancer	*T. aestivum ssp. aestivum*	*NAM-A1a*	*NAM-A1_h1*	T:T	[2]
Kariega	*T. aestivum ssp. aestivum*	*NAM-A1a*	*NAM-A1_h1*	T:T	[2]
Norin61	*T. aestivum ssp. aestivum*	*NAM-A1a*	*NAM-A1_h1*	T:T	[2]
Stanley	*T. aestivum ssp. aestivum*	*NAM-A1a*	*NAM-A1_h1*	T:T	[2]
Claire	*T. aestivum ssp. aestivum*	*NAM-A1a*	*NAM-A1_h1*	T:T	[2]

Jagger	*T. aestivum ssp. aestivum*	*NAM-A1a*	*NAM-A1_h1*	T:T	[2]
T.urartu	*T. urartu*	*NAM-A1a*	-	T:T	[4]
Arinalrfor	*T. aestivum ssp. aestivum*	*NAM-A1c*	*NAM-A1_h3*	C:C	[2]
Landmark	*T. aestivum ssp. aestivum*	*NAM-A1c*	*NAM-A1_h3*	C:C	[2]
Spelt	*T. aestivum ssp. spelta*	*NAM-A1c*	*NAM-A1_h3*	C:C	[5]
Weebill	*T. aestivum ssp. aestivum*	*NAM-A1c*	*NAM-A1_h3*	C:C	[2]
Wild emmer	*T. turgidum ssp. dicoccoides*	*NAM-A1c*	*NAM-A1_h3*	C:C	[6]
Julius	*T. aestivum ssp. aestivum*	*NAM-A1d*	*NAM-A1_h4*	C:C	[2]
Mace	*T. aestivum ssp. aestivum*	*NAM-A1d*	*NAM-A1_h4*	C:C	[2]
Mattis	*T. aestivum ssp. aestivum*	*NAM-A1d*	*NAM-A1_h4*	T:T	[2]
Renan	*T. aestivum ssp. aestivum*	*NAM-A1d*	*NAM-A1_h4*	C:C	[2]
Robigus	*T. aestivum ssp. aestivum*	*NAM-A1d*	*NAM-A1_h4*	C:C	[2]

To investigate the phenotypic effect of *NAM-A1* haplotypes, phenotypes from field trials of the Watkins core collection were categorised by *NAM-A1* haplotype. The haplotype *NAM-A1a* correlated with significantly decreased thousand kernel weight, and significantly smaller grains with reduced grain length, width and area in 2011 (Figure 4.18A, B, C, D). Accessions with *NAM-A1a* also trended towards earlier ear emergence and decreased plot grain mass in 2011 (Figure 4.18E, F). In 2010, *NAM-A1a* correlated again with earlier ear emergence, and more senesced flag leaves at a single time-point, although peduncle senescence score was not significantly different (Figure 4.18G, H, I). As senescence was scored at a single time-point, it is unclear whether there would be a difference in senescence onset relative to heading, or whether this can be fully explained by earlier heading date.

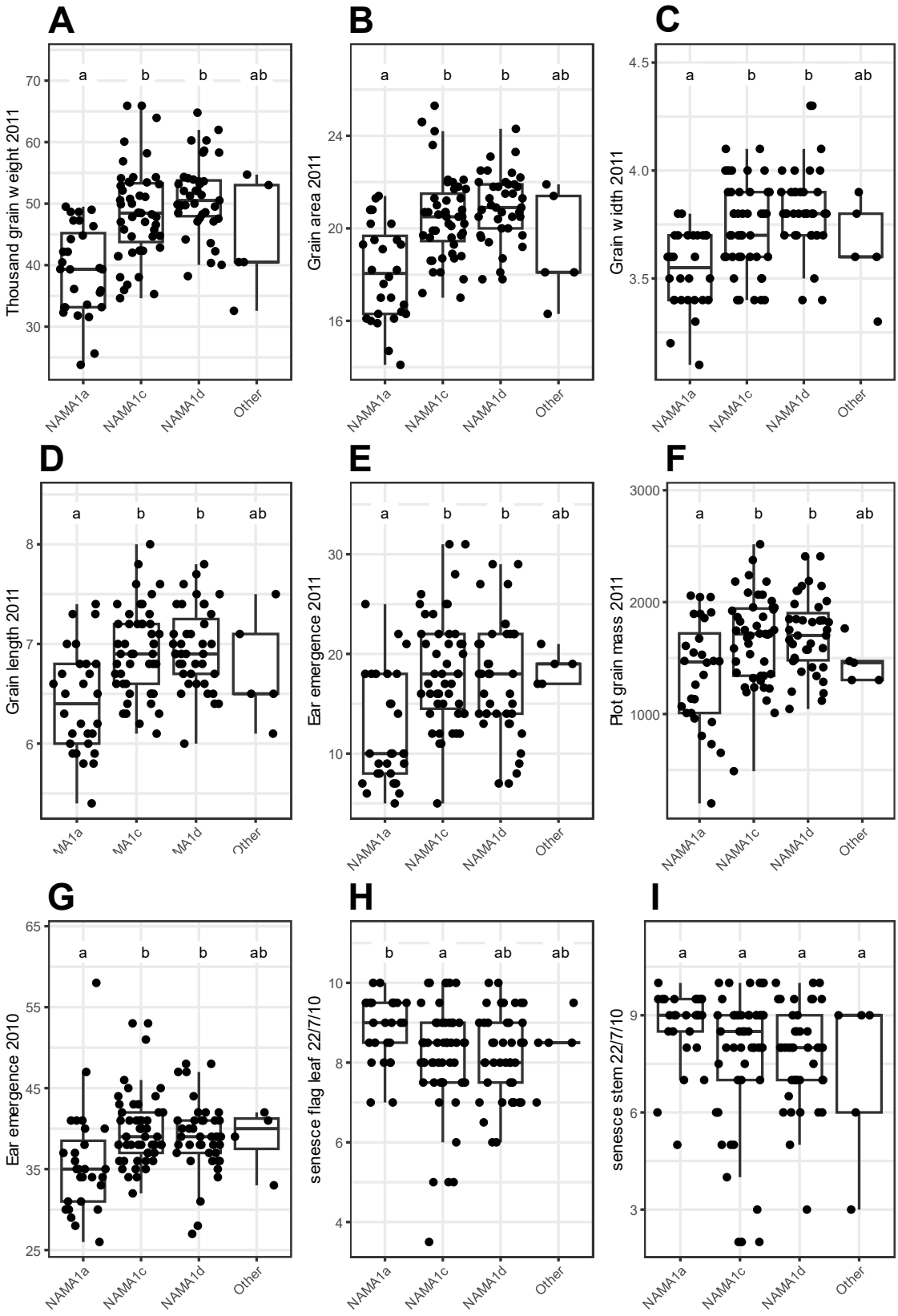

A
Thousand grain weight 2011
70
60
50
40
30
a
b
b
ab
NAMA1a
NAMA1c
NAMA1d
Other
B
Grain area 2011
24
20
16
a
b
b
ab
NAMA1a
NAMA1c
NAMA1d
Other
C
Grain width 2011
4.5
4.0
3.5
a
b
b
ab
NAMA1a
NAMA1c
NAMA1d
Other
D
Grain length 2011
8
7
6
a
b
b
ab
MA1a
MA1c
MA1d
Other
E
Ear emergence 2011
30
20
10
a
b
b
ab
NAMA1a
NAMA1c
NAMA1d
Other
F
Plot grain mass 2011
3000
2000
1000
a
b
b
ab
NAMA1a
NAMA1c
NAMA1d
Other
G
Ear emergence 2010
65
55
45
35
25
a
b
b
ab
NAMA1a
NAMA1c
NAMA1d
Other
H
senesce flag leaf 22/7/10
10
8
6
4
b
a
ab
ab
NAMA1a
NAMA1c
NAMA1d
Other
I
senesce stem 22/7/10
9
6
3
a
a
a
a
NAMA1a
NAMA1c
NAMA1d
Other

Figure 4.18 Haplotype NAM-A1a correlates with decreased thousand grain weight (TGW), earlier ear emergence and earlier senescence in the Watkins core collection. (A) Thousand grain weight (g); (B) Average grain area (mm^2); (C) Average grain length (mm); (D) Average grain width (mm); I Date of ear emergence; (F) Plot grain mass (g); (G) Date of ear emergence; (H) Flag leaf senescence on 22nd July, unknown scale; (I) Stem senescence on 22nd July, unknown scale. (A-F) 2011; (G-I) 2010. Other includes heterozygous/unknown SNP calls; no individuals carried haplotype NAM-A1b. (A-I) ANOVA with post-hoc Tukey test, formula ~ NAMA1_haplotype, letters show significance groups at p<0.05. Phenotypic data re-analysed from field trials at Church Farm, Norwich in 2010 and 2011, with permission (Designing Future Wheat 2018).

4.4 Discussion

4.4.1 *NAM-A1* and *NAM-B1* promote earlier senescence and increased protein content in UK field conditions

The first section of this chapter set out to test the hypothesis that *NAM-A1* and *NAM-B1* promote earlier senescence and increase grain protein content in a UK environment. In a UK winter wheat cultivar, the *Gpc-B1* locus with a functional copy of *NAM-B1* corresponded to earlier overall leaf and ear senescence, while mutation of *NAM-A1* corresponded to later overall leaf and ear senescence across two years of field trials. Functional *NAM-B1* was associated with increased grain protein content, while mutation of *NAM-A1* was associated with decreased grain protein content in one year. This strongly supports the hypothesis, and is consistent with studies showing that the *Gpc-B1* locus promotes earlier senescence in field trials in other environments (Brevis and Dubcovsky 2010; Carter, Santra,Kidwell 2012; Asplund et al. 2013). The increase in protein content of 0.71% (7.1 g kg^{-1}) from *Gpc-B1* was lower than the average 2% increase found in a meta-analysis, but within the range of reported values (Tabbita, Pearce,Barneix 2017; Brevis and Dubcovsky

2010). These results are also consistent with delayed senescence and reduced GPC in *nam-a1/nam-b1* mutants of tetraploid and hexaploid spring wheat in the field in Israel and USA (Pearce et al. 2014; Avni et al. 2014). Here, mutation of *NAM-A1* led to delayed senescence by 2-3 days and reduced protein content by 0.51%, a similar magnitude of effect to the 5 days delay in senescence and 1-7% reduction in GPC in hexaploid spring wheat (Avni et al. 2014). That the effect of mutation of *NAM-A1* was larger in the tetraploid wheat lines implies that in hexaploid wheat, *NAM-D1* acts with *NAM-A1* and *NAM-B1* to also regulate senescence (Pearce et al. 2014).

Homoeologous genes that perform the same function may act together additively, where each homoeolog contributes quantitatively to the phenotype; redundantly, where only loss-of-function of all three homoeologs disrupts the phenotype; or somewhere in between (Borrill, Harrington,Uauy 2019). These results provide evidence that *NAM-A1* and *NAM-B1* act additively to regulate both senescence timing and grain protein content, as the interaction terms were not significant. Homoeologs may also have balanced or divergent expression patterns (Ramírez-González et al. 2018). The difference in senescence timing and grain protein content was the same or slightly greater for *NAM-B1* than *NAM-A1*, which fits with the similar expression levels of *NAM-B1* and *NAM-A1* in *Gpc-B1* introgression lines (Uauy et al. 2006).

While *NAM-A1* and *NAM-B1* promote earlier overall senescence (measured as thermal time to 70% senescence and AUC), how do they affect the onset and duration of senescence? Functional *NAM-A1* and *NAM-B1* promoted earlier onset of both leaf and ear senescence in 2021 and 2022, measured as thermal time to 30% senescence. Conversely, the impact of *NAM-1* on duration of leaf senescence differed between years. In 2021, *nam-a1/nam-b1* double mutants showed the

longest duration of leaf senescence, due to later termination of leaf senescence; in 2022, hot temperatures could have accelerated senescence termination for all lines. In 2022, lines with functional *NAM-A1* showed the longest duration of leaf senescence, due to earlier 10% leaf senescence – this may have been missed in 2021 as some lines had already begun to senesce at the first scoring point. This indicates that both *NAM-A1* and *NAM-B1* promote earlier onset of senescence, for *NAM-B1* with no effect on rate, but for *NAM-A1* potentially counteracted by a slower rate of senescence. Overall, *NAM-1* loss-of-function lines fall most closely into "Type A" stay-green, with later senescence onset (Thomas and Howarth 2000).

4.4.2 Effect of *NAM-A1* and *NAM-B1* on yield

Functional *NAM-B1* was associated with a decrease in yield, while loss-of-function of *NAM-A1* did not affect yield in 2021. The *Gpc-B1* locus was reported to lead to decreased yield in some genotypes (Uauy, Brevis,Dubcovsky 2006) (Carter, Santra,Kidwell 2012; Mishra et al. 2015). However, yield or grain mass per plant did not differ in other studies (Kade et al. 2005; Brevis and Dubcovsky 2008; Kumar et al. 2011; Orlovskaya et al. 2022). Finally, some studies reported a decreased thousand grain weight without a significant decrease in yield (Brevis and Dubcovsky 2010; Eagles et al. 2014). The results in this chapter demonstrate that functional *NAM-B1* corresponds to decreased yield in a UK winter wheat cultivar in UK field conditions. This implies that yield is limited by the reduced duration of leaf photosynthesis in early senescing lines.

The lack of effect on yield of *NAM-A1* is curious given the similar effect that both *NAM-A1* and *NAM-B1* had on senescence and protein content. In *NAM* RNAi lines, delayed senescence did not translate to increased yield as while leaves generated additional sugars, they were not remobilized to the grain (Borrill et al. 2015). The

hypothesis that yield is limited by sink capacity in delayed senescence lines could explain why *nam-a1/nam-b1* double mutants do not have increased yield, but cannot explain why *nam-a1* single mutants have lower yield than *nam-b1* single mutants, which have highly similar senescence profiles. An alternative hypothesis is that with loss-of-function of *NAM-A1,* additional sugars generated by prolonged photosynthesis were offset by increased straw biomass, because of the observed increase in plant height. This would suggest that unlike *NAM-B1, NAM-A1* has an additional role in decreasing plant height and/or partitioning sugars towards grains rather than stems.

Finally, it is important to note that the *nam-b1* single mutant was the “wild-type” genotype, matching the elite cultivar which was the recipient variety used to develop the near-isogenic lines. Therefore, it may not be surprising that this genotype had a higher yield than *nam-a1* single mutants, despite a similar senescence profile. Elite cultivars derive from a long history of selection for yield, so are likely to already contain a combination of loci which enhance yield. The *nam-b1* single mutant NILs may retain this combination of loci, whereas it is possible that in the other NIL genotypes, recombination at chromosome 6A or 6B may have disrupted the yield-enhancing loci of the elite cultivar. The highest protein yield was also observed in wild-type (*nam-b1* single mutant) lines, which had high yield and moderate protein content. Thus, whilst the *Gpc-B1* locus could be employed to increase relative protein content in UK cultivars, *NAM-A1* and *NAM-B1* may not be useful for increasing absolute protein yield.

4.4.3 A pipeline to investigate and track allelic variation

The second section of this chapter demonstrates a pipeline to identify and track allelic variation in senescence-related NAC transcription factors. Variants were

discovered in nine out of twelve copies of *NAM-1*, *NAM-2, NAC5-1* and *NAP-1*, and KASP markers were developed for a subset of variants. By starting with an exome capture dataset of relevant breeding material, 11 out of 14 (78%) functioning KASP markers had a non-zero allele frequency in crossing parents, and 8 could be taken forward to test correlation with yield and protein. As this pipeline uses automated scripts and tools, it could be utilized to identify allelic variation and generate KASP markers for a larger number of genes of interest, and adapted to any exome capture dataset. For example, allelic variation could be identified in candidate hub transcription factors for senescence regulation (Borrill et al. 2019).

4.4.4 Variation in NAC transcription factors

Two types of informative variation were identified with this pipeline. Firstly, variants which alter the protein sequence – missense SNPs and Indels which shift the frame of translation – were identified by variant effect prediction (McLaren et al. 2016). The most common of these variants were deleterious missense mutations D6H in *NAC5-A1* and P40R in *NAM-A2.* The P40R mutation (2A_175467727_C/G) is in subdomain i of the NAC domain, responsible for dimerization (Ernst et al. 2004). It is hypothesized that this mutation would correlate with delayed leaf senescence and decreased GPC, given that a P40S mutation in *NAM-A2* delayed leaf senescence in tetraploid wheat (Borrill et al. 2019). This hypothesis could be tested by genotyping the P40R mutation in lines with available senescence or GPC data, as was carried out for other variants. The KASP marker for the P40R mutation failed marker quality control, probably due to the high GC content of the WT and MUT primers. To overcome this issue with a SNP in a GC-rich region, PCR conditions could be optimised for high GC content primers, or an alternative marker type such as CAPS could be designed. It is not surprising that few deleterious mutations were found in

these transcription factors, as across the wheat genome, transcription factors contain fewer deleterious missense mutations than non-transcription factors (Evans, Arunkumar,Borrill 2022).

Secondly, variants within each gene were connected as gene-level haplotypes. Through this, KASP markers can be used to determine a haplotype and convey additional information. For instance, a SNP in *NAM-B2,* 2B_223155153_G/A, was present in 4% of crossing parents. While this SNP is a synonymous mutation, it indicates that these lines belong to haplotype *NAM-B2_h2,* and therefore also contain three missense mutations in *NAM-B2*. These missense mutations are predicted to be tolerated by SIFT, indicating that they are in less conserved residues, but still alter the peptide sequence. In addition, promoter sequences can contain alleles that affect phenotype through altering gene expression, especially in transcription factors (Mao et al. 2020; Chen et al. 2022). A limitation of exome capture is that it does not capture promoter sequence variation, however promoter variation is likely to be in genetic linkage with coding sequence variation, so could be tracked indirectly through gene-level haplotypes. In addition, a promoter capture array has recently been developed, which would enable the technique to be extended to promoter sequences (Gardiner et al. 2019).

Variants in *NAC5-A1, NAC5-B1, NAC5-D1* and *NAM-D2* did not correlate with yield or GPC in wheat breeding lines. None of these variants altered the sequence of the NAC domain so it is possible that these variants have no effect on transcription factor function. Thus, this does not provide any evidence for or against the hypothesis that *NAC5-1* and *NAM-2* promote increased protein content through earlier senescence. It does indicate that these KASP markers may not add value to a marker-assisted selection pipeline. A more robust test of the added value of a set of

KASP markers for a trait such as GPC could be to compare the accuracy of genomic selection at predicting GPC with and without the addition of KASP genotypes to standard array data.

4.4.5 Implication of allelic variation in *NAM-A1*

What are the implications of this allelic variation in *NAM-A1*? Firstly, *NAM-A1c* and *NAM-A1d* correlated with significantly increased thousand grain weight and later senescence than *NAM-A1a* in the Watkins collection. This indicates that *NAM-A1c* and *NAM-A1d* are reduced function alleles of *NAM-A1,* as the phenotypes match those of loss-of-function of *NAM-A1* or *NAM-B1* (Distelfeld et al. 2012; Uauy, Brevis,Dubcovsky 2006). Allelic variation in the *Triticum timopheevii* ortholog *NAM-G1* was associated with varying transcript levels of *NAM-G1*, which correlated strongly with GPC (Hu et al. 2013). It would be interesting to test whether the transcript levels of *NAM-A1* and its homoeologs are decreased in *NAM-A1c* and *NAM-A1d* haplotypes. *NAM-A1d* was the most common allele of *NAM-A1* in the exome capture panel and crossing parents from a breeding program, which is likely to be the optimal allele for grain yield. For applications where early maturity or increased protein content are required, the *NAM-A1a* allele could be introduced by marker-assisted breeding using the relevant KASP markers.

The existence of a common allelic variant in *NAM-A1* also poses the question: in research involving loss-of-function mutations in *NAM-A1,* what was the “wild-type” allele? In this chapter, loss-of-function of *NAM-A1* delayed senescence in the background RGT Bowen. Previously, mutation of *NAM-A1* delayed senescence in Kronos, Express and Paragon (*Table 2.13*) (Distelfeld et al. 2012; Harrington et al. 2019b; Avni et al. 2014; Chapman et al. 2021b). The Paragon “wild-type” allele is *NAM-A1a,* and the “wild-type” allele for these other backgrounds should be verified.

Crossing a stop-codon mutation in *NAM-A1* into a *NAM-A1c* or *NAM-A1d* background would reveal whether these haplotypes lead to a loss or reduction in the ability of *NAM-A1* to promote early senescence and increased GPC.

4.4.6 Limitations of genetic variation analysis

A major caveat of genetic variation analysis is that recombination rates between wheat cultivars are relatively low, leading to the inheritance of large haplotype blocks of linked genes (Brinton et al. 2020). To better assess the allelic variation in NAC transcription factors, the haplotype analysis should be extended beyond the length of the transcript to understand the genomic context.

At the *NAM-A1* locus, six out of eight pangenome varieties carrying *NAM-A1a* share a haplotype block across chromosome 6A (Brinton et al. 2020). Mattis (*NAM-A1d*) shares most of this haplotype block apart from a 40Mbp region around *NAM-A1,* shared instead with Julius and Robigus *(NAM-A1d)* (Brinton et al. 2020). Sequenced varieties used in this study are reasonably representative of European cultivars – for instance, many UK cultivars derive from Paragon, Claire and Robigus (Shorinola et al. 2022). *NAM-A1a* was previously shown to correlate with increased protein content and reduced thousand grain weight in European cultivars, and a QTL region containing *NAM-A1* was associated with days to ripening in UK cultivars (Cormier et al. 2015; Shorinola et al. 2022). From these alone, it cannot be ruled out that the causal allele of phenotypes correlated with *NAM-A1a* in European cultivars could be another variant from a linked region of up to 40Mbp.

Therefore, the finding in this chapter that *NAM-A1a* also correlates with reduced thousand grain weight and earlier senescence in Watkins landraces is powerful because the Watkins core collection represents much wider genomic diversity than

elite cultivars (Winfield et al. 2018). In addition, Watkins landraces contain novel haplotype blocks not represented in pangenome varieties (Brinton et al. 2020). Hence, this increases the probability that the *NAM-A1a* allele, rather than a linked region, may explain the correlations with reduced thousand grain weight, earlier senescence and increased GPC.

4.4.7 Conclusion

In conclusion, the timing of senescence was successfully phenotyped and analysed in a wheat breeding context. *NAM-A1* and *NAM-B1* promote earlier onset of senescence and increased grain protein content in UK germplasm in UK field conditions, with reduction in yield for *NAM-B1* but not *NAM-A1*. Allelic variation was identified in NAC transcription factors known to be expressed during senescence, and KASP markers were generated to track these variants which would be suitable for use in marker-assisted selection. Overall, this chapter presents a proof-of-concept for applying understanding of senescence, and senescence-regulating transcription factors, to wheat improvement.

5 DISCUSSION

5.1 Summary of main findings

The main aim of this thesis was to investigate the genetic regulation of senescence timing by characterising NAC transcription factors. The key findings of this thesis are as follows: *NAC5-1* was associated with earlier onset of leaf senescence; *NAM-2* was associated with earlier onset of leaf senescence based on two out of six experiments, with no significant difference in four experiments; and *NAP-1* did not correlate with leaf senescence timing. *NAC5-1* and *NAP-1* did not affect total grain mass, while *NAM-2* was associated with decreased grain mass based on one experiment. *NAC5-1* was associated with reduced grain number and grain length. None of the three genes showed any correlation with grain protein content. To demonstrate how senescence-associated NAC transcription factors can be applied in a wheat breeding context, allelic variation was identified in NAC transcription factors in wheat breeding material. Markers were generated to track a subset of allelic variants. Tested variants in *NAC5-1, NAM-2* and *NAP-1* did not correlate with yield or protein content in breeding material, however haplotypes of *NAM-A1* correlated with kernel weight across global landraces. This thesis confirmed that *NAM-A1* and *NAM-B1* correspond to earlier leaf senescence and increased grain protein content and showed that *NAM-B1* corresponds to decreased yield in a UK cultivar in UK field conditions.

5.2 Characterisation of NAC transcription factors

5.2.1 The role of three NAC transcription factors in senescence timing

To investigate the genetic regulation of senescence timing by NAC transcription factors, *NAC5-1, NAP-1* and *NAM-2* were characterised. *NAC5-1* and *NAP-1* were novel candidate senescence regulators in wheat, while *NAM-2* had been linked with the regulation of senescence, but its role in hexaploid wheat and impact on grain protein content had not been characterised (Borrill et al. 2019).

This thesis found that *NAC5-1* was associated with earlier onset of leaf senescence based on both loss-of-function and overexpression. Evidence was mixed for *NAM-2,* as onset of leaf senescence was delayed in two out of three experiments with one mutant line, while there was no significant difference in a second mutant line. Limited evidence was found that *NAC5-1* and *NAM-2* promote peduncle senescence, as *NAC5-1* overexpression lines trended toward earlier peduncle senescence, while *NAM-2* mutant lines trended toward later peduncle senescence in one experiment. While this provides support for the hypothesis that *NAM-2* promotes earlier senescence, it indicates that *NAM-2* has a much more subtle impact than *NAM-1.* This could be explained by the lower expression of *NAM-2* than *NAM-1* homoeologs in senescence (Section 5.2.3). Senescence timing did not differ in *NAP-1* loss-of-function or overexpression lines, indicating that *NAP-1* does not regulate senescence timing.

Secondly, it was hypothesized that transcription factors promoting earlier senescence would also increase grain protein content and decrease grain mass and kernel weight. In support of this, this thesis found increased grain number and grain length in *NAC5-1* mutants with delayed senescence. In one experiment in which

mutation of *NAM-2* delayed senescence, mutant lines also trended toward increased kernel weight. No significant differences in grain protein content were observed in *NAC5-1* or *NAM-2* mutant lines, evidence against the hypothesis that delayed senescence reduces nitrogen remobilization. Allelic variation in *NAM-2* and *NAC5-1* in European wheat breeding populations did not correlate to either yield or grain protein content. This could be because none of the variants tested affected protein function, given that they did not affect the amino acid sequence of the conserved NAC subdomain.

5.2.2 Understanding of senescence regulation applied in a wheat breeding context

The final objective was to explore the potential of senescence-regulating transcription factors to improve grain protein content in a UK wheat breeding context. While *NAM-1* has been well studied, these experiments provided novel and agronomically relevant information about *NAM-1* on three counts (Tabbita, Pearce,Barneix 2017; Cormier et al. 2015; Avni et al. 2014; Uauy, Brevis,Dubcovsky 2006). Firstly, the phenotype of *Gpc-B1* introgression lines had not been reported in a UK environment. The effect of *Gpc-B1,* especially on yield, is subject to gene by genotype and gene by environment interactions, making the phenotype in a novel environment and genetic background hard to predict (Brevis and Dubcovsky 2010). This thesis demonstrated that NILs with functional alleles of *NAM-A1* and *NAM-B1* show earlier onset of leaf senescence, earlier ear senescence and increased grain protein content in a UK elite winter wheat cultivar in UK field conditions. It was concluded that *NAM-A1* and *NAM-B1* regulate leaf senescence primarily by promoting earlier onset, not by increasing the rate (decreasing the duration). This is consistent with a recent study of *NAM-A1* and *NAM-D1* mutations, confirming that all

three homoeologs of *NAM-1* promote senescence and grain protein content in UK germplasm and environment (Chapman et al. 2021b). This thesis found that *NAM-B1* decreases grain yield, while *NAM-A1* has no effect, in this environment.

Secondly, in this thesis the *Gpc-B1* introgression and a *NAM-A1* loss-of-function mutation were combined in a single segregating population. From this, it could be determined that homoeologs *NAM-A1* and *NAM-B1* act additively to regulate senescence and protein content, and that the two genes have quantitatively similar effects. This adds to the previous observation that *NAM-A1* and *NAM-D1* act additively (Avni et al. 2014).

Thirdly, it was shown that *NAM-A1c* and *NAM-A1d* haplotypes correlate with delayed leaf and peduncle senescence and increased kernel weight in the Watkins landrace core collection, compared to *NAM-A1a*. This adds to the finding that *NAM-A1d* correlates with increased yield and decreased grain protein content in cultivars compared to *NAM-A1a,* based on a more genetically diverse panel of wheat than previous studies (Cormier et al. 2015; Leonova et al. 2022; Wingen et al. 2014).

In this thesis the *NAM-A1a* haplotypes were identified in a panel of breeding material. *NAM-A1* haplotypes were not compared with yield and protein content data, as 96% of corresponding crossing parents carried the *NAM-A1d* haplotype, implying that the sample size of *NAM-A1a* and *NAM-A1c* would not be sufficient. If markers could be run on a panel segregating for *NAM-A1* haplotypes, it is predicted that *NAM-A1d* would correlate with increased yield, increased kernel weight and decreased protein content relative to *NAM-A1a.* It is unclear whether the phenotype of *NAM-A1c* would be similar to *NAM-A1d,* as seen in Watkins lines, or intermediate between *NAM-A1a* and *NAM-A1d,* as reported previously (Cormier et al. 2015).

5.2.3 Expression profiles of NAC transcription factors in leaf senescence

The expression profile from anthesis to the first visible leaf yellowing varied between the NAC transcription factors investigated. *NAM-A1* and *NAM-D1* increased in expression more rapidly in early timepoints, then *NAM-D1* expression plateaued, and *NAM-A1* expression decreased after 15 days after anthesis (DAA). *NAM-2* expression increased steadily, while *NAC5-1* and *NAP-1* expression was variable through early timepoints, then increased notably at 23DAA. *NAP-1* paralogs TraesCS2A02G101900/TraesCS2A02G102000 were upregulated late in the time-course. Homoeologs of *NAM-2, NAC5-1* and *NAP-1* shared mostly similar expression patterns, except for peaks in *NAC5-D1* and *NAP-A1* at 15DAA. *NAM-2* homoeologs each showed at least a four-fold lower transcript level than *NAM-A1*. Only *NAM-1* shares the same expression pattern through leaf senescence as its ortholog in barley, *HvNAM-1/HvNAC029* (EU908210), which was also more rapidly upregulated in the early part of senescence (Christiansen and Gregersen 2014). Early upregulation was also shown by *HvNAC030* (DQ869679)*, HvNAC005* (AK251058) and *HvNAC023* (FR821745), contrasting with the gradual or late upregulation of their wheat orthologs *NAM-2, NAP-1* and TraesCS2A02G101900/TraesCS2A02G102000 respectively (Christiansen and Gregersen 2014). *HvNAC020* (FR821742) was upregulated steadily whereas its ortholog *NAC5-1* showed late upregulation (Christiansen and Gregersen 2014). This suggests that NAC transcription factor expression in senescence varies between wheat and barley, although the expression time-course was extended to a later senescence stage in barley than in wheat, meaning that expression profiles are not fully comparable (Christiansen and Gregersen 2014; Borrill et al. 2019).

5.3 Challenges and limitations

5.3.1 Senescence is environmentally variable

A recurring theme throughout experiments in this thesis was that variability in environmental factors impacted the measurement of senescence. The progress of flag leaf yellowing was more rapid in plants under increased light intensity in the glasshouse in *NAC5-1* and *NAP-1* TILLING lines, compared to plants in lower light intensity in the same experiment, and in the higher temperatures of the 2023 *NAM-2* TILLING experiment compared to the 2022 experiment. It is recognised that light, temperature, nitrogen availability and pathogen infection impact the rate of senescence (Yang and Zhang 2006; Lim, Kim,Nam 2007; Schippers 2015). This variability increased the residual variation in statistical analyses of these experiments. In addition, it indicates that the conclusions made above about the effect of mutation and overexpression of *NAC5-1, NAP-1* and *NAM-2* apply only to the conditions in which the experiments were carried out: well-watered, fertilised glasshouse or CER conditions with plants in individual pots.

Thus, researching an environmentally variable trait (senescence) in a field-grown crop (wheat) presents an inherent dilemma. On the one hand, CER-based experiments offer the greatest opportunity to control environmental conditions, minimising the “noise” (including variability in senescence due to environment) and maximising the statistical power to find “signal” (such as effect of genotype). On the other hand, it could be argued that CER-based experiments are not physiologically relevant to agriculture. In this thesis, CER-grown plants restricted to 9cm pots grew 3-9 tillers, fewer than is typical for wheat cultivars grown in the field. For the development of wheat varieties, it is more relevant to test how wheat lines perform

under standard agronomic practice in the field. However, under field conditions variability in temperature, such as was observed in *NAM-1* NILs experiments between 2021 and 2022, and other environmental stresses, such as the unknown factor leading to some *NAM-2* TILLING lines failing to establish in the field, are inevitable.

Another limitation of these experiments is that the yellowing of flag leaf and peduncle, scored in these experiments, is only one aspect of the process of senescence. Senescence also includes biochemical changes such as declining photochemical efficiency, which can be measured as Fv/Fm, cell membrane damage, measured through ion conductivity, and catabolic enzyme activities such as peroxidase activity (Lim, Kim,Nam 2007; Ma, Balazadeh,Mueller-Roeber 2019; Sekhon et al. 2019). Widespread transcriptomic changes occur during senescence, and in *Arabidopsis,* the progress of senescence is often tracked through the expression profiles of senescence-associated genes such as SAG12 (Lim, Kim,Nam 2007). Finally, it is possible to calculate nitrogen remobilization and grain filling rate, although these typically require destructive sampling (Yang et al. 2002; Gaju et al. 2014). Measuring these facets of senescence was outside the scope of this project.

5.3.2 Challenges of TILLING lines

In both Chapter 2 and Chapter 3, TILLING lines were employed to develop mutant lines in *NAM-2, NAC5-1* and *NAP-1.* The polyploid wheat genome created additional challenges in this process. In order to develop mutant lines of *NAM-2* in hexaploid bread wheat, it was necessary to cross together three TILLING lines with mutations in *NAM-A2, NAM-B2* and *NAM-D2.* Due to practical constraints of limited growing space and crossing success rate, for both lines few triple heterozygous (AaBbDd) lines were available after the initial cross, resulting in an additional generation before

a segregating population could be generated with enough individuals to successfully obtain all eight triple homozygous genotype combinations (with a probability of 1/64). Thus, despite the use of speed breeding to accelerate the generation time, the overall time taken to develop the *NAM-2* TILLING plant material with a single backcross with sufficient seed for glasshouse phenotyping was just over two years, more than has been estimated (Watson et al. 2018; Adamski et al. 2020). Thus, additional backcrosses were outside the scope of this thesis.

At this stage, the *NAM-2* TILLING lines still contained significant background mutation load, with each individual having a unique set of background mutations. This could help to explain the inconsistency in senescence and grain traits between 2022 and 2023 experiments, despite progeny of the same parent plants used for both experiments – as well as specific issues noted in Chapter 2. As contrast, the *NAM-1* NILs showed very consistent phenotypes between 2021 and 2022 field experiments. As near-isogenic lines, these lines would be homogeneous across the genome apart from segments of chromosomes 6A and 6B surrounding the *Gpc-B1* locus and *NAM-A1* EMS mutation, as a result of multiple rounds of backcrossing to the recipient elite variety and marker-assisted selection (Tuinstra, Ejeta,Goldsbrough 1997). Both pairs of experiments – *NAM-2* TILLING lines and *NAM-1* NILs – experienced environmental variability, with higher temperatures in one of the two experiments. Therefore, it is likely that the higher genetic heterogeneity of *NAM-2* TILLING lines could explain the more inconsistent phenotypes in those experiments. *NAC5-1* and *NAP-1* TILLING lines were developed in tetraploid Kronos wheat, which reduced crossing time and enabled a second backcross, but means that the material is unsuitable for field trials in a UK climate.

The polyploid wheat genome also means that KASP genotyping primer sets need to include a homoeolog-specific primer, as well as a SNP-specific primer (Ramirez-Gonzalez, Uauy,Caccamo 2015). As *NAM-2, NAC5-1* and *NAP-1* all show >90% similarity between homoeologs, few inter-homoeologous variants were available for KASP primer design. As a result, a compromise was made on primer properties (such as length and GC content) in order to ensure homoeolog-specificity in the manually designed set of *NAM-2* TILLING primers. While non-optimal primers are tractable in the research laboratory (by adjusting PCR settings and manual cluster calling) they may not translate effectively to high-throughput, automated genotyping settings. This is demonstrated in the small proportion (14%) of natural variants in NAC transcription factors for which KASP primers could be designed automatically, and successfully used for genotyping in a wheat breeding setting.

In conclusion, there is a gap between the research materials used for investigation of novel genetic variants in wheat (such as the *NAM-2, NAC5-1* and *NAP-1* TILLING lines and associated KASP primers used in Chapter 2 and Chapter 3), and materials which are potentially suitable for the 'pre-breeding' stage at the start of wheat variety development (such as the *NAM-1* NILs used in Chapter 4). This limits the potential of exploiting, for example, *NAC5-1* TILLING lines to delay leaf senescence in the field. The 'Breeders Diversity Toolkit' project works to narrow this gap between research and breeding practice, by developing near-isogenic lines for trait-linked QTLs and TILLING mutations, documenting markers, and collating a panel of potential pre-breeding material that can be trialled under standard agronomic practices (Designing Future Wheat 2018).

5.4 Implications for regulation of senescence timing in wheat

5.4.1 Understanding the protein-yield trade-off

The characterisation of *NAC5-1* and *NAM-2* in this thesis aids in showing the connection between senescence, yield and protein content. *NAM-1* is frequently used to illustrate the concept that transcription factor regulation of leaf senescence onset alters the balance between photosynthesis and nitrogen remobilization, underpinning the genetic trade-off between yield and grain protein content (Distelfeld, Avni,Fischer 2014; Thomas and Ougham 2014). *NAC5-1* fits into this conceptual framework, as it promotes earlier leaf senescence onset while decreasing grain length. *NAM-2* also provides limited support for this, as it promotes earlier leaf senescence onset, in two out of three experiments of one mutant line, and trends towards promoting decreased thousand kernel weight in one of these two experiments. With every example like these, evidence grows that leaf senescence timing influences the genetic trade-off between yield and grain protein content in wheat as a broader principle, beyond the specific case of *NAM-1*.

5.4.2 The role of *NAM-A1* in wheat

In the experiments in this thesis, loss-of-function of *NAM-A1* did not impact grain mass or kernel weight in the field in two trial years. Across previous studies, *nam-a1/nam-b1* lines grown in the field showed increased kernel weight compared to *nam-b1* lines in one trial year and no significant difference in five trial years (Chapman et al. 2021b; Avni et al. 2014; Harrington et al. 2019b). The lack of effect of *NAM-A1* on yield despite delayed senescence is not consistent with the modulation of yield by the onset of leaf senescence. Sink limitation occurs when the

sink capacity – the maximum grain mass per grain or the maximum starch that can be assimilated into the grain – limits yield. Under sink limitation, even if a delay in senescence prolongs photosynthesis, it does not translate to increased yield or kernel weight, as observed in *NAM* RNAi lines (Borrill et al. 2015). However, *nam-a1* single mutants in this thesis showed reduced yield compared to *nam-b1* single mutants, despite a near-identical time-course of senescence, which is not consistent with sink limitation. It was observed that *nam-a1* single mutants and double mutants were taller, suggesting the hypothesis that more carbohydrates are partitioned to the stem, leaving less for the grain. It is possible that *nam-a1* mutants have increased kernel weight, offset by a negative impact on grain number. Another hypothesis is that the 'wild-type' allele of *NAM-A1* from the winter wheat cultivar is the *NAM-A1d* haplotype, the most common haplotype across European cultivars. In this scenario, the loss-of-function mutant of *NAM-A1* does not differ in kernel weight in comparison to the *NAM-A1d* haplotype, because *NAM-A1d* already confers increased kernel weight relative to *NAM-A1a*. These hypotheses could easily be tested by measuring yield components, leaf and stem sugar contents, and *NAM-A1* haplotype in these lines.

It is interesting that in these experiments, *NAM-A1* affected plant height, whilst *NAM-B1* did not. *GID2* (TraesCS3A02G511800) is among the predicted target genes of *NAM-A1,* but not of *NAM-D1* or *NAM-2* (Harrington et al. 2020). *GID2* increases plant height by promoting the degradation of DELLA proteins to relieve inhibition of growth (Gao and Chu 2020). Could *NAM-A1* decrease plant height by downregulating expression of *GID2?* It is possible, although unlikely to be a direct interaction as *NAM-A1* is a transcriptional activator (Mao et al. 2020). Plant height was not reported for other *nam-a1* mutant lines (Chapman et al. 2021b; Avni et al.

2014; Harrington et al. 2019b). Therefore, it is also possible that the increased height phenotype might result from a background mutation, as hypothesised for unexpected phenotypes encountered in *NAM-2* TILLING lines, but with genetic linkage to *NAM-A1*.

5.4.3 The role of *NAP-1* in wheat

Characterisation of *NAP-1* in wheat in this thesis indicates that *NAP-1* may have diverged in function from its orthologs in both rice and barley in the context of senescence. Overexpression of *NAP-1* had no effect on leaf senescence, whereas overexpression of orthologs *OsNAP* in rice and *HvNAC005* in barley led to premature leaf senescence (Liang et al. 2014; Christiansen et al. 2016). *NAP-1* does not influence grain protein content, whereas *OsNAP* promotes increased grain protein content (Zhou et al. 2013). Interestingly, *OsNAP* is upregulated in dark-induced senescence, whereas *HvNAC005* is not (Christiansen et al. 2016). *HvNAC005* overexpression lines also showed a severe phenotype of stunted growth and poor seed set assessed to result from expression via a strong constitutive promoter (Christiansen et al. 2016). Together this suggests that, despite sharing the same conserved C-terminal motifs, wheat, barley and rice *NAP* may have diverged somewhat in regulatory function (Christiansen et al. 2016).

What alternative function might *NAP-1* perform in wheat? Allelic variants were rare in *NAP-D1* and absent in *NAP-A1* and *NAP-B1*, meaning that correlation of allelic variation in *NAP-1* with phenotypes in breeding lines and Watkins collection could not be used to shed light on this question. *NAP-1* may retain a partially conserved function with *OsNAP* by regulating abiotic stress tolerance. *OsNAP* promotes drought and salt stress tolerance, as well as earlier senescence (Chen et al. 2014; Liang et al. 2014). *NAP-1* homoeologs contain ABA response elements in the

promoter, which would enable differential expression in response to drought and salt stress, although other genes in the *NAC-a* subclade contain similar numbers of ABA response elements (Mao et al. 2020).

NAP-1 may have a role in grain development, as *NAP-A1, NAP-B1* and *NAP-D1* are expressed in the developing wheat grain and specifically in the seed coat, in addition to expression in senescing flag leaves (Ramírez-González et al. 2018; Xiang et al. 2019; Li et al. 2013). This could fit with recent findings that *OsNAP* acts with *OsNAC24* to increase starch contents in rice endosperm by upregulating expression of starch biosynthesis enzymes (Jin et al. 2023). In rice, *osnap* mutants had subtly decreased grain starch contents and increased soluble sugar contents; it would be interesting to test soluble sugar contents in *NAP-1* mutants in wheat (Jin et al. 2023).

5.4.4 The regulatory network of senescence

It is interesting to speculate where *NAM-2* and *NAC5-1* may fit in the senescence regulatory network. On the one hand, a more marked upregulation of *NAC5-1* homoeologs occurs at 23-26DAA, whereas *NAM-2* expression increased gradually throughout early leaf senescence, suggesting that *NAC5-1* may act later in the regulatory cascade. In *Arabidopsis,* three NAC transcription factors negatively regulating senescence had the greatest impact on the regulatory network at the same timepoint that they started to increase in expression (Kim et al. 2018). On the other hand, in this thesis *NAC5-1* double mutants retained higher chlorophyll at 2-5 weeks after heading, whereas *NAM-2* triple mutants retained higher chlorophyll at 4-7 weeks after heading, suggesting that *NAC5-1* promotes chlorophyll degradation (or inhibits chlorophyll synthesis) at an earlier stage than *NAM-2*.

The regulatory interactions of *NAM-1* and *NAM-2* are beginning to be elucidated. To understand the downstream target genes of *NAM-1* and *NAM-2,* an RNA-seq time-course of *NAM* RNAi lines from 3DAA to 26DAA was carried out (Andleeb et al. 2022). Genes upregulated during leaf senescence in wild-type, but not *NAM* RNAi lines, were enriched in GO (Gene Ontology) terms relating to phytohormone signalling, nitrogen metabolism, and metabolism of other nutrients (Andleeb et al. 2022). Genes downregulated during leaf senescence in wild-type, but not *NAM* RNAi lines, were enriched in GO terms relating to housekeeping functions such as chloroplast genes and translation. Nitrate transporters, ammonia transporters, and nitrogen assimilation genes such as wheat orthologs of *Arabidopsis* asparagine synthetase (*ASN1*) and glutamate dehydrogenase (*GDH*) were upregulated in wild-type, but not *NAM* RNAi lines (Andleeb et al. 2022). A previous study also found that ion transport GO terms were enriched among differentially expressed genes in *nam-a1* mutant lines (Pearce et al. 2014). This indicates that *NAM* genes promote nitrogen remobilization by directly or indirectly upregulating the expression of genes involved in nitrogen assimilation and transport (Andleeb et al. 2022).

Downstream of *NAM-1,* transcription factors upregulated in senescence in wild-type but not *NAM* RNAi lines included orthologs of AGL8 and ANAC087, both involved in nitrogen metabolism in *Arabidopsis* (Andleeb et al. 2022). Two of these orthologs of ANAC087 are *NAC3-A1* (TraesCS2A02G101400) and *NAC3-B1* (TraesCS2B02G118500), which promote earlier leaf senescence and programmed cell death, and NAC3-A1 and NAC3-B1 proteins can bind to NAM-A1 and NAM-B1 proteins (Harrington 2019). *NAC3-A1* was also identified using a network inference approach as sharing more predicted targets with differentially expressed genes in *nam-a1* mutants than *NAM-A1* itself (Harrington et al. 2020; Pearce et al. 2014).

Thus, it is possible that *NAC3-1* is upregulated by *NAM* genes, then acts alongside *NAM-1* to promote leaf senescence (Harrington 2019). Upstream of *NAM-1, NAM-A1* expression is upregulated in early-senescing *arf15-a1* loss-of-function lines (Li et al. 2022). Two transcription factors, auxin-responsive ARF15-A1 and jasmonate-responsive MYC2, can bind to the promoter sequence of *NAM-A1* and *NAM-D1 (Li et al. 2022).* MYC2 binding activates *NAM-A1* expression, which is suppressed when ARF15-A1 is added, indicating that ARF15-A1 reduces *NAM-A1* expression by competing with MYC2 at the promoter (Li et al. 2022).

5.4.5 Genetic redundancy and NAC transcription factors

What do these results reveal about genetic redundancy in senescence regulating transcription factors in wheat? There are multiple possible definitions for genetic redundancy (Cusack et al. 2021). Redundancy can be defined at a mechanistic level as two genes which share the same function or partially overlapping functions, such as enzymes catalysing the same reaction or transcription factors regulating some of the same target genes (Cusack et al. 2021). Redundancy can be defined at a phenotypic level as two genes for which double mutants have a phenotype, whereas single mutants have either no phenotype (classic redundancy) or phenotypes less severe than that of the double mutant, even when combined (partial redundancy) (Cusack et al. 2021; Li, Woo,Guo 2018). In hexaploid wheat, homoeologous triads are likely to display a form of redundancy as the diploid ancestors of wheat diverged no more than 7 million years ago, leading to an average 97.2% sequence similarity between homoeologs (Schreiber et al. 2012; Haas, Schreiber,Mascher 2019). Either classic redundancy, or partial redundancy (described here as dosage effect) between homoeologs hides genetic variation from phenotype-based selection, as single mutant phenotypes are subtle or absent (Borrill, Harrington,Uauy 2019).

Conversely, selection can capture variation in a gene with a dominant effect, or an additive effect where the single mutant of each homoeolog shows a phenotype, and double and triple mutants are the quantitative sum of single mutant phenotypes (Borrill, Harrington,Uauy 2019).

All homoeologs of *NAM-1* have additive effects on senescence onset and grain protein content, based on the experiment in this thesis on *NAM-A1* and *NAM-B1,* as well as previous research on *NAM-A1* and *NAM-D1* (Avni et al. 2014). It follows that variation in *NAM-1* is selectable by phenotype-based techniques (Borrill, Harrington,Uauy 2019). This has already been demonstrated, as alleles of *NAM-A1, NAM-B1* and *NAM-D1* were successfully identified in genetic mapping and GWAS for leaf senescence, maturity date, and/or grain protein content (Uauy et al. 2006; Chapman et al. 2021b; Shorinola et al. 2022; Fatiukha et al. 2020; Leonova et al. 2022).

For *NAC5-1,* this thesis showed that single mutants of *NAC5-A1* and *NAC5-B1* as well as double mutants trended towards later leaf senescence onset, decreased overall leaf senescence, and increased grain length in tetraploid wheat – although only double mutants had significantly longer grains. This indicates that *NAC5-1* homoeologs do not show classic redundancy with respect to senescence timing and grain length, although it is not clear whether they have partial redundancy or an additive effect. Variation in *NAC5-A1* is selectable for the trait of seedling drought tolerance based on its discovery in a GWAS (Mao et al. 2022).

For *NAM-2,* triple mutants of cross X50 showed later senescence in two out of three experiments in this thesis. In the field, *NAM-2* X50 triple mutants reached 30% leaf senescence later than *nam-a2* single mutants with similar cover, while in the

glasshouse in 2023, *NAM-2* X50 single mutants were more similar to triple mutants for some senescence traits, and more similar to controls for others. Overall, the subtle differences in senescence, kernel weight and protein content in these mutants makes it difficult to assess whether there is phenotypic redundancy between *NAM-2* homoeologs.

As *NAM-A1* and *NAM-D1* share predicted target genes yet act additively on senescence timing, this shows that partial redundancy at the mechanistic level of transcription factor targets does not automatically produce redundancy at a phenotypic level (Harrington et al. 2020). This fits with the hypothesis that transcription factors are dosage-dependent, where changing the copy number of a transcription factor alters the balance with other components of the regulatory network, and therefore alters gene expression (Birchler et al. 2005). The dosage dependence of transcription factor triads in wheat is supported by their preferential retention after polyploidization (Evans, Arunkumar,Borrill 2022). Nevertheless, partial redundancy is widespread among senescence-regulating transcription factors in *Arabidopsis* (Li, Woo,Guo 2018). In summary, homoeologs of *NAM-1*, *NAC5-1* and *NAM-2* do not show classic redundancy with respect to senescence onset, but *NAC5-1* and *NAM-2* may show partial redundancy.

5.5 Avenues for future research

5.5.1 Testing the impact of *NAC5-1* and *NAM-2* on nitrogen remobilization

One avenue for further research is to explore whether *NAC5-1* and *NAM-2* regulate nitrogen remobilization during senescence. Given that *NAC5-1* and *NAM-2* promote earlier senescence, and genes relating to nitrogen remobilization were differentially expressed in *NAM* RNAi lines, it is hypothesised that *NAC5-1* and *NAM-2* may

promote nitrogen remobilization efficiency (Andleeb et al. 2022). Although loss-of-function of *NAC5-1* did not significantly affect grain protein content in this thesis, this was tested in a single experiment with a small sample size, in well fertilized conditions. Wheat grain protein content depends more on nitrogen remobilization under low nitrogen conditions: if *NAC5-1* and *NAM-2* promote nitrogen remobilization, loss-of-function of *NAC5-1* and *NAM-2* is expected to significantly reduce grain protein content when grown in low nitrogen (Gaju et al. 2014). Alternatively, nitrogen remobilization efficiency in *NAM-2* and *NAC5-1* TILLING lines could be analysed by measuring nitrogen content of the crop component at harvest compared to anthesis (Waters et al. 2009; Gaju et al. 2014).

5.5.2 Characterising novel candidate senescence regulators

There is still more to learn about the role of NAC transcription factors in regulating senescence timing in wheat. This research should be expanded by investigating other candidate senescence regulators, within and beyond the NAC family. For example, it would be interesting to investigate the roles of transcription factors from the CCAAT_HAP1 and RWP-RK families in wheat senescence, as they were enriched among upregulated genes during senescence (Borrill et al. 2019). Individual transcription factors could be investigated through generating TILLING mutants, overexpression or gene-edited loss-of-function, as transgenic and gene-editing technologies become more efficient in wheat (Harwood et al. 2021; Debernardi et al. 2020). In addition, the full list of candidate transcription factors could be put through the pipeline developed in this thesis to discover the allelic variation in wheat populations and generate KASP markers to compare the allelic variation with senescence phenotypes.

How can candidate senescence regulators be prioritized for further research? *NAC5-1* and *NAP-1* were selected as candidate senescence regulators based on orthology with rice genes associated with senescence and expression in flag leaves during early senescence (Borrill et al. 2019; Sperotto et al. 2009; Zhou et al. 2013). One of these two genes was shown to regulate leaf senescence timing, indicating that this is a suitable way to select candidate transcription factors. However, an orthology approach will not be sufficient to discover all transcription factors that regulate senescence timing in wheat, as it misses those which, in rice, do not regulate senescence or have not yet been researched. *NAM-2* was originally picked for characterisation based on both expression in senescing flag leaves and ranking in the top 10% for transcription factor connectivity in a network generated from the senescence time-course data (Borrill et al. 2019). Selecting candidate genes from this network again presents a suitable approach, including *NAM-2* which promotes earlier senescence in tetraploid and hexaploid wheat (at least in some experiments) and excluding *NAP-1*, which does not affect senescence (as it ranks in the bottom 50% of the network for connectivity) (Borrill et al. 2019). Again, this approach would be insufficient to discover all senescence-regulating transcription factors as *NAC5-1* is not in the network (Borrill et al. 2019). Downstream target genes of wheat transcription factors have been predicted *in silico* using a network inference approach (Harrington et al. 2020). Candidate senescence regulators could be selected from predicted downstream targets of a known senescence regulator, such as *NAM-1*, or predicted upstream regulators of senescence-specific catabolic enzymes or transporters, by exploring this *in silico* regulatory network via the online tool Knetminer (Harrington et al. 2020; Hassani-Pak et al. 2021). More than one

method will be needed to prioritise candidate senescence regulators, to work towards understanding the transcriptional regulation of leaf senescence in wheat.

5.5.3 Identifying downstream targets of senescence-regulating NACs

This research prompts the following follow-up questions: How do *NAC5-1* and *NAM-2* regulate the onset of leaf senescence? Given that these results suggest that *NAP-1* does not regulate senescence timing, what is the function of *NAP-1*? A major step toward answering these questions would be to identify the direct downstream target genes which *NAM-2, NAC5-1* and *NAP-1* differentially regulate in the context of leaf senescence. Downstream targets predicted *in silico* cannot distinguish direct versus indirect downstream targets, or the transcription-factor target interactions in a specific tissue (Harrington et al. 2020). To fulfil these criteria, an approach of combining multiple datasets could be taken, described using the example of *NAM-2*.

Direct target genes of *NAM-A2, NAM-B2* and *NAM-D2* could be identified using DAP-seq (DNA Affinity Purification sequencing), which has been successfully applied in polyploid wheat (Bartlett et al. 2017; Zhang et al. 2022). As in ChIP-seq (Chromatin Immunoprecipitation sequencing), the transcription factor protein of interest is immobilized, and genomic DNA fragments which bind to this transcription factor are preferentially retained, resulting in peaks at the transcription factor binding sites in the sequencing output (Bartlett et al. 2017). DAP-seq uses *in vitro* expression of the tagged transcription factor protein, avoiding the necessity for stable transgenic lines for ChIP-seq, which are time-consuming to generate in wheat (Bartlett et al. 2017). A major limitation of DAP-seq is that it does not capture the chromatin state of target tissues (Bartlett et al. 2017). Putative binding sites reported in DAP-seq may be blocked *in vivo* by repressive histone marks, as shown by a comparison of ChIP-seq and DAP-seq (Zhang et al. 2021b). This limitation could potentially be overcome

by filtering DAP-seq peaks based on chromatin state, using available genome-wide datasets such as histone occupancy in wheat flag leaf tissue, or DNAse hypersensitive sites in wheat seedling tissue (Li et al. 2019; Wang et al. 2021b).

Target genes differentially regulated by *NAM-2* in wheat leaf senescence could be identified by RNA-seq analysis, noting genes differentially expressed between TILLING mutant lines – developed in this thesis – and wild-type segregant controls. Flag leaf tissue from the early senescence stage should be used, perhaps from around 14DAA to coincide with the wave of transcriptional upregulation (Borrill et al. 2019). Lines with mutations in single homoeologs and in all homoeologs could both be included, to account for potential redundancy.

Overlapping DAP-seq and RNA-seq datasets would reveal a set of target genes which are both directly bound by *NAM-2 in vitro* and upregulated or downregulated by *NAM-2* in leaf senescence *in vivo.* The functions of these target genes would indicate whether *NAM-2* directly regulates nitrogen remobilization, for example by enrichment of proteases and amino acid transporters. As another example, *NAP-1* had no impact on leaf senescence timing or grain protein content, indicating that *NAP-1* does not regulate leaf senescence, and has diverged in function from its ortholog *OsNAP*. A testable hypothesis following from this is that the direct downstream targets of *NAP-1,* identified by DAP-seq, would have a smaller overlap with differentially expressed genes from a leaf senescence time-course than targets of *NAM-1, NAM-2* or *NAC5-1.* The functions enriched among direct targets of *NAP-1* would shed light on the role this gene performs in wheat. A similar approach of overlapping datasets was taken to identify target genes involved in drought tolerance for *OsNAC5* in rice roots and *NAC5-A1* in wheat seedlings (Chung et al. 2018; Mao et al. 2022).

Identifying transcription factor targets using DAP-seq would also reveal genetic redundancy at the mechanistic level. The overlap between target genes could be compared between *NAM-2* homoeologs, or between *NAM-2* and *NAM-1*, in regulating leaf senescence. In addition, the targets of *NAP-1* could be compared to those of its paralogs TraesCS2A02G101900 and TraesCS2A02G102000, previously published, to assess potential redundancy (Zhang et al. 2022).

Finally, the transcription factors which are direct downstream targets of *NAM-2* would show the position of *NAM-2* in the regulatory network of senescence. It is hypothesised that *NAM-2* will regulate the expression of many transcription factors, as it was identified as a hub gene in a predicted network of senescence regulators (Borrill et al. 2019). In *Arabidopsis,* different hub genes coordinate the senescence regulatory network at each timepoint of senescence (Kim et al. 2018). To take a step further, RNA-seq data could be collected at multiple time points, to show how the targets of *NAM-2* change over the course of senescence and pinpoint the time window in which *NAM-2* acts as a hub gene by regulating other transcription factors. This approach could potentially be explored for *NAM-1* using existing DAP-seq data for *NAM-A1* and *NAM-D1*, and RNA-seq of *NAM* RNAi lines across leaf senescence (Zhang et al. 2022; Andleeb et al. 2022). Overall, identifying target genes would not only reveal the mechanism of senescence regulation by transcription factors such as *NAM-2* and *NAC5-1,* but also advance understanding of the regulatory network of leaf senescence.

5.6 Applications for wheat breeding

5.6.1 A pipeline for applying allelic variation in wheat

A pipeline was demonstrated to investigate allelic variation using the candidate NAC transcription factors in this thesis. Variants were identified using exome capture of wheat breeding material, and KASP markers were generated to track these variants in a larger panel of related breeding lines. Variants were summarized with the effect of each variant on the protein sequence and the gene-level haplotype. This pipeline could be applied beyond senescence, to transfer other sets of candidate genes validated in the lab or selected using gene expression data to a wheat breeding context. A wide range of exome capture data is publicly available that could be used as a starting point (He et al. 2019; Pont et al. 2019; Avni et al. 2017; Gardiner et al. 2018; Singh et al. 2019).

To investigate the connection of a gene family or protein domain of interest to a particular phenotype, all genes in that family or containing that domain could be tested. To achieve this, a wheat panel with relevant phenotypic data is required. Databases with large scale phenotypic data for wheat include the IPK germplasm bank (height, flowering time, kernel weight and yellow rust resistance), the Watkins collection plus linked nested association mapping populations (height, flowering time, kernel weight, grain dimensions, awns), and the CIMMYT germplasm bank (searchable for a wide range of traits including morphology, disease resistances and quality traits) (Schulthess et al. 2022; Philipp et al. 2019; Designing Future Wheat 2018; CIMMYT 2023). Using the pipeline exemplified in this thesis, variants which affect the protein sequence could be shortlisted using the variant effect prediction output, and KASP markers generated to run on a wheat panel with phenotypic data.

The gene-level haplotype feature allows a KASP marker for a linked SNP to be identified if no KASP was returned for the target SNP. It is recommended to run the KASP markers on a small initial sample to verify marker function, as shown in this thesis. This pipeline could also be used as an aid to mapping, based on exome capture data from parental lines: the coordinates of a QTL region could be input instead of transcript coordinates to build haplotypes across the QTL region and generate KASP markers for fine mapping.

5.6.2 Wheat germplasm

A major output of this research is a set of wheat germplasm resources – transgenic overexpression lines and TILLING mutant lines – for *NAC5-1, NAP-1* and *NAM-2.* Firstly, these will be valuable for future research to further characterise these genes. Secondly, TILLING mutant lines in *NAC5-1* and *NAM-2* could be exploited to delay senescence in wheat breeding, and in the case of *NAC5-1,* increase grain length and grain number*. NAC5-1* and *NAM-2* mutations have the potential to increase kernel weight and yield, at least in some environments, through prolonged flag leaf photosynthesis. Introgression of these TILLING mutant lines into a hexaploid wheat cultivar would reduce background mutation load (Uauy, Wulff,Dubcovsky 2017). Field trials like those shown for *NAM-1* in this thesis could be carried out to assess the effect of these mutations on yield. Field trials could be carried out immediately with *NAM-2* lines in Cadenza, and after introgression for *NAC5-1* lines developed in Kronos, as demonstrated for *GW-2* (Simmonds et al. 2016).

5.6.3 Scoring senescence

Measuring the onset of senescence in a wheat breeding context has the potential to provide valuable insight into the protein-yield trade-off and identify novel genetic variation for improving wheat grain protein content. For smaller trials, the onset of

senescence could be scored using a time-course of percentage senescence, as shown in this thesis in *NAM-1* and *NAM-2* field trials. Even more simply, the date of 25% leaf senescence could be estimated as in glasshouse experiments, given that the same trends were obtained from estimates of 25% leaf senescence as from calculation of senescence onset using SPAD data. Equally, the date of 70% leaf senescence, a previously validated metric, could be used to represent overall leaf senescence timing (Chapman et al. 2021a, b). For larger trials, advances in drone imaging systems enable high-throughput phenotyping of senescence in thousands of field plots using metrics such as NDVI (Normalised Difference Vegetation Index) (Haghighattalab et al. 2016; Anderegg et al. 2020). Using this technology, the progress of wheat senescence can be measured at a larger scale and implemented at earlier stages of the breeding funnel. This could provide insights into the protein-yield trade-off for a larger number of plots than are practical to measure for protein content.

5.6.4 Applying understanding of senescence regulation to wheat improvement

Understanding the genetic regulation of senescence opens opportunities to improve the adaptation of wheat varieties to specific environments. Late-senescing lines can have increased photosynthesis – but only when the environment is optimal for continued photosynthesis. If late summer photosynthesis is severely limited by drought or short days, maintaining functional chloroplasts will have minimal effect on yield. Regions with longer growing seasons, such as the UK, may benefit from late-senescing lines, while regions with shorter growing seasons may benefit from early-senescing lines. For example, some *T. aestivum* landraces from Norway and Sweden retained the early-senescing functional *NAM-B1* allele, although it has been

lost in most cultivated bread wheat (Hagenblad et al. 2012). Secondly, the yield benefit of late-senescing lines may be outweighed in certain environments by crop loss due to lodging, or late season pathogens such as stem rust, a re-emerging challenge in the UK (Lewis et al. 2018). Allelic variation in senescence-regulating transcription factors could be harnessed to generate a spectrum of late and early senescing wheat lines, to fit the local conditions and needs of growers.

NAM-A1 haplotypes provide an example of how some of these principles and tools can be applied. The *NAM-A1a* haplotype could be useful for breadmaking wheats requiring high protein content, and for cultivation in environments where early senescence and maturity is beneficial. Conversely, the *NAM-A1d* haplotype would be appropriate for environments with longer growing seasons, where delayed senescence can translate to increased kernel weight and yield, and feed wheats where grain protein content is not a priority. It is therefore unsurprising that most European cultivars carry *NAM-A1d.* However, *NAM-A1d* might be less common in other breeding programs; specifically, it is not yet known whether the *NAM-A1d* haplotype exists in tetraploid wheats. *NAM-A1c* could provide an intermediate haplotype, with balanced yield and protein content. In these results, wheat breeding material in both an exome capture panel and crossing parents were assigned to *NAM-A1* haplotypes, providing a choice of sources which could be used for marker-assisted selection of any of these haplotypes in this breeding program.

If current emissions continue, global carbon dioxide concentrations will increase to 500-1000ppm and ground-level ozone concentrations will increase by 40-60% by 2100 (Feng, Kobayashi,Ainsworth 2008; IPCC 2014). Elevated CO_2 concentration increases yield and decreases protein content through the dilution effect (Al-Hadeethi et al. 2019). Elevated O_3 concentration decreases yield and increases

protein content, but protein yield and micronutrient contents decrease significantly as O_3 is detrimental to nutrient remobilization (Feng, Kobayashi,Ainsworth 2008; Broberg et al. 2021). What will happen when these factors are combined in our future climate? While the combined effect of high CO_2 concentration, warmer temperatures and O_3 pollution on grain protein concentration is unclear, protein yield is predicted to either remain the same or decrease under any of these factors (Jayawardena, Heckathorn,Boldt 2021; Broberg et al. 2021; Al-Hadeethi et al. 2019). Developing wheat varieties with improved nutrient remobilization is more important than ever to counteract the detrimental effects of the changing climate on grain nutritional value.

5.7 Conclusion

In conclusion, the main contribution of this thesis is that the role of three NAC transcription factors in senescence was characterised, a step closer to understanding the regulation of leaf senescence timing in wheat. Results support the model in which the onset of senescence mediates the trade-off between protein content and yield. Future work is needed to identify the downstream targets of these transcription factors and their role within the regulatory network. The allelic variation pipeline, KASP markers and TILLING lines developed in this thesis could be applied to target variation in the studied NAC transcription factors in wheat breeding. Variation in senescence-regulating transcription factors could contribute to improving the efficiency of nitrogen remobilization, increasing wheat grain protein content without additional nitrogen input.

6 References

10+ Consortium (2019) PGSBv2.0_Spelta. http://plants.ensembl.org/Triticum_spelta/Info/Annotation/#assembly. Accessed 25/08/2023

Adamski NM, Borrilr P, Brinton J, Harrington SA, Marchal C, Bentley AR, Bovill WD, Cattivelli L, Cockram J, Contreras-Moreira B, Ford B, Ghosh S, Harwood W, Hassani-Pak K, Hayta S, Hickey LT, Kanyuka K, King J, Maccaferrri M, Naamati G, Pozniak CJ, Ramirez-Gonzalez RH, Sansaloni C, Trevaskis B, Wingen LU, Wulff BBH, Uauy C (2020) A roadmap for gene functional characterisation in crops with large genomes: Lessons from polyploid wheat. Elife 9. doi:10.7554/elife.55646

AHDB (2023a) AHDB Planting and Variety Survey. https://ahdb.org.uk/cereals-oilseeds/planting-variety-survey-results. Accessed 28/08/2023

AHDB (2023b) AHDB Recommended Lists for cereals and oilseeds 2023/24.

AHDB (2023c) Wheat Growth Guide. https://ahdb.org.uk/knowledge-library/wheat-growth-guide. 2023

Aida M, Ishida T, Fukaki H, Fujisawa H, Tasaka M (1997) Genes involved in organ separation in *Arabidopsis*: an analysis of the cup-shaped cotyledon mutant. Plant Cell 9 (6):841-857. doi:10.1105/tpc.9.6.841

Akagi T, Jung K, Masuda K, Shimizu KK (2022) Polyploidy before and after domestication of crop species. Current Opinion in Plant Biology 69:102255. doi:https://doi.org/10.1016/j.pbi.2022.102255

Al-Hadeethi I, Li Y, Odhafa AKH, Al-Hadeethi H, Seneweera S, Lam SK (2019) Assessment of grain quality in terms of functional group response to elevated CO_2 , water, and nitrogen using a meta-analysis: Grain protein, zinc, and iron under future climate. Ecology and Evolution 9 (13):7425-7437. doi:10.1002/ece3.5210

Alhabbar Z, Islam S, Yang RC, Diepeveen D, Anwar M, Balotf S, Sultana N, Maddern R, She MY, Zhang JJ, Ma WJ, Juhasz A (2018) Associations of *NAM-A1* alleles with the onset of senescence and nitrogen use efficiency under Western Australian conditions. Euphytica 214 (10). doi:10.1007/s10681-018-2266-4

Anand L, Rodriguez Lopez CM (2022) ChromoMap: an R package for interactive visualization of multi-omics data and annotation of chromosomes. BMC Bioinformatics 23 (1):33. doi:10.1186/s12859-021-04556-z

Anderegg J, Yu K, Aasen H, Walter A, Liebisch F, Hund A (2020) Spectral Vegetation Indices to Track Senescence Dynamics in Diverse Wheat Germplasm. Frontiers in Plant Science 10. doi:10.3389/fpls.2019.01749

Andleeb T, Ali Z, Mahmood Z, Latif S, Quraishi UM (2022) Wheat Varietal Response to Relative SPAD Index (RSI) and Relative Normalized Difference Vegetation Index (RNDVI) under Variable Nitrogen Application and Terminal Heat Stress along with Yield Repercussion. Agronomy 12 (7):1538

Andleeb T, Knight E, Borrill P (2023) Wheat *NAM* genes regulate the majority of early monocarpic senescence transcriptional changes including nitrogen remobilization genes. G3-Genes Genomes Genetics 13 (2). doi:10.1093/g3journal/jkac275

Appels R, Eversole K, Feuillet C, Keller B, Rogers J, Stein N, Pozniak CJ, Choulet F, Distelfeld A, Poland J, Ronen G, Sharpe AG, Pozniak C, Barad O, Baruch K, Keeble-Gagnere G, Mascher M, Ben-Zvi G, Josselin AA, Himmelbach A, Balfourier F, Gutierrez-Gonzalez J, Hayden M, Koh C, Muehlbauer G, Pasam RK, Paux E, Rigault P, Tibbits J, Tiwari V, Spannagl M, Lang D, Gundlach H, Haberer G, Mayer KFX, Ormanbekova D, Prade V, Simkova H, Wicker T, Swarbreck D, Rimbert H, Felder M, Guilhot N, Kaithakottil G, Keilwagen J, Leroy P, Lux T, Twardziok S, Venturini L, Juhasz A, Abrouk M, Fischer I, Uauy C, Borrill P, Ramirez-Gonzalez RH, Arnaud D, Chalabi S, Chalhoub B, Cory A, Datla R, Davey MW, Jacobs J, Robinson SJ,

Steuernagel B, van Ex F, Wulff BBH, Benhamed M, Bendahmane A, Concia L, Latrasse D, Alaux M, Bartos J, Bellec A, Berges H, Dolezel J, Frenkel Z, Gill B, Korol A, Letellier T, Olsen OA, Singh K, Valarik M, van der Vossen E, Vautrin S, Weining S, Fahima T, Glikson V, Raats D, Cihalikova J, Toegelova H, Vrana J, Sourdille P, Darrier B, Barabaschi D, Cattivelli L, Hernandez P, Galvez S, Budak H, Jones JDG, Witek K, Yu GT, Small I, Melonek J, Zhou RN, Belova T, Kanyuka K, King R, Nilsen K, Walkowiak S, Cuthbert R, Knox R, Wiebe K, Xiang DQ, Rohde A, Golds T, Cizkova J, Akpinar BA, Biyiklioglu S, Gao LL, N'Daiye A, Kubalakova M, Safar J, Alfama F, Adam-Blondon AF, Flores R, Guerche C, Loaec M, Quesneville H, Condie J, Ens J, Maclachlan R, Tan YF, Alberti A, Aury JM, Barbe V, Couloux A, Cruaud C, Labadie K, Mangenot S, Wincker P, Kaur G, Luo MC, Sehgal S, Chhuneja P, Gupta OP, Jindal S, Kaur P, Malik P, Sharma P, Yadav B, Singh NK, Khurana J, Chaudhary C, Khurana P, Kumar V, Mahato A, Mathur S, Sevanthi A, Sharma N, Tomar RS, Holusova K, Plihal O, Clark MD, Heavens D, Kettleborough G, Wright J, Balcarkova B, Hu YQ, Salina E, Ravin N, Skryabin K, Beletsky A, Kadnikov V, Mardanov A, Nesterov M, Rakitin A, Sergeeva E, Handa H, Kanamori H, Katagiri S, Kobayashi F, Nasuda S, Tanaka T, Wu JZ, Cattonaro F, Jiumeng M, Kugler K, Pfeifer M, Sandve S, Xun X, Zhan BJ, Batley J, Bayer PE, Edwards D, Hayashi S, Tulpova Z, Visendi P, Song WN, Cui LC, Du XH, Feng KW, Nie XJ, Tong W, Wang L, IWGSC (2018) Shifting the limits in wheat research and breeding using a fully annotated reference genome. Science 361 (6403):661-+. doi:10.1126/science.aar7191

Asplund L, Bergkvist G, Leino MW, Westerbergh A, Weih M (2013) Swedish Spring Wheat Varieties with the Rare High Grain Protein Allele of *NAM-B1* Differ in Leaf Senescence and Grain Mineral Content. Plos One 8 (3). doi:10.1371/journal.pone.0059704

Asplund L, Hagenblad J, Leino MW (2010) Re-evaluating the history of the wheat domestication gene *NAM-B1* using historical plant material. Journal of Archaeological Science 37 (9):2303-2307. doi:10.1016/j.jas.2010.04.003

Avivi L High protein content in wild tetraploid *Triticum dicoccoides* Korn. In: Proceedings of the 5th International Wheat Genetics Symposium. New Delhi, India: Indian Society of Genetics and Plant Breeding (ISGPB), 1978. pp 372-380

Avni R, Nave M, Barad O, Baruch K, Twardziok SO, Gundlach H, Hale I, Mascher M, Spannagl M, Wiebe K, Jordan KW, Golan G, Deek J, Ben-Zvi B, Ben-Zvi G, Himmelbach A, MacLachlan RP, Sharpe AG, Fritz A, Ben-David R, Budak H, Fahima T, Korol A, Faris JD, Hernandez A, Mikel MA, Levy AA, Steffenson B, Maccaferri M, Tuberosa R, Cattivelli L, Faccioli P, Ceriotti A, Kashkush K, Pourkheirandish M, Komatsuda T, Eilam T, Sela H, Sharon A, Ohad N, Chamovitz DA, Mayer KFX, Stein N, Ronen G, Peleg Z, Pozniak CJ, Akhunov ED, Distelfeld A (2017) Wild emmer genome architecture and diversity elucidate wheat evolution and domestication. Science 357 (6346):93-97. doi:doi:10.1126/science.aan0032

Avni R, Zhao RR, Pearce S, Jun Y, Uauy C, Tabbita F, Fahima T, Slade A, Dubcovsky J, Distelfeld A (2014) Functional characterization of *GPC-1* genes in hexaploid wheat. Planta 239 (2):313-324. doi:10.1007/s00425-013-1977-y

Balfourier F, Roussel V, Strelchenko P, Exbrayat-Vinson F, Sourdille P, Boutet G, Koenig J, Ravel C, Mitrofanova O, Beckert M, Charmet G (2007) A worldwide bread wheat core collection arrayed in a 384-well plate. Theoretical and Applied Genetics 114 (7):1265-1275. doi:10.1007/s00122-007-0517-1

Baloglu MC, Oz MT, Oktem HA, Yucel M (2012) Expression Analysis of *TaNAC69-1* and *TtNAMB-2*, Wheat NAC Family Transcription Factor Genes Under Abiotic Stress Conditions in Durum Wheat (Triticum turgidum). Plant Molecular Biology Reporter 30 (5):1246-1252. doi:10.1007/s11105-012-0445-3

Bang SW, Choi S, Jin XJ, Jung SE, Choi JW, Seo JS, Kim JK (2022) Transcriptional activation of rice CINNAMOYL-CoA REDUCTASE 10 by *OsNAC5*, contributes to drought tolerance by modulating lignin accumulation in roots. Plant Biotechnology Journal 20 (4):736-747. doi:10.1111/pbi.13752

Bartlett A, O'Malley RC, Huang S-sC, Galli M, Nery JR, Gallavotti A, Ecker JR (2017) Mapping genome-wide transcription-factor binding sites using DAP-seq. Nature Protocols 12 (8):1659-1672. doi:10.1038/nprot.2017.055

Beltrano J, Ronco MG, Montaldi ER, Carbone A (1998) Senescence of flag leaves and ears of wheat hastened by methyl jasmonate. Journal of Plant Growth Regulation 17 (1):53-57. doi:10.1007/pl00007012

Benchling (2021). www.benchling.com

Bhattacharjee S (2005) Reactive oxygen species and oxidative burst: Roles in stress, senescence and signal transduction in plants. Current Science 89 (7):1113-1121

Biomatters (2022) Geneious version 2022.2. https://www.geneious.com

Birchler JA, Riddle NC, Auger DL, Veitia RA (2005) Dosage balance in gene regulation: biological implications. Trends in Genetics 21 (4):219-226. doi:10.1016/j.tig.2005.02.010

Boden SA, McIntosh RA, Uauy C, Krattinger SG, Dubcovsky J, Rogers WJ, Xia XC, Badaeva ED, Bentley AR, Brown-Guedira G, Caccamo M, Cattivelli L, Chhuneja P, Cockram J, Contreras-Moreira B, Dreisigacker S, Edwards D, González FG, Guzmán C, Ikeda TM, Karsai I, Nasuda S, Pozniak C, Prins R, Sen TZ, Silva P, Simkova H, Zhang Y, the Wheat I (2023) Updated guidelines for gene nomenclature in wheat. Theoretical and Applied Genetics 136 (4):72. doi:10.1007/s00122-023-04253-w

Bogard M, Allard V, Brancourt-Hulmel M, Heumez E, Machet JM, Jeuffroy MH, Gate P, Martre P, Le Gouis J (2010) Deviation from the grain protein concentration-grain yield negative relationship is highly correlated to post-anthesis N uptake in winter wheat. Journal of Experimental Botany 61 (15):4303-4312. doi:10.1093/jxb/erq238

Bogard M, Allard V, Martre P, Heumez E, Snape JW, Orford S, Griffiths S, Gaju O, Foulkes J, Le Gouis J (2013) Identifying wheat genomic regions for improving grain protein concentration independently of grain yield using multiple inter-related populations. Molecular Breeding 31 (3):587-599. doi:10.1007/s11032-012-9817-5

Bogard M, Jourdan M, Allard V, Martre P, Perretant MR, Ravel C, Heumez E, Orford S, Snape J, Griffiths S, Gaju O, Foulkes J, Le Gouis J (2011) Anthesis date mainly explained correlations between post-anthesis leaf senescence, grain yield, and grain protein concentration in a winter wheat population segregating for flowering time QTLs. Journal of Experimental Botany 62 (10):3621-3636. doi:10.1093/jxb/err061

Bokore FE, Knox RE, DePauw RM, Cuthbert RD, Valerio IP, Clarke FR, Beres BL, Ruan YF, Campbell HL (2019) Validation of the effects of the *Gpc-B1* high grain protein concentration locus from Lillian hard red spring wheat (*Triticum aestivum* L.) using locus specific markers. Euphytica 215 (1). doi:10.1007/s10681-018-2322-0

Borrill P, Adamski N, Uauy C (2015) Genomics as the key to unlocking the polyploid potential of wheat. New Phytologist 208 (4):1008-1022. doi:10.1111/nph.13533

Borrill P, Fahy B, Smith AM, Uauy C (2015) Wheat Grain Filling Is Limited by Grain Filling Capacity rather than the Duration of Flag Leaf Photosynthesis: A Case Study Using NAM RNAi Plants. Plos One 10 (8). doi:10.1371/journal.pone.0134947

Borrill P, Harrington SA, Simmonds J, Uauy C (2019) Identification of transcription factors regulating senescence in wheat through gene regulatory network modelling. Plant Physiology 180 (3):1740-1755. doi:10.1104/pp.19.00380

Borrill P, Harrington SA, Uauy C (2017) Genome-Wide Sequence and Expression Analysis of the NAC Transcription Factor Family in Polyploid Wheat. G3-Genes Genomes Genetics 7 (9):3019-3029. doi:10.1534/g3.117.043679

Borrill P, Harrington SA, Uauy C (2019) Applying the latest advances in genomics and phenomics for trait discovery in polyploid wheat. Plant Journal 97 (1):56-72. doi:10.1111/tpj.14150

Borrill P, Ramirez-Gonzalez R, Uauy C (2016) expVIP: a Customizable RNA-seq Data Analysis and Visualization Platform Plant Physiology 170 (4):2172-2186. doi:10.1104/pp.15.01667

Brevis J, Dubcovsky J Effect of the *Gpc-B1* region from *Triticum turgidum ssp. dicoccoides* on grain yield, thousand grain weight and protein yield. In: Proceedings of 11th International Wheat Genetics Symposium, Brisbane Australia, 2008. pp 24-29
Brevis JC, Dubcovsky J (2010) Effects of the Chromosome Region Including the *Gpc-B1* Locus on Wheat Grain and Protein. Crop Science 50 (1):93-104. doi:10.2135/cropsci2009.02.0057
Brevis JC, Morris CF, Manthey F, Dubcovsky J (2010) Effect of the grain protein content locus *Gpc-B1* on bread and pasta quality. Journal of Cereal Science 51 (3):357-365. doi:10.1016/j.jcs.2010.02.004
Brinton J, Ramirez-Gonzalez RH, Simmonds J, Wingen L, Orford S, Griffiths S, Haberer G, Spannagl M, Walkowiak S, Pozniak C, Uauy C, Project WG (2020) A haplotype-led approach to increase the precision of wheat breeding. Commun Biol 3 (1). doi:ARTN 71 10.1038/s42003-020-01413-2
Broberg MC, Xu YS, Feng ZZ, Pleijel H (2021) Harvest index and remobilization of 13 elements during wheat grain filling: Experiences from ozone experiments in China and Sweden. Field Crops Research 271. doi:10.1016/j.fcr.2021.108259
Buchanan-Wollaston V (1997) The molecular biology of leaf senescence. Journal of Experimental Botany 48 (307):181-199. doi:10.1093/jxb/48.2.181
Burridge AJ, Winfield MO, Wilkinson PA, Przewieslik-Allen AM, Edwards KJ, Barker GLA (2022) The Use and Limitations of Exome Capture to Detect Novel Variation in the Hexaploid Wheat Genome. Frontiers in Plant Science 13. doi:10.3389/fpls.2022.841855
Bushuk W, Briggs KG, Shebeski LH (1969) Protein quantity and quality as factors in the evaluation of bread wheats. Canadian Journal of Plant Science 49 (2):113-122. doi:10.4141/cjps69-022
Cai SG, Yu G, Chen XH, Huang YC, Jiang XG, Zhang GP, Jin XL (2013) Grain protein content variation and its association analysis in barley. Bmc Plant Biology 13. doi:Artn 35 10.1186/1471-2229-13-35
Cantrell RG, Joppa LR (1991) Genetic Analysis of Quantitative Traits in Wild Emmer (*Triticum turgidum L. var. dicoccoides*). Crop Science 31 (3):cropsci1991.0011183X003100030020x. doi:https://doi.org/10.2135/cropsci1991.0011183X003100030020x
Carter AH, Santra DK, Kidwell KK (2012) Assessment of the effects of the *Gpc-B1* allele on senescence rate, grain protein concentration and mineral content in hard red spring wheat (Triticum aestivum L.) from the Pacific Northwest Region of the USA. Plant Breeding 131 (1):62-68. doi:10.1111/j.1439-0523.2011.01900.x
Cauvain SP (2012) Breadmaking : improving quality / edited by Stanley P. Cauvain. 2nd ed. edn. Philadelphia, Pa : Woodhead Pub., Philadelphia, Pa
Chapman EA, Orford S, Lage J, Griffiths S (2021a) Capturing and Selecting Senescence Variation in Wheat. Frontiers in Plant Science 12:17. doi:10.3389/fpls.2021.638738
Chapman EA, Orford S, Lage J, Griffiths S (2021b) Delaying or delivering: identification of novel *NAM-1* alleles that delay senescence to extend wheat grain fill duration. Journal of Experimental Botany 72 (22):7710-7728. doi:10.1093/jxb/erab368
Checovich ML, Galatro A, Moriconi JI, Simontacchi M, Dubcovsky J, Santa-Maria GE (2016) The stay-green phenotype of TaNAM-RNAi wheat plants is associated with maintenance of chloroplast structure and high enzymatic antioxidant activity. Plant Physiology and Biochemistry 104:257-265. doi:10.1016/j.plaphy.2016.03.035
Chee PW, Elias EM, Anderson JA, Kianian SF (2001) Evaluation of a high grain protein QTL from *Triticum turgidum L. var. dicoccoides* in an adapted durum wheat background. Crop Science 41 (2):295-301. doi:DOI 10.2135/cropsci2001.412295x
Chen X, Wang YF, Lv B, Li J, Luo LQ, Lu SC, Zhang X, Ma H, Ming F (2014) The NAC Family Transcription Factor *OsNAP* Confers Abiotic Stress Response Through the ABA Pathway. Plant and Cell Physiology 55 (3):604-619. doi:10.1093/pcp/pct204
Chen XY, Song GQ, Zhang SJ, Li YL, Gao J, Shahidul I, Ma WJ, Li GY, Ji WQ (2017) The allelic distribution and variation analysis of the *NAM-B1* gene in Chinese wheat

cultivars. Journal of Integrative Agriculture 16 (6):1294-1303. doi:10.1016/s2095-3119(16)61459-4
Chen Y, Liu Y, Zhang J, Torrance A, Watanabe N, Adamski NM, Uauy C (2022) The *Triticum ispahanicum* elongated glume locus P2 maps to chromosome 6A and is associated with the ectopic expression of *SVP-A1*. Theoretical and Applied Genetics 135 (7):2313-2331. doi:10.1007/s00122-022-04114-y
Christiansen MW, Gregersen PL (2014) Members of the barley NAC transcription factor gene family show differential co-regulation with senescence-associated genes during senescence of flag leaves. Journal of Experimental Botany 65 (14):4009-4022. doi:10.1093/jxb/eru046
Christiansen MW, Holm PB, Gregersen PL (2011) Characterization of barley (*Hordeum vulgare* L.) NAC transcription factors suggests conserved functions compared to both monocots and dicots. BMC research notes 4 (1):302-302. doi:10.1186/1756-0500-4-302
Christiansen MW, Matthewman C, Podzimska-Sroka D, O'Shea C, Lindemose S, Mollegaard NE, Holme IB, Hebelstrup K, Skriver K, Gregersen PL (2016) Barley plants over-expressing the NAC transcription factor gene *HvNAC005* show stunting and delay in development combined with early senescence. Journal of Experimental Botany 67 (17):5259-5273. doi:10.1093/jxb/erw286
Christopher M, Paccapelo V, Kelly A, Macdonald B, Hickey L, Richard C, Verbyla A, Chenu K, Borrell A, Amin A, Christopher J (2021) QTL identified for stay-green in a multi-reference nested association mapping population of wheat exhibit context dependent expression and parent-specific alleles. Field Crops Research 270. doi:10.1016/j.fcr.2021.108181
Chung PJ, Jung H, Choi YD, Kim JK (2018) Genome-wide analyses of direct target genes of four rice NAC-domain transcription factors involved in drought tolerance. Bmc Genomics 19. doi:10.1186/s12864-017-4367-1
CIMMYT (2023) CIMMYT Wheat germplasm bank. https://wgb.cimmyt.org/gringlobal/search.
Cormier F, Throude M, Ravel C, Gouis J, Leveugle M, Lafarge S, Exbrayat F, Duranton N, Praud S (2015) Detection of *NAM-A1* Natural Variants in Bread Wheat Reveals Differences in Haplotype Distribution between a Worldwide Core Collection and European Elite Germplasm. Agronomy (Basel) 5 (2):143-151. doi:10.3390/agronomy5020143
Cusack SA, Wang P, Lotreck SG, Moore BM, Meng F, Conner JK, Krysan PJ, Lehti-Shiu MD, Shiu S-H (2021) Predictive Models of Genetic Redundancy in Arabidopsis thaliana. Molecular Biology and Evolution 38 (8):3397-3414. doi:10.1093/molbev/msab111
Danecek P, Auton A, Abecasis G, Albers CA, Banks E, DePristo MA, Handsaker RE, Lunter G, Marth GT, Sherry ST, McVean G, Durbin R, Group GPA (2011) The variant call format and VCFtools. Bioinformatics 27 (15):2156-2158. doi:10.1093/bioinformatics/btr330
Davies PJ, Gan S (2012) Towards an integrated view of monocarpic plant senescence. Russian Journal of Plant Physiology 59 (4):467-478. doi:10.1134/s102144371204005x
Debernardi JM, Tricoli DM, Ercoli MF, Hayta S, Ronald P, Palatnik JF, Dubcovsky J (2020) A GRF-GIF chimeric protein improves the regeneration efficiency of transgenic plants.(growth regulating factor-growth interacting factor). Nature biotechnology 38 (11):1274-1279. doi:10.1038/s41587-020-0703-0
Depauw R, Townley-Smith T, Humphreys G, Knox R, Clarke F, Clarke J (2005) Lillian hard red spring wheat. Canadian Journal of Plant Science 85. doi:10.4141/P04-137
Derkx AP, Orford S, Griffiths S, Foulkes MJ, Hawkesford MJ (2012) Identification of Differentially Senescing Mutants of Wheat and Impacts on Yield, Biomass and Nitrogen Partitioning. Journal of Integrative Plant Biology 54 (8):555-566. doi:10.1111/j.1744-7909.2012.01144.x

Designing Future Wheat (2018) DFW WP3 Landraces - Results and Resources. https://designingfuturewheat.org.uk/work-package-3/. Accessed 21/08/2023 2023
Distelfeld A, Avni R, Fischer AM (2014) Senescence, nutrient remobilization, and yield in wheat and barley. Journal of Experimental Botany 65 (14):3783-3798. doi:10.1093/jxb/ert477
Distelfeld A, Cakmak I, Peleg Z, Ozturk L, Yazici AM, Budak H, Saranga Y, Fahima T (2007) Multiple QTL-effects of wheat *Gpc-B1* locus on grain protein and micronutrient concentrations. Physiologia Plantarum 129 (3):635-643. doi:10.1111/j.1399-3054.2006.00841.x
Distelfeld A, Korol A, Dubcovsky J, Uauy C, Blake T, Fahima T (2008) Colinearity between the barley grain protein content (GPC) QTL on chromosome arm 6HS and the wheat *Gpc-B1* region. Molecular Breeding 22 (1):25-38. doi:10.1007/s11032-007-9153-3
Distelfeld A, Pearce SP, Avni R, Scherer B, Uauy C, Piston F, Slade A, Zhao RR, Dubcovsky J (2012) Divergent functions of orthologous NAC transcription factors in wheat and rice. Plant Molecular Biology 78 (4-5):515-524. doi:10.1007/s11103-012-9881-6
Distelfeld A, Uauy C, Fahima T, Dubcovsky J (2006) Physical map of the wheat high-grain protein content gene *Gpc-B1* and development of a high-throughput molecular marker. New Phytologist 169 (4):753-763. doi:10.1111/j.1469-8137.2005.01627.x
Doebley JF, Gaut BS, Smith BD (2006) The Molecular Genetics of Crop Domestication. Cell 127 (7):1309-1321. doi:https://doi.org/10.1016/j.cell.2006.12.006
Dubcovsky J, Dvorak J (2007) Genome plasticity a key factor in the success of polyploid wheat under domestication. Science 316 (5833):1862-1866. doi:10.1126/science.1143986
Eagles HA, McLean R, Eastwood RF, Appelbee MJ, Cane K, Martin PJ, Wallwork H (2014) High-yielding lines of wheat carrying *Gpc-B1* adapted to Mediterranean-type environments of the south and west of Australia. Crop & Pasture Science 65 (9):854-861. doi:10.1071/cp14106
El Mannai Y, Akabane K, Hiratsu K, Satoh-Nagasawa N, Wabiko H (2017) The NAC Transcription Factor Gene *OsY37 (ONAC011)* Promotes Leaf Senescence and Accelerates Heading Time in Rice. International Journal of Molecular Sciences 18 (10). doi:10.3390/ijms18102165
Ernst HA, Olsen AN, Skriver K, Larsen S, Lo Leggio L (2004) Structure of the conserved domain of *ANAC*, a member of the NAC family of transcription factors. Embo Rep 5 (3):297-303. doi:10.1038/sj.embor.7400093
Evans CEB (2023) Github: Scripts used in Catherine Evans' PhD thesis. https://github.com/Borrill-Lab/ThesisCatherineEvans.
Evans CEB, Arunkumar R, Borrill P (2022) Transcription factor retention through multiple polyploidization steps in wheat. G3 (Bethesda) 12 (8). doi:10.1093/g3journal/jkac147
FAOSTAT (2020) http://www.fao.org/faostat/en/. Accessed 01/04/20
Fatiukha A, Filler N, Lupo I, Lidzbarsky G, Klymiuk V, Korol AB, Pozniak C, Fahima T, Krugman T (2020) Grain protein content and thousand kernel weight QTLs identified in a durum x wild emmer wheat mapping population tested in five environments. Theoretical and Applied Genetics 133 (1):119-131. doi:10.1007/s00122-019-03444-8
Feng ZZ, Kobayashi K, Ainsworth EA (2008) Impact of elevated ozone concentration on growth, physiology, and yield of wheat (*Triticum aestivum L*.): a meta-analysis. Global Change Biology 14 (11):2696-2708. doi:10.1111/j.1365-2486.2008.01673.x
Fradgley NS, Gardner K, Kerton M, Swarbreck SM, Bentley AR (2022) Trade-offs in the genetic control of functional and nutritional quality traits in UK winter wheat. Heredity 128 (6):420-433. doi:10.1038/s41437-022-00503-7
Gaju O, Allard V, Martre P, Le Gouis J, Moreau D, Bogard M, Hubbart S, Foulkes MJ (2014) Nitrogen partitioning and remobilization in relation to leaf senescence, grain yield and grain nitrogen concentration in wheat cultivars. Field Crops Research 155:213-223. doi:10.1016/j.fcr.2013.09.003

Gao S, Chu C (2020) Gibberellin Metabolism and Signaling: Targets for Improving Agronomic Performance of Crops. Plant and Cell Physiology 61 (11):1902-1911. doi:10.1093/pcp/pcaa104
Gardiner LJ, Brabbs T, Akhunov A, Jordan K, Budak H, Richmond T, Singh S, Catchpole L, Akhunov E, Hall A (2019) Integrating genomic resources to present full gene and putative promoter capture probe sets for bread wheat. Gigascience 8 (4). doi:10.1093/gigascience/giz018
Gardiner LJ, Joynson R, Omony J, Rusholme-Pilcher R, Olohan L, Lang D, Bai C, Hawkesford M, Salt D, Spannagl M, Mayer KFX, Kenny J, Bevan M, Hall N, Hall A (2018) Hidden variation in polyploid wheat drives local adaptation. Genome Res 28 (9):1319-1332. doi:10.1101/gr.233551.117
Germplasm Resources Unit, John Innes Centre, (2019) SeedStor. https://www.seedstor.ac.uk/. Accessed 01/05/2019
Gong XP, Liu XY, Pan QC, Mi GH, Chen FJ, Yuan LX (2020) Combined physiological, transcriptome, and genetic analysis reveals a molecular network of nitrogen remobilization in maize. Journal of Experimental Botany 71 (16):5061-5073. doi:10.1093/jxb/eraa229
Gregersen PL, Holm PB (2007) Transcriptome analysis of senescence in the flag leaf of wheat (*Triticum aestivum* L.). Plant Biotechnology Journal 5 (1):192-206. doi:10.1111/j.1467-7652.2006.00232.x
Gregersen PL, Holm PB, Krupinska K (2008) Leaf senescence and nutrient remobilisation in barley and wheat. Plant Biology 10:37-49. doi:10.1111/j.1438-8677.2008.00114.x
Groos C, Robert N, Bervas E, Charmet G (2003) Genetic analysis of grain protein-content, grain yield and thousand-kernel weight in bread wheat. Theoretical and Applied Genetics 106 (6):1032-1040. doi:10.1007/s00122-002-1111-1
Gupta PK, Balyan HS, Chhuneja P, Jaiswal JP, Tamhankar S, Mishra VK, Bains NS, Chand R, Joshi AK, Kaur S, Kaur H, Mavi GS, Oak M, Sharma A, Srivastava P, Sohu VS, Prasad P, Agarwal P, Akhtar M, Badoni S, Chaudhary R, Gahlaut V, Gangwar RP, Gautam T, Jaiswal V, Kumar RS, Kumar S, Shamshad M, Singh A, Taygi S, Vasistha NK, Vishwakarma MK (2022) Pyramiding of genes for grain protein content, grain quality, and rust resistance in eleven Indian bread wheat cultivars: a multi-institutional effort. Molecular Breeding 42 (4). doi:10.1007/s11032-022-01277-w
Haas M, Schreiber M, Mascher M (2019) Domestication and crop evolution of wheat and barley: Genes, genomics, and future directions. Journal of Integrative Plant Biology 61 (3):204-225. doi:10.1111/jipb.12737
Hagenblad J, Asplund L, Balfourier F, Ravel C, Leino MW (2012) Strong presence of the high grain protein content allele of *NAM-B1* in Fennoscandian wheat. Theoretical and Applied Genetics 125 (8):1677-1686. doi:10.1007/s00122-012-1943-2
Haghighattalab A, González Pérez L, Mondal S, Singh D, Schinstock D, Rutkoski J, Ortiz-Monasterio I, Singh RP, Goodin D, Poland J (2016) Application of unmanned aerial systems for high throughput phenotyping of large wheat breeding nurseries. Plant Methods 12 (1):35-35. doi:10.1186/s13007-016-0134-6
Harrington SA (2019) Understanding the molecular and genetic mechanisms regulating senescence in wheat. Doctoral, University of East Anglia, https://ueaeprints.uea.ac.uk/id/eprint/74201/
Harrington SA, Backhaus AE, Singh A, Hassani-Pak K, Uauy C (2020) The Wheat GENIE3 Network Provides Biologically-Relevant Information in Polyploid Wheat. G3-Genes Genomes Genetics 10 (10):3675-3686. doi:10.1534/g3.120.401436
Harrington SA, Cobo N, Karafiatova M, Dolezel J, Borrill P, Uauy C (2019a) Identification of a Dominant Chlorosis Phenotype Through a Forward Screen of the Triticum turgidum cv. Kronos TILLING Population. Frontiers in Plant Science 10. doi:10.3389/fpls.2019.00963
Harrington SA, Overend LE, Cobo N, Borrill P, Uauy C (2019b) Conserved residues in the wheat (*Triticum aestivum*) *NAM-A1* NAC domain are required for protein binding and

when mutated lead to delayed peduncle and flag leaf senescence. Bmc Plant Biology 19 (1). doi:10.1186/s12870-019-2022-5
Harwood W, Chen Q-J, Zhang F, Yang B (2021) Editorial: New Genome Editing Tools and Resources: Enabling Gene Discovery and Functional Genomics. Frontiers in Genome Editing 3 (27). doi:10.3389/fgeed.2021.771622
Haseneyer G, Ravel C, Dardevet M, Balfourier F, Sourdille P, Charmet G, Brunel D, Sauer S, Geiger HH, Graner A, Stracke S (2008) High level of conservation between genes coding for the *GAMYB* transcription factor in barley (Hordeum vulgare L.) and bread wheat (Triticum aestivum L.) collections. Theoretical and Applied Genetics 117 (3):321-331. doi:10.1007/s00122-008-0777-4
Hassani-Pak K, Singh A, Brandizi M, Hearnshaw J, Parsons JD, Amberkar S, Phillips AL, Doonan JH, Rawlings C (2021) KnetMiner: a comprehensive approach for supporting evidence-based gene discovery and complex trait analysis across species. Plant Biotechnology Journal 19 (8):1670-1678. doi:10.1111/pbi.13583
Hayta S, Smedley MA, Demir SU, Blundell R, Hinchliffe A, Atkinson N, Harwood WA (2019) An efficient and reproducible Agrobacterium-mediated transformation method for hexaploid wheat (*Triticum aestivum* L.). Plant Methods 15 (1):121. doi:10.1186/s13007-019-0503-z
He F, Pasam R, Shi F, Kant S, Keeble-Gagnere G, Kay P, Forrest K, Fritz A, Hucl P, Wiebe K, Knox R, Cuthbert R, Pozniak C, Akhunova A, Morrell PL, Davies JP, Webb SR, Spangenberg G, Hayes B, Daetwyler H, Tibbits J, Hayden M, Akhunov E (2019) Exome sequencing highlights the role of wild-relative introgression in shaping the adaptive landscape of the wheat genome. Nature Genetics 51 (5):896-+. doi:10.1038/s41588-019-0382-2
Hollmann J, Gregersen PL, Krupinska K (2014) Identification of predominant genes involved in regulation and execution of senescence-associated nitrogen remobilization in flag leaves of field grown barley. Journal of Experimental Botany 65 (14):3963-3973. doi:10.1093/jxb/eru094
Hu XG, Wu BH, Liu DC, Wei YM, Gao SB, Zhen YL (2013) Variation and their relationship of *NAM-G1* gene and grain protein content in *Triticum timopheevii* Zhuk. Journal of Plant Physiology 170 (3):330-337. doi:10.1016/j.jplph.2012.10.009
IPCC (2014) Climate Change 2014: Synthesis Report. Contribution of Working Groups I, II and III to the Fifth Assessment Report of the Intergovernmental Panel on Climate Change [Core Writing Team, R.K. Pachauri and L.A. Meyer (eds.)]. IPCC, Geneva, Switzerland, 151 pp.
Jamar C, Loffet F, Frettinger P, Ramsay L, Fauconnier M-L, du Jardin P (2010) *NAM-1* gene polymorphism and grain protein content in Hordeum. Journal of Plant Physiology 167 (6):497-501. doi:https://doi.org/10.1016/j.jplph.2009.10.014
Jayawardena DM, Heckathorn SA, Boldt JK (2021) A meta-analysis of the combined effects of elevated carbon dioxide and chronic warming on plant %N, protein content and N-uptake rate. AoB PLANTS 13 (4). doi:10.1093/aobpla/plab031
Jeong JS, Kim YS, Redillas M, Jang G, Jung H, Bang SW, Choi YD, Ha SH, Reuzeau C, Kim JK (2013) *OsNAC5* overexpression enlarges root diameter in rice plants leading to enhanced drought tolerance and increased grain yield in the field. Plant Biotechnology Journal 11 (1):101-114. doi:10.1111/pbi.12011
Jiang DG, Zhou LY, Chen WT, Ye NH, Xia JX, Zhuang CX (2019) Overexpression of a microRNA-targeted NAC transcription factor improves drought and salt tolerance in Rice via ABA-mediated pathways. Rice 12 (1). doi:10.1186/s12284-019-0334-6
Jin SK, Xu LN, Leng YJ, Zhang MQ, Yang QQ, Wang SL, Jia SW, Song T, Wang RA, Tao T, Liu QQ, Cai XL, Gao JP (2023) The OsNAC24-OsNAP protein complex activates OsGBSSI and OsSBEI expression to fine-tune starch biosynthesis in rice endosperm. Plant Biotechnology Journal. doi:10.1111/pbi.14124
Joppa LR, Du CH, Hart GE, Hareland GA (1997) Mapping gene(s) for grain protein in tetraploid wheat (*Triticum turgidum* L.) using a population of recombinant inbred

chromosome lines. Crop Science 37 (5):1586-1589. doi:10.2135/cropsci1997.0011183X003700050030x
Jordan KW, Wang S, Lun Y, Gardiner L-J, MacLachlan R, Hucl P, Wiebe K, Wong D, Forrest KL, Sharpe AG, Sidebottom CHD, Hall N, Toomajian C, Close T, Dubcovsky J, Akhunova A, Talbert L, Bansal UK, Bariana HS, Hayden MJ, Pozniak C, Jeddeloh JA, Hall A, Akhunov E, Consortium I (2015) A haplotype map of allohexaploid wheat reveals distinct patterns of selection on homoeologous genomes. Genome Biology 16 (1):48. doi:10.1186/s13059-015-0606-4
Joshi AK, Kumari M, Singh VP, Reddy CM, Kumar S, Rane J, Chand R (2007) Stay green trait: variation, inheritance and its association with spot blotch resistance in spring wheat (*Triticum aestivum* L.). Euphytica 153 (1):59-71. doi:10.1007/s10681-006-9235-z
Jukanti AK, Fischer AM (2008) A high-grain protein content locus on barley (*Hordeum vulgare*) chromosome 6 is associated with increased flag leaf proteolysis and nitrogen remobilization. Physiologia Plantarum 132 (4):426-439. doi:10.1111/j.1399-3054.2007.01044.x
Jukanti AK, Heidlebaugh NM, Parrott DL, Fischer IA, McInnerney K, Fischer AM (2008) Comparative transcriptome profiling of near-isogenic barley (*Hordeum vulgare*) lines differing in the allelic state of a major grain protein content locus identifies genes with possible roles in leaf senescence and nitrogen reallocation. New Phytologist 177 (2):333-349. doi:10.1111/j.1469-8137.2007.02270.x
Kade M, Barneix AJ, Olmos S, Dubcovsky J (2005) Nitrogen uptake and remobilization in tetraploid 'Langdon' durum wheat and a recombinant substitution line with the high grain protein gene *Gpc-B1*. Plant Breeding 124 (4):343-349. doi:10.1111/j.1439-0523.2005.01110.x
Kang K, Shim Y, Gi E, An G, Paek NC (2019) Mutation of *ONAC096* Enhances Grain Yield by Increasing Panicle Number and Delaying Leaf Senescence during Grain Filling in Rice. International Journal of Molecular Sciences 20 (20). doi:10.3390/ijms20205241
Kichey T, Hirel B, Heumez E, Dubois F, Le Gouis J (2007) In winter wheat (*Triticum aestivum* L.), post-anthesis nitrogen uptake and remobilisation to the grain correlates with agronomic traits and nitrogen physiological markers. Field Crops Research 102 (1):22-32. doi:10.1016/j.fcr.2007.01.002
Kichey T, Le Gouis J, Sangwan B, Hirel B, Dubois F (2005) Changes in the cellular and subcellular localization of glutamine synthetase and glutamate dehydrogenase during flag leaf senescence in wheat (*Triticum aestivum* L.). Plant and Cell Physiology 46 (6):964-974. doi:10.1093/pcp/pci105
Kim HJ, Nam HG, Lim PO (2016) Regulatory network of NAC transcription factors in leaf senescence. Current Opinion in Plant Biology 33:48-56. doi:10.1016/j.pbi.2016.06.002
Kim HJ, Park JH, Kim J, Kim JJ, Hong S, Kim JH, Woo HR, Hyeon C, Lim PO, Nam HG, Hwang D (2018) Time- evolving genetic networks reveal a NAC troika that negatively regulates leaf senescence in *Arabidopsis*. Proceedings of the National Academy of Sciences of the United States of America 115 (21):E4930-E4939. doi:10.1073/pnas.1721523115
Kim J (2019) Sugar metabolism as input signals and fuel for leaf senescence. Genes & Genomics 41 (7):737-746. doi:10.1007/s13258-019-00804-y
Kinsella RJ, Kähäri A, Haider S, Zamora J, Proctor G, Spudich G, Almeida-King J, Staines D, Derwent P, Kerhornou A, Kersey P, Flicek P (2011) Ensembl BioMarts: a hub for data retrieval across taxonomic space. Database 2011:bar030. doi:10.1093/database/bar030
Kiszonas AM, Ibba MI, Boehm JD, Morris CF (2021) Effects of the functional *Gpc-B1* allele on soft durum wheat grain, milling, flour, dough, and breadmaking quality. Cereal Chemistry 98 (6):1250-1258. doi:10.1002/cche.10477

Kong LA, Xie Y, Hu L, Feng B, Li SD (2016) Remobilization of vegetative nitrogen to developing grain in wheat (*Triticum aestivum* L.). Field Crops Research 196:134-144. doi:10.1016/j.fcr.2016.06.015
Kong LG, Sun MZ, Xie Y, Wang FH, Zhao ZD (2015) Photochemical and antioxidative responses of the glume and flag leaf to seasonal senescence in wheat. Frontiers in Plant Science 6. doi:10.3389/fpls.2015.00358
Krasileva KV, Vasquez-Gross HA, Howell T, Bailey P, Paraiso F, Clissold L, Simmonds J, Ramirez-Gonzalez RH, Wang X, Borrill P, Fosker C, Ayling S, Phillips AL, Uauy C, Dubcovsky J (2017) Uncovering hidden variation in polyploid wheat. Proceedings of the National Academy of Sciences of the United States of America 114 (6):E913. doi:10.1073/pnas.1619268114
Kumar J, Jaiswal V, Kumar A, Kumar N, Mir RR, Kumar S, Dhariwal R, Tyagi S, Khandelwal M, Prabhu KV, Prasad R, Balyan HS, Gupta PK (2011) Introgression of a major gene for high grain protein content in some Indian bread wheat cultivars. Field Crops Research 123 (3):226-233. doi:https://doi.org/10.1016/j.fcr.2011.05.013
Kumar P, Henikoff S, Ng PC (2009) Predicting the effects of coding non-synonymous variants on protein function using the SIFT algorithm. Nature Protocols 4 (7):1073-1081. doi:10.1038/nprot.2009.86
Kumar U, Joshi AK, Kumari M, Paliwal R, Kumar S, Röder MS (2010) Identification of QTLs for stay green trait in wheat (*Triticum aestivum* L.) in the 'Chirya 3' × 'Sonalika' population. Euphytica 174 (3):437-445. doi:10.1007/s10681-010-0155-6
Kunieda T, Mitsuda N, Ohme-Takagi M, Takeda S, Aida M, Tasaka M, Kondo M, Nishimura M, Hara-Nishimura I (2008) NAC Family Proteins NARS1/NAC2 and NARS2/NAM in the Outer Integument Regulate Embryogenesis in *Arabidopsis*. Plant Cell 20 (10):2631-2642. doi:10.1105/tpc.108.060160
Lee DK, Chung PJ, Jeong JS, Jang G, Bang SW, Jung H, Kim YS, Ha SH, Choi YD, Kim JK (2017) The rice *OsNAC6* transcription factor orchestrates multiple molecular mechanisms involving root structural adaptions and nicotianamine biosynthesis for drought tolerance. Plant Biotechnol J 15 (6):754-764. doi:10.1111/pbi.12673
Leonova IN, Kiseleva AA, Berezhnaya AA, Stasyuk AI, Likhenko IE, Salina EA (2022) Identification of QTLs for Grain Protein Content in Russian Spring Wheat Varieties. Plants-Basel 11 (3). doi:10.3390/plants11030437
Leopold AC (1961) Senescence in plant development - death of plants or plant parts may be of positive ecological or physiological value. Science 134 (349):1727-&. doi:10.1126/science.134.3492.1727
Lewis CM, Persoons A, Bebber DP, Kigathi RN, Maintz J, Findlay K, Bueno-Sancho V, Corredor-Moreno P, Harrington SA, Kangara N, Berlin A, García R, Germán SE, Hanzalová A, Hodson DP, Hovmøller MS, Huerta-Espino J, Imtiaz M, Mirza JI, Justesen AF, Niks RE, Omrani A, Patpour M, Pretorius ZA, Roohparvar R, Sela H, Singh RP, Steffenson B, Visser B, Fenwick PM, Thomas J, Wulff BBH, Saunders DGO (2018) Potential for re-emergence of wheat stem rust in the United Kingdom. Commun Biol 1 (1):13. doi:10.1038/s42003-018-0013-y
Li H, Liu H, Hao C, Li T, Liu Y, Wang X, Yang Y, Zheng J, Zhang X (2022) The auxin response factor *TaARF15-A1* negatively regulates senescence in common wheat (*Triticum aestivum* L.). Plant Physiology. doi:10.1093/plphys/kiac497
Li HZ, Gao X, Li XY, Chen QJ, Dong J, Zhao WC (2013) Evaluation of Assembly Strategies Using RNA-Seq Data Associated with Grain Development of Wheat (Triticum aestivum L.). Plos One 8 (12). doi:ARTN e8353 10.1371/journal.pone.0083530
Li L, He Y, Zhang Z, Shi Y, Zhang X, Xu X, Wu JL, Tang S (2021) *OsNAC109* regulates senescence, growth and development by altering the expression of senescence- and phytohormone-associated genes in rice. Plant Mol Biol 105 (6):637-654. doi:10.1007/s11103-021-01118-y
Li Z, Wang M, Lin K, Xie Y, Guo J, Ye L, Zhuang Y, Teng W, Ran X, Tong Y, Xue Y, Zhang W, Zhang Y (2019) The bread wheat epigenomic map reveals distinct chromatin

architectural and evolutionary features of functional genetic elements. Genome Biology 20 (1):139. doi:10.1186/s13059-019-1746-8
Li ZH, Woo HR, Guo HW (2018) Genetic redundancy of senescence-associated transcription factors in *Arabidopsis*. Journal of Experimental Botany 69 (4):811-823. doi:10.1093/jxb/erx345
Liang C, Wang Y, Zhu Y, Tang J, Hu B, Liu L, Ou S, Wu H, Sun X, Chu J, Chu C (2014) *OsNAP* connects abscisic acid and leaf senescence by fine-tuning abscisic acid biosynthesis and directly targeting senescence-associated genes in rice. Proceedings of the National Academy of Sciences of the United States of America 111 (27):10013. doi:10.1073/pnas.1321568111
Lim PO, Kim HJ, Nam HG (2007) Leaf senescence. In: Annual Review of Plant Biology, vol 58. Annual Review of Plant Biology. pp 115-136. doi:10.1146/annurev.arplant.57.032905.105316
Ling H-Q, Ma B, Shi X, Liu H, Dong L, Sun H, Cao Y, Gao Q, Zheng S, Li Y, Yu Y, Du H, Qi M, Li Y, Lu H, Yu H, Cui Y, Wang N, Chen C, Wu H, Zhao Y, Zhang J, Li Y, Zhou W, Zhang B, Hu W, van Eijk MJT, Tang J, Witsenboer HMA, Zhao S, Li Z, Zhang A, Wang D, Liang C (2018) Genome sequence of the progenitor of wheat A subgenome *Triticum urartu*. Nature 557 (7705):424-428. doi:10.1038/s41586-018-0108-0
Lundstrom M, Leino MW, Hagenblad J (2017) Evolutionary history of the *NAM-B1* gene in wild and domesticated tetraploid wheat. Bmc Genetics 18. doi:10.1186/s12863-017-0566-7
Lv SK, Guo H, Zhang M, Wang QH, Zhang H, Ji WQ (2020a) Large-Scale Cloning and Comparative Analysis of TaNAC Genes in Response to Stripe Rust and Powdery Mildew in Wheat (Triticum aestivumL.). Genes 11 (9):19. doi:10.3390/genes11091073
Lv XM, Zhang Y, Zhang YX, Fan SJ, Kong LG (2020b) Source-sink modifications affect leaf senescence and grain mass in wheat as revealed by proteomic analysis. Bmc Plant Biology 20 (1):17. doi:10.1186/s12870-020-02447-8
Ma XM, Balazadeh S, Mueller-Roeber B (2019) Tomato fruit ripening factor *NOR* controls leaf senescence. Journal of Experimental Botany 70 (10):2727-2740. doi:10.1093/jxb/erz098
Maccaferri M, Harris NS, Twardziok SO, Pasam RK, Gundlach H, Spannagl M, Ormanbekova D, Lux T, Prade VM, Milner SG, Himmelbach A, Mascher M, Bagnaresi P, Faccioli P, Cozzi P, Lauria M, Lazzari B, Stella A, Manconi A, Gnocchi M, Moscatelli M, Avni R, Deek J, Biyiklioglu S, Frascaroli E, Corneti S, Salvi S, Sonnante G, Desiderio F, Marè C, Crosatti C, Mica E, Özkan H, Kilian B, De Vita P, Marone D, Joukhadar R, Mazzucotelli E, Nigro D, Gadaleta A, Chao S, Faris JD, Melo ATO, Pumphrey M, Pecchioni N, Milanesi L, Wiebe K, Ens J, MacLachlan RP, Clarke JM, Sharpe AG, Koh CS, Liang KYH, Taylor GJ, Knox R, Budak H, Mastrangelo AM, Xu SS, Stein N, Hale I, Distelfeld A, Hayden MJ, Tuberosa R, Walkowiak S, Mayer KFX, Ceriotti A, Pozniak CJ, Cattivelli L (2019) Durum wheat genome highlights past domestication signatures and future improvement targets. Nature Genetics 51 (5):885-895. doi:10.1038/s41588-019-0381-3
Madeira F, Pearce M, Tivey ARN, Basutkar P, Lee J, Edbali O, Madhusoodanan N, Kolesnikov A, Lopez R (2022) Search and sequence analysis tools services from EMBL-EBI in 2022. Nucleic acids research 50 (W1):W276-W279. doi:10.1093/nar/gkac240
Maeoka RE, Sadras VO, Ciampitti IA, Diaz DR, Fritz AK, Lollato RP (2020) Changes in the Phenotype of Winter Wheat Varieties Released Between 1920 and 2016 in Response to In-Furrow Fertilizer: Biomass Allocation, Yield, and Grain Protein Concentration. Frontiers in Plant Science 10. doi:10.3389/fpls.2019.01786
Mao CJ, Lu SC, Lv B, Zhang B, Shen JB, He JM, Luo LQ, Xi DD, Chen X, Ming F (2017) A Rice NAC Transcription Factor Promotes Leaf Senescence via ABA Biosynthesis. Plant Physiology 174 (3):1747-1763. doi:10.1104/pp.17.00542

Mao H, Li S, Chen B, Jian C, Mei F, Zhang Y, Li F, Chen N, Li T, Du L, Ding L, Wang Z, Cheng X, Wang X, Kang Z (2022) Variation in cis-regulation of a NAC transcription factor contributes to drought tolerance in wheat. Mol Plant 15 (2):276-292. doi:10.1016/j.molp.2021.11.007
Mao HD, Li SM, Wang ZX, Cheng XX, Li FF, Mei FM, Chen N, Kang ZS (2020) Regulatory changes in *TaSNAC8-6A* are associated with drought tolerance in wheat seedlings. Plant Biotechnology Journal 18 (4):1078-1092. doi:10.1111/pbi.13277
McCallum CM, Comai L, Greene EA, Henikoff S (2000) Targeting Induced LocalLesions IN Genomes (TILLING) for Plant Functional Genomics. Plant Physiology 123 (2):439-442. doi:10.1104/pp.123.2.439
McLaren W, Gil L, Hunt SE, Riat HS, Ritchie GR, Thormann A, Flicek P, Cunningham F (2016) The Ensembl Variant Effect Predictor. Genome Biol 17 (1):122. doi:10.1186/s13059-016-0974-4
Met Office Weather Observations Website (2023) https://wow.metoffice.gov.uk/. Accessed 18/04/2023
Milner MJ, Howells RM, Craze M, Bowden S, Graham N, Wallington EJ (2018) A PSTOL-like gene, *TaPSTOL*, controls a number of agronomically important traits in wheat. BMC Plant Biology 18 (1):115. doi:10.1186/s12870-018-1331-4
Mishra V, Gupta P, Balasubramaniam A, Chand R, Vasistha N, Vishwakarma M, Yadav P, Joshi A (2015) Introgression of a gene for high grain protein content (*Gpc-B1*) into two leading cultivars of wheat in Eastern Gangetic Plains of India through marker assisted backcross breeding.
Nakashima K, Takasaki H, Mizoi J, Shinozaki K, Yamaguchi-Shinozaki K (2012) NAC transcription factors in plant abiotic stress responses. Biochimica Et Biophysica Acta-Gene Regulatory Mechanisms 1819 (2):97-103. doi:10.1016/j.bbagrm.2011.10.005
NCBI (2020) PSSM Viewer https://www.ncbi.nlm.nih.gov/Class/Structure/pssm/pssm_viewer.cgi. Accessed 01/07/2020 (No longer available)
Okumoto S, Pilot G (2011) Amino Acid Export in Plants: A Missing Link in Nitrogen Cycling. Molecular Plant 4 (3):453-463. doi:10.1093/mp/ssr003
Olmos S, Distelfeld A, Chicaiza O, Schlatter AR, Fahima T, Echenique V, Dubcovsky J (2003) Precise mapping of a locus affecting grain protein content in durum wheat. Theoretical and Applied Genetics 107 (7):1243-1251. doi:10.1007/s00122-003-1377-y
Olsen AN, Ernst HA, Lo Leggio L, Skriver K (2005) NAC transcription factors: structurally distinct, functionally diverse. Trends in Plant Science 10 (2):79-87. doi:10.1016/j.tplants.2004.12.010
Orlovskaya OA, Vakula SI, Yatsevich KK, Khotyleva LV, Kilchevsky AV (2022) Productivity and grain nutritional value traits in wheat genotypes with different *NAM-B1* gene allelic variations. Doklady Natsionalnoi Akademii Nauk Belarusi 66 (5):517-524. doi:10.29235/1561-8323-2022-66-5-517-524
Pan WLL, Kidwell KK, McCracken VA, Bolton RP, Allen M (2020) Economically Optimal Wheat Yield, Protein and Nitrogen Use Component Responses to Varying N Supply and Genotype. Frontiers in Plant Science 10. doi:10.3389/fpls.2019.01790
Parrott DL, McInnerney K, Feller U, Fischer AM (2007) Steam-girdling of barley (*Hordeum vulgare*) leaves leads to carbohydrate accumulation and accelerated leaf senescence, facilitating transcriptomic analysis of senescence-associated genes. New Phytologist 176 (1):56-69. doi:10.1111/j.1469-8137.2007.02158.x
Pearce S, Tabbita F, Cantu D, Buffalo V, Avni R, Vazquez-Gross H, Zhao RR, Conley CJ, Distelfeld A, Dubcovksy J (2014) Regulation of Zn and Fe transporters by the *GPC1* gene during early wheat monocarpic senescence. Bmc Plant Biology 14. doi:10.1186/s12870-014-0368-2
Pfaffl MW (2001) A new mathematical model for relative quantification in real-time RT-PCR. Nucleic Acids Res 29 (9):e45. doi:10.1093/nar/29.9.e45

Philipp N, Weise S, Oppermann M, Börner A, Keilwagen J, Kilian B, Arend D, Zhao Y, Graner A, Reif JC, Schulthess AW (2019) Historical phenotypic data from seven decades of seed regeneration in a wheat ex situ collection. Scientific Data 6 (1):137. doi:10.1038/s41597-019-0146-y

Podzimska-Sroka D, O'Shea C, Gregersen PL, Skriver K, Balazadeh S (2015) NAC Transcription Factors in Senescence: From Molecular Structure to Function in Crops. Plants 4 (3):412-448. doi:10.3390/plants4030412

Pont C, Leroy T, Seidel M, Tondelli A, Duchemin W, Armisen D, Lang D, Bustos-Korts D, Goue N, Balfourier F, Molnar-Lang M, Lage J, Kilian B, Ozkan H, Waite D, Dyer S, Letellier T, Alaux M, Russell J, Keller B, van Eeuwijk F, Spannagl M, Mayer KFX, Waugh R, Stein N, Cattivelli L, Haberer G, Charmet G, Salse J, Wheat Barley Legacy B (2019) Tracing the ancestry of modern bread wheats. Nature Genetics 51 (5):905-+. doi:10.1038/s41588-019-0393-z

Qualset C, Vogt H, Borlaug N (1985) Registration of 'Yecora Rojo' Wheat. Crop Science - CROP SCI 25. doi:10.2135/cropsci1985.0011183X002500060069x

Ramírez-González RH, Borrill P, Lang D, Harrington SA, Brinton J, Venturini L, Davey M, Jacobs J, van Ex F, Pasha A, Khedikar Y, Robinson SJ, Cory AT, Florio T, Concia L, Juery C, Schoonbeek H, Steuernagel B, Xiang D, Ridout CJ, Chalhoub B, Mayer KFX, Benhamed M, Latrasse D, Bendahmane A, Wulff BBH, Appels R, Tiwari V, Datla R, Choulet F, Pozniak CJ, Provart NJ, Sharpe AG, Paux E, Spannagl M, Bräutigam A, Uauy C (2018) The transcriptional landscape of polyploid wheat. Science 361 (6403):eaar6089. doi:10.1126/science.aar6089

Ramirez-Gonzalez RH, Uauy C, Caccamo M (2015) PolyMarker: A fast polyploid primer design pipeline. Bioinformatics 31 (12):2038-2039. doi:10.1093/bioinformatics/btv069

Randhawa HS, Asif M, Pozniak C, Clarke JM, Graf RJ, Fox SL, Humphreys DG, Knox RE, DePauw RM, Singh AK, Cuthbert RD, Hucl P, Spaner D (2013) Application of molecular markers to wheat breeding in Canada. Plant Breeding 132 (5):458-471. doi:https://doi.org/10.1111/pbr.12057

Ricachenevsky FK, Menguer PK, Sperotto RA (2013) kNACking on heaven's door: how important are NAC transcription factors for leaf senescence and Fe/Zn remobilization to seeds? Frontiers in Plant Science 4. doi:10.3389/fpls.2013.00226

Roberts IN, Caputo C, Criado MV, Funk C (2012) Senescence-associated proteases in plants. Physiologia Plantarum 145 (1):130-139. doi:10.1111/j.1399-3054.2012.01574.x

Roberts IN, Caputo C, Kade M, Criado MV, Barneix AJ (2011) Subtilisin-like serine proteases involved in N remobilization during grain filling in wheat. Acta Physiologiae Plantarum 33 (5):1997-2001. doi:10.1007/s11738-011-0712-1

Sakuraba Y, Kim D, Han SH, Kim SH, Piao W, Yanagisawa S, An G, Paek NC (2020) Multilayered Regulation of Membrane-Bound *ONAC054* Is Essential for Abscisic Acid-Induced Leaf Senescence in Rice. Plant Cell 32 (3):630-649. doi:10.1105/tpc.19.00569

Sakuraba Y, Piao W, Lim J-H, Han S-H, Kim Y-S, An G, Paek N-C (2015) Rice *ONAC106* Inhibits Leaf Senescence and Increases Salt Tolerance and Tiller Angle. Plant and Cell Physiology 56 (12):2325-2339. doi:10.1093/pcp/pcv144

Sansaloni C, Franco J, Santos B, Percival-Alwyn L, Singh S, Petroli C, Campos J, Dreher K, Payne T, Marshall D, Kilian B, Milne I, Raubach S, Shaw P, Stephen G, Carling J, Pierre CS, Burgueño J, Crosa J, Li H, Guzman C, Kehel Z, Amri A, Kilian A, Wenzl P, Uauy C, Banziger M, Caccamo M, Pixley K (2020) Diversity analysis of 80,000 wheat accessions reveals consequences and opportunities of selection footprints. Nat Commun 11 (1):4572. doi:10.1038/s41467-020-18404-w

Sasaki T, International Rice Genome Sequencing P (2005) The map-based sequence of the rice genome. Nature 436 (7052):793-800. doi:10.1038/nature03895

Schippers JHM (2015) Transcriptional networks in leaf senescence. Current Opinion in Plant Biology 27:77-83. doi:10.1016/j.pbi.2015.06.018

Schreiber AW, Hayden MJ, Forrest KL, Kong SL, Langridge P, Baumann U (2012) Transcriptome-scale homoeolog-specific transcript assemblies of bread wheat. BMC Genomics 13 (1):492. doi:10.1186/1471-2164-13-492

Schulthess AW, Kale SM, Zhao Y, Gogna A, Rembe M, Philipp N, Liu F, Beukert U, Serfling A, Himmelbach A, Oppermann M, Weise S, Boeven PHG, Schacht J, Longin CFH, Kollers S, Pfeiffer N, Korzun V, Fiebig A, Schüler D, Lange M, Scholz U, Stein N, Mascher M, Reif JC (2022) Large-scale genotyping and phenotyping of a worldwide winter wheat genebank for its use in pre-breeding. Scientific Data 9 (1):784. doi:10.1038/s41597-022-01891-5

Scott MF, Fradgley N, Bentley AR, Brabbs T, Corke F, Gardner KA, Horsnell R, Howell P, Ladejobi O, Mackay IJ, Mott R, Cockram J (2021) Limited haplotype diversity underlies polygenic trait architecture across 70 years of wheat breeding. Genome Biology 22 (1):137. doi:10.1186/s13059-021-02354-7

Sekhon RS, Saski C, Kumar R, Flinn BS, Luo F, Beissinger TM, Ackerman AJ, Breitzman MW, Bridges WC, de Leon N, Kaepplere SM (2019) Integrated Genome-Scale Analysis Identifies Novel Genes and Networks Underlying Senescence in Maize. Plant Cell 31 (9):1968-1989. doi:10.1105/tpc.18.00930

Sharma G, Upadyay AK, Biradar H, Sonia, Hittalmani S (2019) *OsNAC*-like transcription factor involved in regulating seed-storage protein content at different stages of grain filling in rice under aerobic conditions. Journal of Genetics 98 (1). doi:10.1007/s12041-019-1066-5

Shorinola O, Simmonds J, Wingen LU, Uauy C (2022) Trend, population structure, and trait mapping from 15 years of national varietal trials of UK winter wheat. G3-Genes Genomes Genetics 12 (2). doi:10.1093/g3journal/jkab415

Simmonds J, Scott P, Brinton J, Mestre TC, Bush M, del Blanco A, Dubcovsky J, Uauy C (2016) A splice acceptor site mutation in *TaGW2-A1* increases thousand grain weight in tetraploid and hexaploid wheat through wider and longer grains. Theoretical and Applied Genetics 129 (6):1099-1112. doi:10.1007/s00122-016-2686-2

Simmonds NW (1995) The relation between yield and protein in cereal grain. Journal of the Science of Food and Agriculture 67 (3):309-315. doi:10.1002/jsfa.2740670306

Singh N, Wu S, Tiwari V, Sehgal S, Raupp J, Wilson D, Abbasov M, Gill B, Poland J (2019) Genomic Analysis Confirms Population Structure and Identifies Inter-Lineage Hybrids in Aegilops tauschii. Frontiers in Plant Science 10. doi:10.3389/fpls.2019.00009

Slade AJ, Fuerstenberg SI, Loeffler D, Steine MN, Facciotti D (2005) A reverse genetic, nontransgenic approach to wheat crop improvement by TILLING. Nature Biotechnology 23 (1):75-81. doi:10.1038/nbt1043

Song SY, Chen Y, Chen J, Dai XY, Zhang WH (2011) Physiological mechanisms underlying *OsNAC5*-dependent tolerance of rice plants to abiotic stress. Planta 234 (2):331-345. doi:10.1007/s00425-011-1403-2

Souer E, van Houwelingen A, Kloos D, Mol J, Koes R (1996) The *No Apical Meristem* Gene of Petunia Is Required for Pattern Formation in Embryos and Flowers and Is Expressed at Meristem and Primordia Boundaries. Cell 85 (2):159-170. doi:https://doi.org/10.1016/S0092-8674(00)81093-4

Sperotto R, Ricachenevsky F, Duarte G, Boff T, Lopes K, Sperb E, Grusak M, Fett J (2009) Identification of up-regulated genes in flag leaves during rice grain filling and characterization of *OsNAC5*, a new ABA-dependent transcription factor. An International Journal of Plant Biology 230 (5):985-1002. doi:10.1007/s00425-009-1000-9

Sun LJ, Huang L, Hong YB, Zhang HJ, Song FM, Li DY (2015) Comprehensive Analysis Suggests Overlapping Expression of Rice *ONAC* Transcription Factors in Abiotic and Biotic Stress Responses. International Journal of Molecular Sciences 16 (2):4306-4326. doi:10.3390/ijms16024306

Tabbita F, Pearce S, Barneix AJ (2017) Breeding for increased grain protein and micronutrient content in wheat: Ten years of the *GPC-B1* gene. Journal of Cereal Science 73:183-191. doi:10.1016/j.jcs.2017.01.003

Takasaki H, Maruyama K, Kidokoro S, Ito Y, Fujita Y, Shinozaki K, Yamaguchi-Shinozaki K, Nakashima K (2010) The abiotic stress-responsive NAC-type transcription factor *OsNAC5* regulates stress-inducible genes and stress tolerance in rice. Molecular Genetics and Genomics 284 (3):173-183. doi:10.1007/s00438-010-0557-0

Tenea GN, Peres Bota A, Cordeiro Raposo F, Maquet A (2011) Reference genes for gene expression studies in wheat flag leaves grown under different farming conditions. BMC Res Notes 4:373. doi:10.1186/1756-0500-4-373

Thomas H, Howarth CJ (2000) Five ways to stay green. Journal of experimental botany 51 (suppl_1):329-337

Thomas H, Ougham H (2014) The stay-green trait. Journal of Experimental Botany 65 (14):3889-3900. doi:10.1093/jxb/eru037

Thorwarth P, Liu GZ, Ebmeyer E, Schacht J, Schachschneider R, Kazman E, Reif JC, Wurschum T, Longin CFH (2019) Dissecting the genetics underlying the relationship between protein content and grain yield in a large hybrid wheat population. Theoretical and Applied Genetics 132 (2):489-500. doi:10.1007/s00122-018-3236-x

Tuinstra MR, Ejeta G, Goldsbrough PB (1997) Heterogeneous inbred family (HIF) analysis: a method for developing near-isogenic lines that differ at quantitative trait loci. Theoretical and Applied Genetics 95 (5):1005-1011. doi:10.1007/s001220050654

Uauy C, Brevis JC, Dubcovsky J (2006) The high grain protein content gene *Gpc-B1* accelerates senescence and has pleiotropic effects on protein content in wheat. Journal of Experimental Botany 57 (11):2785-2794. doi:10.1093/jxb/erl047

Uauy C, Distelfeld A, Fahima T, Blechl A, Dubcovsky J (2006) A NAC gene regulating senescence improves grain protein, zinc, and iron content in wheat. Science 314 (5803):1298-1301. doi:10.1126/science.1133649

Uauy C, Wulff BBH, Dubcovsky J (2017) Combining Traditional Mutagenesis with New High-Throughput Sequencing and Genome Editing to Reveal Hidden Variation in Polyploid Wheat. In: Bonini NM (ed) Annual Review of Genetics, Vol 51, vol 51. Annual Review of Genetics. pp 435-454. doi:10.1146/annurev-genet-120116-024533

UK Flour Millers (2023) Flour Milling in the UK.

United Nations (2022) World Population Prospects 2022: Summary of Results. Department of Economic and Social Affairs Population Division UN DESA/POP/2022/TR/NO. 3.

United Nations (2023) UN Sustainable Development Goals. https://sdgs.un.org/goals. Accessed 07/09/2023

Venske E, dos Santos RS, Busanello C, Gustafson P, de Oliveira AC (2019) Bread wheat: a role model for plant domestication and breeding. Hereditas 156. doi:10.1186/s41065-019-0093-9

Wairich A, Vitali A, Adamski JM, Lopes KL, Duarte GL, Ponte LR, Costa HK, Menguer PK, dos Santos RP, Fett JP, Sperotto RA, Ricachenevsky FK (2023) Enhanced expression of *OsNAC5* leads to up-regulation of *OsNAC6* and changes rice (*Oryza sativa* L.) ionome. Genetics and Molecular Biology 46 (1). doi:10.1590/1678-4685-gmb-2022-0190

Walkowiak S, Gao LL, Monat C, Haberer G, Kassa MT, Brinton J, Ramirez-Gonzalez RH, Kolodziej MC, Delorean E, Thambugala D, Klymiuk V, Byrns B, Gundlach H, Bandi V, Siri JN, Nilsen K, Aquino C, Himmelbach A, Copetti D, Ban T, Venturini L, Bevan M, Clavijo B, Koo DH, Ens J, Wiebe K, N'Diaye A, Fritz AK, Gutwin C, Fiebig A, Fosker C, Fu BX, Accinelli GG, Gardner KA, Fradgley N, Gutierrez-Gonzalez J, Halstead-Nussloch G, Hatakeyama M, Koh CS, Deek J, Costamagna AC, Fobert P, Heavens D, Kanamori H, Kawaura K, Kobayashi F, Krasileva K, Kuo T, McKenzie N, Murata K, Nabeka Y, Paape T, Padmarasu S, Percival-Alwyn L, Kagale S, Scholz U, Sese J, Juliana P, Singh R, Shimizu-Inatsugi R, Swarbreck D, Cockram J, Budak H, Tameshige T, Tanaka T, Tsuji H, Wright J, Wu JZ, Steuernagel B, Small I, Cloutier S, Keeble-Gagnere G, Muehlbauer G, Tibbets J, Nasuda S, Melonek J, Hucl PJ, Sharpe AG, Clark M, Legg E, Bharti A, Langridge P, Hall A, Uauy C, Mascher M, Krattinger SG, Handa H, Shimizu KK, Distelfeld A, Chalmers K, Keller B, Mayer KFX, Poland J, Stein N, McCartney CA, Spannagl M, Wicker T, Pozniak CJ (2020) Multiple

wheat genomes reveal global variation in modern breeding. Nature 588 (7837). doi:10.1038/s41586-020-2961-x
Wang H-L, Zhang Y, Wang T, Yang Q, Yang Y, Li Z, Li B, Wen X, Li W, Yin W, Xia X, Guo H, Li Z (2021a) An Alternative Splicing Variant of *PtRD26* Delays Leaf Senescence by Regulating Multiple NAC Transcription Factors in *Populus*. Plant Cell. doi:10.1093/plcell/koab046
Wang HJ, Schippers JHM (2019) The Role and Regulation of Autophagy and the Proteasome During Aging and Senescence in Plants. Genes 10 (4). doi:10.3390/genes10040267
Wang M, Li Z, Zhang Ye, Zhang Y, Xie Y, Ye L, Zhuang Y, Lin K, Zhao F, Guo J, Teng W, Zhang W, Tong Y, Xue Y, Zhang Y (2021b) An atlas of wheat epigenetic regulatory elements reveals subgenome divergence in the regulation of development and stress responses. The Plant Cell 33 (4):865-881. doi:10.1093/plcell/koab028
Wang N, Xie YZ, Li YZ, Wu SN, Li SX, Guo Y, Wang CS (2020) High-Resolution Mapping of the Novel Early Leaf Senescence Gene *Els2* in Common Wheat. Plants-Basel 9 (6). doi:10.3390/plants9060698
Wang YG, Ren XF, Sun DF, Sun GL (2015) Origin of worldwide cultivated barley revealed by *NAM-1* gene and grain protein content. Frontiers in Plant Science 6. doi:10.3389/fpls.2015.00803
Waters BM, Uauy C, Dubcovsky J, Grusak MA (2009) Wheat (*Triticum aestivum*) NAM proteins regulate the translocation of iron, zinc, and nitrogen compounds from vegetative tissues to grain. Journal of Experimental Botany 60 (15):4263-4274. doi:10.1093/jxb/erp257
Watson A, Ghosh S, Williams MJ, Cuddy WS, Simmonds J, Rey MD, Hatta MAM, Hinchliffe A, Steed A, Reynolds D, Adamski NM, Breakspear A, Korolev A, Rayner T, Dixon LE, Riaz A, Martin W, Ryan M, Edwards D, Batley J, Raman H, Carter J, Rogers C, Domoney C, Moore G, Harwood W, Nicholson P, Dieters MJ, DeLacy IH, Zhou J, Uauy C, Boden SA, Park RF, Wulff BBH, Hickey LT (2018) Speed breeding is a powerful tool to accelerate crop research and breeding. Nature Plants 4 (1):23-29. doi:10.1038/s41477-017-0083-8
Welner DH, Lindemose S, Grossmann JG, Mollegaard NE, Olsen AN, Helgstrand C, Skriver K, Lo Leggio L (2012) DNA binding by the plant-specific NAC transcription factors in crystal and solution: a firm link to WRKY and GCM transcription factors. Biochemical Journal 444:395-404. doi:10.1042/Bj20111742
Wendel JF (2000) Genome evolution in polyploids. Plant Molecular Biology 42 (1):225-249. doi:10.1023/a:1006392424384
Wheat Training (2023) Designing genome specific primers in polyploid wheat. https://www.wheat-training.com/wp-content/uploads/Functional_studies/PDFs/Designing-genome-specific-primers.pdf. Accessed 01/05/2020
Winfield MO, Allen AM, Wilkinson PA, Burridge AJ, Barker GLA, Coghill J, Waterfall C, Wingen LU, Griffiths S, Edwards KJ (2018) High-density genotyping of the AE Watkins Collection of hexaploid landraces identifies a large molecular diversity compared to elite bread wheat. Plant Biotechnology Journal 16 (1):165-175. doi:10.1111/pbi.12757
Winfield MO, Wilkinson PA, Allen AM, Barker GL, Coghill JA, Burridge A, Hall A, Brenchley RC, D'Amore R, Hall N, Bevan MW, Richmond T, Gerhardt DJ, Jeddeloh JA, Edwards KJ (2012) Targeted re-sequencing of the allohexaploid wheat exome. Plant Biotechnol J 10 (6):733-742. doi:10.1111/j.1467-7652.2012.00713.x
Wingen LU, Orford S, Goram R, Leverington-Waite M, Bilham L, Patsiou TS, Ambrose M, Dicks J, Griffiths S (2014) Establishing the A. E. Watkins landrace cultivar collection as a resource for systematic gene discovery in bread wheat. Theor Appl Genet 127 (8):1831-1842. doi:10.1007/s00122-014-2344-5

Wojciechowska N, Sobieszczuk-Nowicka E, Bagniewska-Zadworna A (2018) Plant organ senescence - regulation by manifold pathways. Plant Biology 20 (2):167-181. doi:10.1111/plb.12672

Xiang D, Quilichini TD, Liu Z, Gao P, Pan Y, Li Q, Nilsen KT, Venglat P, Esteban E, Pasha A, Wang Y, Wen R, Zhang Z, Hao Z, Wang E, Wei Y, Cuthbert R, Kochian LV, Sharpe A, Provart N, Weijers D, Gillmor CS, Pozniak C, Datla R (2019) The Transcriptional Landscape of Polyploid Wheats and Their Diploid Ancestors during Embryogenesis and Grain Development. The Plant Cell 31 (12):2888-2911. doi:10.1105/tpc.19.00397

Xie Q, Mayes S, Sparkes DL (2016) Early anthesis and delayed but fast leaf senescence contribute to individual grain dry matter and water accumulation in wheat. Field Crops Research 187:24-34. doi:10.1016/j.fcr.2015.12.009

Xue GP, Bower NI, McIntyre CL, Riding GA, Kazan K, Shorter R (2006) *TaNAC69* from the NAC superfamily of transcription factors is up-regulated by abiotic stresses in wheat and recognises two consensus DNA-binding sequences. Functional Plant Biology 33 (1):43-57. doi:10.1071/fp05161

Yang JC, Zhang JH (2006) Grain filling of cereals under soil drying. New Phytologist 169 (2):223-236. doi:10.1111/j.1469-8137.2005.01597.x

Yang JC, Zhang JH, Wang ZQ, Zhu QS, Liu LJ (2002) Abscisic acid and cytokinins in the root exudates and leaves and their relationship to senescence and remobilization of carbon reserves in rice subjected to water stress during grain filling. Planta 215 (4):645-652. doi:10.1007/s00425-002-0789-2

Yang LT, Mickelson S, See D, Blake TK, Fischer AM (2004) Genetic analysis of the function of major leaf proteases in barley (*Hordeum vulgare* L.) nitrogen remobilization. Journal of Experimental Botany 55 (408):2607-2616. doi:10.1093/jxb/erh267

Yang XL, Lu YL, Ding Y, Yin XF, Raza S, Tong YA (2017) Optimising nitrogen fertilisation: A key to improving nitrogen-use efficiency and minimising nitrate leaching losses in an intensive wheat/maize rotation (2008-2014). Field Crops Research 206:1-10. doi:10.1016/j.fcr.2017.02.016

Yates Andrew D, Allen J, Amode RM, Azov AG, Barba M, Becerra A, Bhai J, Campbell Lahcen I, Carbajo Martinez M, Chakiachvili M, Chougule K, Christensen M, Contreras-Moreira B, Cuzick A, Da Rin Fioretto L, Davis P, De Silva Nishadi H, Diamantakis S, Dyer S, Elser J, Filippi CV, Gall A, Grigoriadis D, Guijarro-Clarke C, Gupta P, Hammond-Kosack Kim E, Howe KL, Jaiswal P, Kaikala V, Kumar V, Kumari S, Langridge N, Le T, Luypaert M, Maslen GL, Maurel T, Moore B, Muffato M, Mushtaq A, Naamati G, Naithani S, Olson A, Parker A, Paulini M, Pedro H, Perry E, Preece J, Quinton-Tulloch M, Rodgers F, Rosello M, Ruffier M, Seager J, Sitnik V, Szpak M, Tate J, Tello-Ruiz Marcela K, Trevanion Stephen J, Urban M, Ware D, Wei S, Williams G, Winterbottom A, Zarowiecki M, Finn Robert D, Flicek P (2022) Ensembl Genomes 2022: an expanding genome resource for non-vertebrates. Nucleic Acids Research 50 (D1):D996-D1003. doi:10.1093/nar/gkab1007

Yuan Z, Cao Q, Zhang K, Ata-Ul-Karim ST, Tian Y, Zhu Y, Cao W, Liu X (2016) Optimal Leaf Positions for SPAD Meter Measurement in Rice. Front Plant Sci 7:719. doi:10.3389/fpls.2016.00719

Zhang Y, Li Z, Liu J, Zhang Ye, Ye L, Peng Y, Wang H, Diao H, Ma Y, Wang M, Xie Y, Tang T, Zhuang Y, Teng W, Tong Y, Zhang W, Lang Z, Xue Y, Zhang Y (2022) Transposable elements orchestrate subgenome-convergent and -divergent transcription in common wheat. Nat Commun 13 (1):6940. doi:10.1038/s41467-022-34290-w

Zhang YJ, Geng HM, Cui ZC, Wang HY, Liu DQ (2021a) Functional Analysis of Wheat NAC Transcription Factor, *TaNAC069*, in Regulating Resistance of Wheat to Leaf Rust Fungus. Frontiers in Plant Science 12. doi:10.3389/fpls.2021.604797

Zhang YY, Li ZJ, Zhang YE, Lin KD, Peng Y, Ye LH, Zhuang YL, Wang MY, Xie YL, Guo JY, Teng W, Tong YP, Zhang WL, Xue YBA, Lang ZB, Zhang YJ (2021b) Evolutionary rewiring of the wheat transcriptional regulatory network by lineage-specific

transposable elements. Genome Research 31 (12):2276-2289. doi:10.1101/gr.275658.121
Zhang ZL, Liu C, Guo YF (2020) Wheat Transcription Factor *TaSNAC11-4B* Positively Regulates Leaf Senescence through Promoting ROS Production in Transgenic *Arabidopsis*. International Journal of Molecular Sciences 21 (20):18. doi:10.3390/ijms21207672
Zhao D, Derkx AP, Liu DC, Buchner P, Hawkesford MJ (2015) Overexpression of a NAC transcription factor delays leaf senescence and increases grain nitrogen concentration in wheat. Plant Biology 17 (4):904-913. doi:10.1111/plb.12296
Zhao X, Guo Y, Kang L, Yin C, Bi A, Xu D, Zhang Z, Zhang J, Yang X, Xu J (2023) Population genomics unravels the Holocene history of bread wheat and its relatives. Nature Plants 9 (3):403-419
Zhou Y, Huang WF, Liu L, Chen TY, Zhou F, Lin YJ (2013) Identification and functional characterization of a rice NAC gene involved in the regulation of leaf senescence. Bmc Plant Biology 13. doi:10.1186/1471-2229-13-132
Zhu TT, Nevo E, Sun DF, Peng JH (2012) Phylogenetic analyses unravel the evolutionary history of NAC proteins in plants. Evolution 66 (6):1833-1848. doi:10.1111/j.1558-5646.2011.01553.x